University of Sheffield

Extracellular matrix receptors of the integrin family control cancer cell growth under nutrient starvation

Bian Yanes

A thesis submitted in partial fulfilment of
the requirements for the degree of
Doctor of Philosophy

The University of Sheffield
Faculty of Science

May 2025

Abstract

Alterations in cell metabolism is one of the hallmarks of cancer, where cancer cells have a different metabolic behaviour than normal cells and they are able to find alternative ways to obtain energy. Due to the high tumour growth rate and the limited blood supply, the tumour microenvironment has been found to be hypoxic and deprived of nutrients. Therefore, cancer cells reprogram their metabolism and adopt new strategies to survive. One of these strategies is to uptake macromolecules from the tumour microenvironment, degrade them and use them as a source of nutrients.

Here we showed that different types of ECM supported highly invasive breast cancer cell growth under amino acids starvation, through a pathway that required ECM internalisation followed by lysosomal degradation. The uptake and degradation of collagen I increased the intracellular amino acids content, leading to the upregulation of metabolic pathways including phenylalanine and tyrosine catabolism. The inhibition of this pathway abolished ECM dependent cell growth under amino acids starvation.

Cells interact with the ECM through plasma membrane receptors of the integrin family. Here we showed that $\alpha 2\beta 1$ integrin was required for ECM internalisation. Moreover, inhibiting $\alpha 2$ strongly impaired ECM-dependent cell growth under amino acids starvation. Furthermore, ECM was also shown to support the growth of breast cancer cells under glucose starvation in an $\alpha 2\beta 1$ integrin dependent mechanism. ECM was also shown to increase the intracellular amino acids content under glucose starvation suggesting that cells rely on amino acids when they are deprived.

Interestingly, amino acids starvation significantly upregulated $\alpha 2\beta 1$ integrin expression in breast and pancreatic cancer cells. This upregulation of $\alpha 2$ integrin expression was shown to be mediated by KRAS/MEK/ERK pathway.

Overall, our data highlight the role of the ECM receptor $\alpha 2\beta 1$ integrin in promoting ECM-dependent cell growth and identify a mechanism that regulates its expression under starvation.

Acknowledgment

Completing this PhD would have not been possible without the support and encouragement of many people.

First and foremost, I would like to express my deepest gratitude to my supervisor Dr. Elena Rainero, her continuous support, expertise and insightful feedback made this project very enjoyable. I truly appreciate the trust that she put in me and allowing me to carry on my project freely which helped me to grow both as a researcher and as an individual. Also, I would like to thank my advisers Prof. Andy Furley and Dr. Mark Bass for their countless advice and constructive comments during my PhD journey.

Many thanks to Dr. Hellen Matthews for providing the pancreatic cancer cells and for her advice and suggestions during lab meetings. I would like to also thank the staff at the Wolfson Light Microscopy Facility Dr Darren Robinson, Dr Nick van Hateren, Dr Heather Walker at the University of Sheffield Mass Spectrometry Centre and Dr Stephen Brown for his help at the Sheffield RNAi facility.

I am also deeply thankful to all Rainero and Matthews lab members for making the lab environment so much fun and enjoyable to work in. Many thanks to Mona and Vic for all the mature discussions during lunch time and for being great workout buddies. Thanks to Rachele for all the amazing stories that she shares with me, for the help in organising the lab and for her delicious cakes that she always makes. Thanks to Shahd, Sherry, Haya, Zhe, Ife, Eric, Bella, and Rachel for all their support, intellectual and scientific conversations.

On a personal note, I would like to express my heartfelt gratitude to my family (my dad, my mum, and my sisters) who despite being miles away, they have always been very supportive and motivated me to keep going. Their love, encouragement and believe in me gave me strength throughout this challenging journey.

Lastly, thanks to all my friends and loved ones who without them this achievement would have not been possible.

Declaration

I declare that this thesis has been solely the result of my own work and has not been submitted for any other degree at the University of Sheffield or any other institution. I can confirm that where I have quoted from the work of others, the source is always given.

Bian Yanes

Table of contents

Abstract 1
Acknowledgment 2
Declaration 3
Table of contents 4
List of Figures 9
List of Tables 12
Abbreviations 13
1 Introduction 17
1.1 Sustained proliferative signalling 18
1.2 Breast cancer: 18
1.2.1 Breast cancer progression and subtypes: 18
1.2.2 Genetic alterations in breast cancer 20
1.2.3 Breast cancer treatment: 22
1.2.3.1 Early breast cancer: 22
1.2.3.2 Advanced breast cancer: 23
1.3 Pancreatic cancer: 24
1.3.1 Pancreatic cancer progression: 24
1.3.2 Genetic alterations in PDAC: 25
1.3.3 Pancreatic cancer treatments: 26
1.3.3.1 Targeting KRAS to treat PDAC: 27
1.4 The tumour microenvironment (TME): 29
1.4.1 Immune cells: 29
1.4.2 Endothelial cells: 30
1.4.3 Cancer associated fibroblasts (CAFs): 30
1.4.4 The Extracellular matrix (ECM): 33
1.4.4.1 Collagens: 34
1.4.4.2 Fibronectin: 37
1.4.4.3 Basement membrane (BM): 39
1.5 ECM remodelling: 41
1.5.1 ECM stiffness: 42
1.5.2 ECM degradation: 43

1.5.3 ECM endocytosis: 45
1.6 ECM receptors: Integrins 47
1.7 Integrin trafficking: 49
1.8 Cancer metabolism: 51
1.8.1 Glycolysis: 51
1.8.2 Amino acids metabolism: 52
1.8.2.1 Glutamine metabolism: 53
1.8.2.2 Branched-Chain amino acids (BCAA): 55
1.8.2.3 Asparagine and Aspartate: 56
1.8.2.4 Serine and Glycine: 56
1.8.3 The role of CAFs in cancer metabolism: 58
1.8.4 Surviving under nutrient deprivation: 59
1.9 Aim of the project: 62
2 Materials and Methods: 63
2.1 Materials: 63
2.1.1 Cell culture media 63
2.1.2 Reagents 63
2.1.3 Solutions 64
2.2 Methods: 64
2.2.1 Cell culture 64
2.2.1.1 Starvation media composition 65
2.2.2 ECM production 68
2.2.2.1 Collagen I and Matrigel preparation: 68
2.2.2.2 Cell derived matrices (CDM): 69
2.2.3 ECM uptake: 69
2.2.4 Cell proliferation assays: 71
2.2.5 ECM cross-linking: 73
2.2.6 Immunofluorescence: 73
2.2.6.1 2D culture: 73
2.2.6.2 3D culture 75
2.2.7 Western blotting (WB) 75
2.2.8 EdU incorporation assays 76
2.2.9 Cell apoptosis assays 77
2.2.9.1 Caspase 3/7 assays: 77

2.2.9.2 Propidium iodide (PI) assays: 77
2.2.10 siRNA knockdown 78
2.2.11 Metabolite profiling 79
2.2.11.1 Non-targeted metabolomics: 79
2.2.11.2 Targeted metabolomics: 79
2.2.12 RT-qPCR 80
2.2.13 Cell adhesion 82
2.2.14 Statistical analysis 82
2.2.15 Survival analysis 82
3 The extracellular matrix promoted breast cancer cell growth under amino acid starvation 83
3.1 Introduction: 83
3.2 Results: 85
3.2.1 ECM partially rescued the growth of MCF10CA1 breast cancer cells under AA starvation 85
3.2.2 ECM induced MCF10CA1 cell division but did not affect cell death under AA starvation. 87
3.2.3 Chemical crosslinking prevented collagen I-dependent cell growth under AA starvation. 90
3.2.4 ECM uptake and ECM-dependent cell growth were mediated by macropinocytosis 93
3.2.5 Intracellular metabolites were upregulated on collagen I under AA starvation and Gln starvation 95
3.3 Discussion: 100
4 The ECM supported cell growth under glucose starvation 105
4.1 Introduction: 105
4.2 Results: 106
4.2.1 ECM partially rescued the growth of MCF10CA1 cells under glucose starvation 106
4.2.2 ECM partially rescued the growth of MCF10CA1 cells under glucose & glutamine starvation 107
4.2.3 ECM induced MCF10CA1 cell division and reduced cell apoptosis under Glc starvation 108
4.2.4 Chemical cross-linking had a small effect on collagen I- mediated cell growth under Glc starvation 109
4.2.5 ECM-dependent cell growth might be independent of macropinocytosis ... 110

4.2.6 α2β1 integrin is required for ECM dependent cell growth under Glc starvation. 111

4.2.7 ECM-dependent cell growth under Glc starvation is associated with upregulation of amino acid-related metabolic pathways. 113

4.3 Discussion: 116

5 Oncogenic RAS mutations drive a2 integrin expression under amino acid starvation 123

5.1 Introduction: 123

5.2 Results: 126

5.2.1 α2β1 integrin was required for collagen I uptake under amino acid starvation 126

5.2.2 α2β1 integrin was required for ECM-dependent MCF10CA1 cell growth under amino acid starvation. 127

5.2.3 Amino acid starvation strongly increased α2 integrin expression at the mRNA level 128

5.2.4 α2 integrin expression significantly increased at the protein level under AA starvation 129

5.2.5 β1 integrin expression at the mRNA level varies under AA starvation in cancer cells 130

5.2.6 α5 integrin expression increased at the mRNA level, but not at the protein level, in pancreatic but not breast cancer cells 131

5.2.7 The expression of α2, but not α5, was significantly increased in physiological starvation conditions in pancreatic cancer cells. 132

5.2.8 Amino acid starvation promoted α2 integrin expression in a RAS-dependent and GCN2-independent manner. 134

5.2.9 ERK phosphorylation rapidly increased under AA starvation in breast and pancreatic cancer cells 137

5.2.10 α2 integrin expression was regulated by MEK under amino acid starvation 138

5.2.11 The expression of α2 integrin increased in MCF10A mammary epithelial cells under AA starvation via growth factors stimulation 140

5.2.12 Amino acid starvation promoted α2 integrin expression in a RAS-dependent manner in SW1990 cells grown in 3D. 141

5.2.13 Amino acid starvation promoted α2 integrin expression in MCF10CA1 breast cancer cells in a MAPK dependent manner in 3D. 143

5.2.14 Amino acid starvation promoted SW1990 pancreatic cancer cell adhesion to collagen I and spreading. 144

5.2.15 Integrin α2 is upregulated in pancreatic cancer and correlates with poor prognosis 146

5.3 Discussion: 147

6 General discussion 152
6.1 Summary: 152
6.2 ECM partially rescued highly invasive breast cancer cell growth under different starvation conditions 153
6.3 The ECM promotes cell division and prevents cell apoptosis in different starvation conditions 154
6.4 The ECM promotes cell growth via different mechanisms 155
6.5 ECM modified the intracellular metabolite content under starvation 157
6.6 ECM-dependent cell growth is mediated by integrins 159
6.7 The expression of integrins under amino acid starvation is regulated by the RAS-MEK-Erk pathway 161
6.8 Therapeutic opportunities 163
6.9 Conclusion and future directions 164
7 References: 166

List of Figures

Chapter 1

Figure 1-1 The hallmarks of cancer. 17
Figure 1-2 Breast cancer progression. 19
Figure 1-3 Advanced breast cancer treatment approaches 24
Figure 1-4 Pancreatic ductal adenocarcinoma (PDAC) progression. 25
Figure 1-5 RAS activation mechanism 28
Figure 1-6 KRAS incidences and treatment in PDAC. 29
Figure 1-7 The composition of ECM 34
Figure 1-8 Collagen synthesis.. 35
Figure 1-9 The role of collagens in different types of cancer.. 37
Figure 1-10 Fibronectin structure.. 38
Figure 1-11 the basement membrane structure. 41
Figure 1-12 The effect of MMPs on cancer progression. 44
Figure 1-13 The extracellular matrix proteins endocytosis.. 46
Figure 1-14 Integrins activation.. 49
Figure 1-15 Glucose metabolism in cancer.. 52
Figure 1-16 Glutamine metabolism in cancer. 55
Figure 1-17 Amino acids metabolism. 58
Figure 1-18 Macromolecules scavenging in cancer under nutrient deprivation.. 61

Chapter 2

Figure 2-1 ECM uptake analysis using Image J software.. 70
Figure 2-2 Cell number analysis using CME software.. 72
Figure 2-3 Integrin intensity analysis method using Image J software.. 74

Chapter 3

Figure 3-1 Collagen I and Matrigel partially rescued MCF10CA1 cells growth under AA starvation 86
Figure 3-2 CDM partially rescued MCF10CA1 cells growth under AA starvation. 87
Figure 3-3 ECM increased MCF10CA1 cells division under AA starvation. 88
Figure 3-4 ECM did not affect MCF10CA1 cells death under AA starvation. 89
Figure 3-5 MCF10CA1 collagen I uptake was induced under AA starvation. 91
Figure 3-6 Crosslinking completely abolished ECM-dependent cell growth. 92
Figure 3-7 ECM-dependent MCF10CA1 cell growth was mediated by macropinocytosis 94
Figure 3-8 Intracellular AA were higher on collagen I compared to on plastic under AA starvation. 96
Figure 3-9 Intracellular AA were upregulated on collagen I under Gln starvation. 97
Figure 3-10 phenylalanine, tyrosine and fumarate were upregulated on coll I under AA starvation. 99
Figure 3-11 HPDL knockdown reduced coll I-dependent cell growth under starvation. 99
Figure 3-12 Schematic representation of ECM-dependent cell growth under AA starvation 100

Chapter 4

Figure 4-1 Collagen I and Matrigel partially rescued MCF10CA1 cell growth under Glc starvation. 106
Figure 4-2 CDM partially rescued MCF10CA1 cell growth under Glc starvation. 107
Figure 4-3 Collagen I and Matrigel partially rescued MCF10CA1 cell growth under Glc & Gln starvation. 108
Figure 4-4 ECM increased MCF10CA1 cell division and decreased apoptosis under Glc starvation. 109
Figure 4-5 Collagen I cross-linking slightly reduced MCF10CA1 cell growth under Glc or (Glc & Gln) starvation. 110
Figure 4-6 ECM-dependent MCF10CA1 cell growth might be macropinocytosis independent. 111
Figure 4-7 $\alpha 2\beta 1$ integrin inhibition opposed the ECM-dependent cell growth. 112
Figure 4-8 MCF10CA1 cells on collagen I switch to amino acid metabolism at day 1 of Glc starvation. 114
Figure 4-9 MCF10CA1 cells on collagen I switch to amino acid metabolism at day 6 of GLC starvation. 115
Figure 4-10 Glycine, serine, and threonine metabolism..... 120
Figure 4-11 Working model of ECM-dependent cell growth under Glc starvation. 122

Chapter 5

Figure 5-1 Integrated stress response signalling pathway. 124
Figure 5-2 The inhibition of $\alpha 2\beta 1$ integrin reduced collagen I uptake under AA starvation..126
Figure 5-3 MCF10CA1 cells growth on collagen I was strongly reduced upon inhibition of $\alpha 2\beta 1$ integrin under starvation. 127
Figure 5-4 The expression of ITGA2 increased significantly at the mRNA level under AA starvation compared to complete media. 128
Figure 5-5 The expression of ITGA2 increased at the protein level under AA starvation.....129
Figure 5-6 The expression of ITGA2 increased in MCF10CA1 on collagen I.. 130
Figure 5-7 The expression of ITGB1 increased at the mRNA level under AA starvation in some cell lines. 131
Figure 5-8 The expression of $\alpha 5$ integrin increased significantly at the mRNA level in pancreatic cancer cells but not at the protein level and in breast cancer cells under AA starvation. 132
Figure 5-9 The expression of $\alpha 2$, but not $\alpha 5$, integrin increased significantly at the mRNA level in TIFM media compared to complete media.. 133
Figure 5-10 GCN2 inhibitor completely abolished the expression of ASNS under AA starvation 134
Figure 5-11 GCN2 inhibition significantly decreased the expression of $\alpha 2$ integrin in MCF7, but not in MCF10CA1 or MDA-MB-231 breast cancer cells under AA starvation, while no effect was detected in complete media.. 135
Figure 5-12 KRAS, but not GCN2, was required for $\alpha 2$ integrin expression in pancreatic cancer cells under AA starvation, while in complete media, KRAS inhibition decreased $\alpha 2$ integrin expression a cell line-dependent manner. 136
Figure 5-13 The phosphorylation of ERK was increased within 5 minutes of AA starvation in both breast and pancreatic cancer cells.. 137
10Figure 5-14 MEK inhibition reduced the expression of $\alpha 2$ integrin at both the mRNA and the

protein level..... 139
Figure 5-15 Amino acid starvation promoted α2 integrin expression in MCF10A in the presence of growth factors. 141
Figure 5-16 Amino acid starvation promoted α2 integrin expression in 3D, in a KRAS-dependent manner.. 142
Figure 5-17 Amino acid starvation promoted α2 integrin expression in 3D, in a MAPK-dependent manner.. 144
Figure 5-18 Amino acid starvation promoted SW1990 cell adhesion to collagen I and spreading.. 145
Figure 5-19 α2 integrin was over-expressed in pancreatic cancer patients and correlated with poor overall and disease-free survival.. 146

Chapter 6

Figure 6-1 Working model. 153
Figure 6-2 Venn diagram of the upregulated metabolites on collagen I under complete media and starvation conditions. 158

List of Tables

Chapter 1

Table 1-1 Breast cancer molecular subtypes 20
Table 1-2 The percentages of cases with most mutated genes 21
Table 1-3 Early breast cancer therapy options 22
Table 1-4 Collagen types, their tissue distribution and association with cancer.....36
Table 1-5 Amino acids classification in cancer 53

Chapter 2

Table 2-1 Cell culture media, supplier and Catalogue number 63
Table 2-2 List of reagents and suppliers 63
Table 2-3 List of solutions and their recipes 64
Table 2-4 Composition of starvation media used for each cell line 65
Table 2-5 DMEM media formulation 66
Table 2-6 DMEM/F-12 media formulation 67
Table 2-7 List of inhibitors, the concentration used and the supplier 71
Table 2-8 List of antibodies, the dilution used and the supplier 75
Table 2-9 List of antibodies used in (WB) 76
Table 2-10 List of siRNAs and the supplier 79
Table 2-11 Master mix composition 80
Table 2-12 The thermal cycle running program 80
Table 2-13 QPCR master mix composition..... 81
Table 2-14 PCR system running program 81
Table 2-15 List of targeted genes primers 81
Table 2-16 List of inhibitors, their concentration and the supplier 81

Chapter 6

Table 6-1 suggested treatment combinations for KRAS driven cancers 164

Abbreviations

AA	Amino Acid
ATP	Adenosine Triphosphate
AMPK	AMP-activated protein kinase
ATF4	activating transcription factor 4
ASNS	asparagine synthetase
ATER	ataxia telangiectasia and Rad 3 related kinase
ADM	acinar to ductal metaplasia
ApCAFs	antigen-presenting CAFs
ADAMs	disintegrin and metalloproteinase
ADAMTs	disintegrin and metalloproteinases with thrombospondin motifs
Asn	Asparagine
Asp	Aspartate
ASNase	asparaginase
BRPC	borderline resectable pancreatic cancer
BM	basement membrane
BCAAs	branched-chain amino acids
BCKAs	branched chain a-keto acids
BCAT 1/2	BCAA transaminases 1 and 2
BCKDH	branched-chain α-keto acid dehydrogenase
BCKDK	BCKDH kinase
BSA	bovine serum albumin
CDM	cell derived matrices
CAFs	Cancer associated fibroblasts
Coll I	Collagen I
Complete	Com
CYRI	CYFIP-related RAC1 interacting
CDKN2A	cyclin-dependent kinase inhibitor 2A
cCAFs	cycling CAFs
cFN	cellular FN
CTHRC1	Collagen triple helix repeat containing-1 gene
DUSP6	dual-specificity protein phosphatase
DCIS	Ductal carcinoma in situ
dCAFs	developmental CAFs
DDRs	discoidin domain receptors
EdU	5-ethynyl-2'-deoxyuridine
eIF2α	eukaryotic translation initiation factor 2 alpha
ER	Endoplasmic reticulum
ER	oestrogen receptor
EGFR	epithelial growth factor receptor
ECM	extracellular matrix
EMT	epithelial to mesenchymal transition

EAA	essential amino acids
FAK	focal adhesion kinase
5-FU	5-flurouracil
FSP1	fibroblast-specific protein
FAP	fibroblasts activated protein
FGF5	fibroblasts growth factor 5
FACITs	fibrillar-associated collagens with interrupted triple helices
FN	Fibronectin
FA	focal adhesion
Gln	Glutamine
Glc	Glucose
GCN2	Amino acids deprivation activates general control non-derepressible 2
GEM	Gemcitabine
GEFs	guanine nucleotide exchange factors
GAPs	GTP-activating proteins
GEO	the Gene Expression Omnibus
GLUD1	glutamate dehydrogenase
GOT1	oxaloacetate aspartate transaminase
HPD	4-hydroxyphenylpyruvate dioxygenase
HPDL	4-hydroxyphenylpyruvate dioxygenase like
HA	Hyaluronan
Haase	hyaluronidase
HRI	Heme-regulated eIF2a kinase
HGEC	human glomerular epithelial cells
HER 2	human epidermal growth factor receptor 2
HRAS	Harvey rat sarcoma viral oncogene homolog
HNSCC	head and neck squamous cell cancer
HEK2	hexokinase 2
IDC	invasive ductal carcinoma
ISR	integrated stress response
IPMNs	intraductal papillary mucinous neoplasms
iCAFs	inflammatory CAFs
IM	interstitial matrix
ITGBL1	integrin subunit beta like 1
Ile	isoleucine
IFNg	interferon g
KRAS	Kirasten rat sarcoma viral oncogene homolog
a-KG	a-ketoglutaric acid
LAPC	locally unresectable pancreatic cancer
LOX	lysyl oxidase
LARGE	like acetylglucosaminyltransferase
Loxl3	Lysyl oxidase-like 3

Leu	leucine
Matr	Matrigel
MMPs	metalloproteinases enzymes
MEF	mouse embryonic fibroblast
MM	multiple myeloma
MPM	malignant pleural mesothelioma
mTOR	mammalian target of rapamycin
MAP3K21	Mitogen-Activated Protein Kinase 21
MSCs	mesenchymal stem cells
mCAFs	matrix CAFs
myCAFs	myofibroblasts like CAFs
MAPK	mitogen-activated protein kinase
MACITs	membrane anchored collagens
MT1-MMP	membrane type matrix metalloproteinase 1
MCT	monocarboxylate
mTORC1	mTOR complex 1
mTORC2	mTOR complex 2
NSCLC	non-small cells lung cancer
NAT	neoadjuvant therapy
NRAS	neuroblastoma RAS viral oncogene homolog
NFs	Normal fibroblasts
Net4	Netrin 4
NMMIIA	non-muscle myosin IIA
NEAA	non-essential amino acids
NMDA	N-methyl-D-aspartate
OS	overall survival
OAA	oxaloacetate
PDAC	pancreatic ductal adenocarcinoma
PRODH1	proline oxidase
PI	propidium Iodide
PERK	PKR-like ER Kinase
Pca	prostate cancer
PI3K	phosphatidylinositol-3-OH kinase
PR	progesterone receptor
AKT	protein kinase B
PARP	poly (ADP- ribose) polymerase
PanIN	pancreatic intraepithelial neoplasia
PDGFRa	PDGF receptor a
PDGFRβ	PDGF receptor β
pCAFs	tumour-promoting CAFs
pFN	plasma FN
POSTN	Periostin
PSCs	pancreatic stellate cells

PKD1	protein kinase D1
PPM1K	protein phosphatase 1 K
PHGDH	phosphoglycerate dehydrogenase
P4HA	prolyl-4-hydroxlase
RTKs	receptor tyrosine kinases
rCAFs	tumour-restraining CAFs
ROS	reactive oxygen species
a-SMA	a-smooth muscle actin
STAT3	Signal transduce and activator of transcription 3
SSP	serine synthesis pathway
SHMT	Serine hydroxymethyltransferase
TCA	Tricarboxylic acid cycle
TFE3	transcription factor enhancer 3
TIFM	tumour interstitial fluid media
TNBC	Tripel negative breast cancer
TP53	tumour protein 53
TGFb	transforming growth factor b
TME	tumour microenvironment
ATF4	transcription factor 4
TIPMs	tissue inhibitors of metalloproteinases
TKI	tyrosine kinase inhibitor
UPLC-MS/MS	ultra-performance liquid chromatography- tandem mass spectrometry
vCAFs	vascular CAFs
Val	valine
Cross-linked collagen I	x-linked coll I

1 Introduction

Cancer is a disease characterised by an uncontrollable growth and proliferation of cells. This growth abnormality leads to the formation of tumours which are complex-like structures composed of different types of cells residing in a supportive microenvironment. Hanahan and Weinberg proposed 10 functional capabilities called "the hallmarks of cancer" that cancer cells acquire during cancer progression to be able to proliferate, survive and migrate **(Figure 1-1)**. These traits are shared in all types of human tumours and understanding them will be quite beneficial to develop cancer therapeutic treatments (Hanahan and Weinberg, 2011).

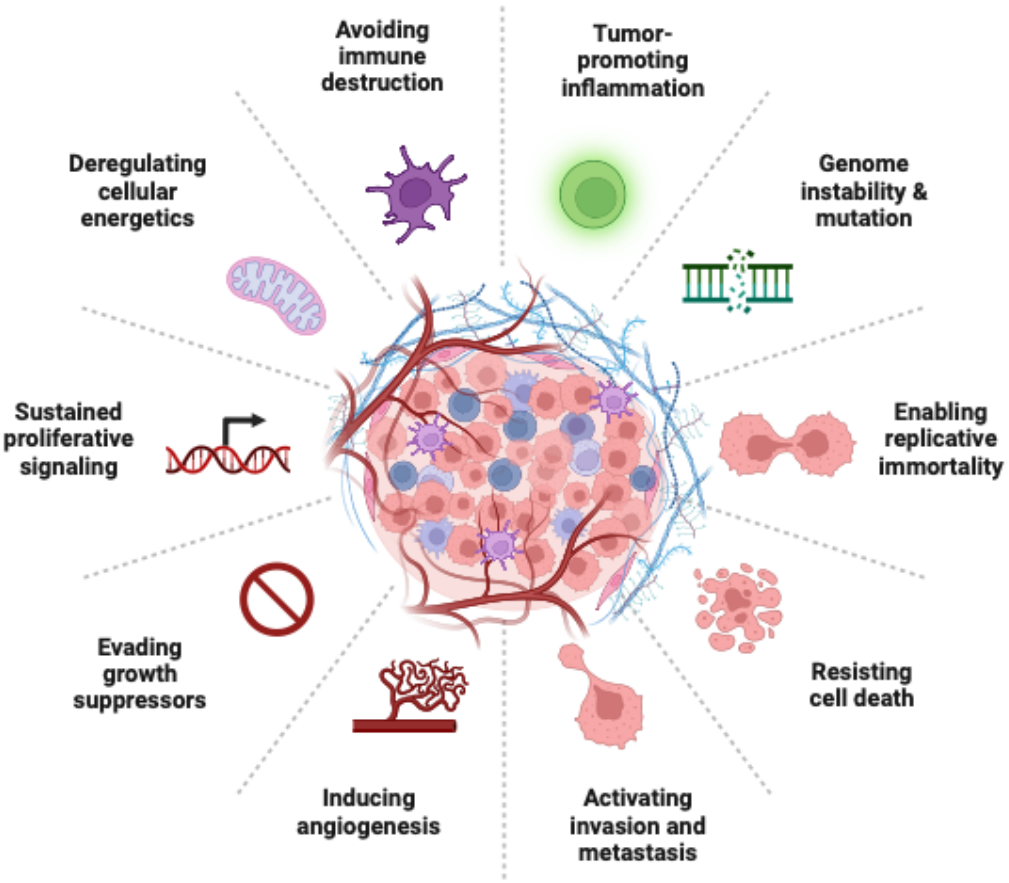

Figure 1-1 The hallmarks of cancer. Researchers suggest that there are ten hallmarks of cancer which most or all cancer cells acquire to grow and survive during cancer progression through different mechanistic strategies. Adapted from (Hanahan and Weinberg, 2011). "Created in BioRender.com".

1.1 Sustained proliferative signalling

One of the main cancer cells traits is their ability to sustain proliferation due to the deregulation of growth signalling. Growth factors binding to their cell surface receptors, normally tyrosine kinases, can trigger signalling cascades which stimulate cell growth. Plenty of cancer cells can secrete growth factors themselves which can promote the neighbouring normal cells to further release more growth factors to enhance their growth, this term is called autocrine signalling (Hanahan and Weinberg, 2000, Hanahan and Weinberg, 2011). In addition, the expression of growth factor receptors is found to be increased in cancer which might promote cancer cells to trigger signalling cascades independently of growth factors stimulation (Hanahan and Weinberg, 2000).

Furthermore, multiple signalling pathways involved in cells proliferation are mutated in cancer. Such as mutations involved in the RAS-RAF-MEK-ERK (MAPK) pathway and the uncontrolled expression of Myc which can cause cell cycle deregulation (Evan and Vousden, 2001).

1.2 Breast cancer:

According to the global cancer statistics in 2022, breast cancer is the second most common type of cancer and the fourth cause of cancer death worldwide, with around 2.3 million new cases diagnosed and 666,000 deaths in 2022 (Bray et al., 2024). It is the most commonly diagnosed cancer in women with nearly one in four cases and one in six cancer deaths around the world (Bray et al., 2024). In the UK, 15% of the new cancer cases are breast cancer making it the most common cancer in the UK (CRUK, 2017-2019a). Drinking alcohol, smoking, obesity, family history, oral contraceptive, hormonal therapies, late menopause, early puberty, and the density of the breast tissue are all considered risk factors (BreastCancerNow, 2024).

1.2.1 Breast cancer progression and subtypes:

Most breast cancer types are carcinomas and less than 1% are sarcomas (Feng et al., 2018). Breast cancer can be divided into three stages according to their invasiveness: Ductal carcinoma in situ (DCIS) **(Figure 1-2, A)** is a non-invasive type of breast cancer, it develops inside the normal ducts, and it is surrounded by a layer of myoepithelial cells and a layer of basement membrane. Even though DCIS is non-invasive, it has the potential to become invasive, and it can progress to invasive ductal carcinoma (IDC) **(Figure 1-2, B)**. IDC is the invasive type of

breast cancer, and it comprises around 80% of breast cancer cases (Feng et al., 2018). IDC develops when cancer cells breach the basement membrane, reach the surrounding tumour microenvironment and start migrating towards nearby tissues (Kaushik et al., 2016). Metastatic breast cancer is developed when cancer cells spread to another organ in the body **(Figure 1-2,C)**. Usually, breast cancer spreads to the brain, liver, lungs and bone. Around 30% of women diagnosed with breast cancer develop the metastatic form (Feng et al., 2018).

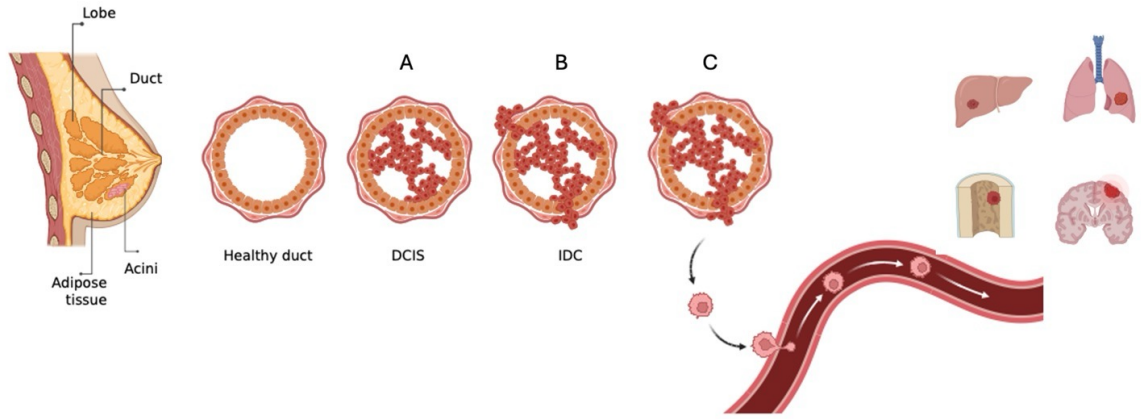

Figure 1-2 Breast cancer progression (A) The first stage of breast cancer is ductal carcinoma in situ (DCIS) where cancer cells start to proliferate inside the normal duct, followed by (B) invasive ductal carcinoma (IDC) as cancer cells break the basement membrane and start invading the surrounding tumour microenvrroenmnt, then (C) metastatic breast cancer when breast cancer cells spread to other organs usually liver, lungs, bone and brain. "Created in BioRender.com".

Breast cancer can be classified into different molecular subtypes, based on the expression of a set of receptors: oestrogen receptor (ER), progesterone receptor (PR), and human epidermal growth factor receptor 2 (HER2). There are five molecular subtypes. Luminal A is ER and/or PR positive; it forms around 40% of breast cancer cases and it is considered low grade with the best prognosis. Luminal B subtype is ER and/ or PR positive, HER2 positive or negative, it forms less than 20% of breast cancer cases, it progresses slightly faster than luminal A and it has a slightly worse prognosis. HER2-enriched breast cancer subtype is characterised by high expression of HER2 gene. It accounts for 10%-15% of breast cancer cases; it grows faster than the luminal types of breast cancer and its prognosis is worse. Triple negative/basal like breast cancer (TNBC) is a high grade more aggressive type of breast cancer and it accounts for around 20% of breast cancer cases. TNBC is characterised by the lack of ER, PR and HER2 expression (Feng et al., 2018) **(Table 1-1).**

Table 1-1 Breast cancer molecular subtypes: The table shows the differences between breast cancer subtypes in terms of gene expression, their prognosis, the percentage of cases for each subtype and the 5 years survival rate.

Subtypes	*Gene expression*	*Prognosis*	*Diagnosis*	*5 years survival rate*
Luminal A	ER+, PR±, HER2–	Best prognosis	~40%	94.4%
Luminal B	ER+, PR±, HER2±	Slightly worse than Luminal A	~20%	90.7%
HER2 enriched	ER–, PR–, HER2+	worse than Luminal A	10-15%	84.8%
TNBC	ER–, PR–, HER2–	Most aggressive and worst prognosis	20%	77.1%

1.2.2 Genetic alterations in breast cancer

Family history is one of breast cancer risk factors (around 10% of breast cancers are inherited). Mutations in *BRCA1* and *BRCA2* genes, which are involved in DNA repair, can be inheritable (Harbeck et al., 2019). Tumours with mutated *BRCA1* tends to form the TNBC subtype, while tumours with *BRCA2* are sporadic tumours (Cancer Genome Atlas, 2012). *BRCA* mutation carriers have a high risk of ovarian cancer too (Shiovitz and Korde, 2015). There are other high penetrance genes but quite rare, also associated with hereditary breast cancer such as *PTEN, TP53, CDH1, and STK11* (Harbeck et al., 2019, Shiovitz and Korde, 2015). Additional moderate-penetrance genes have been identified to be associated with a predisposition to breast cancer; *CHEK2, PALB2, ATM*, and *BRIP1* are genes usually interact with BRCA genes and are involved in DNA repair mechanisms (Shiovitz and Korde, 2015).

Genetic and epigenetic abnormalities have also been detected in breast cancer patients. A study in 507 patients identified 30,626 somatic mutations in the four subtypes of breast cancer (Cancer Genome Atlas, 2012). The most frequently mutated genes are shown in **(Table 1-2)**. Luminal breast cancer subtypes have the largest number of mutated genes with the highest mutation frequency being in *PIK3CA* (Cancer Genome Atlas, 2012). However, the analysis of protein and mRNA signatures showed that proteins associated with phosphatidylinositol-3-OH kinase (PI3K) pathway activation, such as phospho-protein kinase B (pAKT), and pS6, were highly expressed in TNBC and HER2+ subtypes compared to luminal subtypes. In TNBC, the most commonly mutated gene is *TP53* Followed by *PIK3CA.* Furthermore, many genes involved in the PI3K and RAS-RAF-MEK pathways were identified to be amplified in TNBC such as *KRAS* (32%) and *BRAF* (30%) (Cancer Genome Atlas, 2012). RAS is another gene which has been

identified to be a breast cancer driver although <5% of breast cancer cases harbour a RAS mutated gene (Eckert et al., 2004, Galie, 2019).

Table 1-2 The percentages of cases with most mutated genes identified in all breast cancer subtypes in a study on 507 patients (Cancer Genome Atlas, 2012)

Gene	Luminal A	Luminal B	HER2+	TNBC
PIK3CA	45%	29%	39%	9%
GATA3	14%	15%	2%	2%
MAP3K1	13%	5%	4%	Absent
TP53	12%	29%	72%	80%
CDH1	9%	5%	5%	Absent
MLL3	8%	6%	7%	5%
MAP2K4	7%	2%	2%	Absent
PTEN	4%	4%	2%	1%
AKT1	4%	2%	2%	Absent
PIK3R1	0.4%	2%	4%	Absent

1.2.3 Breast cancer treatment:

Even though breast cancer is one of the most common types of cancer and its treatment is quite advanced, some types are more aggressive indicating that they grow and spread rapidly and are often resistant to therapy. Those types are harder to treat than others, hence it is important to find new treatments. Patients can either be given these therapies as a monotherapy or as a combination of two or more therapies (Wang and Minden, 2022)

1.2.3.1 Early breast cancer:

For early breast cancer, local treatment including surgery is one of the primary options, together with ablation therapy, regardless of the subtype. Usually, neoadjuvant therapy (NAT) such as systemic therapy enhances the surgery efficacy and minimise the local tumour invasiveness (Xiong et al., 2025). Adjuvant therapies such as chemotherapy, radiotherapy, endocrine therapy, and targeted therapy can also be given depending on the subtype and the tumour burden (Harbeck et al., 2019). After surgery, all ER and PR positive patients receive endocrine adjuvant therapy, such as Tamoxifen, for at least 5 years and chemotherapy is recommended if patients at a high risk of recurrence. For HER2+ and TNBC, neoadjuvant therapy before surgery is a must (Harbeck et al., 2019, Xiong et al., 2025). Table 1-3 shows the treatment approaches for early breast cancer depending on the breast cancer subtype.

Table 1-3 Early breast cancer therapy options: The table shows the treatment options for early breast cancer cases given according to the subtype (Harbeck et al., 2019).

Subtype	Surgery	Neoadjuvant		Adjuvant			
		Chemo	Endocrine	Chemo	Radio	Anti HER2	Endocrine
Luminal A	Yes	Anthracycline-Taxine sequence or docetaxel and cyclophosphamide	Yes, for low-risk recurrence	Anthracycline-Taxine sequence or docetaxel and cyclophosphamide	Yes/No		Yes Tamoxifen (a selective oestrogen modulator)
Luminal B	Yes	Anthracycline-Taxine sequence or docetaxel and cyclophosphamide	Yes, for low-risk recurrence	Anthracycline-Taxine sequence or docetaxel and cyclophosphamide			
HER2+	Yes	Anthracycline-Taxine sequence or docetaxel and carboplatin +HER2 blockade		Paclitaxel		Trastuzumab (Herceptin) for 1 year	
TNBC	Yes	Yes, Anthracycline-Taxine sequence		Capecitabine			

1.2.3.2 Advanced breast cancer:

Advanced or metastatic breast cancer is when the tumour has spread to another organ. It is the most aggressive type of breast cancer and currently the treatments aim to relieve the symptoms and prolong the life expectancy of the patient. The recurrent metastatic tumour is more aggressive than the De novo one (Harbeck et al., 2019). Surgery might be an option, but it is not applicable to all patients. Endocrine therapy, radiotherapy, chemotherapy, and targeted therapy can all be given to metastatic breast cancer patients as monotherapy or in combinations. Many breast cancer tumours are immune cold tumours; however, immunotherapy is an option especially in metastatic TNBC with immune markers PD1/PDL1 (Xiong et al., 2025). Interestingly, radiotherapy and anti HER2 drugs such as Trastuzumab can induce immune responses, hence the microenvironment can be primed by those therapies (Harbeck et al., 2019, Xiong et al., 2025). In luminal types of breast cancer, endocrine therapies such as the selective ER degraders (tamoxifen, an aromatase inhibitor or fulvestrant) can be used until endocrine resistance emerges. In that case, CDK4/6 inhibitors such as palbociclib, abemaciclib and ribociclib can be given. Targeting the phosphatidyl protein 3-kinase (PI3K)-protein kinase B (AKT) – mammalian target of rapamycin (mTOR) pathway is also an option in treating advanced breast cancer patients, as it has been shown that this pathway plays a role in endocrine therapy resistance. mTOR inhibitors such as everolimus and the AKT inhibitor capivasertib have been approved to be used (Harbeck et al., 2019). As mentioned earlier, BRCA mutations are common in the TNBC subtype. Hence, the poly (ADP- ribose) polymerase (PARP) inhibitors Olaparib and talazoparib are also an optional treatment (Harbeck et al., 2019, Xiong et al., 2025, Lebert et al., 2018). **Figure 1-3** shows the current treatment approaches for advanced breast cancers according to the subtype (Harbeck et al., 2019, Xiong et al., 2025, Wang and Minden, 2022).

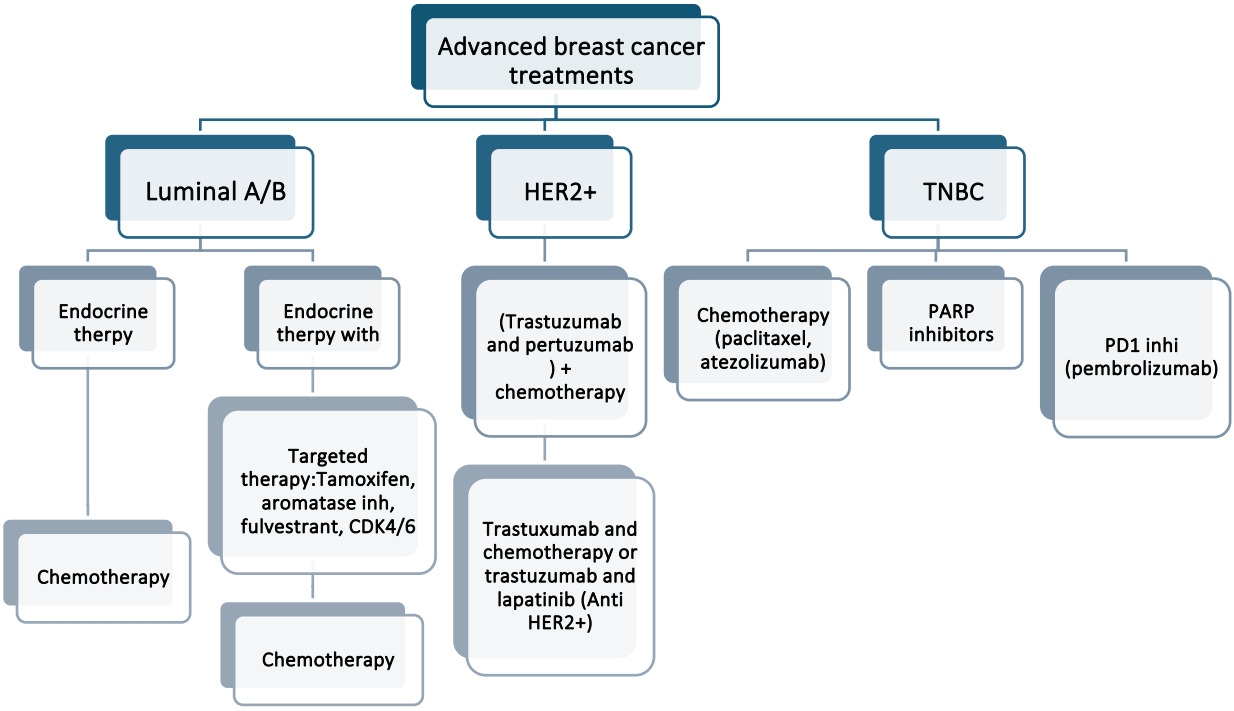

Figure 1-3 Advanced breast cancer treatment approaches: The treatment options for advanced breast cancer cases given according to the subtype (Xiong et al., 2025, Harbeck et al., 2019).

1.3 Pancreatic cancer:

Pancreatic cancer is the 10th most common type of cancer and the 5th leading cause of cancer death in the UK with nearly 10,800 new cases every year (CRUK, 2017-2019b). Elderly people are at the highest risk of getting pancreatic cancer as it is less common before the age of 40. In addition to age, smoking, drinking alcohol, obesity, and diabetes are among the pancreatic cancer risk factors (Bray et al., 2024).

1.3.1 Pancreatic cancer progression:

The most common malignant pancreatic cancer type is adenocarcinoma and more specifically pancreatic ductal adenocarcinoma (PDAC). Other types include 15-20% neuroendocrine tumours, 2% colloid carcinomas, 2% solid-pseudopapillary tumours, 1% acinar cell carcinomas, and 0.5% pancreatoblastomas (Kleeff et al., 2016). Similarly to breast cancer, PDAC progresses from normal to invasive to ductal carcinoma (Hruban et al., 2000). It is usually generated from pancreatic intraepithelial neoplasia (PanIN) or less frequently from mucinous cystic neoplasms

and intraductal papillary mucinous neoplasms (IPMNs) (Kleeff et al., 2016, Hruban et al., 2000). **(Figure 1-4)**.

1.3.2 Genetic alterations in PDAC:

The progression of PanIN to PDAC is associated with genetic alterations and activating mutations in certain genes in each stage including the four main driver genes *KRAS* which has been found to be mutated in around 90% of PDAC patients, the loss of tumour protein 53 (*TP53*) in 80%, the loss of cyclin-dependent kinase inhibitor 2A (*CDKN2A*) in 60% and the loss of SMAD4 in 40% of PDAC patients, in addition to telomere shortening and structural changes (Connor and Gallinger, 2022) **(Figure 1-4)**. These genetic alterations in particular can affect PDAC proliferation, migration, antiapoptotic behaviour and response to treatment (Zhou et al., 2025). Furthermore, some genes are altered but at low individual prevalences such as transforming growth factor β (*TGF-β*), Mitogen-Activated Protein Kinase 21 (*MAP3K21*), and *BRAF*. There are usually around 40 mutated genes in a PDAC exome with *KRAS* being the main driver gene. However, some tumours can have wildtype *KRAS*, in that case other genes in the RAS pathway were found to be altered such as *BRAF*, and *mTOR* (Connor and Gallinger, 2022). Similarly to breast cancer, 10% of PDAC patients have a family history with *BRCA1/2*, *PALB2, ATM* and *STK11* being mutated (Kleeff et al., 2016).

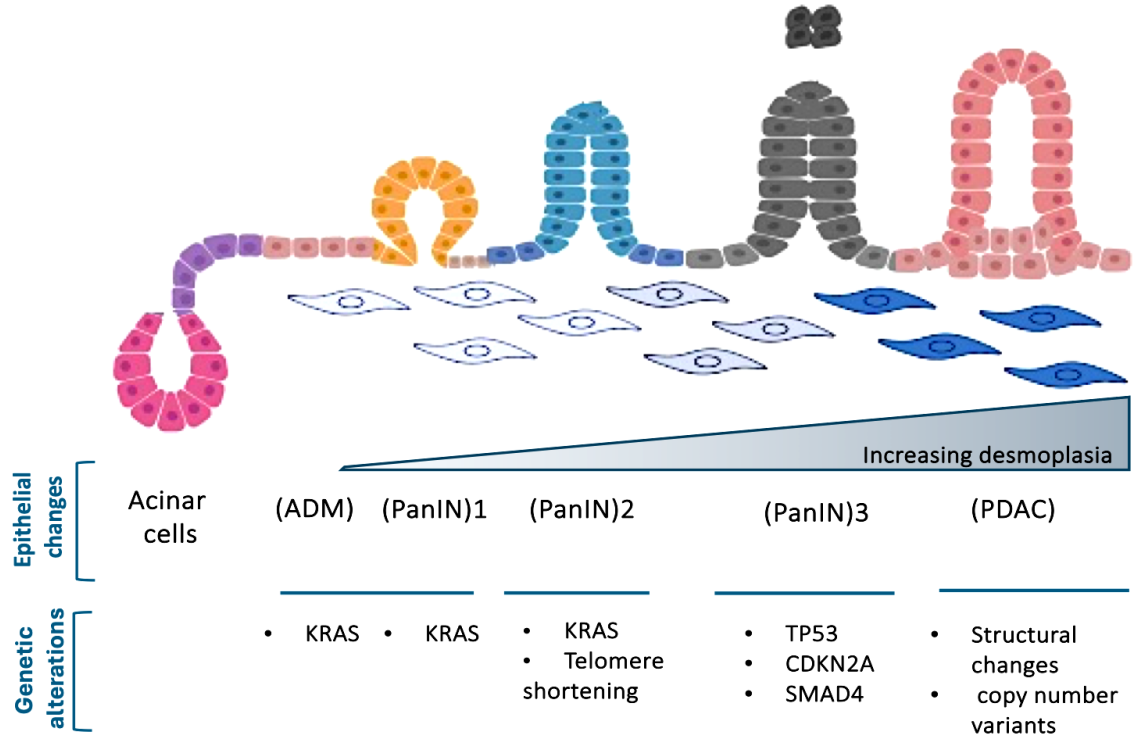

Figure 1-4 Pancreatic ductal adenocarcinoma (PDAC) progression PDAC arises from normal ductal epithelium to acinar to ductal metaplasia (ADM), followed by the formation of pancreatic intraepithelial neoplasia (PanINs) with genetic alterations and microenvironmental stimulation with an increase in desmoplasia leading to the development of PDAC. Low grades (PanIN 1 and 2) acquire KRAS mutations and telomere shortening. While the high grade PanIN3 acquire inactivation of TP53, CDKN2A and/or SMAD4 followed by structural changes and copy number variants forming the invasive PDAC. Adapted from (Orth et al., 2019, Connor and Gallinger, 2022) "Created in BioRender.com".

1.3.3 Pancreatic cancer treatments:

PDAC is an aggressive type of cancer with a 5-year overall survival rate of only 11%. The lack of symptoms and the difficulties of identifying specific tumour markers lead to advanced stage diagnosis. In addition to that, the tumour usually grows in a vascularised area of the pancreas, which facilitated distant metastasis, mainly to the liver and peritoneum. This leads to the tumour being unresectable for around 80% of patients (Kleeff et al., 2016). Due to the location of PDAC tumour and its late diagnosis, less than 20% of patients can have surgery as a first treatment option, followed by adjuvant therapy. Unfortunately, a big number (~80%) of those patients who undergo resection can relapse (Kleeff et al., 2016). 30-40% of patients are diagnosed with borderline resectable pancreatic cancer (BRPC) or locally unresectable pancreatic cancer (LAPC) and 50-60% with metastatic PDAC (Kleeff et al., 2016). Chemotherapy is the first option for PDAC treatment such as Gemcitabine (GEM), Folfirinox, Paclitaxel, Capecitabine and 5-flurouracil (5-FU) which can be given as a monotherapy or in combinations (Kleeff et al., 2016, Zhou et al., 2025). Neoadjuvant chemotherapy showed treatment optimisation and better patients' overall survival especially in the BRPC cases. Adjuvant chemotherapy also showed better overall survival and reduction in disease recurrence. Chemoresistance is a challenge in PDAC as it can arise due to the overexpression of proteins which promote several cell survival mechanisms. Furthermore, the metabolic reprogramming in PDAC and fibrosis also contribute to the PDAC chemotherapy resistance (Zhou et al., 2025)
Immunotherapy is another approach for treating PDAC and it is currently being tested in clinical trials. However, this approach is challenging due to the highly immunosuppressive tumour microenvironment. Targeted therapies are another possible treatment for PDAC as some signalling pathways have been shown to be dysregulated in PDAC and play a critical role in PDAC progression. These include epithelial growth factor receptor (EGFR), TGF-β, Wnt, NOTCH, RAS/RAF/ERK and PI3K/AKT/mTOR signalling pathways (Zhou et al., 2025). Preclinical studies showed that targeting these pathways can inhibit PDAC progression (Zhou et al., 2025). Furthermore, Olaparib, an FDA approved PARP inhibitor, has been proven to be effective in

metastatic PDAC patients who have mutations in the DNA damage repair genes BRCA1 or BRCA2. Also, due to KRAS being mutated in ~90% of PDAC patients, targeting it is an interesting approach for PDAC treatment and different KRAS inhibitors are currently in the preclinical/ clinical phase (Hosein et al., 2022, Zhou et al., 2025).

1.3.3.1 Targeting KRAS to treat PDAC:

RAS is a small GTPase which cycles between a GDP bound inactive state and a GTP bound active state. There are three members of the RAS gene family: KRAS (Kirasten rat sarcoma viral oncogene homolog), HRAS (Harvey rat sarcoma viral oncogene homolog), and NRAS (neuroblastoma RAS viral oncogene homolog). Normally, when extracellular signals are transmitted to the cells via receptor tyrosine kinases (RTKs) such as EGFR, guanine nucleotide exchange factors (GEFs) and GTP-activating proteins (GAPs) regulate the activation of RAS, as GEFs such as SOS1 and 2 promote the loading of the GTP in RAS GTPase domain where RAS binds to GTP with high affinity, whereas GAPs regulate the GTP hydrolysis. In cancer, RAS mutations decrease the GTP hydrolysis causing RAS always binding to GTP and constitutively active (Takacs et al., 2020) **(Figure 1-5)**. RAS has been found to be mutated in different types of cancer including PDAC and the mutations are located at G12, G13, or Q61 amino acid residues, which play a role in nucleotide binding. The activation of RAS signalling pathways then promotes cell proliferation, and migration (Yang and Wu, 2024).

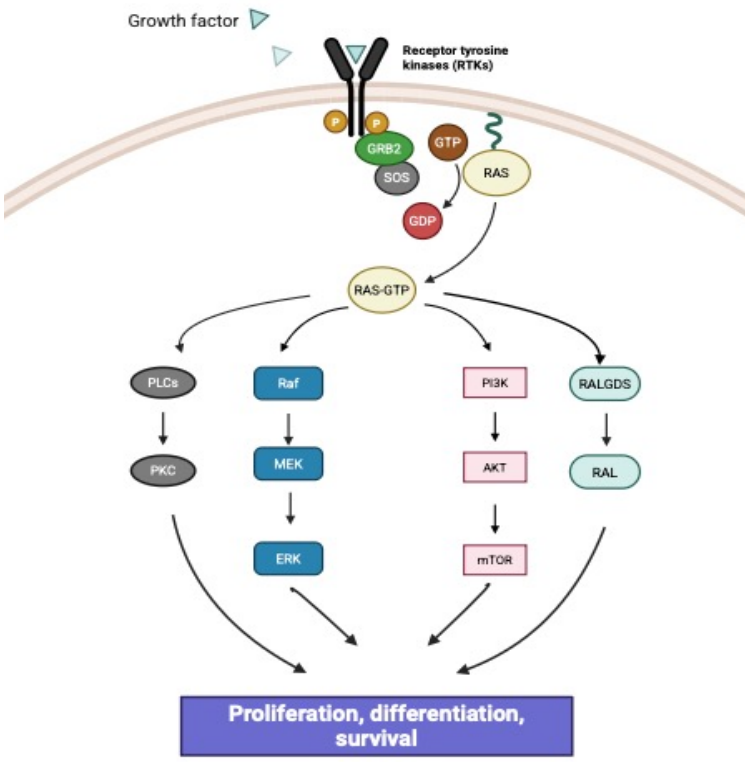

Figure 1-5 RAS activation mechanism RAS is activated downstream of receptor tyrosine kinases (RTKs). GEFs and GAPs accelerate the GDP-GTP switch. The activation of RAS triggers various signalling pathways promoting cells proliferation, differentiation and survival. "Created in BioRender.com"

In PDAC, KRAS is the most commonly mutated RAS, and the mutations were identified to be located at different hotspots. $KRAS^{G12D}$ is the most common one (35%) followed by $KRAS^{G12V}$ (30%), $KRAS^{G12R}$ (13%) and less frequently $KRAS^{Q61H}$ and $KRAS^{G12C}$ (Hosein et al., 2022) **(Figure 1-6).** Targeting KRAS as a treatment for PDAC is a very promising approach and multiple drugs are currently being tested. For instance, the $KRAS^{G12C}$ inhibitors (Sotorasib and Adagrasib) have been approved for the treatment of non-small cell lung cancer (NSCLC) and colorectal cancer (CRC). In PDAC, these inhibitors showed promising results for patients with a $KRAS^{G12C}$ mutation, as the response to Adagrasib showed 5.4 months progression free survival (PFS) and 8 months median overall survival (OS) (Bekaii-Saab et al., 2023) while the response to Sotorasib showed slightly lower PFS of 4 months and OS of 6.9 months (Strickler et al., 2023). Some drugs have been developed to target $KRAS^{G12D}$ mutation such as MRTX1133 and RMC-9805, currently in clinical trials. Pan-RAS inhibitors, inhibiting all RAS isoforms, have also been developed; however, these drugs showed higher toxicity. They can target either all RAS isoforms or each isoform separately, such as BI-2865 which is a Pan-KRAS inhibitor (Yang and Wu, 2024). Targeting pathways upstream of RAS or downstream of RAS are also being considered such as

RTKs inhibitors, SOS, PI3K and MEK inhibitors (Yang and Wu, 2024). **Figure 1-6** shows the KRAS targeted therapeutic approaches in PDAC.

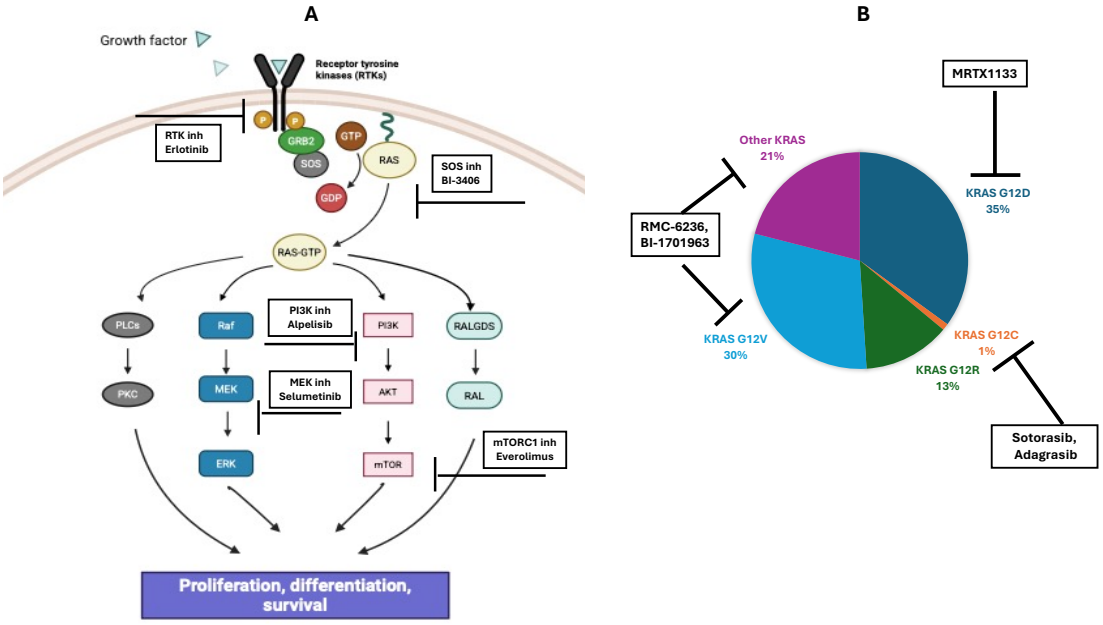

Figure 1-6 KRAS incidences and treatment in PDAC A) Targeted pathways upstream and downstream of RAS. B) KRAS incidences in PDAC with some KRAS inhibitors currently in clinical trials (Yang and Wu, 2024, Hosein et al., 2022)." A was created in BioRender.com".

1.4 The tumour microenvironment (TME):

Cancer is not just defined as an uncontrolled proliferation of cells, but it is a complex disease with the tumour being surrounded by multiple cells that form the tumour microenvironment (TME), such as immune cells, endothelial cells, adipocytes, fibroblasts and stellate cells in addition to the extracellular matrix (ECM) (Anderson and Simon, 2020). The TME support tumour progression from early growth to invasion and advanced metastatic stages (Hanahan and Weinberg, 2011). Understanding the effect of the TME on cancer cells is important as targeting the TME or the interaction between cancer cells and the surrounding cells is one of the approaches to treat cancer (Baghban et al., 2020).

1.4.1 Immune cells:

Immune cells can either be tumour promoter or tumour suppressor. There are several types of T-cells which can promote tumour progression such as cytotoxic T cells ($CD8^+$) which can targets abnormal antigen on the tumours and destroy them. On the other hand, cytotoxic T cells can supress angiogenesis by secreting interferon gamma (IFN-γ) (Anderson and Simon, 2020). Some types of cancers such as breast, colorectal and ovarian are highly infiltrated with tumour

associated macrophages (TAMs) which play an important role in their growth and metastasis (Larionova et al., 2020). They can stimulate cancer cells migration by producing factors such as IL6 which was shown to promote EMT in colorectal cancer. In addition, the chemokines produced by TAMs can enhance cancer cells stemness (Baghban et al., 2020). Furthermore, M2 macrophages can induce angiogenesis by enhancing blood vessels formation and producing VEGF and TNFα (Baghban et al., 2020).

1.4.2 Endothelial cells:

Endothelial cells form the inner layer of the blood vessels. The oxygen and nutrients supply at the early stages of tumorigenesis is not sufficient for the tumour growth. However, when tumours become hypoxic, they start secreting factors that support angiogenesis such as vascular endothelial factor A (VEGFA) and platelet derived growth factors (PDGF) to promote neo-angiogenesis which is the formation of new blood vessels from existing ones and is regulated by the proliferation of TECs (Nagl et al., 2020). The tumour endothelial cells (TECs) are differentiated from normal endothelial cells as they have irregular morphology and phenotype, in addition to stemness gene signature. They play multiple roles not only in angiogenesis but also in cancer cells growth and migration (Baghban et al., 2020). Furthermore, TECs can affect the tumour immunogenicity by guiding the adhesion and extravasation of immune cells from the blood vessels into the stroma. They can also promote T cells activation and inactivation as TECs can upregulate molecules which enhance T cell arrest (Nagl et al., 2020). Moreover, many angiocrine factors such as the growth factors PDGF, and TGFβ and interlukins (IL-3,6,8) can promote cancer cells progression and metastasis (Nagl et al., 2020).

1.4.3 Cancer associated fibroblasts (CAFs):

Normal fibroblasts (NFs) are activated into myofibroblasts to initiate a regenerative response during the wound healing process (Yang et al., 2023). Myofibroblasts are mesenchymal-like shaped cells highly expressing α-smooth muscle actin (α-SMA). Cancer is known as “the wound that never heals”, hence cancer associated fibroblasts (CAFs) are the myofibroblasts of a tumour (Yang et al., 2023, Hu et al., 2022). They are one of the most important cells in the TME and they differ from NFs by expressing certain proteins including α-SMA, Vimentin, fibroblast-specific protein (FSP1), PDGF receptor α (PDGFRα) and β (PDGFRβ), and fibroblasts activated protein (FAP) (Wang et al., 2021). However, the expression of CAFs markers can also vary

according to the type of tumour. For instance, it was shown that in breast cancer α-SMA is upregulated and α-SMA-positive CAFs promote cell proliferation and breast cancer progression (Hu et al., 2022); while in PDAC, it was found that 75% of CAFs are α-SMA positive which 50% of them express PDGFRα , 9% express only PDGFRα but not α-SMA and 16% lack both PDGFRα and α-SMA (Helms et al., 2020).

CAFs may originate from different types of cells in the TME, such as fibroblasts, immune cells, mesenchymal stem cells (MSCs), or epithelial cells. Hence, they are quite heterogeneous where their heterogeneity varies according to their origin. In addition, their type and function differ between different tumours as the cancer type and stage also affect CAFs heterogeneity (Ping et al., 2021, Yang et al., 2023). In breast cancer, four subpopulations of CAFs were identified; 1) vascular CAFs (vCAFs) which mainly express genes involved in angiogenesis such as *Col18a1*, *Notch3*, *Nr2f2*, and *Epas1*, 2) matrix CAFs (mCAFs) which express genes related to the extracellular matrix (ECM) such as collagens (*Col14a*), glycoproteins (*Vcan*, and *Dcn*), and matrix remodelling enzymes (*Lox* and *Lox1)* , 3) cycling CAFs (cCAFs) are the proliferative version of vCAFs and they express cell cycle genes, and 4) developmental CAFs (dCAFs) which express ECM genes and genes related to stem cells such as *Sox9*, *Sox10* and *Scrg1* (Bartoschek et al., 2018, Hu et al., 2022). Furthermore, a study showed that the gene expression of the aforementioned CAFs changes during breast cancer progression where CAFs become more supportive for tumour growth and development over time. The study identified 906 differentially expressed genes between the early and late tumour stage making vCAFs the dominant (~47% of stromal cells) at the late stage, while the mCAFs level was decreased, dCAFs level did not change and cCAFs level was barely detectable. Hence, the mammary tumour progression is associated with changes in CAFs gene expression (Elwakeel et al., 2019). In PDAC, CAFs were classified into three subgroups; 1) myofibroblasts-like CAFs (myCAFs) highly expressing α-SMA, ECM related components and contractility factors; 2) inflammatory CAFs (iCAFs), lacking α-SMA and overexpressing chemokines and cytokines; 3) antigen-presenting CAFs (ApCAFs), which express major histocompatibility complex class II (MHCII) (Yang et al., 2023, Helms et al., 2020).

CAFs play an essential role in tumour development, as they promote cancer cells proliferation, invasion, migration, and stemness. They also contribute to the remodelling of ECM, drug resistance and cancer metabolism (Ping et al., 2021). CAFs secrete multiple factors, such as growth factors, cytokines and different enzymes, that participate in cancer cells stemness,

invasion, migration, angiogenesis, immune response, and metabolic response. CAFs also secrete ECM proteins, therefore they regulate ECM composition and remodelling (Ping et al., 2021). For instance, it was previously shown that CAF secreted-TGF-β increased breast cancer cells motility by promoting the expression of the metalloproteases MMP2 and MMP9, vimentin and fibronectin (Hu et al., 2022). Furthermore, fibroblasts growth factor 5 (FGF5) secreted by CAFs was shown to promote HER2-positive breast cancer cell resistance to HER2 targeted therapies (Trastuzumab and Lapatinib), where FGF5 was shown to activate FGFR2 in breast cancer cells leading to the activation of HER2 via c-Src (Fernandez-Nogueira et al., 2020). Similarly, CAFs secreted-TGF-β was shown to promote PDAC progression and chemoresistance in a mechanism mediated by TGFβ/ SMAD 2/3 / activating transcription factor 4 (ATF4) pathway (Zhang et al., 2022, Wei et al., 2021). CAFs can also play a role in cancer cells metabolic reprograming by secreting various metabolites to support cancer cells growth, more details are in Section 1.6.4. Moreover, CAFs play an essential role in ECM remodelling as well via secreting both ECM proteins and ECM remodelling enzymes such as MMPs and lysyl oxidase (LOX) (Ping et al., 2021). The interaction between CAFs and immune cells have also been shown to enhance tumour progression. In both breast cancer and pancreatic cancer, CAFs have been reported to secrete chemokines and cytokines, which promote the recruitment of immune cells such as monocytes and their transformation into M2-like macrophages, which are known for their role in tumour progression (Hu et al., 2022, Zhang et al., 2022).

CAFs can also affect the heterogeneity of the tumours. (Ligorio et al., 2019) investigated the changes in PDAC cell gene expression by co-culturing them in the presence of different ratios of CAFs. They identified 135 upregulated genes, and 51 downregulated genes when PDAC cells were co-cultured with CAFs in a 10:90 ratio compared to PDAC cells alone. By using gene enrichment analysis, they identified two PDAC subpopulations; epithelial to mesenchymal transition (EMT) and proliferative (Pro). PDAC cells cultured in the 10:90 ratio were expressing both Pro and EMT genes simultaneously, while 65% of PDAC cells did not express both genes when they were cultured in the absence of CAFs. However, in the 50:50 ratio, there was a mixture of cells expressing EMT, Pro or both, suggesting an effect of CAF abundance on PDAC heterogeneity. In addition, culturing PDAC cells in CAF-conditioned media trigged the activation of mitogen-activated protein kinase (MAPK) and Signal transduce and activator of transcription 3 (STAT3) pathways, which are important for the EMT and Proliferative PDAC behaviour. Finally, co-culturing CAFs with PDAC cells increased the proliferation of PDAC cells *in*

vitro and tumour growth and metastatic burden *in vivo* (Ligorio et al., 2019). On the contrary, some studies showed that CAFs have a tumour suppressive effect, mediated by the secretion of anti-tumorigenic factors, such as Slit2, and Asporin. Hence, CAFs can be divided into tumour-restraining CAFs (rCAFs) and tumour-promoting CAFs (pCAFs). Both can be distinguished by the expression of different markers where rCAFs do not express α-SMA but rather they express CAV1, CD271, Mefilin and Saa3 and it is believed that the two types of CAFs can convert into each other according to the tumour stage (Wang et al., 2021).

1.4.4 The Extracellular matrix (ECM):

The ECM is a complex and dynamic three-dimensional network of cross-linked proteins. Mass-spectrometry characterisation elucidated the ECM composition, defined as the 'matrisome'. The matrisome consists of ~300 core proteins, such as collagens, proteoglycans and glycoproteins; ECM associated proteins, consisting of secreted factors such as cytokines, growth factors, and ECM regulators such as MMPs and LOXs; and ECM affiliated proteins such as Galectins, and Mucins (Naba et al., 2012). There are two types of the ECM: the basement membrane (BM), mainly composed of collagen IV, laminins and nidogen, separates the epithelium from the stroma. The interstitial matrix (IM) is mostly composed of collagen I, proteoglycans and fibronectin and it is considered as the tissue structural scaffolding (Cox, 2021) **(Figure 1-7)**. The ECM represents a significant component in the TME, as the ECM forms up to 60% of the tumour mass and is mainly secreted by CAFs. Its composition varies between tissues and tumour stage; for instance, more collagens were shown to be expressed in the ECM of metastatic melanoma cells compared to non-metastatic ones (Naba et al., 2012). In addition, elastin was highly expressed in the metastatic cells compared to non-metastatic ones and emilins, which are ECM proteins binding to elastin, were only expressed in the metastatic cells (Naba et al., 2012). In cancer, the ECM is involved in tumour development at all stages, and it plays a critical role in cancer cells proliferation, invasion and migration (Sleeboom et al., 2024). In the following sections, I will introduce the main IM components, collagens and fibronectins and the BM components laminins and collagen IV.

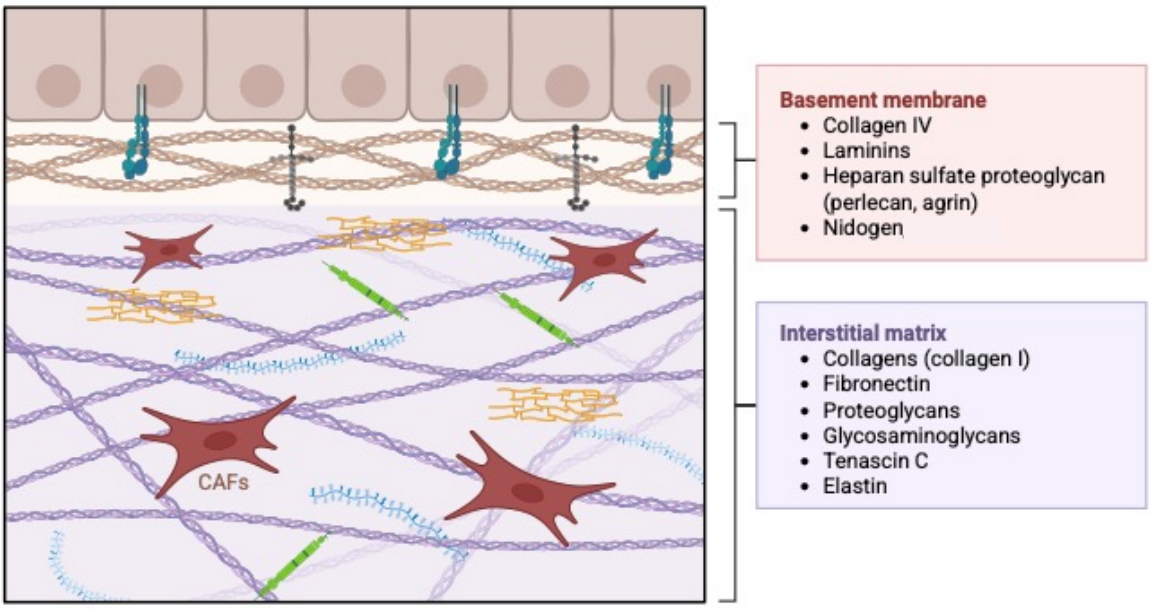

Figure 1-7 The composition of ECM The figure shows the two types of ECM which mainly secreted by CAFs; the basement membrane which mainly consists of collagen IV, laminins and nidogen and the interstitial matrix which mainly consists of collagen I, fibronectin and proteoglycans "Created in BioRender.com".

1.4.4.1 Collagens:

The most abundant proteins in the ECM are collagens and they form ~ 30% of the total protein mass in the human body. 28 types of collagens have been identified so far, and they are structured as a right-handed triple helix of α chains, each one characterized by left-handed polyproline II helices and a one residue stagger between the α chains. The amino acid sequence of the α chains consist of repeats of Gly-X-Y where Gly is Glycine to stabilise the triple helix, and the X and Y are proline and 4-hydroxyproline respectively. However, in non-fibrillar collagen, this sequence can be disrupted (Ricard-Blum, 2010, Xu et al., 2019) **(Figure 1-8).** The formation of collagen starts by the translation of the procollagen molecule. The procollagen molecule then undergoes posttranslational modifications in the endoplasmic reticulum (ER) including hydroxylation and glycosylation and binds with chaperon proteins such as heat shock protein 47, protein disulfide isomerase and prolyl hydroxylase for stabilisation. The procollagen is then hydrolysed by proteinases to form collagen (Ricard-Blum, 2010, Xu et al., 2019, De Martino and Bravo-Cordero, 2023).

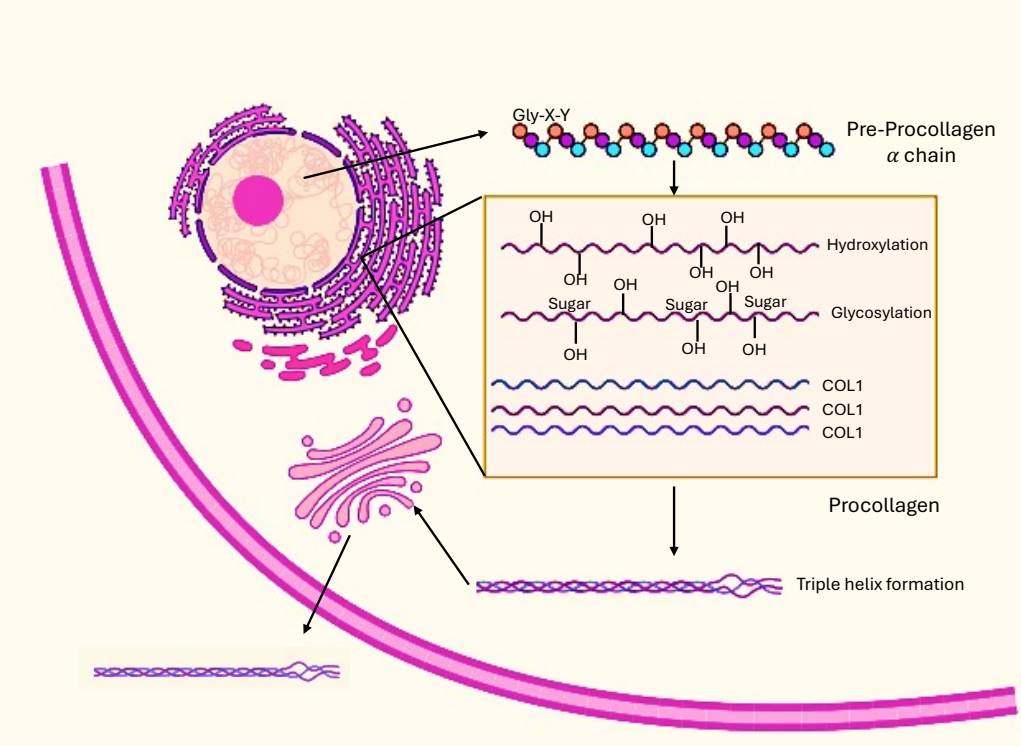

Figure 1-8 Collagen synthesis. The collagen synthesis starts with the formation of the procollagen α chain which is an amino acids sequence consisting of repeats of glycine, proline and 4-hydroxyproline. The procollagen then undergoes posttranslational modifications in the ER such as hydroxylation and glycosylation, followed by the formation of a triple helix collagen which is then secreted to the extracellular space. "Created in BioRender.com".

According to their structure, collagens can be divided into four subgroups: fibrillar-forming collagens, mostly present in the IM; network-forming collagens, found in the BM; fibrillar-associated collagens with interrupted triple helices (FACITs); and membrane anchored collagens (MACITs) (Xu et al., 2019). Several collagens have been implicated in different cancer types **(Table 1-6)**. To be stabilised and to form fibres or networks, collagen molecules are crosslinked extracellularly via LOX, which promotes the formation of intermolecular and intramolecular linkages between the same types or different types of collagen (Ricard-Blum, 2010). Collagens are extensively remodelled during cancer progression, and they impact on tumour proliferation, invasion, migration, dissemination, and metabolism (De Martino and Bravo-Cordero, 2023) **(Figure 1-9)**.

Table 1-4 Collagen types, their tissue distribution and association with cancer: Four collagen types have been identified so far (fibrillar forming collagen, Network forming collagen, fibrillar-associated collagens with interrupted triple helices (FACITs); and membrane anchored collagens (MACITs). The four types can differ in their ECM localisation, their distribution in healthy tissues and the types of cancers that they are associated with (Fang et al., 2014, Nissen et al., 2019, Zhang et al., 2023).

Structure	Type	ECM	Tissue distribution	Cancer
Fibrillar-forming	I	IM	Blood vessels, skin, ligaments, tendon, sclera, and cornea	Lung, colorectal, pancreas, ovarian, and breast cancer
	II	IM	cartilage	Bone cancer
	III	IM	Lung, skin, intestine, vascular systems, and liver	Colorectal, pancreas, breast, and head and neck squamous cell cancer (HNSCC)
	V	IM	Skin, ligaments, tendon, sclera, and cornea, Lung, intestine, vascular systems, and liver	Breast cancer
	XI		Lung, brain, placenta, skeletal muscle, articular cartilage, trabecular bone, tendons, trachea, and testis.	Breast, pancreatic, colon, non-small lung cancer, gastric, and HNSCC
	XXIV	IM	Bone, muscle, liver, lung, ovaries, spleen, testis, and kidney	HNSCC
	XXVII	IM	Cartilage	unknown
Network -forming	IV	BM	Broadly distributed	Pancreatic, breast, gastric and colorectal cancer
	VI	Between IM and BM	Lung, skin, dermis, cartilage, tendon, adipose, cornea, and skeletal muscle.	Ovarian, breast, pancreatic, colon cancer melanomas and glioblastomas.
FACIT	XII	IM	Weight bearing tissues Skeletal muscle	Colorectal, colon cancer, breast, PDAC
	XX	IM	It is distributed within many tissues	Prostate cancer
MACIT	XIII	Between IM and BM	Epithelia, muscle and nerves	Bladder cancer, Breast cancer

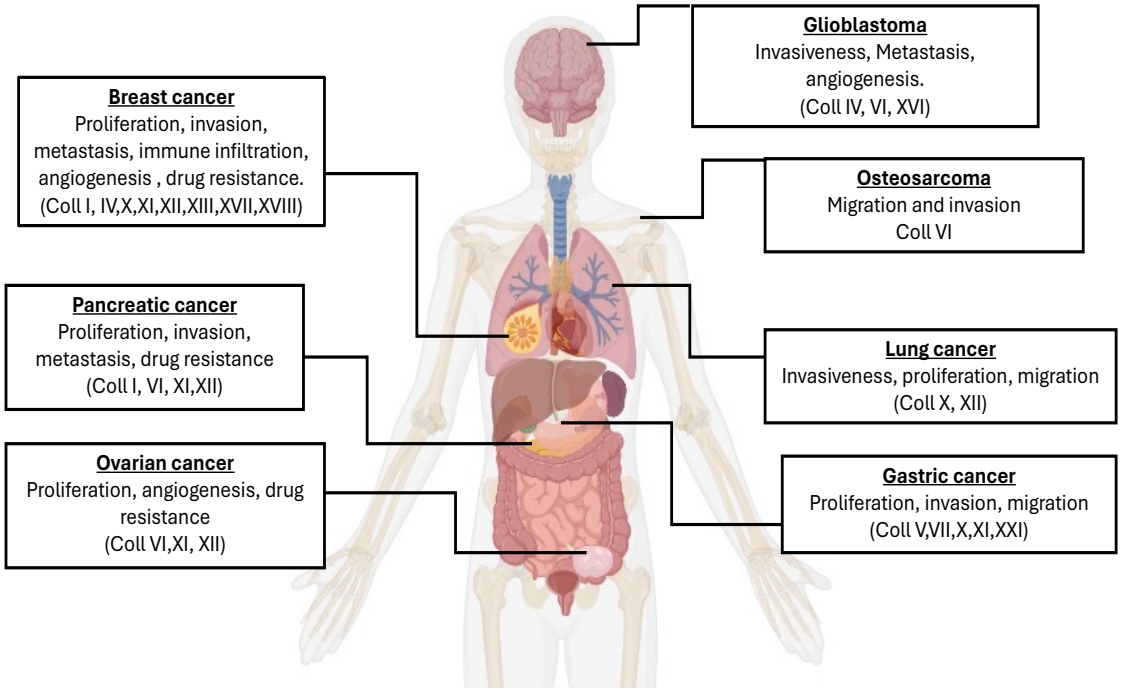

Figure 1-9 The role of collagens in different types of cancer. Collagens play multiple roles in cancer, promoting invasiveness, proliferation, migration, angiogenesis and drug resistance (Zhang et al., 2023, Buglio et al., 2024) "Created in BioRender.com".

1.4.4.2 Fibronectin:

Fibronectin (FN) is one of the main ECM glycoproteins. There is the plasma FN (pFN), a soluble form which exists in the blood, synthesised and secreted by hepatocytes, and the cellular FN (cFN), a fibrillar form which exists in tissues, synthesised and secreted by multiple cells such as endothelial cells and monocytes, but mainly by fibroblasts. FN is encoded by the FN1 gene. It is a 440kD protein formed of two monomers of 230-270 kDa linked together at the C-terminal by two disulfide bonds. Each FN monomer consists of repeats of three different types of FN motifs (FNI, FNII, and FNIII). The FN structure has 12 FNI at the N-terminal and C-terminal, two FNII and 15 FNIII in the central and in the heparin binding (HEPII) domains. The structure also contains three FNIII with different splicing; the extra domains A and B (EDA-EDB), the type III connecting segment region (IIICS) which is a non-homologous variable (V) (Spada et al., 2021, Guerrero-Barbera et al., 2024) **(Figure 1-10)**. The extra three FNIII splice sites can differentiate the cFN from the pFN (Rick et al., 2019).

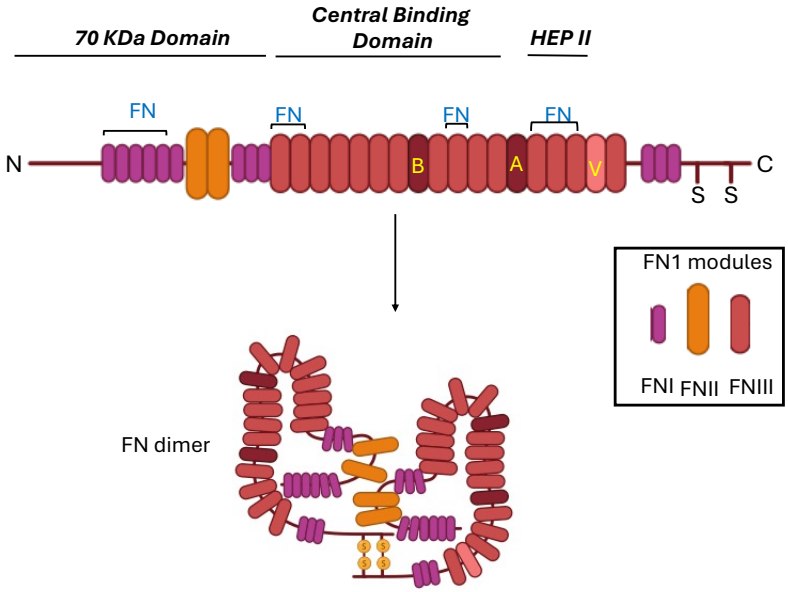

Figure 1-10 Fibronectin structure. Each FN monomer consists of repeats of three different types of FN motifs (FNI, FNII, and FNIII). The FN structure has 12 FNI at the N-terminal and C-terminal, two FNII and 15 FNIII in the central and in the heparin binding (HEPII) domains in addition to three FNIII with different splicing (B-A-and V). "Created in BioRender.com".

The binding of multiple FN molecules forms FN fibrils. The formation of FN fibrils and their assembly are essential for ECM deposition and organization, as FN assembly is crucial for the deposition of other ECM proteins such as collagen type I and thrompospondin-1 (Spada et al., 2021). FN plays an essential role in cancer invasion and metastasis as the alignments of the FN fibres can guide cancer cells to invade away from their primary site (Rick et al., 2019). Indeed, head and neck squamous cancer (HNSCC) cells have been shown to collectively migrate on ECM derived from HNSCC-associated fibroblasts. Fibronectin was found to be the main component of this ECM, and the FN-rich fibres promoted the directional migration of HNSCC cells (Gopal et al., 2017). Similarly, co-culturing prostate cancer cells or HNSCC cells with prostate CAFs induced their directional migration but not when they were co-cultured with NFs. Interestingly, the expression of FN was 50% higher in CAF derived ECM comparing to the NF one and FN was aligned in organised fibres in CAF ECM (Erdogan et al., 2017). FN promotes cancer cells migration not only by providing aligned fibres, but also by triggering signalling after binding to its receptors. A previous study showed that FN enhanced the migration and invasion of lung adenocarcinoma cells due to the activation of the focal adhesion kinase (FAK), which triggered downstream signalling pathways leading to ECM degradation via the ECM degrading enzyme MMP9 (Meng et al., 2009, Efthymiou et al., 2020). Furthermore, FN has also been

shown to regulate cancer cells proliferation in different type of cancers such as colorectal (Yi et al., 2016), breast (Ghura et al., 2021), and ovarian cancer (Mitra et al., 2011).

1.4.4.3 Basement membrane (BM):

The BM is a thin (50-100 nm) ECM layer that separates the epithelia from the stroma. Insoluble molecules such as collagen IV, laminins, nidogen and heparan-sulphate proteoglycans come together in a self-assembly process to form the BM. The BM is also considered as a reservoir for growth factors which can be released once it is degraded (Engbring and Kleinman, 2003). Collagen IV forms 50% of the BM and is a network forming type of collagen. There are six isoforms of collagen IV which are all assembled from α chain polypeptides. Each α chain consists of three domains: an amino-terminal 7S domain, a carboxy-terminal globular non-collagenous (NC)-1 domain, and a middle triple-helical domain. To form the network, three α chains connect to each other via the NC1 domain to form a trimer, followed by the formation of a dimer by connecting two trimers via their NC1 domains. The final structure of collagen IV is formed by the assembly of four dimers via their amino-terminal 7S domain (Kalluri, 2003, Ricard-Blum, 2010) **(Figure 1-11)**.

Laminin is the second major component of the BM and is a big molecule (400-900 KDa) composed of three chains, α, β, and γ, that connect to each other via disulfide bonds to form a heterotrimer. There are 16 isoforms of cross shaped laminins which are formed from different combination of five α, three β, and three γ chains and this composition would give the laminin its name, for example Laminin 111 is formed from a combination of α1, β1, and γ1 chains. The C-termini of the three chains form the long arm of the cross arranged in a coiled-coil structure where laminin binds to its receptors and triggers cell signalling events. On the opposite side, laminin binds with other BM components, such as nidogens, collagens and perlecans, via its short arm which is formed from the N-terminal of the chains (Nonnast et al., 2025) **(Figure 1-11)**.

Both laminin and collagen IV can initiate their self-assembly and then the assembly of the BM starts when laminin binds to cell surface receptors, integrins and dystroglycans, which then promote the production of more laminin polymers; this is followed by the deposition of laminin polymers which interact with collagen IV polymers. Nidogen facilitates the interaction between laminin and collagen IV and the other BM components, fibulin and perlecan, stabilise it more (Kalluri, 2003). Hence laminin deposition and binding to the cell are quite important for the

formation of the BM. Moreover, the absence of collagen IV leads to the formation of a structurally unstable BM (Chang and Chaudhuri, 2019). Indeed, it was found that breast cancer cell proliferation was increased when cells were not able to anchor laminin to their surface. The loss of laminin anchoring was due to dystoglycan dysfunction which was as a result of a reduction in the expression of the glycosyltransferase like acetylglucosaminyltransferase (LARGE), which regulate dystroglycan glycosylation. Interestingly the loss of LARGE expression was observed in the aggressive type of breast cancer "basal-like breast cancer" and it was associated with poor overall survival (Akhavan et al., 2012).

In the early stage of tumour progression, the BM is tumour suppressive, as it restrains both tumour growth and migration. However, it becomes tumour promoter at later stages. When cancer cells start to proliferate, the tumour volume increases, and this puts pressure on the BM. The forces generated from the expansion of the tumour result in weakening the BM. Eventually cancer cells break through the BM and start invading and migrating towards the IM (Chang and Chaudhuri, 2019). Interestingly, the stiffness of the BM has also been shown to facilitate the invasion of cancer cells. A former study showed that the expression of the BM protein Netrin 4 (Net4) regulates the stiffness of the BM. High levels of Net4 decreased the stiffness of the BM due to binding to laminin and softening its complex. The softening of the BM led to a decrease in cancer cells invasion and therefore increase patients' survival (Reuten et al., 2021). Altogether, the BM can play a critical role in cancer cells proliferation, invasion and metastasis.

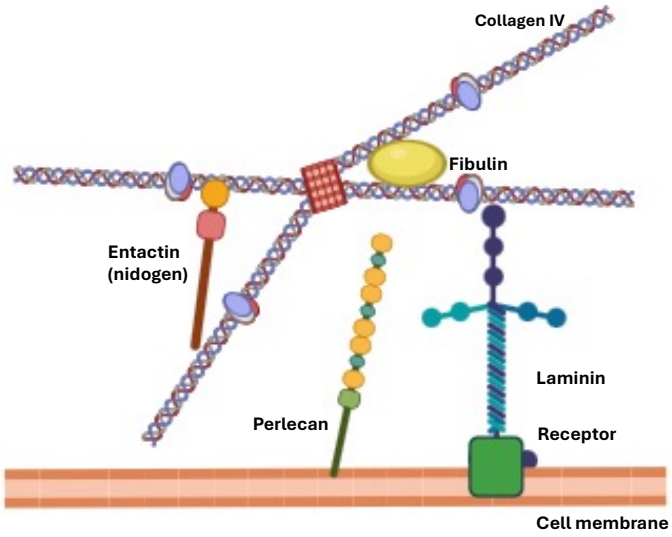

Figure 1-11 the basement membrane structure. Laminin binds to cell surface receptors which promote the formation of laminin polymers. Laminin polymers interact with collagen IV polymers. Nidogen (also known as entactin) facilitates the interaction between laminin and collagen IV, and fibulin and perlecan, stabilise the BM "Created in BioRender.com".

1.5 ECM remodelling:

The ECM is dysregulated in cancer. It undergoes continuous remodelling and composition changes, which promote tumour progression. A previous study by Bergamaschi et al identified the changes in the expression of ECM related genes in breast cancer tumours from 28 patients and showed that breast cancer can be classified into four distinct groups according to these changes. The density of the ECM in the four groups was variable however, most tumours in group three and four had soft ECM while group one and two had mixed ECM densities. Most of basal-like breast cancer tumours belonged to group one which also showed an upregulation in PI3K pathway, while Luminal A/B tumours were scattered in all groups. Moreover, the groups showed different disease outcome, with group one resulting in the worst outcome (Bergamaschi et al., 2008). Similarly in pancreatic cancer, by using proteomics, Tian et al detected various changes in ECM during PDAC progression where fibrosis and inflammation markers were found to be upregulated. The most abundant ECM proteins during all stages of PDAC progression were identified to be fibrillar collagens with type I and III forming 90% of all collagens. Moreover, the collagen mass was enhanced by 2.6-fold during the progression from normal pancreas to PDAC (Tian et al., 2019). Furthermore, a pan-cancer analysis of 1027 matrisome genes in 30 types of cancer, including breast and pancreatic cancer, identified 23 upregulated and 17 downregulated genes compared to normal tissues. Collagen triple helix repeat containing-1 gene (CTHRC1) had the highest score as it was upregulated and affected

patient survival in 9 types of cancer including breast cancer. Furthermore, 19 genes were identified to be upregulated in the 9 CTHRC1 dependent cancers including Coll10A1, Coll11A1, Periostin (POSTN) and integrin subunit beta like 1 (ITGBL1), ADAMTS16, and MMP13 and the enrichment analysis of these gens showed that they are involved in ECM adhesion and organisation. Interestingly the authors showed that CTHRC1, MMP13, and POSTN were highly expressed in breast cancer compared to normal tissues (Harikrishnan et al., 2022).

Therefore, an increase in ECM protein expression is observed during cancer development and tumour cell-ECM interaction is a fundamental factor that enhances tumorigenicity.

1.5.1 ECM stiffness:

The expression of ECM proteins and its stiffness are increased in various types of cancer, including breast and pancreatic cancer, causing fibrosis. For instance, mammary epithelial cells are normally encased by the BM which is surrounded by fibrillar collagen. The expression of type I, III and IV collagens increase during tumour progression, which in turn increases the stiffness of the ECM and this is considered one of the major breast cancer risk factors (Martinez and Smith, 2021). Being in a collagen rich environment, tumours switch to a more malignant phenotype with invasive and metastatic features (Provenzano et al., 2008).

ECM stiffness applies mechanical forces and tension on the tumour affecting its growth. It keeps changing during tumour progression and it plays a role in a variety of cell functions (Deng et al., 2022). For instance, the stiffness of ECM and collagen I crosslinking have been shown to affect breast cancer cell invasion. It was shown that invasive breast cancer cells collectively invaded in densely aligned collagen I fibres and this invasion was prompted by the collagen crosslinker Lysyl oxidase-like 3 (Loxl3), which was found to be upregulated in invasive breast cancer cells (Koorman et al., 2022). Interestingly, a previous study by Nagoc et al showed that despite expressing all the required genes for dissemination, cancer cells do not become invasive until the BM is disrupted, and they become in contact with the collagen I matrix (Kauppila et al., 1998; Nguyen-Ngoc et al., 2012). Moreover, ECM stiffness regulates cell proliferation and cancer cells morphological properties. A study in 14 different cancer cell lines found out that the cells can be split into two categories according to their response to ECM rigidity where the growth of some cells was increased on stiff substrates hence they were identified as rigidity dependent such as (MDA-MB-231 breast cancer cells and A549 lung cancer cells) while other cells were considered as rigidity independent such as (PC-3 prostate cancer cells and mPanc96

pancreatic cancer cells) where their growth was not affected by changing the ECM stiffness (Tilghman et al., 2010). Interestingly, the growth of the rigidity dependent cells was decreased when they were seeded on soft substrate, and this was shown to be at least in part due to cell cycle progression alteration and apoptosis induction. In addition, the cells spreading and migration was also reduced on soft substrates compared to stiff ones (Tilghman et al., 2010). Furthermore, ECM stiffness also plays a role in PDAC cells progression where it was shown previously that ECM rigidity can promote the epithelial mesenchymal transition (EMT) in PDAC cells due to a decrease in E-Cadherin expression and an increase in Vimentin expression. In addition, ECM rigidity was shown to increase PDAC resistance to chemotherapy, specifically to paclitaxel (Rice et al., 2017). Overall, the changes in ECM expression and its stiffness play a critical role in cancer cells progression and development.

1.5.2 ECM degradation:

The degradation of the ECM is a major process of ECM remodelling, and it is essential not just for the reorganisation of ECM proteins but also for the release of multiple factors such as growth factors and cytokines. The ECM can be degraded in two different ways; extracellularly via proteases such as the matrix metalloproteinases (MMPs), disintegrin and metalloproteinase (ADAMs), and disintegrin and metalloproteinases with thrombospondin motifs (ADAMTs); or intracellularly, where ECM components bind to their receptors, are internalised via different endocytic pathways and degraded into the lysosomes (Winkler et al., 2020).

MMPs are a family of at least 23 zinc-dependent endopeptidases in humans. They are usually in an inactive state, and they get activated via multiple proteinases such as furin, plasmin and other active MMPs. Their activity can be inhibited via the tissue inhibitors of metalloproteinases (TIPMs). Both MMPs and TIMPs can be released in the extracellular space by various stromal cells. The role of MMPs in tumour progression has been widely studied and MMPs do not only regulate ECM degradation, but they also control signalling pathways (Kessenbrock et al., 2010). Different MMPs have been shown to regulate tumour growth, angiogenesis, cells apoptosis, invasion and metastasis (Kessenbrock et al., 2010) **(Figure 1-12)**. For instance, MMP9 was shown to regulate cell growth proteolytically by activating TGF-β (Kessenbrock et al., 2010). In breast cancer the expression of MMPs such as MMP1, MMP7, MMP9, MMP11, MMP12, MMP14 and MMP15 was found to be increased, and this correlated with a decrease in patient survival. Some of these MMPs have been found to play a role in breast cancer metastasis, such

as MMP1 which enhances TNBC metastasis to the brain by degrading the brain blood barrier (Wu et al., 2015). Similarly, MMP2 enhances breast cancer metastasis to the brain, while MMP13 plays a role in breast cancer metastasis to the bone and MMP14 to the lung (Kwon, 2022). Some MMPs play a dual role according to the stage of cancer, for instance at the early stages of breast cancer MMP11 enhances tumour formation while it supresses tumour metastasis at the late stage (Kwon, 2022). Similarly to breast cancer, a recent study compared MMPs expression in PDAC using the Gene Expression Omnibus (GEO) and GEPIA databases and found that 10 MMPs were upregulated in PDAC compared to normal pancreas: MMP1, MMP2, MMP3, MMP7, MMP9, MMP10, MMP11, MMP12, MMP14, and MMP28, while five of them were correlated with poor overall survival MMP1, MMP3, MMP11, MMP14, and MMP28 (Luan et al., 2023).

Multiple MMP inhibitors have been generated, however due to the dual role of MMPs in cancer, they failed in clinical trials. For instance, MMP8 was found to play a pro-tumorigenic effect, and its high expression correlated with poor patient survival in both ovarian cancer and hepatocellular carcinoma. On the contrary, in oral tongue squamous cell carcinoma, its low expression correlated with decreased patient survival (Winkler et al., 2020).

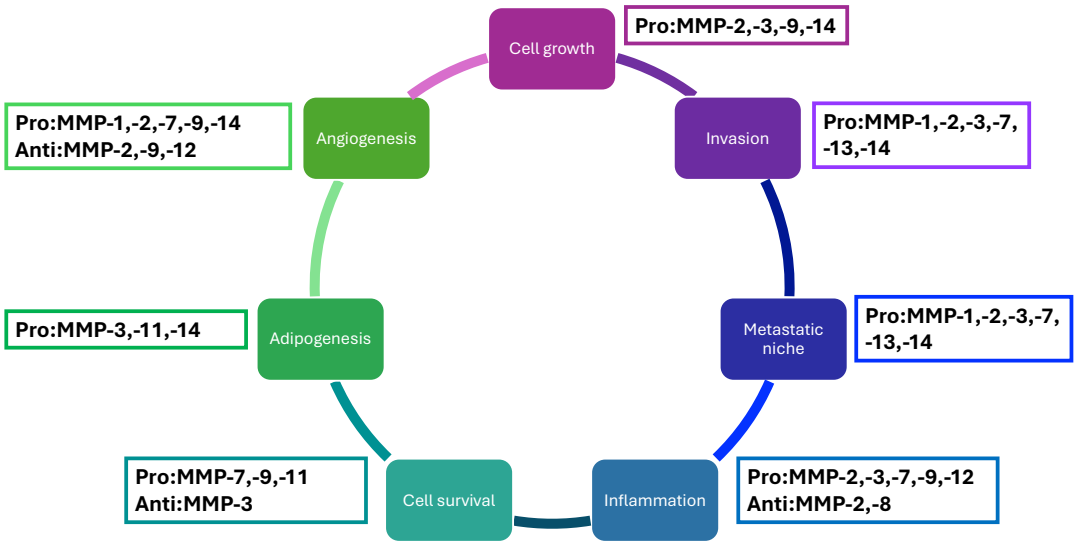

Figure 1-12 The effect of MMPs on cancer progression. A number of MMPs regulate (promote (Pro), or supress (Anti)) cellular processes in cancer such as cell growth, invasion, metastasis, inflammation, cell survival, adipogenesis and angiogenesis, adapted from (Kessenbrock et al., 2010).

ADAMTSs are another family of ECM degradation enzymes. There are 19 ADAMTSs identified so far and most of them are highly expressed in breast cancer, ovarian cancer and pancreatic cancer. Similarly to MMPs, ADAMTSs can play a role in ECM remodelling and cancer progression. In breast cancer, ADAMTS 4 and 5 are associated with increased cancer invasion and metastasis (Bacchetti et al., 2024). Furthermore, recent work in our lab showed that ADAMTS5 promotes ovarian cancer invasion, and its high expression is correlated with poor overall patient survival (Yuan et al., 2025). Hence, degrading the ECM extracellularly plays a critical role in cancer progression.

1.5.3 ECM endocytosis:

The second ECM degradation mechanism is the internalisation of its components via different endocytic pathways, followed by lysosomal degradation. This mechanism has also been found to promote cancer progression (Rainero, 2016). Collagen I can be internalised via different mechanisms. In fibroblasts, collagen I coated beads were found to bind to $\alpha 2\beta 1$ integrin receptor and get internalised in a phagocytosis dependent mechanism (Lee et al., 1996). The binding of collagen to $\alpha 2\beta 1$ integrin enhanced Ca^{2+} entry, which is essential for the interaction between Gelsolin and non-muscle myosin IIA (NMMIIA) leading to the actin assembly at the collagen adhesion site and therefore promoting collagen phagocytosis (Arora et al., 2013). Solubilised collagen can also be internalised by a clathrin-dependent mechanism after binding to one of the mannose receptor family members, Endo180 and be transferred to early endosomes then lysosomes to be degraded, while the receptor is recycled back to the cell surface (Wienke et al., 2003). This collagen internalisation route was observed in mesenchymal cells but not epithelial cells, consistent with the fact that the expression of Endo180 is lower in epithelial cells (Madsen et al., 2011). Indeed, the expression of Endo 180 was found to be upregulated in mesenchymal basal-like breast cancer cells, and it is correlated with increases in tumour volume *in vivo* (Wienke et al., 2007). Similarly, pancreatic stellate cells (PSCs) were shown to internalise collagen via Endo180 but not via $\alpha 2\beta 1$ integrin and this internalisation enhanced their invasive behaviour (Ikenaga et al., 2012). The third possible route of collagen internalisation is via macropinocytosis (Yamazaki et al., 2020). A recent paper from our lab showed that cancer cells internalised collagen I, Matrigel and cell derived matrices (CDM) via macropinocytosis during cell migration. To migrate, cancer cells internalised collagen I, in an

α2β1 integrin-dependent manner, via macropinocytosis and degraded it into the lysosomes. This process was shown to be regulated by the MAPK/p38 pathway, and it promoted tumour invasion and migration (Martinez et al., 2024) **(Figure 1-13)**.

FN can also be endocytosed and degraded into the lysosomes. Previous studies showed that FN internalisation is mediated by its receptor α5β1 integrin, in a caveolin 1 dependent manner (Sottile and Chandler, 2005, Shi and Sottile, 2008). A later study showed that the turnover of FN is regulated by the membrane type matrix metalloproteinase 1 (MT1-MMP/ MMP14) as FN is extracellularly cleaved by MT1-MMP before it is internalised via α5β1 integrin, leading to increased cell migration due to the disruption of FN polymerisation (Shi and Sottile, 2011) **(Figure 1-13)**.

Laminin has also been shown to be internalised via phagocytosis. Coopman et al showed that MDA-MB-231 breast cancer cells could uptake and degrade FITC-Matrigel via phagocytosis in an α3β1 integrin-dependent mechanism (Coopman et al., 1996) **(Figure 1-13).** Hence, the endocytosis of ECM proteins can be differentially regulated, and this varies according to multiple factors such as the ECM protein itself, its structure and the cell type. In addition, both extracellular degradation and endocytosis can work together to promote ECM remodelling and the turnover of ECM proteins.

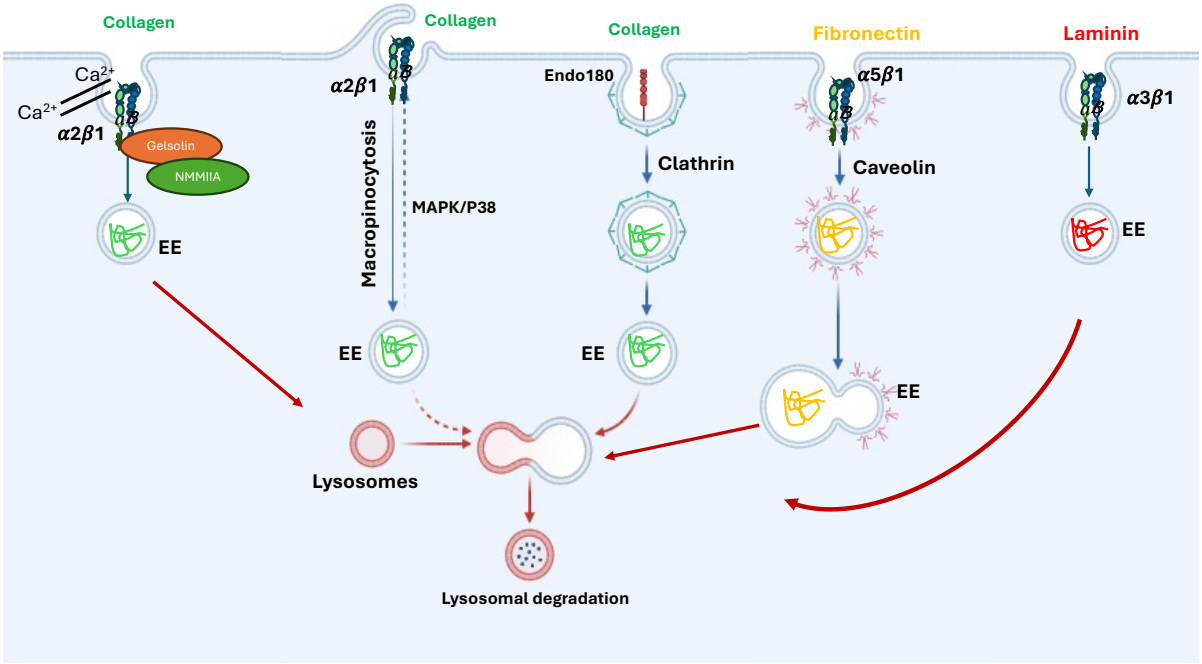

Figure 1-13 The extracellular matrix proteins endocytosis. From left to right, the binding of collagen to α2β1 integrin promotes Ca^{2+} entry, which is essential for the interaction between Gelsolin and non-muscle myosin IIA (NMMIIA) which further triggers the phagocytosis of collagen. Collagen can also be internalised via macropinocytosis mediated by MAPK/P38. After binding to its receptor Endo180, collagen can be internalised in a clathrin-dependent mechanism. After binding to its receptor α5β1, Fibronectin can be internalised in a caveolin-mediated mechanism. Laminin can be internalised in a phagocytosis process after binding to its receptor α3β1. After their internalisation, ECM proteins are eventually degraded in the lysosomes "Created in BioRender.com".

1.6 ECM receptors: Integrins

The attachment of cancer cells to the ECM is crucial for their survival and development. This attachment is called cell-ECM adhesion. There are multiple plasma membrane receptors that interact with the ECM, such as syndecans, dystroglycan, discoidin domain receptors (DDRs) and integrins (Sleeboom et al., 2024). Integrins are the major ECM adhesion receptors. They are heterodimers cell surface receptors consisting of two subunits, α & β. So far, there are 18 α subunits and 8 β subunits identified in mammals, which can form at least 24 integrins. Integrins are transmembrane receptors, and the structure of each subunit is characterised by three domains: a small cytoplasmic tail, a transmembrane domain and a large extracellular domain. They can bind different ECM proteins either via a specific site on the α subunit or via a combination of epitopes on both subunits (Kechagia et al., 2019, Moreno-Layseca et al., 2019). Some integrins can bind to a specific ECM protein such as α5β1 integrin binding to FN, while others can bind to multiple ECM proteins such as α2β1 and α4β1 (Moreno-Layseca et al., 2019).

Integrins exist in three confirmations: a low affinity bent (inactive), an extended with a closed headpiece and high affinity extended with an open headpiece (active) (Takagi et al., 2002) (Figure 1-14). Integrins can be activated either from inside or from outside the cells. The inside-out activation is triggered when the talin/paxillin/kindlin complex binds to the cytoplasmic domain of the β subunit via their FERM domains. This binding disrupts the α/β connection leading to the opening of the receptor head to interact with the ECM ligands (Lu et al., 2022, Sun et al., 2019). Binding to ECM ligands can trigger the outside-in activation of integrins. This then triggers the recruitment of the focal adhesion (FA) proteins called "the integrin adhesome", which were identified by proteomic analysis as more than 2000 proteins, defined as the meta adhesome, induced on a fibronectin substrate. 60 meta adhesome proteins were identified as core/consensus adhesion proteins, including FAK, talin, vinculin and paxillin (Robertson et al., 2015, Horton et al., 2015). Adhesion complexes connect integrins to the actin

cytoskeleton and this facilitates adherence and spreading of the cell (Sun et al., 2019) **(Figure 1-14).** After the recruitment of adhesion proteins, integrins clustering is triggered to stabilise the binding. Integrins clustering distributes the tensile forces extending the adhesions lifetime (Sun et al., 2019).

The integrin-ECM binding initiates intracellular signalling cascades essential for cell's behaviours such as differentiation, proliferation, invasion, and migration. Therefore, the expression of integrins on the cell surface can determine the cell behaviour towards a variety of extracellular changes (Hamidi and Ivaska, 2018).

Seeding MCF7 epithelial breast cancer cells on an ECM derived from the highly aggressive MDA-MB-231 breast cancer cells led to MCF7 cells becoming more aggressive and more migratory. Seeding MCF7 on MDA-MB-231 ECM induced EMT and increased integrins signalling by an $\alpha v\beta 3$ integrin-dependent mechanism (Machado Brandao-Costa et al., 2020). Integrins are also involved in drug resistance; for instance, tyrosine kinase inhibitor (TKI) resistance in NSCLC was found to be due to an increase in the expression of $\alpha 5$ integrin and its downstream FAK-STAT3-AKT signalling pathway. The upregulation of $\alpha 5$ integrin expression caused an increase in NSCLC invasion and migration (Yang et al., 2021). Furthermore, $\alpha v\beta 6$ integrin expression was high in PDAC cells and blocking it reduced cells proliferation, invasion and migration *in vitro*. Moreover, combining the $\alpha v\beta 6$ integrin blocking antibody 264RAD with Gemcitabine strongly reduced tumour volume *in vivo* and increased the overall survival of PDAC mice (Reader et al., 2019). Hence, integrins regulate different mechanisms which can affect cancer progression and targeting them can improve the efficiency of cancer therapies.

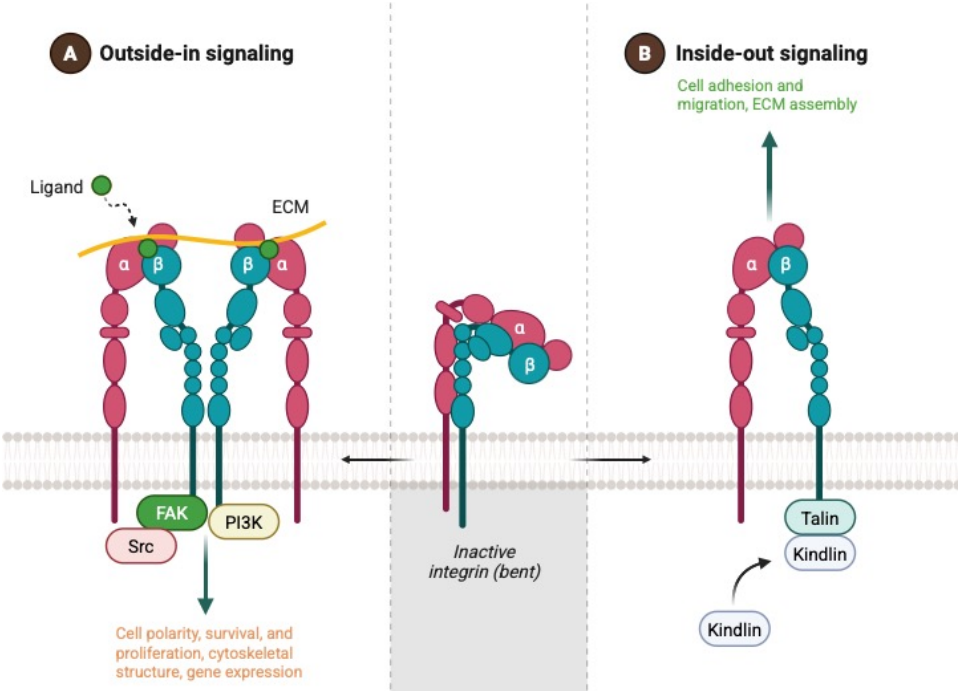

Figure 1-14 Integrin activation. Integrins can be activated either in an inside-out process when Talin and kindlin bind to the integrin cytoplasmic tail which in turn promotes binding to its ECM ligand and therefore increases cell adhesion and migration. Integrins can also be activated in an outside-in process; after binding to ECM ligands, adhesion complexes are clustered which triggers signalling cascades promoting various cell functions "Created in BioRender.com".

1.7 Integrin trafficking:

Integrins not only localise to the cell surface, but they are also transported through the endosomal system. Inactive and active integrins can be endocytosed, trafficked, degraded in the lysosomes or recycled back to the cell surface. Integrins trafficking is an important mechanism that cells undertake to regulate cell adhesion and migration, by controlling the availability of certain integrins at the cell surface (De Franceschi et al., 2015, Moreno-Layseca et al., 2019). Integrins internalisation occurs via different routes, both clathrin-dependent and clathrin-independent. Several regulators have been found to be involved in integrin trafficking, including small GTPases of the Rab, Arf and Rho families (De Franceschi et al., 2015, Moreno-Layseca et al., 2019). After internalisation, the majority of integrins recycle back to the plasma membrane via two different mechanisms: a short-loop pathway regulated by Rab4 or a long-loop pathway regulated by Rab11 (De Franceschi et al., 2015). Meecham et al showed that 90% of the ligand bound αvβ6 integrin is internalised via both clathrin-dependent and caveolin-dependent pathways. 60% of internalised integrins are recycled back to the plasma membrane in a Rab11-dependent mechanism, while they are still bound to their ligand (Meecham et al.,

2022). The expression of Rab25, an epithelial-specific member of the Rab11 family, was found to be increased in ovarian cancer and breast cancer and this upregulation was associated with increased in the tumour volume and its aggressiveness (Cheng et al., 2004). Caswell et al later showed that in A2780 ovarian cancer cells, seeded on a fibronectin-rich 3D matrix, Rab25, but not Rab11a, binds to $\alpha5\beta1$ integrin at the cytoplasmic domain of the $\beta1$ subunit. This in turn promoted ovarian cancer cells persistent migration due to the continuous recycling of $\alpha5\beta1$-containing vesicles to the membrane of pseudopodial tips (Caswell et al., 2007).

The recycling of integrins is known for playing a key role in cell motility. For instance, it was previously shown that after growth factor stimulation, $\alpha v\beta3$ integrin, a vitronectin and fibronectin receptor, is internalised and recycled back to the plasma membrane via a Rab4, protein kinase D1 (PKD1) and its substrate Rabaptin-5 dependent mechanism. The recycling of $\alpha v\beta3$ promoted directional cell migration and interestingly, it inhibited the Rab 11 mediated recycling of $\alpha5\beta1$ integrin. The inhibition of $\alpha v\beta3$ recycling could significantly restore the recycling of $\alpha5\beta1$ leading to random cell migration. This can show the crosstalk between the integrin receptors and how the expression profile or recycling of the receptors that bind the same ligand can predict the migration behaviour of the cells (White et al., 2007, Christoforides et al., 2012). In addition, the activity of integrins can determine their trafficking behaviour. A former study showed that the inactive and active $\beta1$ integrin are internalised via clathrin-dependent and dynamin-dependent mechanisms to early endosomes. Here, the inactive $\beta1$ integrin is recycled back to the plasma membrane in a Rab4 fast loop mediated manner, while the active one is transferred to Rab7 compartments. Furthermore, the trafficking of the active $\beta1$ integrins was slower than the inactive ones and the net of their endocytosis was higher, resulting in an accumulation in the internal pool (Arjonen et al., 2012).

1.8 Cancer metabolism:

Altered cell metabolism is considered one of the hallmarks of cancer, as cancer cells have the ability to reprogramme their metabolism to support their growth according to the availability of nutrients in the TME (DeBerardinis and Chandel, 2016). The metabolic alterations can also depend on the tumour stage, as some metabolic pathways are activated at the early stages of cancer while others can be more beneficial for the metastatic behaviour of the cells (DeBerardinis and Chandel, 2016). Some of the metabolic alterations commonly observed in cancer are described below.

1.8.1 Glycolysis:

Glucose is a source of carbon which mammalian cells use to obtain energy. Normally, growth factors stimulate the cells to uptake glucose from the extracellular space and convert it to pyruvate in a process called glycolysis; pyruvate then is metabolised into CO_2 via oxidative phosphorylation in the mitochondria through the Tricarboxylic acid cycle (TCA), also known as the Krebs cycle. This process is called aerobic glycolysis as it requires the presence of oxygen, and it can generate 36 moles of Adenosine Triphosphate (ATP) per mole of glucose. However, in the 1920s Otto Warburg discovered that in the presence or absence of oxygen, cancer cells increase the uptake of glucose, convert it to pyruvate, which is then converted to lactate - this is called the Warburg effect. Lactate is secreted into the extracellular space, causing an increase in the acidity of the TME. The increased H^+ ions from lactate secretion can alter the TME by diffusing into the surrounding microenvironment, increase its remodelling and therefore, the invasiveness of cancer cells. Warburg effect generates only 2 moles of ATP per mole of glucose, but it also generates intermediates for several anabolic pathways leading to the production of lipids, nucleotides and proteins (Liberti and Locasale, 2016). Previous studies showed that the Warburg effect occurs as a result of multiple genetic mutations. For instance, the proliferation of normal cells is usually stimulated by growth factors-mediated activation of PI3K-Akt-mTOR pathway. However, the growth of cancer cells is independent of growth factors stimulation as genetic alterations in cancer cells lead to the constitutive activation of this pathway. This promotes glycolysis by increasing the cell surface level of glucose receptors including GLUT1 and GLUT4, which in turn enhance the uptake of glucose. Furthermore, AKT can phosphorylate and activate glycolysis enzymes such as hexokinase 2 (HEK2) (Hoxhaj and

Manning, 2020). A former study showed that lymphoma cells rely on glycolysis to proliferate, and that glucose uptake is regulated by PI3K-mTOR pathway and MYC. The inhibition of PI3K and MYC reduced glucose uptake and the viability of the cells. Therefore, a combination of a glycolysis inhibitor and a MYC inhibitor might represent a suitable treatment for lymphoma (Broecker-Preuss et al., 2017, Hoxhaj and Manning, 2020) **(Figure 1-15).**

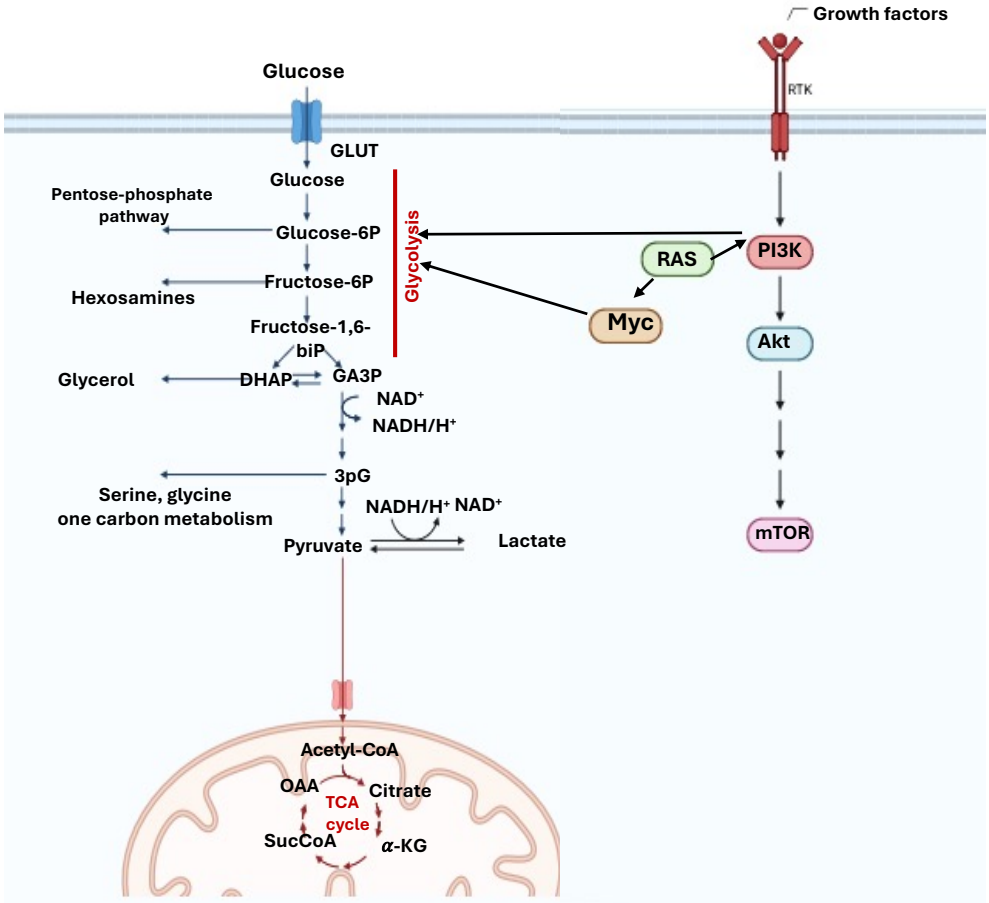

Figure 1-15 Glucose metabolism in cancer. Cancer cells uptake more glucose than normal cells, the uptaken glucose via the glucose transporter GLUT is converted it into pyruvate in a process called glycolysis via multiple steps, must of pyruvate is converted into lactate and some feeds into the TCA cycle. Glycolysis can also generate intermediates for several anabolic pathways such as pentose phosphate pathway (PPP) and the one Carbone metabolism. The sustained activation of PI3K-AKT-mTOR and MYC pathways in cancer cells enhance the glycolysis process "Created in BioRender.com".

1.8.2 Amino acids metabolism:

Amino acids (AA) are biomacromolecules which play an essential role in regulating cancer cells proliferation. There are 20 amino acids, divided into two groups, non-essential amino acids (NEAA) and essential amino acids (EAA). Amino acids are fundamental for the synthesis of proteins. Cells can only synthesise NEAA, while they rely on extracellular sources of EAA. However, cancer cells rely on the extracellular uptake of some NEAA, referred to conditional

EAA, such as glutamine and arginine. Therefore, in cancer, amino acids are grouped into EAAs, NEAA, and conditional EAAs (Chen et al., 2024) (Table 1-5).

Table 1-5 Amino acids classification in cancer: 20 amino acids are identified which can be classified in cancer into three categories; essential amino acids (EAAs), non-essential amino acids (NEAAs) and conditional essential amino acids (conditional EAAs) (Chen et al., 2024).

EAAs	NEAA	Conditional EAAs
Tryptophan	Asparagine	Glutamine
isoleucine	Aspartate	Arginine
Leucine	Alanine	
Valine	Cysteine	
Methionine	Glutamic acid	
Threonine	Glycine	
Phenylalanine	Proline	
Histidine	Serine	
Lysine	Tyrosine	

1.8.2.1 Glutamine metabolism:

In addition to glucose, cancer cells require amino acids and glutathione, which are essential for the synthesis of nucleic acids and redox homeostasis (Choi and Park, 2018). The most abundant amino acid in the blood is glutamine. Some cancer cells are addicted to it, as it provides nitrogen for the synthesis of nucleic acids and the synthesis of other amino acids (Choi and Park, 2018, Geck and Toker, 2016). After entering the cells, glutamine is converted into glutamate in a process called glutaminolysis. Glutamate then is converted into α-ketoglutarate via different enzymes: glutamate dehydrogenase (GLUD1), which leads to the release of ammonium, or aminotransferases, which transfer amino nitrogen to generate another amino acid such as aspartate, alanine and phosphoserine. α-ketoglutarate then feed into the TCA cycle for the production of ATP (Choi and Park, 2018) (Figure 1-16). It has now been established that the majority of ATP is not derived from aerobic glycolysis, but it is generated from mitochondria, and glutamine is one of the main contributors in this process. A study by Fan et al showed that in RAS and Akt driven cancer cells, the glycolytic flux is increased, however the majority of ATP is generated from glutamine and not glucose via oxidative phosphorylation in both normoxic and hypoxic conditions (Fan et al., 2013). Similarly, it was previously shown that PDAC cells rely on both glucose and glutamine to grow. However, PDAC cells rely on a non-canonical pathway, different from the one mentioned earlier, to generate

ATP from glutamine, where glutamine is converted into aspartate, aspartate is then converted in the cytoplasm into oxaloacetate (OAA) via the oxaloacetate aspartate transaminase (GOT1), followed by the production of pyruvate. This pathway was shown to be triggered due to the reduction of GLUD1 expression and the increase of GOT1 expression via oncogenic KRAS. Interestingly, the pathway is specific to PDAC cells but not to non-transformed normal pancreatic ductal cells (HPDEs) and it is essential for cancer cell growth, while the inhibition of GOT1 did not affect the growth of HPDEs (Son et al., 2013) **(Figure 1-16).** Furthermore, the addiction of cancer cells to glutamine, which indicate their heightened reliance on it, was found to be correlated with their invasiveness. A former study showed, by using isotope tracer and bioenergetic analysis, that highly invasive ovarian cancer cells are more addicted to glutamine comparing to low invasive ones. The authors found that glutamine in high invasive ovarian cancer cells contribute to 40% of the TCA cycle fluxes while in low invasive cells glutamine contribute to only 15% of it. This was shown to be essential for the proliferation and invasion of the highly invasive cells in a STAT3 dependent mechanism. In high invasive cells, glutamine was shown to activate ERK1/2 which led to STAT3 serine phosphorylation which in turn increased TCA cycle activation, while in low invasive cells, glucose plays a role in STAT3 tyrosine phosphorylation by activating JAK1, which in turn was shown to regulate glycolysis. The addiction of ovarian cancer cells to glutamine also affected patient survival as the high expression of genes involved in glutaminolysis and TCA cycle was correlated with poor patient survival (Yang et al., 2014). Hence, cancer cells rely on different metabolites to survive during cancer progression, and this varies according to many factors such as cancer type, cancer stage and the nutrient availability in the TME.

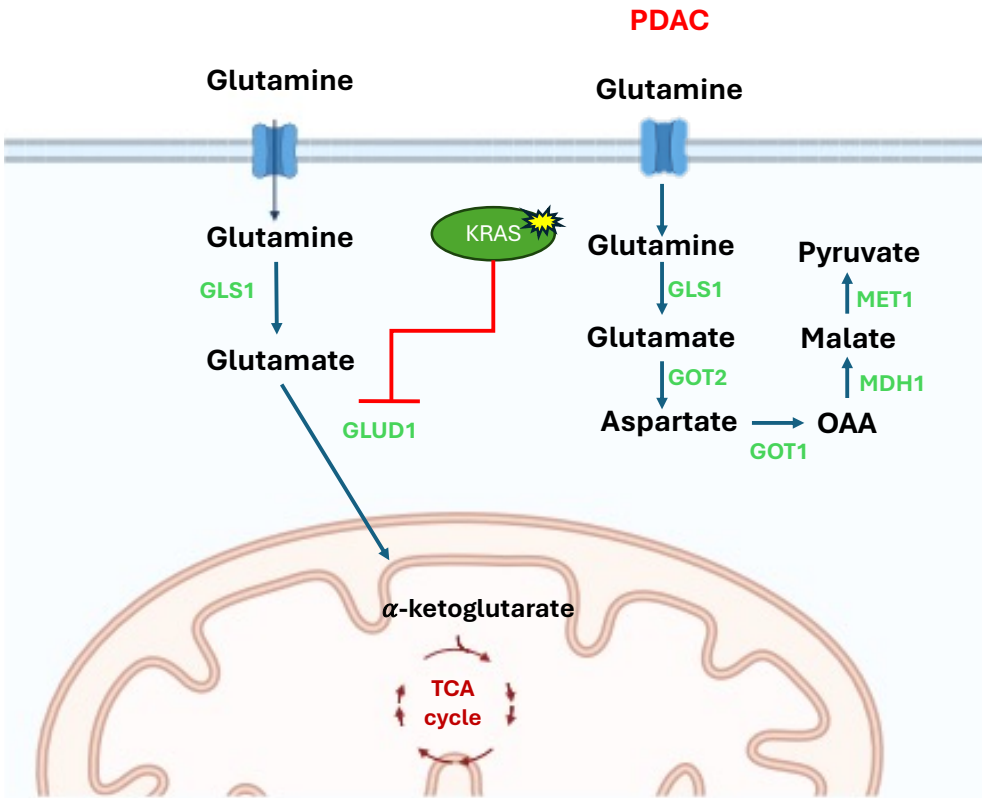

Figure 1-16 Glutamine metabolism in Cancer. After entering the cells, glutamine is converted into glutamate via GLS1 in a process called glutaminolysis. Glutamate then is converted into α-ketoglutarate via GLUD1 which feeds into the TCA cycle. In PDAC, oncogenic KRAS inhibits GLUD1 and alternatively glutamine is converted into glutamate then aspartate via GOT2 followed by the production of OAA via GOT1, malate then pyruvate. "Created in BioRender".

1.8.2.2 Branched-Chain amino acids (BCAA):

Leucine (Leu), isoleucine (Ile), and valine (Val) are EAAs known as branched-chain amino acids (BCAAs). They are interconnected where changes in the level of any of these AAs can affect the level of the other two as the enzymes involved in the catabolism of these AAs can use any of them as a substrate, hence a reduction in any of the enzymes might affect these three amino acids (Chen et al., 2024). BCAAs are transported into the cells via LAT1/2, BCAAs then are converted into branched chain α-keto acids (BCKAs) via BCAA transaminases 1 and 2 (BCAT 1/2). BCAT can also transfer nitrogen into α-ketoglutaric acid (α-KG) to produce glutamate. The keto acids produced will then be metabolised into Acetyl-CoA via the branched-chain α-keto acid dehydrogenase (BCKDH) whose activity is regulated by BCKDH kinase (BCKDK) and the protein phosphatase 1 K (PPM1K) (Ling et al., 2023) **(Figure 1-17, A)**. In hepatocellular carcinoma (HCC), the catabolism of BCAAs was found to be disrupted as their accumulation was observed in HCC but not in regenerative liver tissues, due to the reduction in the expression

of enzymes involved in BCAAs degradation. Accumulation of BCAAs activated mTORC1 therefore increasing the proliferation of HCC cells. Interestingly, as BCAAs derived from the diet, the tumour volume and the overall survival were associated with diet rich of BCAAs in an HCC mouse model. The reduced expression of BCAAs catabolic enzymes was also observed in other types of cancer such as stomach, kidney and colon cancers, however, it is unknown if this would promote their proliferation in an mTORC1 dependent mechanism (Ericksen et al., 2019).

1.8.2.3 Asparagine and Aspartate:

Asparagine (Asn) and Aspartate (Asp) are NEAAs which play a critical role in tumour metastasis. Aspartate can be converted into asparagine by the asparagine synthase (ASNS), and aspartate can be generated from asparagine by asparaginase (ASNase) (Chen et al., 2024) **(Figure 1-17, B)**. In breast cancer, ASNS expression was found to be increased in aggressive tumours and its expression strongly correlated with metastatic relapse to the brain, lungs and liver, therefore poor patient survival. The authors suggested that this effect might be due to the induction of EMT as silencing ASNS led to a reduction in the expression of genes involved in EMT and this was also shown when the transcription factor ATF4, which regulate ASNS expression, was reduced. This effect was confirmed *in vivo* where feeding mice with low asparagine diet led to a decrease in the metastatic burden (Knott et al., 2018). Similarly, Doglioni et al found that in breast cancer lung metastasis, aspartate in the lung environment activates the *N*-methyl-D-aspartate (NMDA) receptor, which in turn triggers the activation of eIF5A and TGFβ signalling leading to increased collagen synthesise. Interestingly, aspartate level was found to be increased in the lungs' interstitial fluid of breast cancer patients (Doglioni et al., 2025).

1.8.2.4 Serine and Glycine:

The other NEAAs which can play a role in cancer progression are serine and glycine. These two AAs can donate one carbon to the folate cycle, and they are essential for nucleotide synthesis and redox homeostasis. Serine can be synthesised from glucose during glycolysis as a branched pathway. By serine hydroxy methyltransferases, glycine is generated from serine where one carbon is then donated to the folate cycle. Even though serine can be generated from glucose, the uptake of exogeneous serine is increased in cancer cells making it the second most used amino acid (Lukey et al., 2017, Chen et al., 2024) **(Figure 1-17, C)**. Indeed, it was previously

shown that cancer cells upregulate serine uptake and the lack of exogenous serine can affect cell proliferation. However, the tumour suppressor protein p53 was shown to support cancer growth under serine deprivation and reactivate the cell cycle, while cancer cells lacking p53 did not survive the absence of serine (Maddocks et al., 2012). Another study showed that PDAC cells can use tryptophan as a one carbon source instead of serine when serine is deprived. The expression of IDO1, an enzyme regulates the production of a one carbon unit from tryptophan, was highly increased in pancreatic cancer cells. Interestingly this was shown to be regulated by immune cells, where the activation of IDO1 can be induced by the immune cytokine interferon γ (IFNγ) (Newman et al., 2021). Cancer cells can also adapt to extracellular serine deprivation by increasing its synthesis from glucose, as it was found that the inhibition of phosphoglycerate dehydrogenase (PHGDH), the first enzyme in the serine synthesis pathway (SSP), reduced colorectal cancer cells growth in the absence of serine and glycine. This was shown to be mediated by ATF4, as the depletion of serine activated ATF4 which increased the expression of SSP enzymes including PHGDH. Furthermore, combining both a diet lacking serine and glycine with a PHGDH inhibitor impeded tumour growth *in vivo* (Tajan et al., 2021). Hence, serine is an essential amino acid for tumour growth, but some tumours can compensate its deficiency by generating it intracellularly from glucose.

Overall, amino acids are important for cancer cell growth and metastasis. However, cancer cells might be able to adapt and reprogramme their metabolism when they face a reduction in any of the amino acids and this depends on multiple factors including the cancer type, genetic characterisation and the TME that they reside in which will be discussed in the next section.

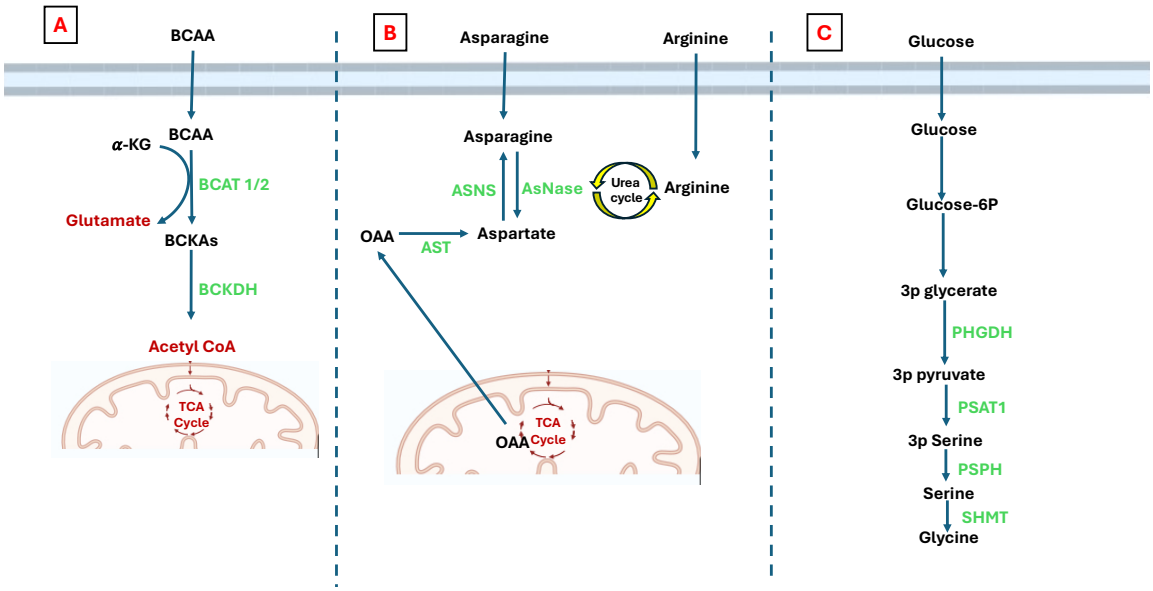

Figure 1-17 Amino acids metabolism. (A) After entering the cell, branched chain amino acids (BCAAs) are converted into α-keto acids (BCKAs) via BCAT 1/2, BCKAs are then converted into Acetyl CoA via BCKDH which then feeds into the TCA cycle. (B) Asparagine and aspartate are interconnected; aspartate to asparagine via ASNS and asparagine can be converted into aspartate via ASNase which is generated from arginine via the urea cycle. Aspartate can also be generated from oxaloacetate (OAA) via AST. (C) Serine is produced from glucose during the glycolysis process. Serine can also be converted into glycine by serine hydroxy methyltransferase (SHMT). "Created in BioRender.com".

1.8.3 The role of CAFs in cancer metabolism:

CAFs have been shown to affect the metabolism of cancer cells, as they secrete several metabolites to support tumour growth and development (Nazemi and Rainero, 2020). CAFs also undergo aerobic glycolysis, similarly to cancer cells, and secrete lactate and pyruvate which can then be used by cancer cells. This behaviour of cancer cells is called "the reversed Warburg effect" and it was shown to be induced in epithelial cancer cells (Pavlides et al., 2014). Co-culturing lymphoma cells with CAFs or growing them in CAF conditioned media supported their survival. This was found to be due to pyruvate secretion by CAFs. Pyruvate was found to be the highest metabolite in the media, its effect on cancer cells survival was due to the reduction of reactive oxygen species (ROS) and increase in energy production via the TCA cycle. The inhibition of monocarboxylate (MCT), a pyruvate transporter, reduced cell survival (Sakamoto et al., 2018). Another study showed that breast cancer cells use pyruvate in the TME to support ECM remodelling in the lung metastatic niche. Pyruvate can be converted into α-ketoglutarate, which increases the activation of prolyl-4-hydroxlase (P4HA), an enzyme involved in collagen synthesis. The activation of P4HA promotes collagen hydroxylation, leading to collagen stabilisation and increased breast cancer cell growth. The inhibition of MCT2 reduced collagen hydroxylation and deposition (Elia et al., 2019). Furthermore, the crosstalk between CAFs and

cancer cells was also observed in ovarian cancer. Curtis et al showed that co-culturing ovarian cancer cells with CAFs induced their proliferation, invasion and metastasis. CAFs, in a p38/MAPK-dependent mechanism, secrete chemokines and cytokines which in turn promote the utilisation of glycogen by cancer cells. Glycogen is fuelled into glycolysis, leading to energy production (Curtis et al., 2019). As it was mentioned earlier, the ECM is stiff in different types of cancer, including pancreatic and breast cancer. The stiffness of the ECM and its composition are regulated by CAFs. Studies showed that the stiffness of ECM can affect cancer cell metabolism. For instance, seeding highly invasive breast cancer cells on a dense collagen I matrix altered various metabolic genes, where an upregulation in the expression of the TCA cycle genes was observed. In addition, there was a reduction in using glucose as a source of nutrients while the glutamine utilisation was increased (Morris et al., 2016). Furthermore, the architecture of the ECM can also modulate cancer metabolism. Culturing breast cancer cells on 3D-collagen increased the intracellular ATP:ADP ratio, compared to culturing cells on 2D-matrices. This was identified as a result of an increase in the uptake of glucose, as for cancer cells to be able to migrate in a dense 3D matrix they need to consume more energy (Zanotelli et al., 2018). Overall, CAFs can play a pivotal role in cancer metabolism via different mechanisms including secreting metabolites which cancer cells can use, sending signals to cancer cells to modulate their metabolism or modulating ECM composition and structure which in turn can affect the metabolism of cancer cells.

1.8.4 Surviving under nutrient deprivation:

The tumour blood vessels are different from the healthy ones as they are known for being larger and abnormal due to the lack of the tight endothelial monolayer and the irregular branching. This can cause leakiness, which could lead to a lack of nutrients in the TME (Nagy et al., 2010, Baluk et al., 2005). In addition, cancer cells consume more nutrients than normal cells as a result of their high proliferation rate. This leads to a deficiency in the availability of the extracellular nutrients. In fact, the TME in PDAC was found to be hypoxic and lack glucose and amino acids, such as glutamine and serine (Kamphorst et al., 2015). In addition to the support from CAFs which was described above, cancer cells themselves can adopt different strategies to obtain nutrients, such as scavenging.

Scavenging is a process where cancer cells uptake macromolecules from the TME, degrade them into the lysosomes and use the resulting components to produce metabolites (Finicle et

al., 2018). Tumours can obtain extracellular nutrients via receptor mediated scavenging, macropinocytosis, or entosis (Finicle et al., 2018). Indeed, it was shown that mutated KRAS induced the uptake of extracellular proteins such as albumin via macropinocytosis, to be used as source of amino acids. Culturing transformed NIH3T3 $KRAS^{V12}$ cells for 24 hours in a media supplemented with 2% albumin increased the intracellular levels of both glutamate and α-ketoglutarate. Furthermore, while culturing PDAC cells in a low glutamine media reduced their proliferation, the addition of albumin significantly suppressed this effect and enhanced the growth of the cells in a macropinocytosis dependent mechanism, which was regulated by KRAS as KRAS knockdown significantly reduced the rescuing effect of albumin (Commisso et al., 2013). Similarly, Kamphorst et al showed that $KRAS^{G12D}$ pancreatic cancer cells did not survive in the absence of one of the essential amino acids leucine, lysine or phenylalanine without the addition of bovine serum albumin (BSA). The addition of 5% albumin to the media enhanced the intracellular level of essential amino acids and promoted cell growth (Kamphorst et al., 2015) **(Figure 1-18).**

Some signalling pathways have been found to be upregulated in cancer which have a pivotal role in cancer metabolism. mTOR is a fundamental regulator of cell growth, and its major role is controlling anabolic and catabolic processes. mTOR is found inside the cells in two forms; mTOR complex 1 (mTORC1) regulates cell metabolism, and its activity depends on stimulation via growth factors and the availability of the intracellular amino acids and glucose. mTOR complex 2 (mTORC2) plays a role in controlling cytoskeleton dynamics, but it has also recently been implicated in glucose metabolism, as it can phosphorylate Akt which in turn increases the expression of GLUT and the glycolytic enzyme hexokinase 2 (HEK2) (Nazemi and Rainero, 2020, Masui et al., 2014). A study by Palm et al showed that inhibiting mTORC1 in amino acids deprived conditions enhanced the endocytosis of albumin and its lysosomal degradation (Palm et al., 2015). Another study by Rainero et al showed that glucose starvation of ovarian cancer cells decreased the activity of mTORC1, which in turn promoted the tensin-dependent internalisation of fibronectin bound-α5β1 integrin (Rainero et al., 2015) **(Figure 1-18)**. This study suggests that ECM components and their internalisation under nutrient starvation conditions could be used as source of nutrients. Indeed, PDAC cells have been shown to internalise collagen I and collagen IV under glucose or glutamine starvation conditions via macropinocytosis dependent and independent pathways, respectively, and use collagen derived proline as source of nutrients to survive (Olivares et al., 2017). In addition, the

expression of β4 integrin and its internalisation with its ligand laminin have been found to be induced in mammary epithelial cells *in vitro* under nutrient depleted conditions and *in vivo* in dietary restricted mice. Also in this context, mTORC1 was activated as a result of increased intracellular amino acids which were released from the lysosomal digestion of laminin (Muranen et al., 2017).

AMP-activated protein kinase (AMPK) is another metabolic sensor in the cells, activated in response to energy stress and promoting catabolism. It has been observed that the activation of AMPK in fibroblasts decreased the expression of the adhesion protein tensin 1 and 3, which in turn reduced the activity of α5β1 integrin (Georgiadou et al., 2017). However, more studies are needed to identify the role of AMPK in cancer cell metabolism in terms of integrins activity and their trafficking.

All together, these findings elucidate the role of the extracellular macromolecules, including ECM proteins, in cancer cell metabolism. However, more studies are needed to understand how the nutrient depleted microenvironment triggers receptor-mediated ECM uptake in 3D microenvironment and what is the role of the ECM receptors in this process.

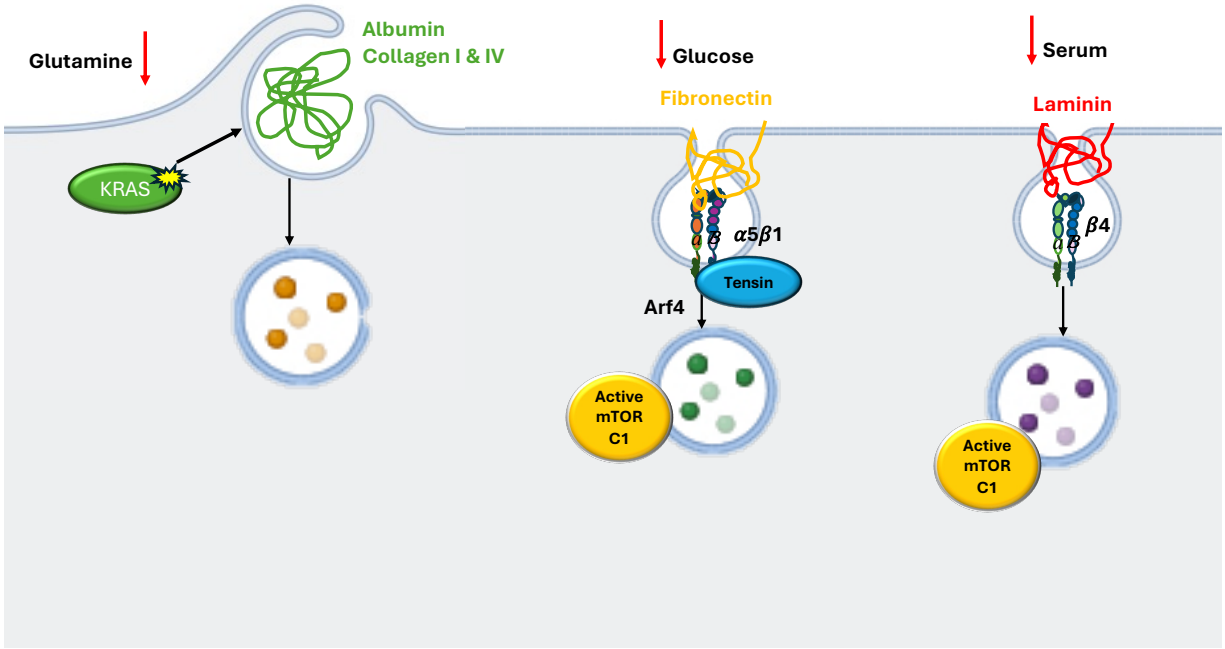

Figure 1-18 Macromolecules scavenging in cancer under nutrient deprivation. Under glutamine starvation, oncogenic KRAS triggers the uptake of albumin and collagen I & IV via macropinocytosis. Under glucose starvation, fibronectin is internalised with its receptor α5β1 integrin in a tensin and Arf4 dependent mechanism which reactivate mTORC1. Under serum starvation, laminin and its receptor β4 get internalised which was shown to reactivate mTORC1 "Created in BioRender.com".

1.9 Aim of the project:

Some types of cancer are surrounded by dense ECM, and the interaction with ECM proteins via integrin receptors can support cancer cells proliferation. We hypothesise that cancer cells use ECM proteins in an environment deprived of nutrients as an energy source and that this process is regulated by integrins. We also hypothesise that nutrient limitation stimulates ECM uptake by controlling ECM-receptor expression.

To test these hypotheses, the role of different types of ECM on the growth of highly invasive breast cancer cells under amino acids, glucose, and glutamine starvation was examined. in addition, I tested the impact of nutrient starvation in controlling ECM uptake and integrin expression.

The aims of the project were:

- Comparing the effect of different types of ECM on breast cancer cell growth under starvation.

- Identifying the requirement for ECM internalisation in ECM-dependent cell growth.

- Determining the changes in the intracellular metabolites in the presence or absence of ECM under starvation.

- Assessing the role of integrins in ECM-dependent cell growth.

- Characterising integrin expression under starvation in cancer.

2 Materials and Methods:

2.1 Materials:

2.1.1 Cell culture media

Table 2-1 Cell culture media, supplier and Catalogue number

Media	Supplier	Catalogue number
DMEM, high glucose, pyruvate	Gibco	41966-029
DMEM/F-12, glutamax	Gibco	31331-093
DMEM/F-12, no glutamine	Gibco	21331-020
SILAC advanced DMEDM/F-12 Flex	Gibco	A24943-01
DMEM,no amino acids	US Biological life science	D9800-13-USB-10L

2.1.2 Reagents

Table 2-2 List of reagents and suppliers

Reagent	Supplier
10cm petri dishes	Greiner bio-one
6-well tissue culture plates	Greiner bio-one
96-well glass bottom plates	Greiner bio-one
96-well plastic bottom plates	FALCON
3.5cm2 glass-bottom dishes	SPL Life Science
0.45µm filter	Gilson
Ambion ™ Nuclease-Free water	Invitrogen
Ammonium hydroxide (NH4OH)	Sigma
Bovine Serum albumin	Sigma-Aldrich
CellEvent™ Caspase-3/7 Green Detection	Invitrogen
Collagen type I (Rat tail high concentration)	Corning
Click-iT™ EdU Alexa FlourTM 555 Imaging Kit	Invitrogen
D-glucose anhydrase	Fisher chemical
DharmaFect 1 (DF1) Reagent	Dharmacone
Dialyzed FBS	Gibco
Dimethyl sulfoxide (DMSO)	Fisher Scientific
Deoxyribonuclease I/DN25 (DNase I)	Sigma
DRAQ5™	ThermoFisher
Epidermal growth factor (EGF)	Sigma
Fatal bovine serum (FBS)	Gibco
Gelatin	Sigma
Glutaraldehyde solution	Sigma Aldrich
Glutamine stable 100x	biowest
Glycine	Sigma
High-Capacity cDNA Reverse Transcription kit	Applied biosystems
Horse serum (HS)	Gibco
Hoechst 33342	Invitrogen
Hydrocortisone	Sigma
Insulin solution human	Sigma
L-Ascorbic acid	Sigma
Matrigel	Corning
Microplate PCR 384 well	Alpha laboratories

4-15% Mini Protean TGX stain Free Protein gels	BioRad Laboratories
NHS-Fluorescein	Thermo Scientific
PVDF membrane	IMMOBILON-FL
Propidium Iodide (PI)	ThermoFisher
Penicillin/ Streptomycin (Pen/strep)	Life Technologies
PBS containing calcium and magnesium	Sigma
Phalloidin Alexa Fluor 555	ThermoFisher
Paraformaldehyde	Thermo scientific
Protein ladder "Color Prestained Protein Standard"	New England Biolabs
pHrodo™ iFL Red STP ester	ThermoFisher
QiaShredder columns	QIAGEN
qPCRBIO SyGreen Blue Mix Lo-ROX	PCR BIOSYSTEMS
RNase free water	Cleaver scientific
RNAse mini-Kit (50)	QIAGEN
Sodium chloride	Sigma-Aldrich
Tris(hydroxymethyl)aminomethane (Tris)	Sigma-Aldrich
Triton-X100	Sigma
Trypan blue stain 0.4%	Gibco by life technologies
Trypsin EDTA solution 1x	Sigma
Tween-20	Sigma
Vectashield mounting reagent with DAPI	VECTOR laboratories

2.1.3 Solutions

Table 2-3 List of solutions and their recipes

Solution	Recipe
Running buffer	25mM Tris, 192mM Glycine and 1% SDS in dH2O
Towbin buffer 10x	1.92M Glycine, 0.25M Tris
Transfer buffer	10% 10X Towbin buffer, 20% methanol
TBS	10mM Tris-HCl PH7.4, 150mM NaCl
TBS-T	TBS,0.1% Tween-20 (v/v)
1% SDS lysis buffer	1% SDS (v/v), 50mM Tris-HCl PH7.0
Loading buffer	1mM DTT, 1x NuPAGE
Metabolite extraction buffer	5 MeOH: 3 ACN: 2 H_2O
Cell extraction buffer	20mM NH_4OH,0.5% Triton X-100 (v/v) in PBS containing calcium (Ca^{2+}) and magnesium (Mg^{2+})
EdU staining	1x Click-iT, 4mM CuSO4, 0.25% (v/v) Alexa Flour azide and 1x Reaction buffer additive in dH2O

2.2 Methods:

2.2.1 Cell culture

MCF10A and MCF10-CA1 cells were cultured in high glucose Dulbecco's Modified Eagle's Medium (DMEM) /F12 medium supplemented with 2.5% or 5% horse serum, 1% penicillin and streptomycin (Pen/strep), 0.2μg/ml Hydrocortisone, 20 ng/ml EGF and 10 μg/ml Insulin. MDA-MB-231, CAFs, MCF7, Panc1 and SW1990 cells were cultured in high glucose DMEM supplemented with 10% Fatal bovine serum (FBS) and 1%(pen/strep). All cells were kept at 37°C and 5% CO_2 incubator at all times and passaged twice a week. MCF10A and MCF10CA1

cells were kindly provided by Prof Giorgio Scita, IFOM, Milan (Italy), Panc1 and SW1990 cells were kindly provided by Dr Helen Matthews (The University of Sheffield). MCF7 cells were kindly provided by Professor Penelope Ottewell (The University of Sheffield). CAFs were extracted from breast tumour and generated in Professor Akira Orimo's lab, Paterson Institute, Manchester. To starve the cells, starvation media listed in table (Table 2-4) were used. In all conditions where FBS was used, FBS was replaced with dialysed FBS (DFBS). To passage the cells, the medium was removed, cells were washed twice with PBS, and 500 µl/ 10cm dish of 0.25% trypsin was added. Cells were incubated at 5% CO_2, 37°C for 5-7 minutes until detached then they were resuspended in growth media and replated in 10 cm tissue culture dishes at the desired density.

For long time storing, cryofreezing of the cells was used. Cells were washed with PBS and trypsinised as mentioned above. Cells were resuspended in complete medium and centrifuged at 1000rpm for 3 minutes at room temperature. The cell pellet was resuspended in a freezing solution of 50% medium and 50% serum (500µl) then pipetted in a cryo-vial. A solution of 80% serum+ 20% DMSO (500µl) was pipetted gently on top, and the vial was inverted to mix. The cells were kept at-80C° for a couple of days before storing in liquid nitrogen.

2.2.1.1 Starvation media composition

Table 2-4 Composition of starvation media used for each cell line

Cell line	Starvation condition	Media composition
1. MCF10CA1 2. MCF10A 3. MDA-MB-231 4. MCF7 5. SW1990 6. Panc1	Amino acid starvation	1.2 (+) DMEM, (+) 4.5 g/L D-glucose, (+) 2.5% or 5% HS, (+) 1% Pen/Strep, (+) 20 ng/ml EGF, (+) 10 ug/ml insulin, (+) 0.2 ug/ml hydrocortisone 3.4.5.6 (+) DMEM, (+) 4.5 g/L D-glucose, (+) 10% DFBS, (+) 1% pen/strep
MCF10CA1	Glucose starvation	(+) DMEM/F12, (+) L-glutamine, (+) 2.5% HS, (+) 1% Pen/Strep, (+) 20 ng/ml EGF, (+) 10 ug/ml insulin, (+) 0.2 ug/ml hydrocortisone
MCF10CA1	Glutamine starvation	(+) DMEM/F12, (+) 2.5% HS, (+) 1% Pen/Strep, (+) 20 ng/ml EGF, (+) 10 ug/ml insulin, (+) 0.2 ug/ml hydrocortisone
SW1990	Tumour Interstitial Fluid Medium (TIFM)	TIFM kindly provided by Muir lab and it was developed as in (Saab et al., 2023) + 10% DFBS, (+) 1% pen/strep

Table 2-5 DMEM media formulation

	DMEM, high glucose, pyruvate	DMEM, low glucose, (W/O) amino acid, Pyruvic acid
Amino Acids		
Glycine	30	Absent
L-Arginine hydrochloride	84	Absent
L-Cystine 2HCl	63	Absent
L-Glutamine	580	Absent
L-Histidine hydrochloride-H2O	42	Absent
L-Isoleucine	105	Absent
L-Leucine	105	Absent
L-Lysine hydrochloride	146	Absent
L-Methionine	30	Absent
L-Phenylalanine	66	Absent
L-Serine	42	Absent
L-Threonine	95	Absent
L-Tryptophan	16	Absent
L-Tyrosine disodium salt dihydrate	72	Absent
L-Valine	94	Absent
Vitamins		
Choline chloride	4	4
D-Calcium pantothenate	4	4
Folic Acid	4	4
Niacinamide	4	4
Pyridoxine hydrochloride	4	4
Riboflavin	0.4	0.4
Thiamine hydrochloride	4	4
i-Inositol	7.2	7.2
Inorganic Salts		
Calcium Chloride (CaCl2-2H2O)	264	265
Ferric Nitrate (Fe(NO3)3"9H2O)	0.1	0.1
Magnesium Sulfate (MgSO4-7H2O)	200	97.67
Potassium Chloride (KCl)	400	400
Sodium Bicarbonate (NaHCO3)	3700	Absent
Sodium Chloride (NaCl)	6400	6400
Sodium Phosphate monobasic (NaH2PO4-2H2O)	141	109

Other Components		
D-Glucose (Dextrose)	4500	1000
Phenol Red	15	15.9
Sodium Pyruvate	110	Absent

Table 2-6 DMEM/F-12 media formulation

	DMEM/F-12 Glutamax (mg/L)	DMEM/F-12 no glutamine (mg/L)	SILAC Advanced DMEM/F12 Flex Media, no glucose (mg/L|)
Amino Acids			
Glycine	18.75	18.75	18.75
L-Alanine	4.45	4.45	4.45
L-Alanyl-L-Glutamine	542	Absent	Absent
L-Arginine hydrochloride	147.5	147.5	7.5
L-Asparagine-H2O	7.5	7.5	6.65
L-Aspartic acid	6.65	6.65	17.56
L-Cysteine hydrochloride-H2O	17.56	17.56	31.29
L-Cystine 2HCl	31.29	31.29	7.35
L-Glutamic Acid	7.35	7.35	Absent
L-Histidine hydrochloride-H2O	31.48	31.48	31.48
L-Isoleucine	54.47	54.47	54.47
L-Leucine	59.05	59.05	59.05
L-Lysine hydrochloride	91.25	91.25	Absent
L-Methionine	17.24	17.24	17.24
L-Phenylalanine	35.48	35.48	35.48
L-Proline	17.25	17.25	17.25
L-Serine	26.25	26.25	26.25
L-Threonine	53.45	53.45	53.45
L-Tryptophan	9.02	9.02	9.02
L-Tyrosine disodium salt dihydrate	55.79	55.79	55.79
L-Valine	52.85	25.85	25.85
Vitamins			
Biotin	0.0035	0.0035	0.0035
Choline chloride	8.98	8.98	8.98
D-Calcium pantothenate	2.24	2.24	2.24
Folic Acid	2.65	2.65	2.65
Niacinamide	2.02	2.02	2.02
Pyridoxine hydrochloride	2.031	2	2

Riboflavin	0.219	0.219	0.219
Thiamine hydrochloride	2.17	2.17	2.17
Vitamin B12	0.68	0.68	0.68
i-Inositol	12.6	12.6	12.6
Inorganic Salts			
Calcium Chloride (CaCl2) (anhyd.)	116.6	116.6	116.6
Cupric sulfate (CuSO4-5H2O)	0.0013	0.0013	0.0013
Ferric Nitrate (Fe(NO3)3"9H2O)	0.05	0.05	0.05
Ferric sulfate (FeSO4-7H2O)	0.417	0.417	0.417
Magnesium Chloride (anhydrous)	28.64	28.64	28.64
Magnesium Sulfate (MgSO4) (anhyd.)	48.84	48.84	48.84
Potassium Chloride (KCl)	311.8	311.8	311.8
Sodium Bicarbonate (NaHCO3)	2438	2438	2438
Sodium Chloride (NaCl)	6999.5	6995.5	6995.5
Sodium Phosphate dibasic (Na2HPO4) anhydrous	71.02	71.02	71
Sodium Phosphate monobasic (NaH2PO4-H2O)	62.5	62.5	62.5
Zinc sulfate (ZnSO4-7H2O)	0.432	0.432	0.432
Other Components			
D-Glucose (Dextrose)	3151	3151	Absent
Hypoxanthine Na	2.39	2.39	2.39
Linoleic Acid	0.042	0.042	0.042
Lipoic Acid	0.105	0.105	0.105
Phenol Red	8.1	8.1	Absent
Putrescine 2HCl	0.081	0.081	0.081
Sodium Pyruvate	55	55	55
Thymidine	0.365	0.365	0.365

2.2.2 ECM production

2.2.2.1 Collagen I and Matrigel preparation:

A solution of 2 mg/ml collagen I or 3 mg/ml Matrigel in PBS were prepared, 15 µl/ well were added to a 96 well plate and left to polymerise at 5% CO_2, 37°C. PBS was added after 4 hrs, and plates were kept in the incubator overnight. For 35mm glass-bottom dishes, a solution of 0.5-1 mg/ml collagen I in PBS was prepared, the dishes were coated with 100 µl/dish and kept at 37°C to polymerise. PBS was added after 1hr, and dishes were kept in the incubator overnight.

2.2.2.2 Cell derived matrices (CDM):

CDMs were generated in 96 well plates or 35mm glass-bottom dishes. Plates/dishes were coated with 0.2% gelatine and incubated at 5% CO_2, 37°C for 1 hour. Gelatine was washed twice with PBS and crosslinked with 1% sterile glutaraldehyde in PBS for 30 minutes at room temperature (RT). Plates/dishes were washed twice with PBS, quenched with 1 M sterile glycine in water for 20 minutes at RT, washed twice with PBS and incubated with complete media for 30 minutes at 5% CO_2, 37°C. The media was removed and 6 x 10^3 or 2x10^5 CAF cells /dish were seeded, and plates were incubated at 5% CO_2, 37°C until confluent. Media was changed every other day for 7 days with complete media containing 50μg/ml ascorbic acid. After 7 days, media was removed and CDM was washed twice with PBS containing calcium (Ca^{2+}) and magnesium (Mg^{2+}).

To extract the CDM, an extraction buffer containing 20mM NH_4OH and 0.5% Triton X-100 in PBS Ca^{2+} and Mg^{2+} was gently added to the wells for ~2 minutes at RT. After CDM extraction, CDM was washed twice with PBS Ca^{2+} and Mg^{2+} and the DNA residues were digested with 15μg/ml DNase I in PBS Ca^{2+} and Mg^{2+} for 1 hour at 5% CO_2, 37°C. CDM was washed twice with PBS Ca^{2+} and Mg^{2+} and stored at 4°C in PBS Ca^{2+} and Mg^{2+} with Pen/strep for up to 1 month.

2.2.3 ECM uptake:

35mm glass-bottom dishes were coated with collagen I and polymerised as in **Section 2.2.2.** Collagen I was labelled with 10 μg/ ml NHS fluorescein in PBS and incubated for 1 hour at RT. Alternatively, collagen I was labelled with 20μg/ml pHRodo iFL red in PBS containing 0.1 M $NaHCO_3$ and incubated for 1 hour at RT. Then, collagen I was washed twice with PBS. PBS was added and the dishes were left at 5% CO_2, 37°C overnight. Where indicated, cells were incubated in starvation media **(Table 2-4)** overnight. The day after 2x 10^5 cells were seeded in the presence of DMSO or 20 μM E64d **(Table 2-7)** and incubated at 5% CO_2, 37°C for 6 hours. Where indicated, cells were incubated for 2 hours then 15μM BTT-3033 **(Table 2-7)** was added to the cells for 4 hours. Cells were fixed with 4% paraformaldehyde (PFA) in PBS for 15 minutes at RT. After fixing, cells were permeabilised with 0.25% Triton X-100 for 5 minutes, washed twice with PBS, and actin was stained with 1:400 phalloidin Alexa fluor 555 in PBS for 10 minutes. Samples were washed twice with PBS and once with distilled water. To finish, 2 drops of Vectashield containing DAPI were added. Dishes were sealed and left at 4°C until imaging. Cells

were imaged with a Nikon A1 confocal microscope using 40x oil objective. Z stacks were taken to cover the cells from bottom to top with 1 μm interval. In case of pHRodo labelling, 1:1000 Hoechst 33342 was spiked into the media and incubated for 15 minutes. Media was changed with fresh media, and cells were imaged live with a Nikon A1 confocal microscope, 60x oil objective. Image J software (https://imagej.net/ij/) was used to quantify ECM uptake as in (Commisso et al., 2014). Briefly, the cell area was measured by drawing around the cells using the phalloidin staining as a reference and saved in the region of interest (ROI). The cell area was measured **(Figure 2-1,A)**. The image relative to the ECM staining then was thresholded to remove the background signal, and the total area of the internalised ECM was measured **(Figure 2-1, B)**.

ECM uptake index = Total area of the internalised ECM/ cell area X 100

For CDM labelling, CDMs were generated as in **Section 2.2.2**, labelled with 20μg/ml pHRodo iFL red in PBS containing 0.1 M $NaHCO_3$ and incubated for 1 hour at RT. CDMs were washed 3 times with PBS and $2x10^5$ cells were seeded and incubated for 5 hours at 5% CO_2, 37°C. 1:1000 SPY620 actin probe was spiked into the media and the dishes were incubated for 1 hour at 5% CO_2, 37°C. To finish, 1:1000 Hoechst 33342 was spiked into the media and incubated for 15 minutes. Media was changed with fresh media, and cells were imaged live with a Nikon A1 confocal microscope, 40x oil objective. CDM uptake index was quantified with image J as above. Where indicated, cells were seeded on CDM for two hours then 1 μM FRAX597 or DMSO were added. Cells were stained as above and imaged live after a 3-hour incubation.

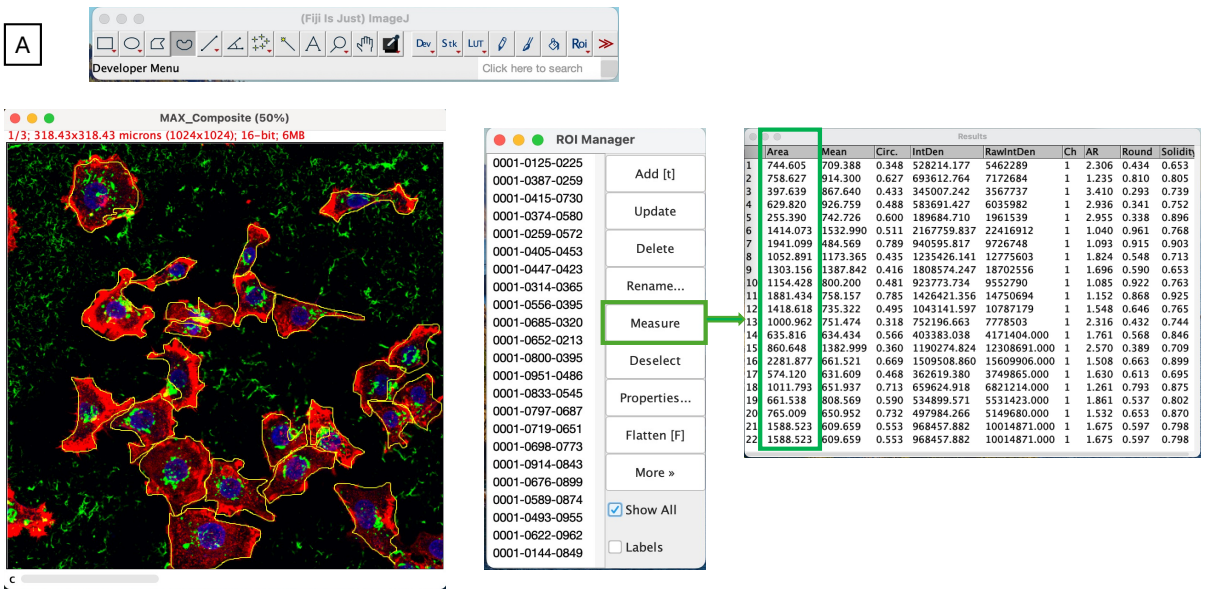

B

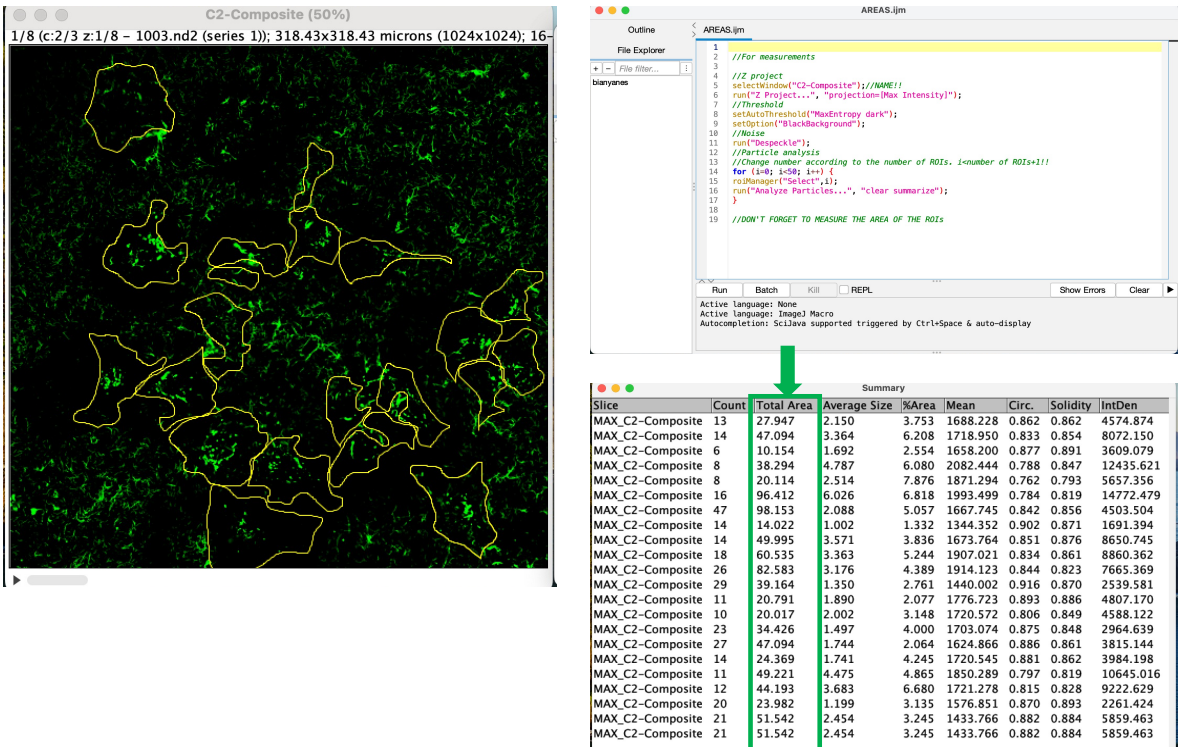

Slice	Count	Total Area	Average Size	%Area	Mean	Circ.	Solidity	IntDen
MAX_C2-Composite	13	27.947	2.150	3.753	1688.228	0.862	0.862	4574.874
MAX_C2-Composite	14	47.094	3.364	6.208	1718.950	0.833	0.854	8072.150
MAX_C2-Composite	6	10.154	1.692	2.554	1658.200	0.877	0.891	3609.079
MAX_C2-Composite	8	38.294	4.787	6.080	2082.444	0.788	0.847	12435.621
MAX_C2-Composite	8	20.114	2.514	7.876	1871.294	0.762	0.793	5657.356
MAX_C2-Composite	16	96.412	6.026	6.818	1993.499	0.784	0.819	14772.479
MAX_C2-Composite	47	98.153	2.088	5.057	1667.745	0.842	0.856	4503.504
MAX_C2-Composite	14	14.022	1.002	1.332	1344.352	0.902	0.871	1691.394
MAX_C2-Composite	14	49.995	3.571	3.836	1673.764	0.851	0.876	8650.745
MAX_C2-Composite	18	60.535	3.363	5.244	1907.021	0.834	0.861	8860.362
MAX_C2-Composite	26	82.583	3.176	4.389	1914.123	0.844	0.823	7665.369
MAX_C2-Composite	29	39.164	1.350	2.761	1440.002	0.916	0.870	2539.581
MAX_C2-Composite	11	20.791	1.890	2.077	1776.723	0.893	0.886	4807.170
MAX_C2-Composite	10	20.017	2.002	3.148	1720.572	0.806	0.849	4588.122
MAX_C2-Composite	23	34.426	1.497	4.000	1703.074	0.875	0.848	2964.639
MAX_C2-Composite	27	47.094	1.744	2.064	1624.866	0.886	0.861	3815.144
MAX_C2-Composite	14	24.369	1.741	4.245	1720.545	0.881	0.862	3984.198
MAX_C2-Composite	11	49.221	4.475	4.865	1850.289	0.797	0.819	10645.016
MAX_C2-Composite	12	44.193	3.683	6.680	1721.278	0.815	0.828	9222.629
MAX_C2-Composite	20	23.982	1.199	3.135	1576.851	0.870	0.893	2261.424
MAX_C2-Composite	21	51.542	2.454	3.245	1433.766	0.882	0.884	5859.463
MAX_C2-Composite	21	51.542	2.454	3.245	1433.766	0.882	0.884	5859.463

Figure 2-1 ECM uptake analysis using Image J software. The cell area was identified by drawing around each cell using the phalloidin staining as a reference and recording the area in ROI manager. Then the cell area was measured (A). The image corresponding to the ECM channel then was thresholded, and the total area of the internalised ECM was measured (B).

Table 2-7 List of inhibitors, the concentration used and the supplier

Inhibitors	Concentration	Catalogue number	Supplier
E64d (Aloxistatin)	20uM	A13259	AdooQ Bioscience
BTT3033	15uM	4724	Tocris
FRAX597	1uM	6029	Tocris

2.2.4 Cell proliferation assays:

96 well plates were coated with ECM as described in **Section 2.2.2**. 400 cells/ well were seeded in complete media and plates were incubated for 4 hours at 5% CO_2, 37°C. Media was removed, cells were washed twice with PBS and media was changed to the complete or starvation media. Plates were incubated at 5% CO_2, 37°C and fixed after 2, 4, or 6 days with 4% PFA, washed twice with PBS, and stained with 5mM DRAQ5 in PBS (40µl/well) for 1 hour at RT. Cells were washed twice with PBS, cells were incubated in the second wash for 30 minutes at RT to remove background. Cells were imaged with a Licor Odyssey Sa imager (700 nm for DRAQ5, offset 3mm,

intensity 5, 169µm resolution) and the signal intensity (the total intensity minus the total background) was measured using Image Studio Lite software. Alternatively, 800 cells/well were seeded on ECM in complete media, after 4 hours the media was changed to complete or starvation media containing DMSO, 15 µM BTT-3033, or 1 µM FRAX597 **(Table 2-7)**. Inhibitors were added every other day for 4 days. Cells were fixed with 4 % PFA for 15 minutes at RT, stained with 1:1000 Hoechst 33342 for 15 minutes and imaged with an ImagesXpress micro, 2x objective and DAPI filter in the Sheffield RNAi Screening Facility (SRSF). The images were obtained by acquiring multiple sites to cover the entire wells (4 sites/well for the 2x objective). The cell number was measured using MetaXpress and Costume Module Editor software (CME) by designing an algorithm that could detect the nuclei by covering the range of nuclei size and intensity **(Figure 2-2)**.

For cells proliferation on CDM, cells were fixed with 4% PFA and stained with 1:1000 Hoechst 33342 in PBS for 15 minutes at RT, washed twice with PBS and imaged with ImageXpress micro 2X objective. Cell number was measured using MetaXpress and CME software as above.

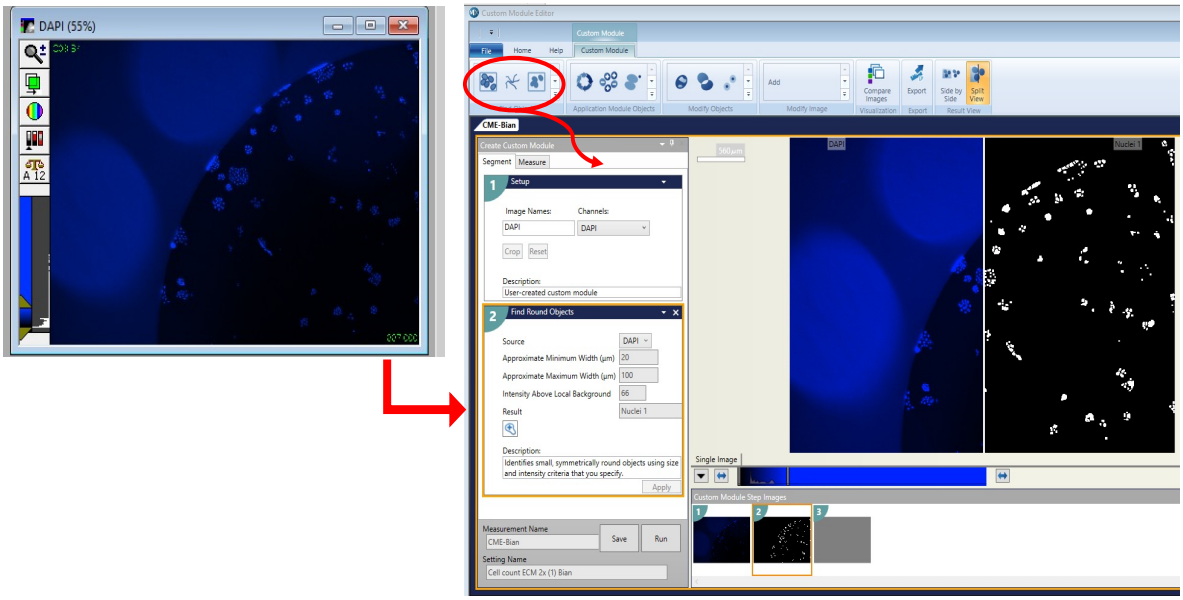

Figure 2-2 Cell number analysis using CME software. The algorithm is based on identifying the round objective in a range of small and large nuclei using the DAPI staining. After finding the best settings that could cover the whole area, the same algorithm was tested on other images to check if it was suitable for all conditions. The algorithm then was run on all the wells to get the total cell number. This analysis was done for every experiment.

2.2.5 ECM cross-linking:

35mm glass-bottom dishes were coated with 1mg/ml collagen I and polymerised for 1 hour at 5% CO_2, 37°C. Collagen I was labelled with 10 μg/ ml NHS fluorescein and incubated for 1 hour at RT. Collagen I was washed twice with PBS and crosslinked with 10% sterile glutaraldehyde in PBS for 30 minutes at RT, washed twice with PBS and quenched with 1M sterile glycine in water for 20 minutes at RT. Collagen I was washed twice with PBS then covered with PBS and left at 5% CO_2, 37°C overnight. The day after, $2x10^5$ cells were seeded in complete media or starvation media containing 20μM E64d and cells were incubated at 5% CO_2, 37°C. 20μM E64d was added every other day and cells were fixed at day 3 with 4% PFA for 15 minutes at RT, permeabilised with 0.25% Triton X-100 for 5 minutes at RT, washed twice with PBS and actin was stained with 1:400 phalloidin Alexa fluor 555 in PBS for 10 minutes at RT. To finish, two drops of Vectashield containing DAPI were added. Dishes were sealed and images with a Nikon A1 confocal microscope, 40x oil objective. Z stacks were taken to cover the cell from bottom to top with 1μm interval. Collagen I uptake was measured as described in **Section 2.2.3.**

For the cell proliferation assays, 96 well plates were coated with 2 mg/ml collagen I and collagen I was polymerised at 5% CO_2, 37°C overnight. Collagen I was crosslinked with 10% sterile glutaraldehyde for 30 minutes at RT, washed twice with PBS, quenched with 1M sterile glycine for 20 minutes at RT, washed twice with PBS. 800 cells/well were seeded and plates were incubated at 5% CO_2, 37°C for 4 hrs. Media was removed, cells were washed twice with PBS, media was changed to complete or starvation media and cells were incubated at 5% CO_2, 37°C. Cells were fixed with 4% PFA for 15 minutes at RT after 2 or 6 days and stained with 1:1000 Hoechst 33342 for 15 minutes at RT. PBS was added, cells were imaged with an ImageXpress micro, 2x objective and the cell number was quantified as described in **Section 2.2.4**.

2.2.6 Immunofluorescence:

2.2.6.1 2D culture:

35 mm glass-bottomed dishes were coated with collagen I as in **Section 2.2.1** and $2x10^5$ cells were seeded. Dishes were incubated for 1 hour at 5% CO_2, 37°C. Cells were fixed with 4% PFA, permeabilised with 0.25% Triton X-100, washed twice with PBS then blocked with 1% Bovine Saline Albumin (BSA) for 1 hour at RT. Cells were washed twice with PBS and incubated for 1 hour at RT with 1:200 of anti-human FITC-conjugated α2 integrin antibody or anti-human Alexa

647-conjugated β1 integrin antibody **(Table 2-8)** in PBS. Cells were washed twice with PBS and two drops of Vectasheild containing DAPI were added. Dishes were sealed and imaged with a Nikon A1 confocal microscope, 40x oil objective. The fluorescent intensity was measured using Image J software. The cell area was identified by drawing around the cell and saving the selection in the region of interest ROI manager. Then the mean intensity in each cell was measured as in **(Figure 2-3)**.

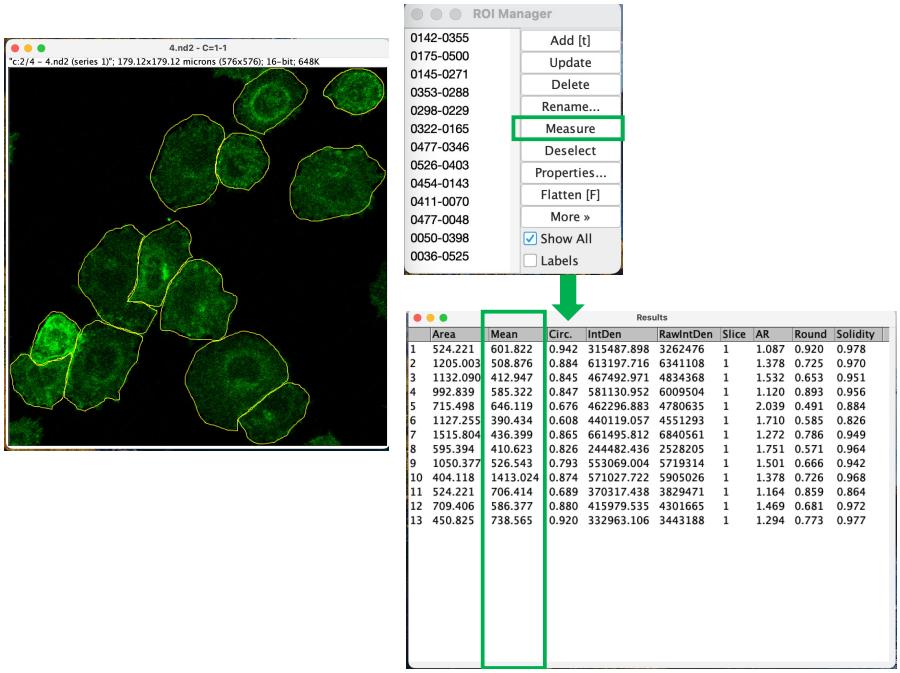

Figure 2-3 Integrin intensity analysis method using Image J software. The cell area was identified by drawing around each cell and recorded in ROI. Then the mean intensity was measured.

2.2.6.2 3D culture

5μl of growth factor reduced Matrigel was added to each well of an 8 well glass-bottom chamber slide. The Matrigel was spread evenly, and the chamber was incubated at 5% CO_2, 37°C for 15-30min. Cells were trypsinised, counted and diluted in a solution of media containing 2% Matrigel. 400 μl of cells per well were seeded on the Matrigel coated wells to a final concentration of 1.25 x 10^4 cells/ml. The day after, media was changed to complete media or starvation media in the presence or absence of the indicated inhibitors and cells were incubated at 5% CO_2, 37°C for 2 days. Cells were fixed with 4% PFA, permeabilised with 0.25% Triton X-100, washed twice with PBS then blocked with 1% Bovine Saline Albumin (BSA) for 1 hour at RT. Cells were washed twice with PBS and incubated for 1 hour at RT with 1:200 of anti-human FITC-conjugated α2 integrin antibody in PBS. Cells were washed twice with PBS and two drops of Vectasheild containing DAPI were added. Chambers were sealed and imaged with a Nikon A1 confocal microscope, 60x oil objective. The fluorescence intensity was measured using Image J software as in Section 2.2.6.1.

Table 2-8 List of antibodies, the dilution used and the supplier

Antibody	Dilution ratio	Catalogue number	Supplier
FITC-Anti Human CD49b Antibody (α2)	1:200	359306	Biolegend
Alexa Fluor 647 anti-human CD29 Antibody (β1)	1:200	303017	Biolegend

2.2.7 Western blotting (WB)

10^6 cells/well were seeded in 6 well plates. After a 4-hour incubation at 5% CO_2, 37°C, cells were washed twice with PBS, media was changed to complete or starvation media and cells were incubated at 5% CO_2, 37°C overnight. The day after, media was removed, cells were washed twice with ice cold PBS and 100 μl/ well ice cold lysis buffer (50mM Tris and 1% SDS in water) was added. Cells were scraped; the lysate was transferred to a QiaShredder column and spun at full speed for 5 minutes at RT. The flowthrough was transferred to a clean Eppendorf tube. Loading buffer (1mM DTT in 1x NuPage) was added to the samples and it was heated at ~70°C for 5 minutes. The samples were loaded in a gradient gel and the gel was run at 100V for 1 hour 15 minutes. The gel was transferred to an IMMOBILON-FL-PVDF membrane. The membrane was blocked for 1 hour with 5% BSA in TBS-T at RT then blocked with primary

antibodies (Table 2-9) with GAPDH in 5% BSA in TBS-T overnight in a cold room. The day after, the membrane was washed 3 times with TBS-T, 10 minutes each, and incubated with Licor secondary antibodies (Table 2-9) in TBS-T+ 0.01% SDS for 1 hour at RT on a rocker. Membrane was washed 3 times with TBS-T, 10 minutes each, rinsed with water a couple of times and imaged with Licor Odyssey Sa imager. The signal intensity was measured using Image Studio Lite software.

To measure ERK phosphorylation, 10^6 cells/well were seeded in 6 well plates. After a 4-hour incubation at 5% CO_2, 37°C, cells were washed twice with PBS, media was changed with media without serum and growth factors and cells were incubated at 5% CO_2, 37°C overnight. The day after, media was removed, cells were washed with PBS and media was changed to complete or starvation media, without serum and growth factors. The cells were lysed after 5, 10, or 15 minutes and samples were analysed as described above.

Table 2-9 List of antibodies used in (WB)

Primary antibodies	Supplier	Dilution
Mouse anti-human CD49b (ITGA2) antibody	BD biosciences 611017	1:1000
Rabbit polyclonal CD49e (ITGA5) antibody	Proteintech 10569-1-AP	1:1000
P44/42 MAPK (ERK1/2) antibody	Cell signalling (#9102)	1:1000
Phosphor-p44/42 MAPK (ERK1/2) antibody	Cell signalling (#9101)	1:1000
Rabbit PAK1 polyclonal antibody	Proteintech (21401-1-AP)	1:1000
GAPDH	Santa Cruz Biotechnology (SC-47724)	1:1000

Secondary antibodies	Supplier	Dilution
IR Dye 680LT anti-Rabbit antibody	LICOR Biosciences	1:20000
IR Dye 800LT anti-Mouse antibody	LICOR Biosciences	1:30000

2.2.8 EdU incorporation assays

96 well plates were coated with ECM as described in Section 2.2.2. 400 MCF10CA1 cells/well were seeded and plates were incubated for 4 hours at 5% CO_2, 37°C. Media was removed, cells were washed twice with PBS and media was changed to complete or starvation media. Plates were kept at 5% CO_2, 37°C for 4 days, cells were then incubated with 5μM Edu for 2 days. At day 6 post-starvation, cells were fixed with 4% PFA for 15 minutes, washed twice with PBS, permeabilised with 0.25% Triton-X 100 for 5 minutes and stained with 1:1000 Hoechst 33342

for 15 minutes at RT. Cells were washed twice with PBS and twice with 3% BSA in PBS then incubated with Invitrogen Click-iT reaction cocktail (1x Click-it reaction buffer, $CuSO_4$, Alexa Fluor 555 azide, reaction buffer additive) for 30 minutes at RT with gentle rocking. Cells were washed twice with PBS and imaged with an ImageXpress micro, 10x objective detecting DAPI and Cy3 wavelength and the nuclei number was measured as described in **Section2.2.4**. An algorithm was designed to detect the total nuclei number and the nuclei that were Edu positive.

2.2.9 Cell apoptosis assays

2.2.9.1 Caspase 3/7 assays:

96 well plates were coated with ECM as described in **Section 2.2.2**. 400 MCF10CA1 cells/well were seeded and plates were incubated for 4 hours at 5% CO_2, 37°C. Media was removed, cells were washed twice with PBS and media was changed to complete or starvation media. Plates were incubated at 5% CO_2, 37°C for 3 or 6 days then media was removed, and cells were incubated in PBS Ca^{2+} and Mg^{2+} containing 5% horse serum and 5μM Cell Event Caspase-3/7 Green Detection Reagent for 1 hour 30 minutes at 5% CO_2, 37°C. Cells then were fixed with 4% PFA and stained with 1:1000 Hoechst 33342 for 15 minutes at RT. Images were obtained with an ImageXpress micro, 10x objective and the cells positive for Caspase 3/7 were measured by designing an algorithm to detect the nuclei (DAPI wavelength) to measure the total cell number and, as Caspase 3/7 is a cytoplasmic protein, the cytoplasm was covered to measure the cells positive for Caspase 3/7 (GFP wavelength).

2.2.9.2 Propidium iodide (PI) assays:

96 well plates were coated with ECM as described in **Section 2.2.2**. $1x10^3$ MCF10CA1 cells/well were seeded and plates were incubated at 5% CO_2, 37°C. The day after, media was removed, cells were washed twice with PBS and media was changed to complete or starvation media. After 3 or 6 days of incubation at 5% CO_2, 37°C, cells were incubated with 1:1000 Hoechst 33342 and 1 μg/ml PI for 30 minutes at 5% CO_2, 37°C. Cells were then washed twice with PBS and left in media without phenol red. Cells were imaged live with an ImageXpress micro, 10x objective and the cells positive for PI were measured by designing an algorithm to detect the nuclei (DAPI wavelength) to measure the total cell number and the nuclei positive for PI (Cy3 wavelength).

2.2.10 siRNA knockdown

96 well plates were coated with ECM as described in **Section 2.2.2**. A mix of 5 μl serum free media and a 5 μl of 5 μM siRNA **(Table 2-10)** was added to each well and the plate was incubated for 5 minutes at RT. A mix of 0.2μl of Dharmafect 1 (DF1) and 4.8 μl of serum free media was prepared and incubated for 5 minutes at RT. The DF1 mix was added to each well of the 96 well plate. The plate was incubated for 20 minutes at RT on a gentle rocker (Final concentration of siRNA is 30nM). $2x10^3$ MCF10CA1 cells in 80μl media containing 5% horse serum were added and the cells were incubated at 5% CO_2, 37°C overnight. The day after, the media was removed, cells were washed twice with PBS and media was changed to complete or starvation media. After 4 days of incubation at 5% CO_2, 37°C, cells were fixed with 4 % PFA for 15 minutes and stained with 1:1000 Hoechst 33342. Cells were imaged with an ImageXpress micro, 2x objective and the cell number was measured using MetaXpress and CME software by designing an algorithm to detect the nuclei (DAPI wavelength) to measure the total cell number as described in **Section 2.2.4**. Alternatively, a mix of 197 μl of serum free media and 3 μl of 5 μM siRNA was added to each well of a 6 well plate and the plate was incubated for 5 minutes at RT. A mix of 4 μl of Dharmafect 1 (DF1) and 196 μl of serum free media was prepared and incubated for 5 minutes at RT. The DF1 mix was added to each well of the 6 well plate. The plate was incubated for 20 minutes at RT on a gentle rocker. $5x10^5$ MCF10CA1 cells in 1.6 ml of media containing 5% horse serum were added and the cells were incubated at 5% CO_2, 37°C for 72hrs. Cells were collected, and WB was run as in **Section 2.2.7**.

Table 2-10 List of siRNAs and the supplier

siRNA	Catalogue number	Supplier
ON-TARGETplus SMARTpool Human ITGA2 siRNA	L-004566-00-0005	Dharmacon™
ON-TARGETplus SMARTpool Human PAK1 siRNA	L-003521-00-0005	Dharmacon™
ON-TARGETplus SMARTpool Human HPDL siRNA	L-014985-01-0005	Dharmacon™
ON-TARGETplus SMARTpool Human PAK1 siRNA	L-003521-00-0005	Dharmacon™
On TARGET plus control siRNA non-targeting siRNA	D-001810-04-20	Dharmacon™

2.2.11 Metabolite profiling

2.2.11.1 Non-targeted metabolomics:

$2.4x10^4$ MCF10CA1 cells/well were plated in 6 well plates coated with 2 mg/ml collagen (400 µl/well) or on plastic. After a 4-hour incubation at 5% CO_2, 37°C, media was changed to complete or starvation media and cells incubated for 6 days. Media was removed, the plate was placed on ice and cells were washed twice with ice cold PBS. 500 µl/well of ice-cold extraction solution (5 MeOH: 3 ACN: 2 H_2O) was added for 5 minutes with gentle rocking. Metabolites were transferred to an Eppendorf tube and centrifuged at 4°C, 14000 rpm for 10 minutes. Samples were kept at -80°C. Samples were run at the Faculty of Science biOMICS Facility using a Waters G2 Synapt mass spectrometer in electrospray mode. 3 replicates of each condition were combined and run at both positive and negative modes. The data is binned into 0.2 amu m/z bins and the m/z in each bin is used to identify putative IDs using the HumanCyc database (P.Romero., 2005). The data were analysed using Perseus software at S0 0.1 and False Discovery rate (FDR) 0.05. The metabolic pathways upregulated on ECM compared to plastic were obtained using MetaboAnalyst 5.0 (https://www.metaboanalyst.ca), by comparing the data to the Homo sapiens KEGG pathway library.

2.2.11.2 Targeted metabolomics:

$2.4x10^4$ MCF10CA1 cells/well were plated in 6 well plates coated with 2 mg/ml collagen (400 µl/well) or on plastic. After a 4-hour incubation at 5% CO_2, 37°C, media was changed to complete or starvation media and cells incubated for 6 days. Cells were extracted, and samples were collected as described in **Section2.2.11.1**. Samples were run using a Waters Synapt G2-Si mass spectrometer coupled to Water Acquity UPLC. Tyrosine, phenylalanine, and fumarate

were separated using Column Waters BEH Amide 150 x 2.1 mm. Samples were run in the negative mode and identified by comparing the compounds mass and retention time with the standards.

2.2.12 RT-qPCR

$1x10^6$ cells/well were plated in 6 well plates, after 4 hours of incubation at 5% CO_2, 37°C, media was changed to complete, or starvation media in the presence or absence of inhibitors **(Table 2-16)** and the cells were incubated overnight. The day after, media was removed, the cells were washed twice with PBS and trypsinised. 3.5 ml of media was added, the cells were collected and centrifuged at 1000 rpm for 5 minutes. The supernatant was removed, and the cell pellet was resuspended with 1 ml PBS and centrifuged at 1400rpm for 5 minutes. The PBS was removed, and the pellet was kept at-80°C. Using QIAGEN RNA extraction kit, the mRNA was extracted according to the manufacturers' protocol. The concentration of the extracted mRNA was measured by Nanodrop LITE Spectrophotometer (Thermo Scientific), and the extracted mRNA was used to synthesise cDNA. The following master mix was prepared by using High-Capacity cDNA Reverse Transcription kit **(Table 2-11)**:

Table 2-11 Master mix composition

Component	Volume per sample
10x RT Random Primers	2.0 µl
25x dNTP Mix	0.8µl
10x RT buffer	2.0µl
MultiScribe™ Reverse Transcriptase (RT)	1.0µl

5.8µl per sample of the master mix was added to a 14.2 µl mix of nuclease free water + 1000 ng of RNA (a-RT control was prepared using the sample with the highest RNA concentration). The samples were run in a thermal cycler with the program in **(Table 2-12)**:

Table 2-12 The thermal cycle running program

	Step 1	Step 2	Step 3	Step 4
Temperature °C	25	37	85	4
Time (min)	10	120	5	∞

The synthesised cDNA was kept at-80°C. The cDNA was then diluted 1:10 in nuclease free water and 3 µl of the cDNA solution was added to the master mix, which was prepared using qPCRBIO SyGreen Blue Mix (Table 2-13).

Table 2-13 QPCR master mix composition

	Volume	Final concentration
2x SYBR Green PCR Master Mix	5µl	1x
10x QuantiTect Primer Assay	1µl	1x
Water	1µl	

The samples were loaded in a 384 well plate (3 technical replicates per sample) including the-RT control and a water control for each tested gene. The plate was sealed and spun down for few seconds. The samples then were run using a QuantStudio 12K Flex Real-Time PCR System, with the settings in (Table 2-14).

Table 2-14 PCR system running program

	Hold Stage	PCR Stage		Met Curve stage		
Temperature (°C)	95	95	60	95	60	95
Time (min:sec)	2:00	00:10	00:30	00:15	1:00	00:15

The results were obtained using the following equation:

$$2^{-\Delta CT} = 2^{-(\text{Ct Target gene-Ct GAPDH})}$$

Table 2-15 List of targeted genes primers

Primer	GeneGlobe Id	Catalogue number	Supplier
Hs_ITGA2_1_SG QuantiTect Primer Assay	QT00086695	249900	Qiagen
Hs_ITGB1_1_SG QuantiTect Primer Assay	QT00068124	249900	Qiagen
Hs_ITGA5_1_SG QuantiTect Primer Assay	QT01008126	249900	Qiagen
Hs_GAPDH_1_SG QuantiTect Primer Assay	QT00079247	249900	Qiagen

Table 2-16 List of inhibitors, their concentration and the supplier

Inhibitor	Concentration	Catalogue number	Supplier
MRTX1133	200nM	HY-134813	MedChem
Selumetinib	10uM	S1008	SelleckChem
GCN2iB	5uM	HY-112654	MedChem

2.2.13 Cell adhesion

96 well plates were coated with ECM as described in **Section 2.2.2**. Cells were starved in amino acid-free media or kept in complete media for 18 hours. $2x10^4$ SW1990 cells were seeded on ECM or plastic and after 15 minutes, 30 minutes, or 1 hour, cells were washed twice with PBS, fixed 4% PFA and stained with 1:1000 Hoechst 33342 for 15 minutes at RT. Cells were washed twice with PBS and imaged with an ImageXpress micro, 2x objective. Cell number was measured using MetaXpress and CME software as described in **Section 2.2.4**.

2.2.14 Statistical analysis

Graphs were created in GraphPad prism software using the super-plots method (Lord et al.,2020) where each coloured dote represent a biological repeat and the black dotes represent the means of the repeats. One-way ANOVA (Kruskal-Wallis, Dunn's multiple comparisons test) was applied to compare between three or more groups with one variable. Two-way ANOVA (Tukey's multiple comparisons test) was applied to compare between groups with two independent variables. Mann-Whitney test was used to compare between two groups with one variable. Perseus software was used for non-targeted metabolomics statistical analysis by performing student *t*-test where SO was 0.1 and FDR was 0.05.

2.2.15 Survival analysis

The survival analysis was performed using GEPIA2 (Gene Expression Profiling Interactive Analysis) website (http://gepia2.cancer-pku.cn/#survival). The analysis was done using the RNA sequencing expression data of 9,736 tumours and 8,587 normal samples from the TCGA and the GTEx projects, using a standard processing pipeline (Tang et al.,2019).

3 The extracellular matrix promoted breast cancer cell growth under amino acid starvation

Figures: (1)-(2-A, C)-(4)-(6-A, C)-(7-B, D)-(8-A, B)-(10-B) and (11-A, B) have been published in (Nazemi et al., 2024) under the Creative Common Attribution Licence (CC BY 4.0)

3.1 Introduction:

Cancer cells consume more nutrients than normal cells due to their high proliferation rate. Previous studies showed that glucose uptake in cancer cells is increased comparing to normal cells, which in turn triggers alternative metabolic pathways (DeBerardinis and Chandel, 2016). The most consumed nutrients by cancer cells are glucose and glutamine (Lukey et al., 2017). However, amino acids other than glutamine, such as serine, has been found to be the major contributor for the proliferating cell carbon mass (Hosios et al., 2016). Cancer cells rapid nutrient consumption leads to a deficiency in the availability of the extracellular nutrients, which is also driven by an insufficient blood supply. In fact, the TME in pancreatic ductal adenocarcinoma (PDAC) was found to be hypoxic and limited in glucose and most amino acids, including glutamine, alanine, cysteine and serine (Kamphorst et al., 2015). Therefore, cancer cells reprogram their metabolism and adopt new strategies to be able to survive under nutrient scarcity. On the other hand, tumours can also shift their energy production from glycolysis to the mitochondria oxidative phosphorylation. On the other hand, cancer cells can uptake macromolecules from the surrounding microenvironment, degrade them and use them as source of nutrients. Indeed, it has been discovered that cancer cells under starvation conditions can internalise albumin, the most abundant protein in the blood, and use it as source of amino acids (Finicle, Jayashankar and Edinger, 2018).

The ECM components can also be a source of glucose and amino acids. Indeed, PDAC cells were shown to uptake collagens under both glucose and glutamine starvation and use the derived proline to grow under these nutrient limited conditions. The catabolism of the derived proline via the proline oxidase (PRODH1) increased the proliferation of the cells under nutrient deprivation (Olivares et al., 2017). In addition, the glucose starvation of ovarian cancer cells enhanced the tensin-dependent internalisation of $\alpha 5\beta 1$ integrin and its ligand fibronectin,

which triggered ovarian cancer cells migration (Rainero et al., 2015). Similarly, mammary epithelial cells under serum starvation internalised β4 integrin and its ligand laminin, preventing cell death. The internalised laminin enhanced mTORC1 activity and increased the intracellular levels of essential amino acids (Muranen et al., 2017). This promoted us to investigate the role of ECM in breast cancer metabolism in more details. Breast cancer cells are surrounded by thick ECM, and it is well established that the ECM can promote breast cancer progression via multiple mechanisms (Kaushik et al., 2016). However, the full picture of the role of ECM in breast cancer metabolism is still unclear. Understanding the contribution of ECM in cancer metabolic reprograming and its use as a source of nutrients is essential especially in the types of cancer where ECM stiffness is high, such as in breast and pancreatic cancer. In this chapter we show that highly invasive breast cancer cells internalised and degraded different types of matrices under full amino acid (AA) and glutamine starvation (Gln). This uptake was shown to be macropinocytosis dependent, led to an increase in the intracellular amino acid levels and upregulated multiple metabolic pathways, including phenylalanine and tyrosine metabolism. The downregulation of HPDL, an enzyme in this pathway, strongly reduced ECM dependent cell growth.

3.2 Results:

3.2.1 ECM partially rescued the growth of MCF10CA1 breast cancer cells under AA starvation

To test whether breast cancer cells were able to use the ECM proteins to survive under nutrient deprivation, we seeded MCF10CA1 highly invasive breast cancer cells on Collagen I (a key component of the interstitial matrix) vs plastic **(Figure 3-1,A,B)** or Matrigel (a basement membrane preparation) vs plastic **(Figure 3-1,C,D)** in AA free media or Gln free media. The growth of the cells was monitored for up to six days. The results show that both collagen I and Matrigel partially rescued the growth of the cells, as the number of cells remained lower than compared media, under both AA (20% rescue) and Gln (50% rescue) starvation compared to plastic. These results suggest that ECM promoted breast cancer cell growth and/or survival under nutrient deprivation. Interestingly, the cells grew regardless of seeding them on both types of matrices vs on plastic for up to 6 days in complete media **(Figure 3-1, E, F)** which indicates that the cells relied more on ECM when they were under starvation.

To test the effect of ECM on cells growth in a more physiological environment, we generated cell derived matrices (CDMs) from CAFs. CDMs are 3D matrices that mimic the physiological ECM. The composition and the stiffness of CDMs have been found to be very close to the in vivo matrix (Kaukonen et al., 2017). CDMs were generated from CAFs as shown in **Section 2.2.2** and MCF10CA1 cells were seeded on top of them vs on plastic under both AA starvation or Gln starvation conditions and cell growth was monitored for up to six days **(Figure 3-2, A, B)**. The results show that the CDM partially rescued cell growth under both starvation conditions compared to plastic. Similarly to collagen I and Matrigel, cells grew regardless of seeding them on CDM or plastic in complete media **(Figure 3-2, C)**. Overall, the data show that different types of ECM partially rescued the growth of invasive breast cancer cells under both AA starvation and Gln starvation conditions.

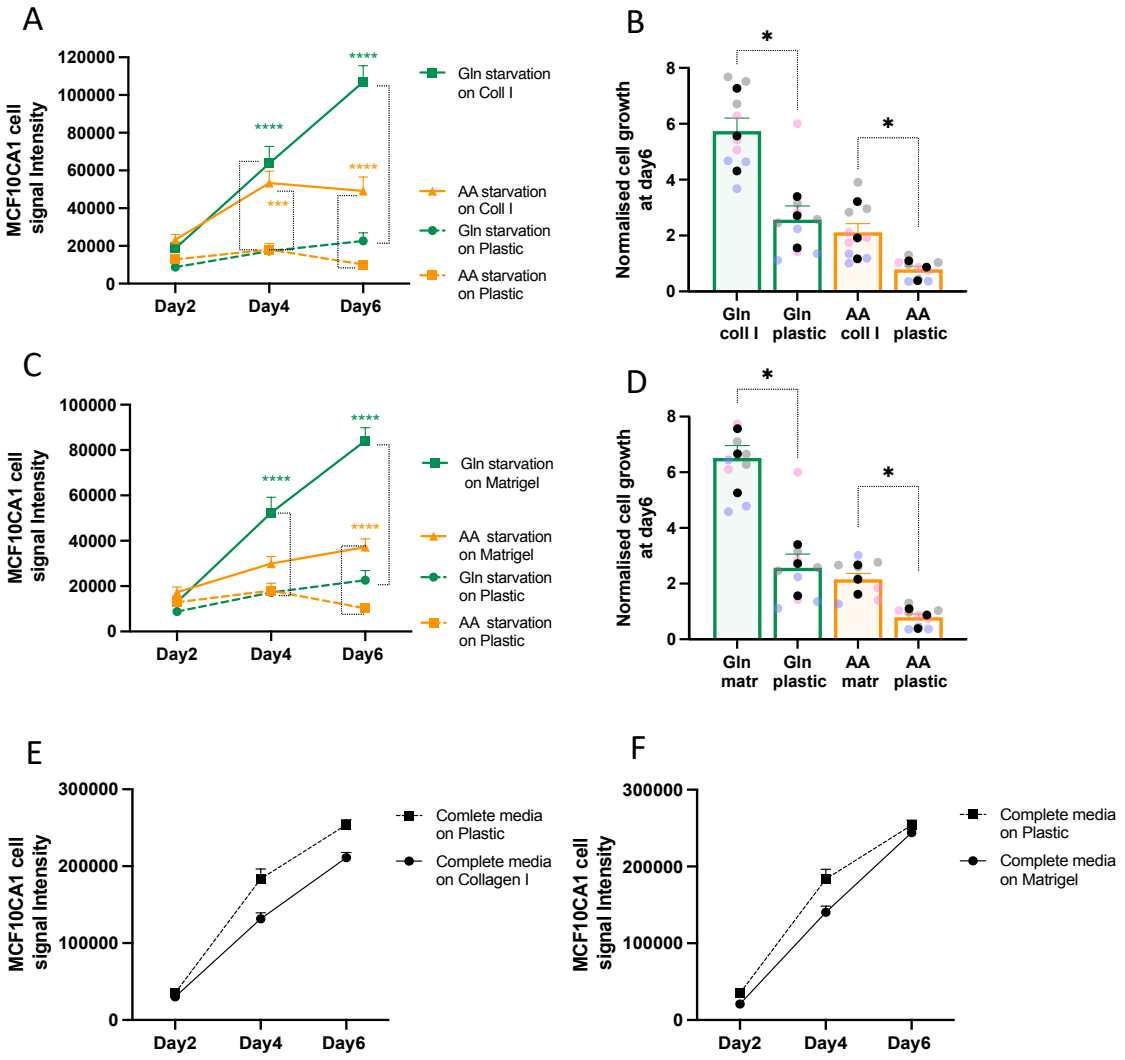

Figure 3-1 Collagen I and Matrigel partially rescued MCF10CA1 cells growth under AA starvation (Nazemi et al., 2024). MCF10CA1 cells were seeded on 2 mg/ml collagen I vs plastic (A-B) and on 3 mg/ml Matrigel vs plastic (C-D) under both amino acid (AA) or glutamine (Gln) free media for 6 days. MCF10CA1 cells were seeded on 2 mg/ml collagen I vs plastic (E) and on 3 mg/ml Matrigel vs plastic (F) under complete media for 6 days. Cells were fixed in day 2, 4, and 6 and the nuclei were stained with DRAQ5. The signal intensity was measured using a Licor Odyssey Sa system and quantified with Image Studio Lit software. N=3 independent experiments, values represent the Mean± SEM, the coloured dots for biological repeats, the black dots represent the mean of the individual experiments. (A-C-E-F) Two-Way ANOVA, Tukey's multiple comparisons test. (B-D) Kruskal-Wallis, Dunn's multiple comparisons test. *p < 0.05, **p < 0.01, ****p < 0.0001

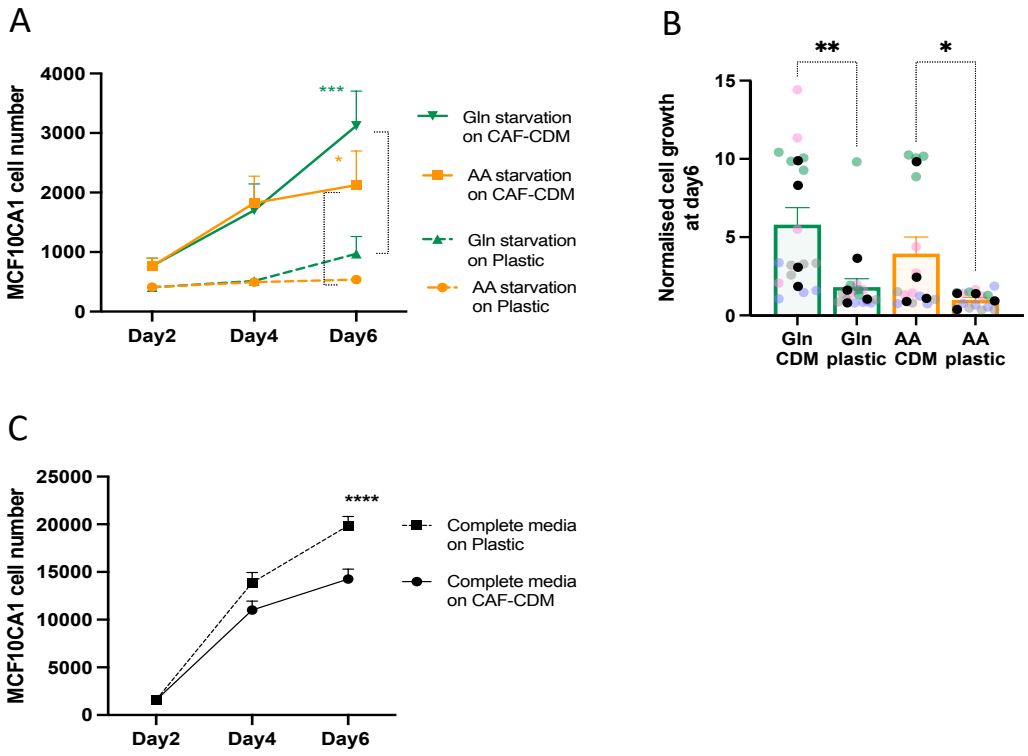

Figure 3-2 CDM partially rescued MCF10CA1 cells growth under AA starvation. MCF10CA1 cells were seeded on CAF-CDM vs plastic (A-B) under both AA free media and Gln free media for 6 days. MCF10CA1 cells were seeded on CAF-CDM vs plastic (C) in complete media for 6 days. Cells were fixed at day 2, 4, and 6 and the nuclei were stained with Hoechst 33342. The cells were imaged using an Image Xpress micro system and cell numbers were quantified with MetaXpress and CME software. N=4 independent experiments, values represent the Mean ± SEM, the coloured dots for biological repeats, the black dots represent the mean of the individual experiments. (A-C) Two-Way ANOVA, Tukey's multiple comparisons test. (B) Kruskal-Wallis, Dunn's multiple comparisons test. *p < 0.05, **p < 0.01, ***p < 0.001, ****p < 0.0001

3.2.2 ECM induced MCF10CA1 cell division but did not affect cell death under AA starvation.

The ECM mediated cell growth shown above could be due to an increase in cell division or a decrease in cell death, or a combination of both. To investigate this, we seeded MCF10CA1 cells on collagen I, Matrigel or plastic for 4 days under AA starvation **(Figure 3-3,A)**, Gln starvation **(Figure 3-3,B) or** complete media **(Figure 3-3,C)** for 4 days, followed by a two day incubation in the presence of EdU (5-ethynyl-2'-deoxyuridine), which is a thymidine analogue that is incorporated into the DNA during DNA synthesis. The results show that under both AA and Gln starvation, cell division was increased on both collagen I and Matrigel compared to plastic, while there was no difference when cells were seeded in complete media.

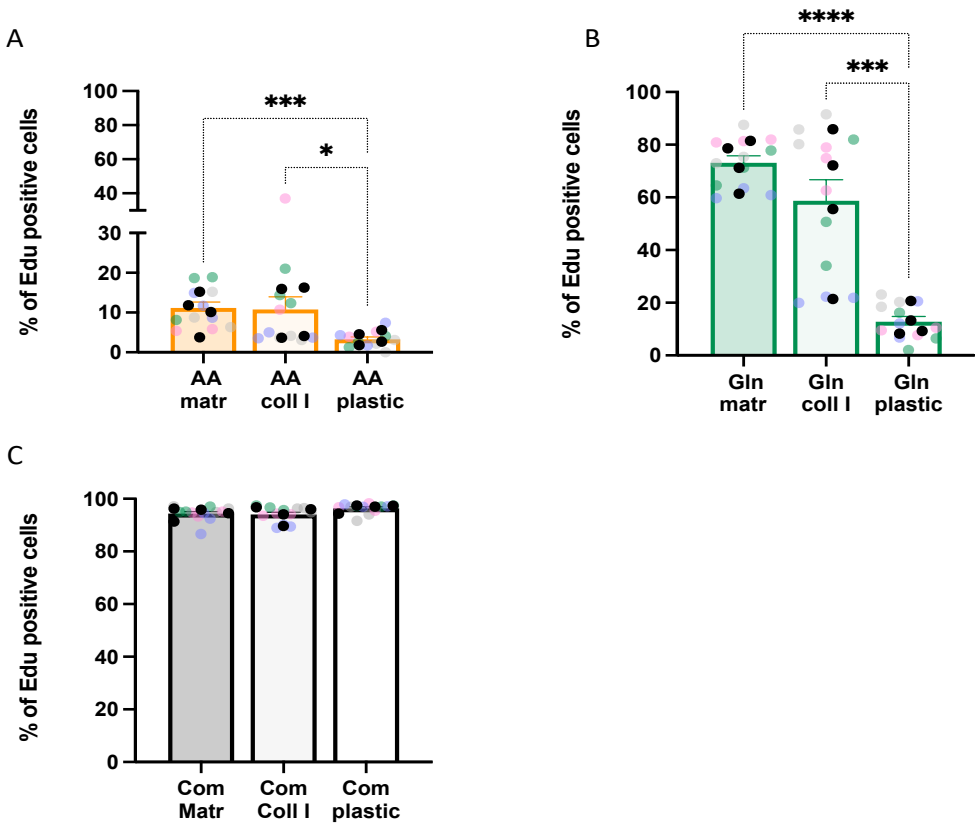

Figure 3-3 ECM increased MCF10CA1 cells division under AA starvation. MCF10CA1 cells were seeded on 2 mg/ml collagen I, 3 mg/ml Matrigel or plastic under AA free (A), Gln free (B) or complete media (Com, C) for 4 days followed by 2 days in the presence of 5μM EdU. Cells were fixed and stained with Click iT EdU Kit and Hoechst 33342. The cells were imaged using an Image Xpress micro system and cell numbers were quantified with MetaXpress and CME software. N=4 independent experiments, and values represent the Mean± SEM, the coloured dots for biological repeats, the black dots represent the mean of the individual experiments. Kruskal-Wallis, Dunn's multiple comparisons test. *p < 0.05, ***p < 0.001****p < 0.0001.

It was shown previously that nutrients deprivation can cause cell death (Graham et al., 2012, Kang et al., 2023). To test whether the ECM also affected MCF10CA1 cells death under starvation, first cell apoptosis was measured by assessing the number of cells positive for cleaved caspase 3/ 7, which is an apoptotic marker. Apoptosis is a type of cell death where the mitochondria release different proteins such as cytochrome c leading to the activation of caspases which in turn cleave multiple proteins and cause cell death (Yanes and Rainero, 2022). Cells were seeded on collagen I, Matrigel or on plastic in complete or AA free media for up to 6 days. Cells then were stained with cleaved caspase 3/7 and the number of cells positive for this apoptotic marker was measured at day3 **(Figure 3-4, A)** or day6 **(Figure 3-4, B)**. Interestingly, the results show that both collagen I and Matrigel did not affect cell death at both time points, regardless of whether cells were seeded in complete or AA starvation media. As expected, on plastic AA starvation significantly increased cell apoptosis compared to complete

media. There are different types of cell death and apoptosis is one of them. Hence, to test whether other types of cell death were involved, another cell death marker was used. MCF10CA1 cells were seeded on collagen I or plastic in complete or AA free media for up to 6 days and cells were stained with propidium Iodide (PI). PI is a cell viability marker that binds to DNA of damaged cells as it can penetrate their permeable membrane but not live cells. The number of cells positive for PI was measured at day 3 **(Figure 3-4, C)** and day 6 **(Figure 3-4, D)**. Similarly to the apoptosis data, the ECM did not significantly affect cells death under both AA starvation and complete media.

To conclude, the results shown in this section indicate that the ECM-mediated cell growth was due to an increase in cell division rather than a decrease in cell death.

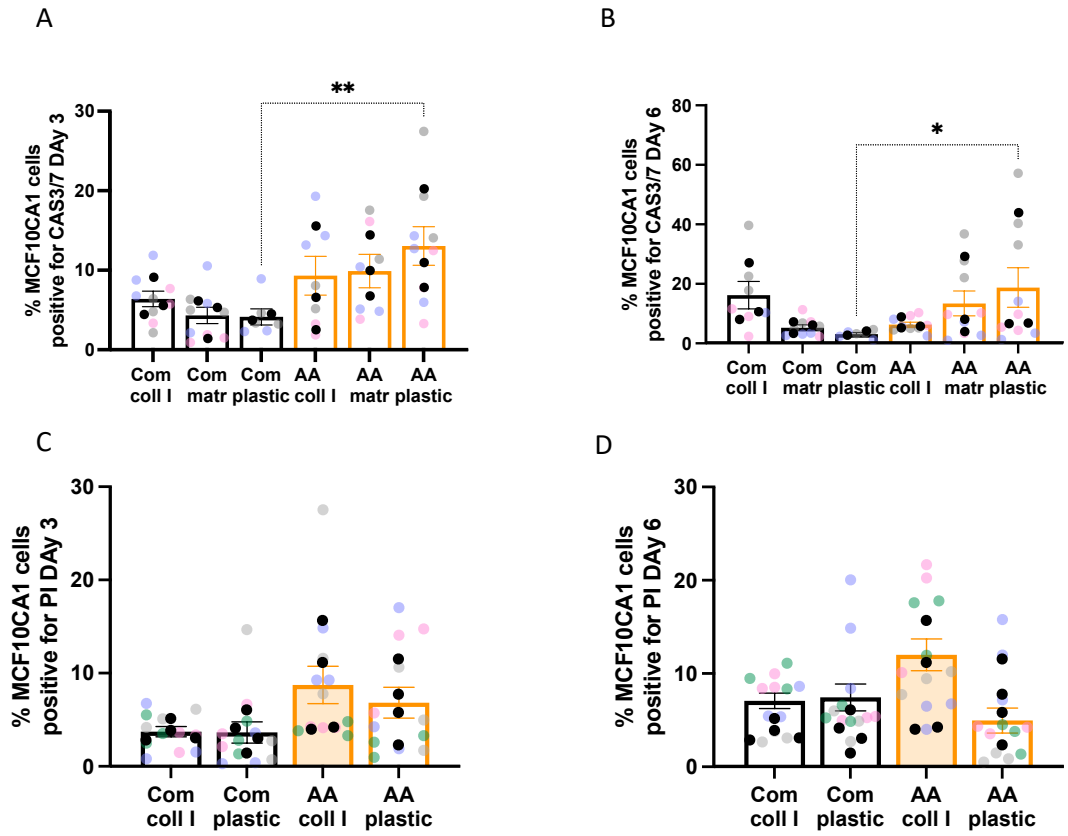

Figure 3-4 ECM did not affect MCF10CA1 cells death under AA starvation. MCF10CA1 cells were seeded on 2 mg/ml collagen I, 3 mg/ml Matrigel or plastic in AA free and complete media (Com) for 3 (A) or 6 (B) days, then media was changed to PBS containing 5µM Cell Event Caspase-3/7 Green Detection Reagent. Cells were fixed and stained with Hoechst 33342. MCF10CA1 cells were seeded on 2mg/ml collagen I or plastic in AA free and complete media for 3 (C) or 6 (D) days. Media was changed to media containing Hoechst 33342 and 1µg/ml PI. The cells were imaged using an Image Xpress micro system and the number of cells positive for CAS3/7 or PI was quantified with MetaXpress and CME software. N≥3 independent experiments, values represent the Mean ± SEM, the coloured dots for biological repeats, the black dots represent the mean of the individual experiments. Kruskal-Wallis, Dunn's multiple comparisons test. *$p < 0.05$, **$p < 0.01$.

3.2.3 Chemical crosslinking prevented collagen I-dependent cell growth under AA starvation.

Previous studies showed that under nutrient deprivation cancer cells can uptake macromolecules from the tumour microenvironment in a process called scavenging (Finicle et al., 2018). And previous studies in our lab showed that MDA-MB-231 cells, which are highly invasive breast cancer cells, internalise and degrade ECM components (Martinez et al., 2024). To investigate if MCF10CA1 cells could also uptake ECM components, the cells were seeded on fluorescently labelled collagen I for 6 hours in complete media in the presence or absence of E64d, which is a lysosomal protease inhibitor **(Figure 3-5, A)**. The results indicate that MCF10CA1 cells internalised and degraded collagen I in complete media, as the collagen I uptake index was increased by adding the lysosomal inhibitor. To test whether the cells were also able to uptake and degrade collagen I under starvation, MCF10CA1 cells were seeded on fluorescently labelled collagen I for 6 hours in the presence of E64d in complete or AA free media **(Figure 3-5, B)**. The results show that in the absence of AAs, the uptake and the degradation of collagen I in breast cancer cells were significantly increased compared to complete media.

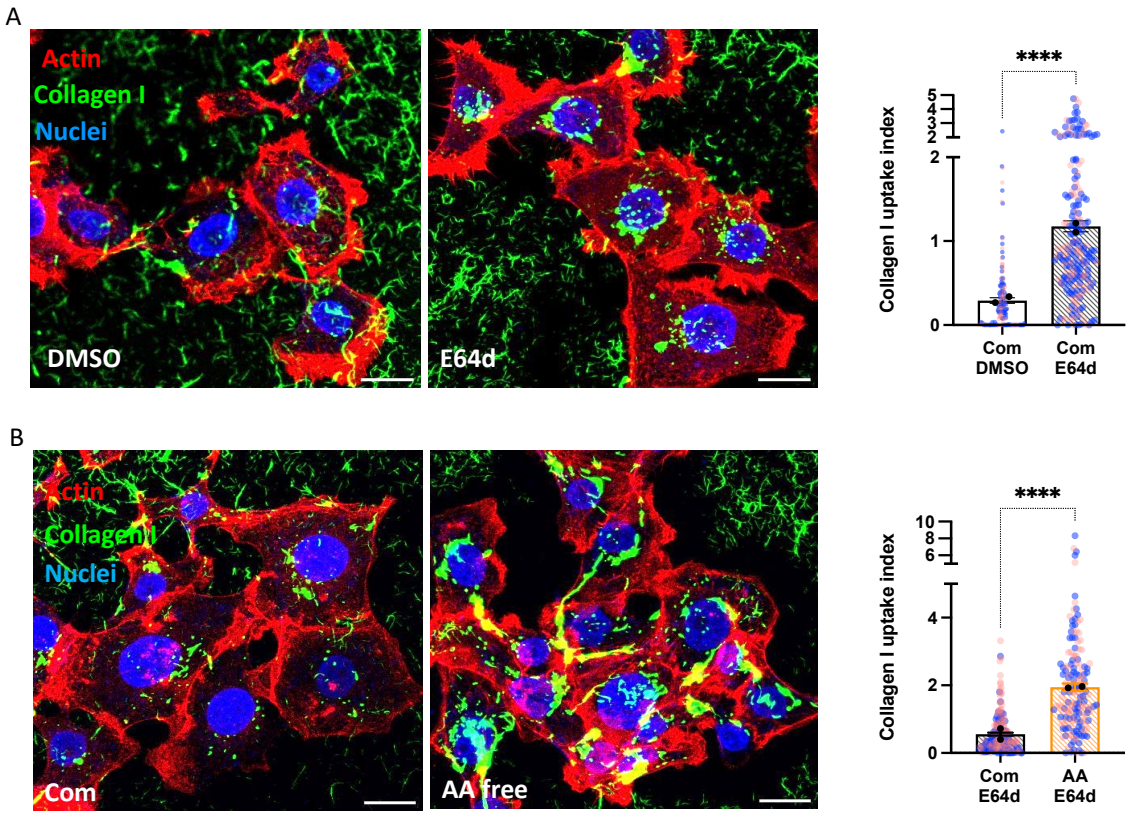

Figure 3-5 MCF10CA1 collagen I uptake was induced under AA starvation MCF10CA1 cells were seeded on 0.5 mg/ml collagen I , labelled with NHS fluorescein (green), under complete media in the presence of DMSO or 20µM E64d (A), cells were fixed after 6 hours and stained with phalloidin (red) and DAPI (blue). MCF10CA1 cells were seeded on 0.5 mg/ml collagen I labelled with NHS fluorescein (green), under complete media or AA starvation media in the presence of 20µM E64d (B). Cells were fixed after 6 hours and stained with phalloidin (red) and DAPI (blue). Cells were imaged with a Nikon A1 confocal microscope 40x objective. Collagen I uptake index was calculated with Image J software. Scale bar 20µm. N=2 independent experiments, values represent the Mean± SEM, the coloured dots for biological repeats, the black dots represent the mean of the individual experiments. Mann-Whitney test. ****$p < 0.0001$.

Glutaraldehyde is a widely used collagen crosslinking agent which binds to the collagen amine groups (L. H. H. OLDE DAMINK et al., 1995). To test the effect of crosslinking on collagen I uptake, MCF10CA1 cells were seeded on fluorescently labelled collagen I or chemically crosslinked collagen I under AA starvation for 3 days in the presence of E64d **(Figure 3-6, A)**. The results show that the cells were unable to internalise the crosslinked collagen I. To investigate whether stopping collagen I uptake and degradation by crosslinking would affect the ECM-dependent cell growth shown in **Section 3.1.2**, MCF10CA1 cells were seeded on plastic, collagen I or crosslinked collagen I under both AA **(Figure 3-6, B, C)** or Gln starvation **(Figure 3-6,D,E)** for up to 6 days. The results show that the ECM-dependent cell growth was completely abolished under both starvation conditions when collagen I was crosslinked.

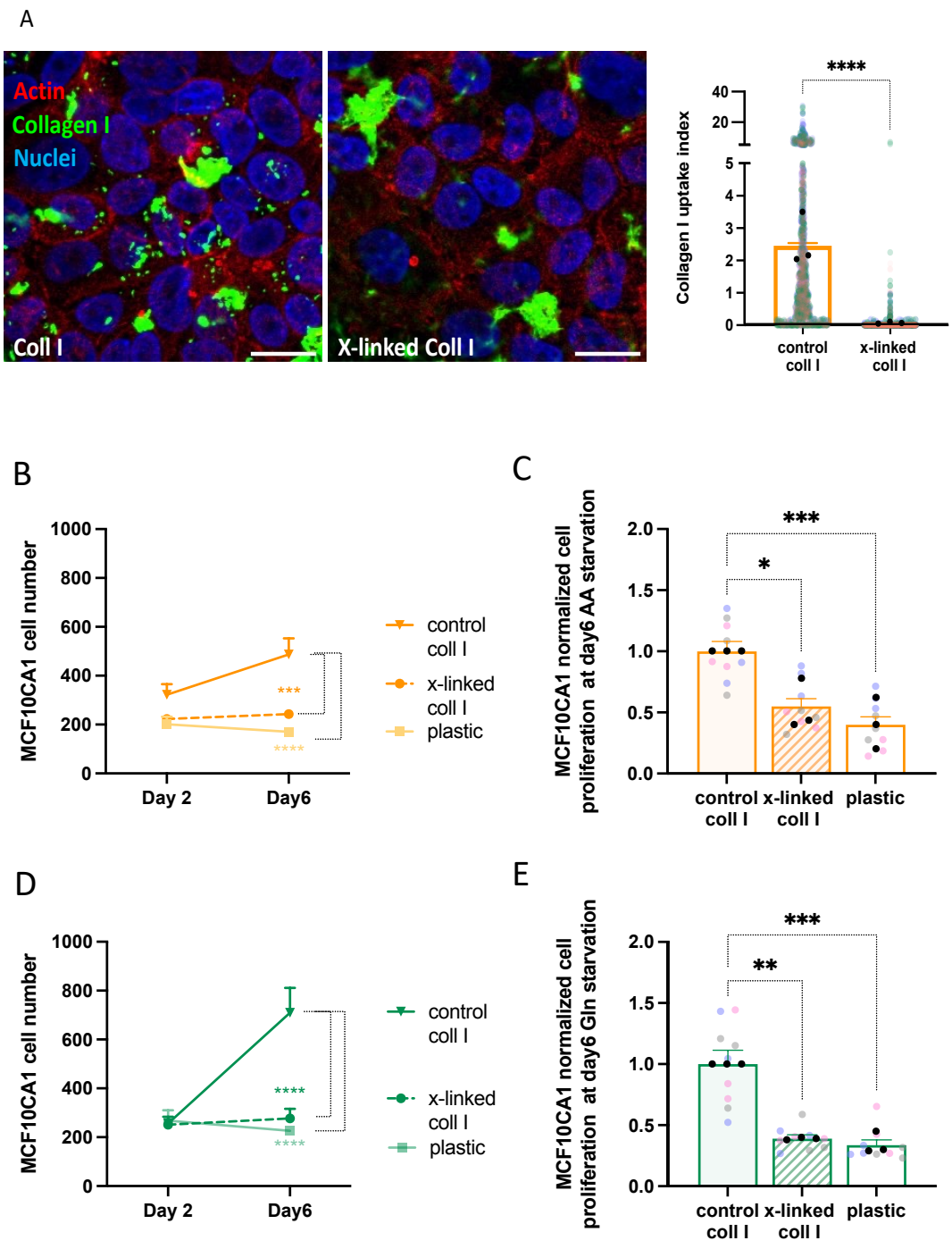

Figure 3-6 Crosslinking completely abolished ECM-dependent cell growth. MCF10CA1 cells were seeded on 1 mg/ml collagen I or crosslinked collagen I (x-linked coll I) labelled with NHS fluorescein (green) in AA free media containing 20μM E64d (A). Cells were fixed after 3 days and stained with phalloidin (red) and DAPI (blue). Cells were imaged with a Nikon A1 confocal microscope, 40x objective. Collagen I uptake index was calculated with Image J software. Scale bar 20μm. MCF10CA1 cells were seeded on 2mg/ml collagen I or crosslinked collagen I (x-linked coll I) vs plastic under AA free media (B-C) or Gln free media (C-E) for 6 days. Cells were fixed at day 2, and 6 and the nuclei were stained with Hoechst 33342. The cells were imaged using an Image Xpress micro system and cell numbers were quantified with MetaXpress and CME software. N=3 independent experiments, values represent the Mean± SEM, the coloured dots for biological repeats, the black dots represent the mean of the individual experiments. (A) Mann-Whitney test. (B-D) Two-Way ANOVA, Tukey's multiple comparisons test. (C-E) Kruskal-Wallis, Dunn's multiple comparisons test. *p < 0.05, **p < 0.01, ***p < 0.001, ****p < 0.0001

3.2.4 ECM uptake and ECM-dependent cell growth were mediated by macropinocytosis

Previous studies showed that PDAC cells internalised collagen I and collagen IV under glucose or glutamine starvation conditions in a macropinocytosis-dependent and a macropinocytosis independent pathway, respectively (Olivares et al., 2017). Macropinocytosis is a non-selective endocytosis mechanism, where cells generate large structures called endocytic cups to uptake fluids and macromolecules from the extracellular space. The closure of the endocytic cups form macropinosomes, which eventually fuse with endosomes and lysosomes for degradation (Finicle et al., 2018).

To invistigate whether ECM uptake under starvation was mediated by macropinocytosis, we assessed if inhibiting macropinocytosis affected ECM uptake under starvation. MCF10CA1 cells were seeded on CDM in the presence of DMSO or FRAX597 (a macropinocytosis inhibitor which inhibits group I PAKs) under AA starvation for 5 hours **(Figure 3-7,A)**. The results show that by inhibiting macropinosytosis, the uptake of CDM was significantly reduced. To test the effect of macropinocytosis inhibition on ECM-depenedent cell growth, MCF10CA1 cells were seeded on collagen I for up to 4 days in the presence of DMSO or FRAX597 under AA **(Figure 3-7,B)** or Gln starvation **(Figure 3-7,C)**. MCF10CA1 cells were also seeded on collagen I, after performing a PAK1 siRNA knockdown, under both AA **(Figure 3-7,D)** or Gln starvation **(Figure 3-7,E)** for up to 4 days. Consistent with previous results showing that ECM uptake was mediated by macropinoytosis, cell growth was impaired by desrupting this endocytic pathway. Indeed, both pharmachological inhibition and knocking-down of PAK1 significantly reduced the collagen I-dependent cell growth under both starvation conditions **(Figure 3-7)**. These results indicate that ECM-dependent breast cancer cell growth under nutrient deprevation was mediated by macropinocytosis.

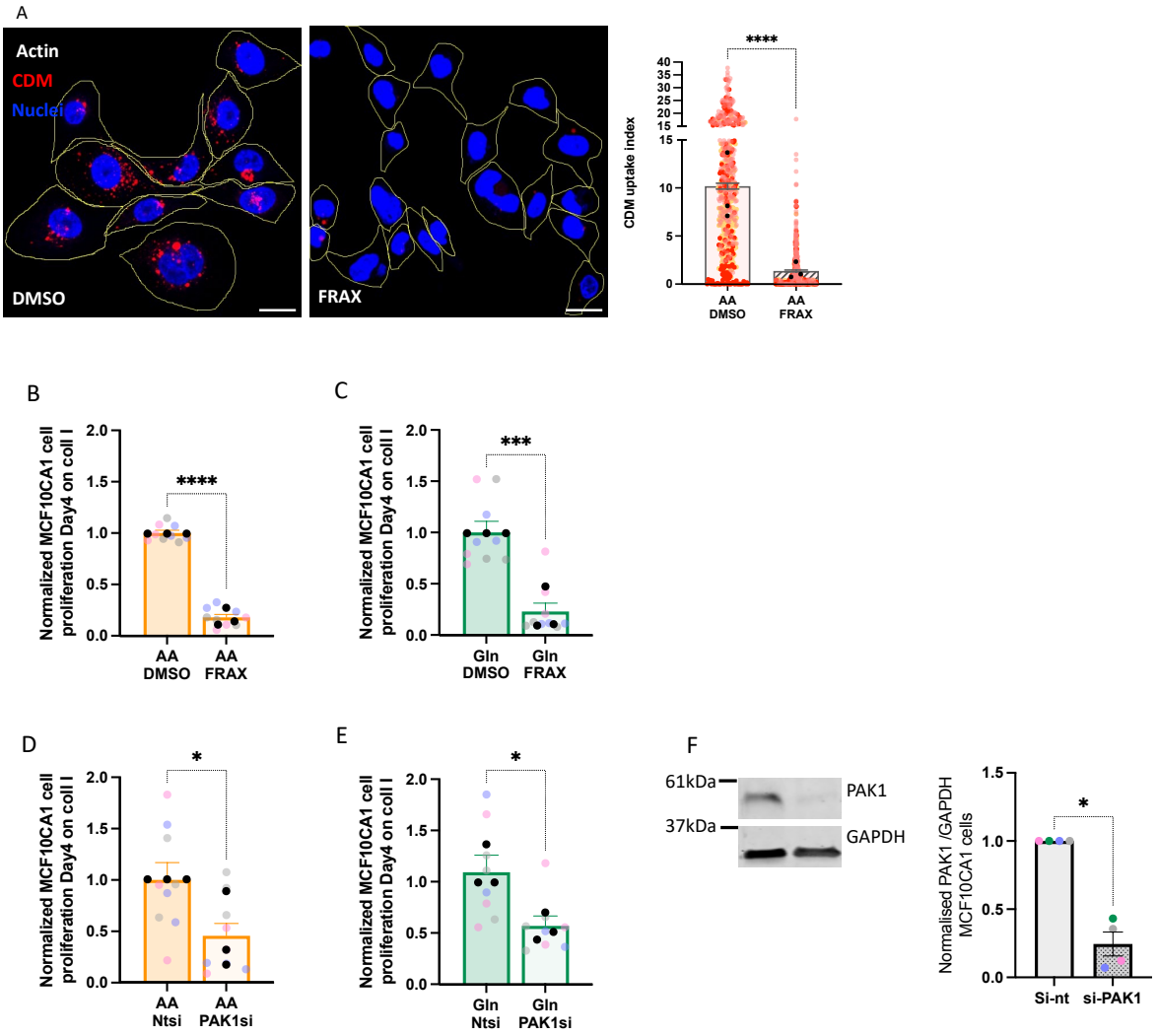

Figure 3-7 ECM-dependent MCF10CA1 cell growth was mediated by macropinocytosis MCF10CA1 cells were seeded in AA free media for 5 hours on CAF-CDM labelled with pH-Rodo (red). DMSO or 1μM FRAX 597 were added two hours after seeding. Cells were stained with Hoechst 33342 (Blue), Spy actin (white, not shown) and imaged live with a Nikon A1 confocal microscope, 40x objective. CDM uptake index was calculated with Image J software. Scale bar 20μm. (A). MCF10CA1 cells were seeded on 2 mg/ml collagen I in AA free (B) and or Gln free media (C) in the presence of DMSO or 1μM FRAX 597, which were added every other day for up to 4 days. Cells were fixed at day 4 and stained with Hoechst 33342. MCF10CA1 cells were seeded on 2 mg/ml collagen I, transfected with non- targeted siRNA (Ntsi) or PAK1-siRNA (PAK1si), in AA free (D) or Gln free media (E) for 4 days. Cells were fixed and stained with Hoechst 33342. The cells were imaged using an Image Xpress micro system and cell numbers were quantified with MetaXpress and CME software. MCF10CA1 cells were seeded on plastic, transfected with an siRNA targeting PAK1 integrin (si-PAK1) or a non-targeting siRNA (si-nt) as a control. Cell lysates were collected after 72 hours, samples were run by Western Blotting, membranes were stained for PAK1 and GAPDH and imaged with a Licor Odyssey system. The protein band intensity was measured with Image Studio Lite software (F). N≥3 independent experiments, values represent the Mean± SEM, the coloured dots for biological repeats, the black dots represent the mean of the individual experiments. Mann-Whitney test *p < 0.05, ***p < 0.001, ****p < 0.0001

3.2.5 Intracellular metabolites were upregulated on collagen I under AA starvation and Gln starvation

A previous study by Muranen et al showed that the uptake of laminin in MCF10A mammary epithelial cells under nutrient starvation increased the intracellular amino acid levels (Muranen et al., 2017). To assess whether this was the case in our study, we seeded MCF10CA1 cells on plastic or on collagen I for 6 days under AA starvation **(Figure 3-8)** or Gln starvation **(Figure 3-9)** and then performed metabolomics via non targeted infusion mass spectrometry to measure the intracellular metabolite content. Under AA starvation, the results show that (1610) metabolites were upregulated on collagen I. The pathway enrichment analyses showed that purine metabolism, arginine biosynthesis, and phenylalanine, tyrosine and tryptophan biosynthesis were among the highest upregulated metabolic pathways on collagen I under AA starvation **(Figure 3-8, B)**. Indeed, when we assessed the amino acid levels, phenylalanine and tyrosine were the most upregulated amino acids on coll I compared to plastic **(Figure 3-8, C)**. Similarly, when cells were grown under Gln starvation, (975) metabolites were upregulated on coll I. The pathway enrichment analyses showed that galactose metabolism, arginine and proline metabolism and, similarly to AA starvation, phenylalanine, tyrosine and tryptophan biosynthesis were among the highest upregulated metabolic pathways on collagen I under Gln starvation **(Figure 3-9, B)**. Assessing the amino acid levels showed that arginine, phenylalanine and tyrosine were the most upregulated amino acids on coll I compared to plastic **(Figure 3-9, C)**. Comparing our two datasets shows that (556) metabolites were upregulated on collagen I under both full AA starvation and Gln starvation **(Figure 3-9, D)**.

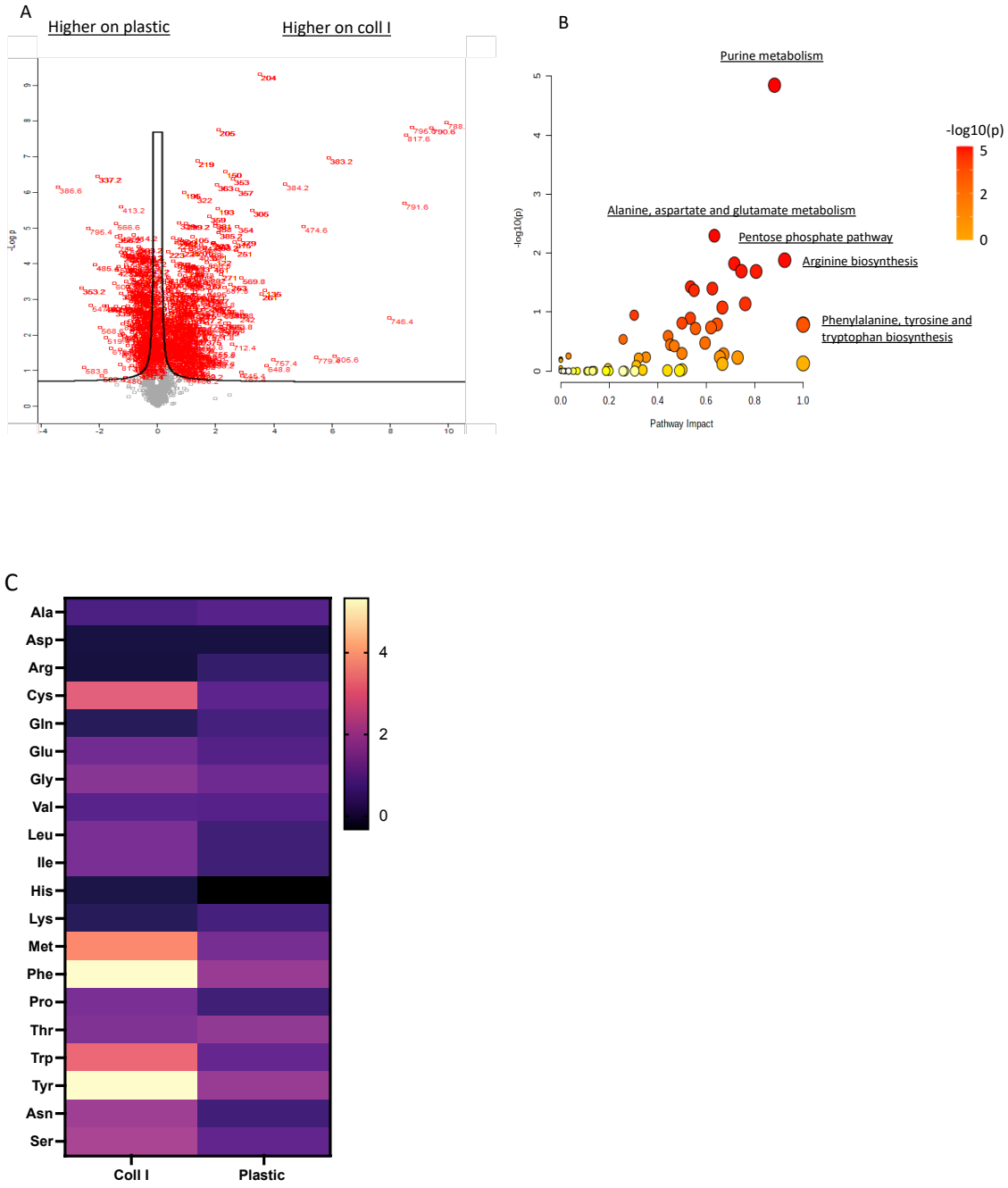

Figure 3-8 Intracellular AA were higher on collagen I compared to on plastic under AA starvation. MCF10CA1 cells were seeded in AA free media on 2 mg/ml collagen I vs on plastic for 6 days. Metabolites were extracted and quantified with non-targeted mass spectrometry. Volcano blot (A) enriched metabolic pathways (B). Heatmap of amino acid intracellular content on collagen I (coll I) vs plastic (C). (A) analysed using Perseus software at S0 0.1. (B) analysed using MetaboAnalyst 5.0 https://www.metaboanalyst.ca.

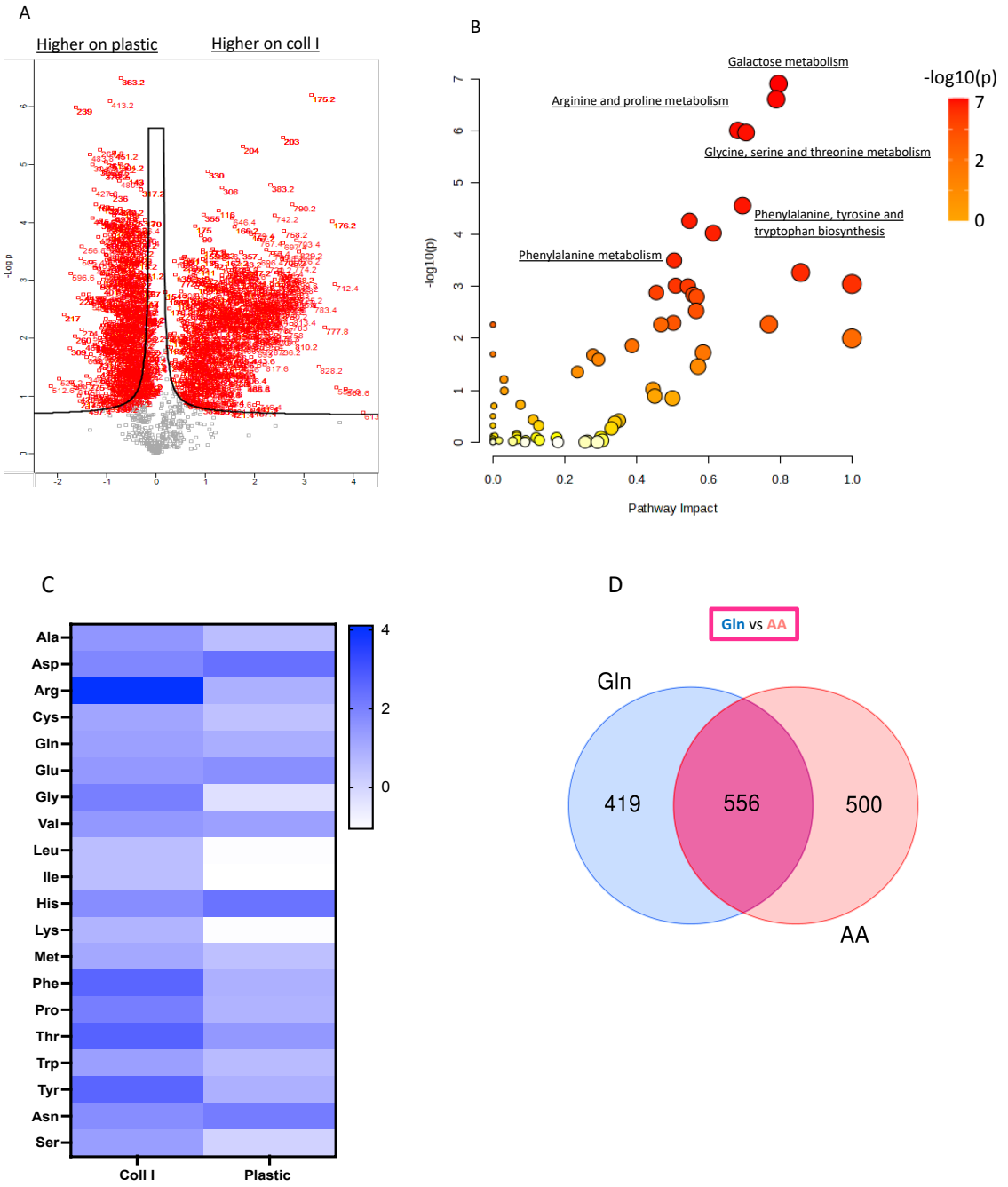

Figure 3-9 Intracellular AA were upregulated on collagen I under Gln starvation MCF10CA1 cells were seeded in Gln free media on 2 mg/ml collagen I vs on plastic for 6 days. Metabolites were extracted and quantified with non-targeted mass spectrometry. Volcano blot (A) enriched metabolic pathways (B). Heatmap of amino acids changes on coll I vs plastic (C). Venn diagram of upregulated metabolites on 2 mg/ml coll I in AA free vs Gln free (D). (A) analysed using Perseus software at S0 0.1. (B) analysed using MetaboAnalyst 5.0 https://www.metaboanalyst.ca.

To further investigate and confirm the increase of phenylalanine and tyrosine metabolism, we performed targeted ultra-performance liquid chromatography- tandem mass spectrometry (UPLC-MS/MS) and the results show that the intracellular level of phenylalanine, tyrosine and fumarate was increased on collagen I compared to plastic under AA starvation **(Figure 3-10, B)**. consistently, phenylalanine and tyrosine were also upregulated when MDA-MB-231 cells were seeded on both CAF-CDM or coll I under AA starvation (Nazemi et al., 2024). Therefore, phenylalanine and tyrosine metabolism was shown to be upregulated in different cell lines when they were seeded on two types of ECM. Fumarate is the final product of the phenylalanine and tyrosine metabolism which can then be fed into the TCA cycle to produce energy **(Figure 3-10, A)**. 4-hydroxyphenylpyruvate dioxygenase (HPD) and its paralog 4-hydroxyphenylpyruvate dioxygenase like (HPDL) are enzymes involved in the phenylalanine/ tyrosine metabolic pathway **(Figure 3-10, A)**. To assess whether the ECM dependent cell growth was mediated by an increase in phenylalanine/ tyrosine catabolism, cells were seeded on collagen I under AA **(Figure 3-11, B)** and Gln **(Figure 3-11, C)** starvation for 4 days after performing HPDL siRNA knockdown. The efficiency of the knockdown was tested via Immunofluorescence, demonstrating a significant reduction in HPDL fluorescence in the knock down cells **(Figure 3-11, A).** The results show that HPDL siRNA knockdown significantly reduced cell growth on collagen I under both starvation conditions. The same results were observed in MDA-MB-231 cells (Nazemi et al., 2024). Overall, these results indicate that ECM uptake sustained cell proliferation under AA starvation by promoting phenylalanine and tyrosine catabolism. Therefore, HPDL might be a novel therapeutic target to inhibit ECM-dependent breast cancer cell growth.

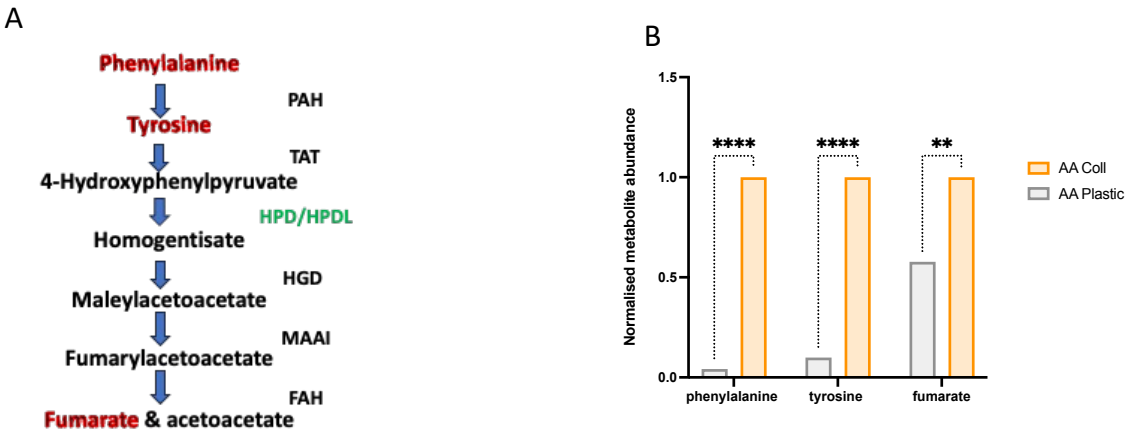

Figure 3-10 phenylalanine, tyrosine and fumarate were upregulated on coll I under AA starvation MCF10CA1 cells were seeded in AA free media on 2 mg/ml collagen I vs on plastic for 6 days. Metabolites were extracted at day 6 and quantified with targeted mass spectrometry. Phenylalanine and tyrosine metabolism diagram (A). Levels of phenylalanine, tyrosine and fumarate on collagen I vs on plastic under AA free media measeared by targeted metabolites (B). N= 3 independent experiments, values represent the Mean± SEM, the black dots represent the mean of the individual experiments. Two-Way ANOVA, Tukey's multiple comparisons test. **p < 0.01, ****p < 0.000.

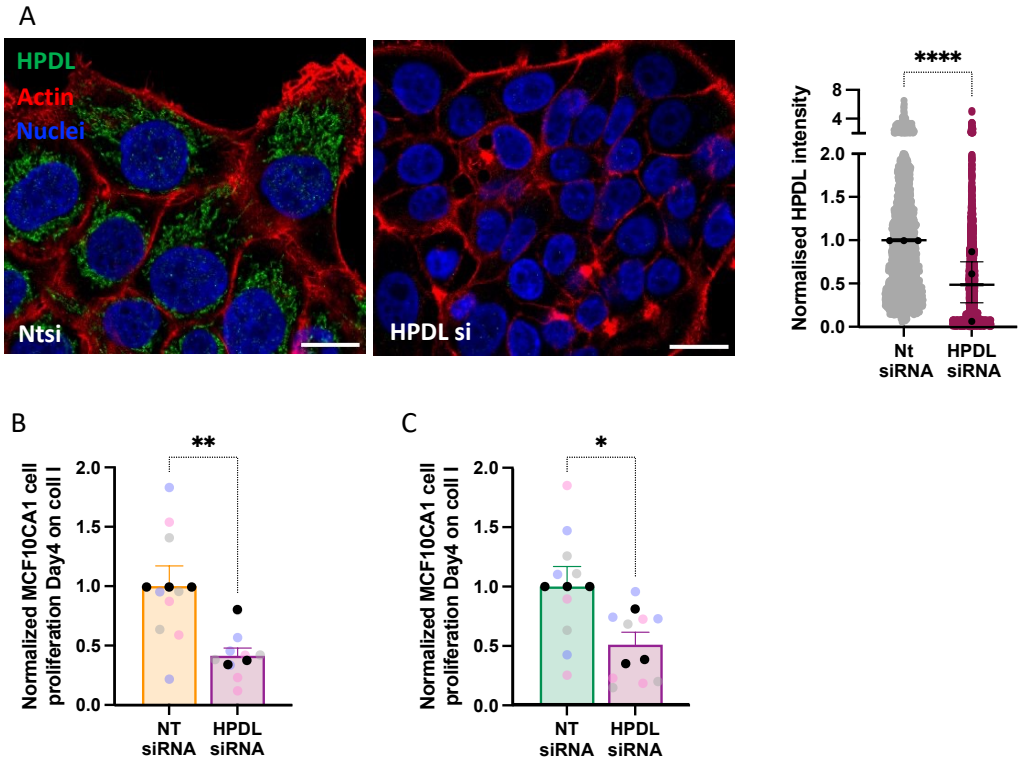

Figure 3-11 HPDL knockdown reduced coll I-dependent cell growth under starvation. MCF10CA1 cells were seeded on plastic in complete media in the presence of a non-targeting siRNA (Ntsi) or HPDL-siRNA (HPDLsi) (A). Cells were fixed and stained with HPDL (green), phalloidin (red) and DAPI (blue). Scale bar 20µm. HPDL mean intensity was measured using ImageJ software. N=3 independent experiments. MCF10CA1 cells were seeded on 2mg/ml collagen I, transfected with a non-targeting siRNA (Ntsi) or HPDL-siRNA (HPDLsi), under AA free (B) or Gln free media (C) for 4 days. Cells were fixed and stained with Hoechst 33342. The cells were imaged using an Image Xpress micro system and cell numbers were quantified with MetaXpress and CME software. N=3 independent experiments, values represent the Mean± SEM, the coloured dots for biological repeats, the black dots represent the mean of the individual experiments. Mann-Whitney test. *p < 0.05, **p < 0.01, ****p < 0.000.

3.3 Discussion:

According to the global cancer statistics in 2022, breast cancer is the second most common type of cancer worldwide with approximately 2.3 million new cases and 666,000 deaths (Bray et al., 2024). The development of breast cancer has been found to be accompanied by ECM remodelling which include changes in its composition and stiffness. This remodelling also plays an essential role in metastasis and drug resistance (Kaushik et al., 2016). For instance, the expression of procollagen I and III has been found to be increased during breast cancer malignancy and these are mainly produced by fibroblasts (Kauppila S et al., 1998). Collagen fibre reorganization changes during tumour progression, where they become more aligned in invasive carcinoma to facilitate the cells invasion and migration (Provenzano et al., 2006, Provenzano et al., 2008). However, little is known about the role of ECM in breast cancer metabolism. Herein we showed that invasive breast cancer cells under both AA and Gln starvation internalised ECM via macropinocytosis and degraded it into the lysosome, which in turn supported cells proliferation by promoting phenylalanine and tyrosine metabolism (Figure 3-12).

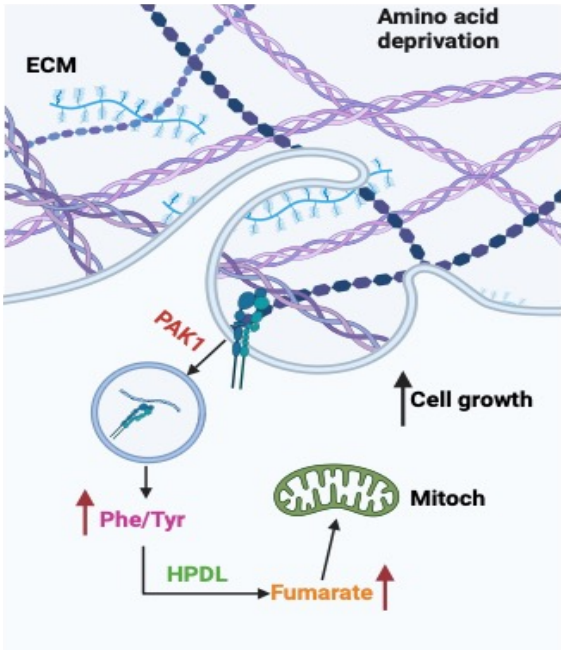

Figure 3-12 Schematic representation of ECM-dependent cell growth under AA starvation. Invasive breast cancer cells internalise and degrade ECM under AA starvation in a macropinocytosis dependent mechanism. The degradation of ECM increased phenylalanine and tyrosine metabolism leading to an HPDL-dependent cell growth. "Created in BioRender.com".

Here we showed that invasive breast cancer cells used collagen I, Matrigel and CDM as sources of nutrients when they were grown in media lacking either all AA or Gln. These results are in line with a previous study by Muranen et al where starved MCF10A mammary epithelial cells were shown to uptake laminin (Muranen et al., 2017). However, in their study a soluble laminin was used, while in ours we could show that MCF10CA1 cells internalised different types of 2D and 3D complex polymerised matrices, to better mimic the physiological ECM. MCF10CA1 cells are highly invasive breast cancer cells, and they were able to use both types of ECM, Matrigel (representing the basement membrane) and collagen I (representing the interstitial matrix). Suggesting that this process might favour both the breach through the basement membrane in the early stages of cancer invasion as well as the migration through the interstitial matrix during later stages. MCF10CA1 cells were derived from the mammary epithelial cells MCF10A, and they are part of a series of cells modelling breast cancer progression (Rhee et al., 2008). Our latest publication showed that collagen I did not enhance the growth of the mammary epithelial cells MCF10A or the non-invasive breast cancer cells MCF10A-DCIS under AA or Gln starvation. However, Matrigel significantly enhanced the growth of MCF10A-DCIS under Gln starvation (Nazemi et al., 2024). Hence, breast cancer cells start using the ECM during breast cancer progression gradually.

Most of ECM is secreted by cancer associated fibroblasts (CAFs). CDMs are 3D complex matrices that mimic the in vivo ECM, and they are naturally produced by fibroblasts (Cukierman E et al., 2001, Kaukonen et al., 2017). Our results showed that under starvation conditions the cells grew better on CDM as well compared to plastic. This indicate that our findings are also applicable in a more physiological environment. However, cell growth on collagen I and Matrigel was higher compared to the CDM. Similar results were observed in MDA-MB-231 breast cancer cells (Nazemi et al., 2024). This might be due to the need of the cells to rely on a specific type of ECM protein under certain conditions or due to the different physical and mechanical properties of 2D vs 3D matrices. In addition, the fibroblasts quality and the time of ECM production can play a role in the CDMs composition and stiffness (Kaukonen et al., 2017).

Our data shows that the ECM increased the division rate of MCF10CA1 cells under both starvation conditions. However, there was no effect on cell apoptosis. Similar results observed in MDA-MB-231 cells (Nazemi et al., 2024). A previous study by Badaoui et al showed that

under serum starvation, collagen I decreased MCF7 and T47D cells apoptosis. However, in their study, they measured the apoptotic rate after 24 hr and 48 hr (Badaoui M et al., 2018), while in our case we looked at a later time points (3 and 6 days) and this could indicate that the cells might have had more time to adapt to the starvation conditions. Another study by Maquoi et al showed that MCF7 apoptosis rate was increased when they were impeded in 3D collagen I gel for 7 days, however, there was no effect on MDA-MB-231 cells apoptosis (Maquoi et al., 2012). Both MCF7 and T47D cells are known for being less aggressive and poorly invasive, while MDA-MB-231 and MCF10CA1 cells are highly invasive breast cancer cells. Therefore, this might be the reason why the cell lines behave differently. Further studies are needed to confirm that the ECM does not affect cell apoptosis under AA starvation.

ECM can be degraded in two different ways; extracellularly via matrix metalloproteinases enzymes (MMPs) or intracellularly where ECM components can bind to their receptors, be internalised via different endocytic pathways and degraded into the lysosomes (Rainero, 2016). A recent study in our lab showed that invasive breast cancer cells internalise and degrade different types of ECM while they are migrating (Martinez et al., 2024). Our results confirm that as MCF10CA1 cells internalised and degraded collagen I in both complete and AA free media. Interestingly, the collagen uptake index was higher under AA starvation compared to complete media. This indicates that the cells require more ECM to be able to survive when they are starved.

Different approaches have been used to induce collagen crosslinking *in vitro*. Glutaraldehyde is one of the most commonly used, where the aldehyde groups bind to the amine groups in collagen to form a stable Schiff base (L. H. H. OLDE DAMINK et al., 1995). Glutaraldehyde can be toxic to the cells at long incubation time points, however, studies showed that short time points up to 6 hours can lead to efficient crosslinking results. Moreover, quenching glutaraldehyde with glycine can minimise its toxicity (Lai and Ma, 2013). Here we showed that crosslinking collagen I with glutaraldehyde for 30 min could completely abolish collagen I uptake under AA starvation. In addition, the cells were not able to grow under AA and Gln starvation when they were seeded on crosslinked collagen I. Crosslinking can also affect the ECM degradation via MMPs. However, inhibiting MMPs did not reduce the ECM-dependent

MDA-MB-231 cell growth (Nazemi et al., 2024). Overall, these results indicate that the ECM-dependent cell growth is, at least in part, due to its internalisation.

Macropinocytosis is a non-selective clathrin-independent endocytic pathway which can be induced by growth factors. Recently few studies showed that under nutrient deprivation, cancer cells uptake extracellular proteins via macropinocytosis (Recouvreux and Commisso, 2017). For instance, PDAC cells internalise albumin, the most abundant protein in the blood vessels, under glutamine starvation (Commisso et al., 2013). In addition, being surrounded by collagen rich matrices, PDAC cells also internalise collagen I and collagen IV under glucose or glutamine starvation conditions via macropinocytosis dependent and macropinocytosis independent pathways, respectively (Olivares et al., 2017). Furthermore, recent studies in our lab showed that MDA-MB-231 cells internalise different types of matrices via macropinocytosis (Nazemi et al., 2024, Martinez et al., 2024). PAK1 is a macropinocytosis regulator (Dharmawardhane S et al., 2000), it is overexpressed in some types of cancer, including breast cancer, and it is known for playing different roles during cancer progression. Therefore, several PAK1 inhibitors have been developed (Yao et al., 2020). Here we showed that inhibiting macropinocytosis via a PAK inhibitor (FRAX597) significantly reduced the uptake of CDM under AA starvation. Moreover, collagen I dependent cell growth was reduced after inhibiting and knocking-down PAK1 under both AA and Gln starvation. These results indicate that the ECM effects on cell growth are macropinocytosis dependent.

Studies showed that the composition and the stiffness of ECM can affect breast cancer metabolism. Indeed, highly metastatic breast cancer cells (4T1) demonstrated a reprograming in their metabolism in a high-density collagen matrix compared to a low density one. This was observed by an increase in the expression of the Tricarboxylic acid cycle (TCA) genes leading to an enhancement in Gln metabolism and use of Gln to fuel the TCA cycle. By contrast there was a decrease in the glycolysis gene expression (Morris et al., 2016). In addition, breast cancer progression from benign tumour to invasive ductal carcinoma (IDC) is accompanied by a metabolic adaptation. It has been observed that in IDC tissues, the level of some amino acids such as tyrosine and phenylalanine was increased which in turn increased tyrosine catabolism, while their concentration in the IDC serum was decreased, indicating that the demand for these metabolites is boosted during breast carcinoma progression (H. More T et al., 2018). Our

results also showed that under AA starvation, culturing cells on collagen I upregulated the intracellular AA levels under both AA and Gln starvation. Furthermore, phenylalanine/ tyrosine metabolism was increased in both conditions, which was confirmed by an increase in phenylalanine, tyrosine, and fumarate levels via targeted mass spectrometry. These results were also shown in MDA-MB-231 cells under AA starvation (Nazemi et al., 2024).

HPD and its paralog HPDL are enzymes involved in multiple metabolic pathways, including the phenylalanine/ tyrosine catabolism. The expression of both enzymes has been found to be increased in different types of cancer, and they affect cancer cell growth in breast cancer (Wang et al., 2019) and in Pancreatic cancer (Ye et al., 2020). Similarly in our study, HPDL knockdown significantly reduced MCF10CA1 and MDA-MB-231 cells proliferation on collagen I under both AA and Gln starvation. Furthermore, HPDL knockdown reduced the fumarate level on collagen I under AA starvation in MDA-MB-231 cells (Nazemi et al., 2024). Fumarate was not the only TCA metabolite which was detected in our metabolic profile but also malate, citrate and isocitrate were among the metabolites that were identified to be increased on collagen I compared to plastic under AA starvation, indicating that collagen I could be a source to fuel the TCA cycle under nutrient starvation.

In this chapter we showed that under AA starvation, the ECM supported invasive breast cancer cell growth. This growth was shown to be due to an increase in ECM uptake via macropinocytosis, which in turn upregulated phenylalanine/ tyrosine catabolism leading to the production of fumarate to fuel the TCA cycle.

4 The ECM supported cell growth under glucose starvation

4.1 Introduction:

Normal cells obtain energy by transforming glucose to pyruvate via the glycolysis process and then pyruvate is converted into CO_2 in the mitochondria through the Tricarboxylic acid cycle (TCA); this process generates 36 moles of Adenosine Triphosphate (ATP) per mole of glucose. Usually this is regulated by growth factors stimulation driving cell growth in the presence of oxygen. (Pelicano et al., 2006). One of the alterations in cancer is that cancer cells heavely rely on the glycolysis process to obtain energy. In cancer cells, the uptaken glucose is not only used to generate ATP but also to activate new metabolic pathways which eventually produce precursors that can be used to build lipids, nucleic acids and proteins (Thompson, 2011). The increase in glucose uptake is believed to be due to different alterations in cancer cells such as mitochondria defects and oncogenes stimulations (Pelicano et al., 2006). For instance, KRAS G12D oncogene in PDAC cells inhances the uptake of glucose via GLUT1 (encoding glucose transporter 1) and this has been found to be regulated by MAPK pathway and the cMYC transcription factor (Ying et al., 2012). Similarly in colorectal cancer, GLUT1 was upregulated in mutated KRAS or BRAF cells and these cells survived in low glucose conditions compared to the wild type ones (Yun et al., 2009). In addition, the activation of AKT downstream of PI3K via insulin stimulation increases the translocation of GLUT4 to the cell surface (Cong Li-Na et al., 1997). Furthermore, the activation of AKT has been shown to increase the expression of GLUT1 which in turn led to the inhibition of cell apoptosis (Barthel et al., 1999). This increase in the glucose demand by cancer cells can lead to a glucose scaricity in the tumour microenvironment. Indeed, it was previously shown that glucose concentration was extremly low in colon cancer, stomach cancer tissues (Hirayama et al., 2009) and in pancreatic cancer (Kamphorst et al., 2015).

However, studies showed that cancer cells can reprogarm their metabolism and continue to grow under glucose deprivation. For instance, Endo et al showed that glucose withdrwal activated LKB1-AMPK pathway in cancer cells, which in turn induced autophagy leading to an increase in cell migration and invasivness, which was mediated by an increase in Nrf2 activation and MMP9 expression (Endo et al., 2018). Moreover in ovarian cancer cells, glucose deprivation

triggered the internalisation and lysosomal degradation of α5β1 intergin bound to fibronectin, which in turn promoted cell migration (Rainero et al., 2015).

In this chapter, we investigated the role of different types of ECM on breast cancer cell growth under glucose starvation and we found that ECM enhanced cell growth. This effect could be a combination of ECM uptake and a signalling effect mediated by integrins, and was associated with an increase in intracellular amino acid content.

4.2 Results:

4.2.1 ECM partially rescued the growth of MCF10CA1 cells under glucose starvation

We previously showed that the ECM partially rescued breast cancer cell growth under AA starvation **(Chapter 3)** (Nazemi et al., 2024). To investigate the effect of ECM on breast cancer cell growth under glucose (Glc) starvation MCF10CA1 cells were seeded on plastic vs collagen I **(Figure 4-1, A-B)** or plastic vs Matrigel **(Figure 4-1, C-D)** under Glc starvation. The growth of the cells was monitored for up to 6 days. Both collagen I and Matrigel significantly increased cell growth under Glc starvation compared to plastic.

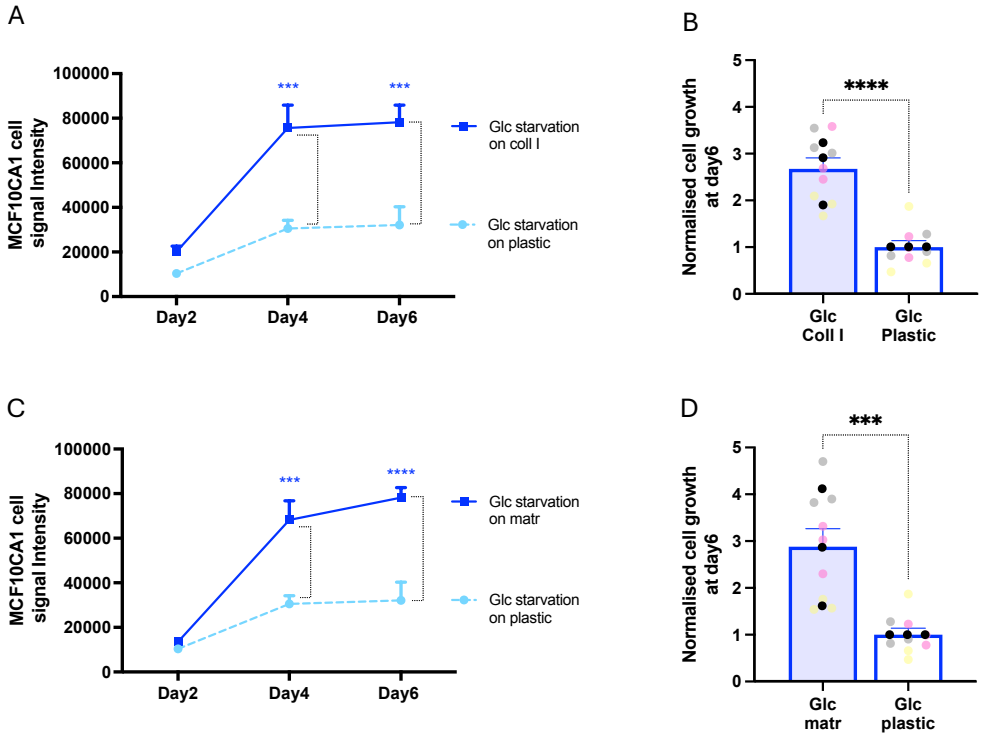

Figure 4-1 Collagen I and Matrigel partially rescued MCF10CA1 cell growth under Glc starvation. MCF10CA1 cells were seeded on 2 mg/ml collagen I vs plastic (A-B) and on 3 mg/ml Matrigel vs plastic (C-D) under glucose (Glc) free media for 6 days. Cells were fixed at day 2, 4, and 6, the nuclei were stained with DRAQ5, the signal intensity was measured using a Licor Odyssey system and quantified with Image Studio Lit software. N=3 independent experiments, values represent the Mean± SEM, the coloured dots for biological repeats, the black dots represent the mean of the individual experiments. (A, C) Two-Way ANOVA, Tukey's multiple comparisons test. (B, D) Mann-Whitney test. ***$p < 0.001$, ****$p < 0.0001$.

To further invistigate the role of ECM on cell growth in a more physiological environment, MCF10CA1 cells were seeded on plastic vs CAF-CDM **(Figure 4-2, A-B)** under Glc starvation for up to 6 days. The results show that seeding cells on CDM trasiently promoted their growth under Glc starvation compared to plastic. Indeed, we detected a significant increase in cell numbers at day 4, followed by drastic decrease at day 6. Interestingly, the effect of collagen I and Matrigel was stronger than CDM. This could be due to the complextiy of CDM composition and indicating that the cells might more rely on some ECM components than others when they are starved.

Overall, the results show that the ECM plays a role in supporting cell growth under Glc starvation.

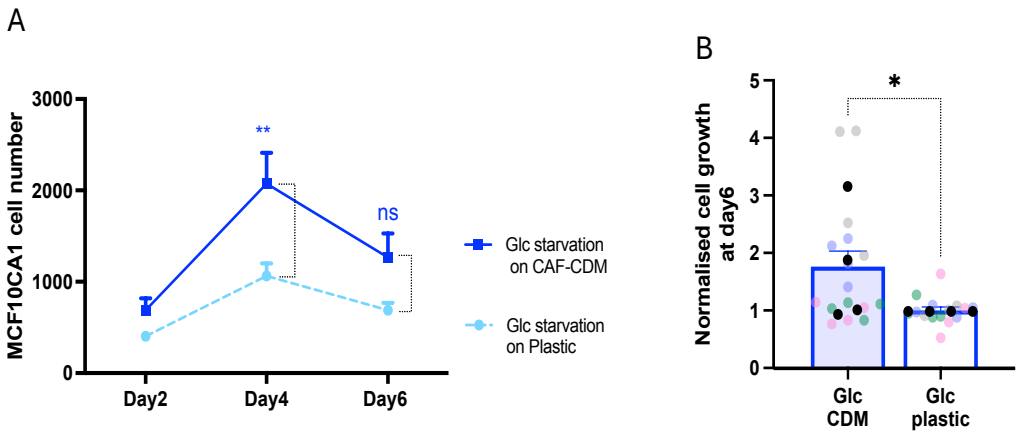

Figure 4-2 CDM partially rescued MCF10CA1 cell growth under Glc starvation. MCF10CA1 cells were seeded on CAF-CDM vs plastic in Glc free media for 6 days. Cells were fixed at day 2, 4, and 6 and the nuclei were stained with Hoechst 33342. The cells were imaged using an Image Xpress micro system and cell numbers were quantified with MetaXpress and CME software. N=4 independent experiments, values represent the Mean ± SEM, the coloured dots for biological repeats, the black dots represent the mean of the individual experiments. (A) Two-Way ANOVA, Tukey's multiple comparisons test. (B) Mann-Whitney test. ns: non-significant, *$p < 0.05$, **$p < 0.01$.

4.2.2 ECM partially rescued the growth of MCF10CA1 cells under glucose & glutamine starvation

Glc and Gln are the most important nutrients that cancer cells rely on to grow. To investigate whether the ECM also supported the growth of cancer cells in an environment lacking both Glc and Gln, MCF10CA1 cells were seeded on plastic vs collagen I **(Figure 4-3, A-B)** or plastic vs Matrigel **(Figure 4-3, C-D)** under Glc & Gln starvation. Cell growth was monitored for up to 6 days. Both collagen I and Matrigel increased cell numbers under Glc & Gln starvation compared to plastic. The normalised cell growth rate at day 6 showed that both matrices significantly

enhanced cell growth; however, collagen I was more efficient than Matrigel. Hence, even under harsh starvation conditions, the ECM supported cancer cell growth.

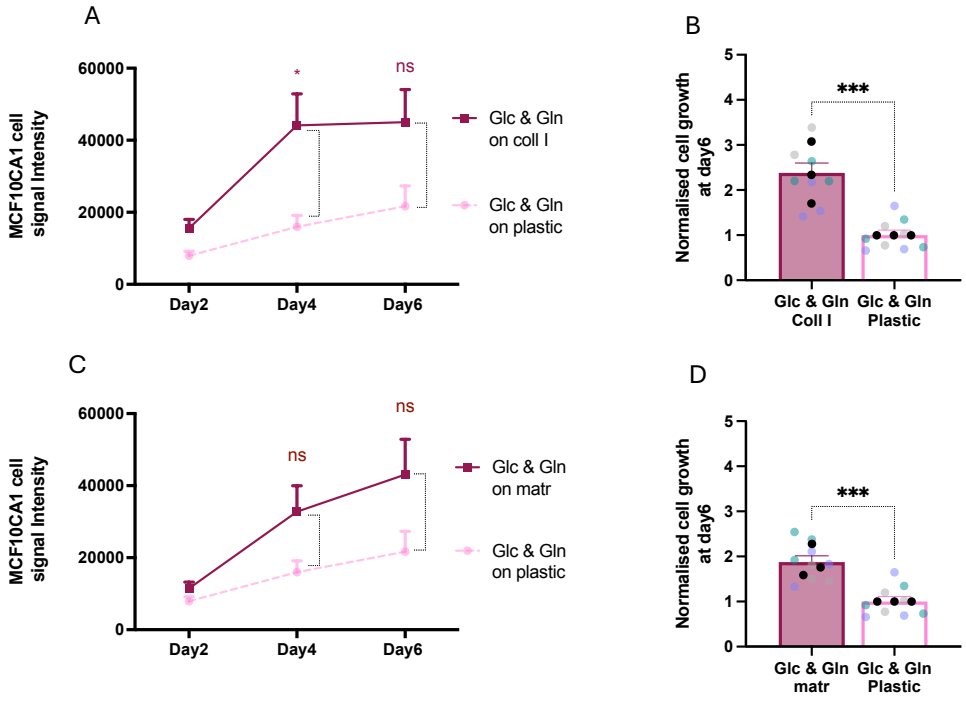

Figure 4-3 Collagen I and Matrigel partially rescued MCF10CA1 cell growth under Glc & Gln starvation. MCF10CA1 cells were seeded on 2 mg/ml collagen I vs plastic (A-B) and on 3 mg/ml Matrigel vs plastic (C-D) under glucose (Glc) & glutamine (Gln) free media for 6 days. Cells were fixed at day 2, 4, and 6, the nuclei were stained with DRAQ5, the signal intensity was measured using a Licor Odyssey system and quantified with Image Studio Lit software. N=3 independent experiments, values represent the Mean ± SEM, the coloured dots for biological repeats, the black dots represent the mean of the individual experiments. (A, C) Two-Way ANOVA, Tukey's multiple comparisons test. (B, D) Mann-Whitney test. ns: non-significant, *p < 0.05, ***p < 0.001.

4.2.3 ECM induced MCF10CA1 cell division and reduced cell apoptosis under Glc starvation

Previously we showed that the ECM enhanced breast cancer cell proliferation under amino acid starvation, without affecting apoptosis **(Chapter 3)** (Nazemi et al., 2024). To test whether this was the case under Glc starvation, MCF10CA1 cells were seeded on collagen I, Matrigel or plastic in Glc free media for 4 days, followed by a two-day incubation in the presence of EdU. Both collagen I and Matrigel significantly enhanced the percentage of EdU positive cells under Glc starvation **(Figure 4-4, A)**. Alternatively, cells were seeded on collagen I, Matrigel or plastic in Glc free media for up to 6 days. Cells were then stained for cleaved caspase 3/7 and the number of cells positive was measured at day 3 **(Figure 4-4, B)** and day 6 **(Figure 4-4, C).** The quantifications show that both matrices reduced the percentage of cleaved caspase 3/7 positive cells after 6 days incubation in Glc free media, while no change was detected at day 3

(Figure 4-4). Overall, our data show that ECM resulted in increased cell numbers under Glc starvation via both promoting cell division and reducing apoptosis.

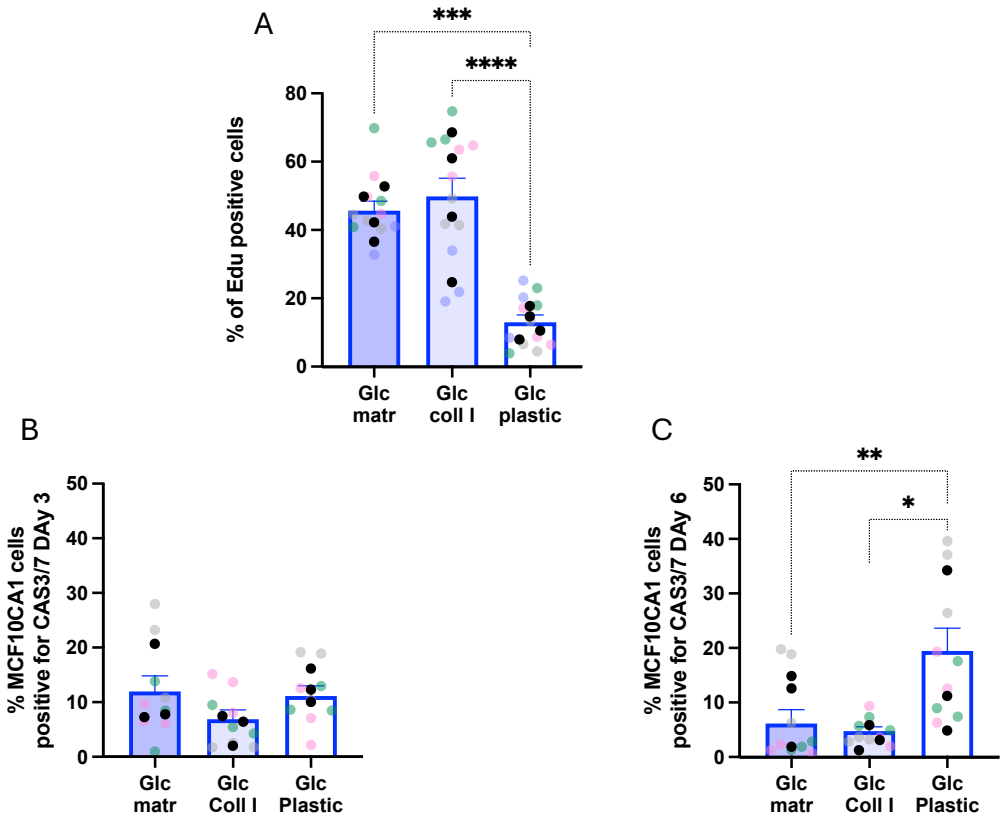

Figure 4-4 ECM increased MCF10CA1 cell division and decreased apoptosis under Glc starvation. MCF10CA1 cells were seeded on 2 mg/ml collagen I, 3 mg/ml Matrigel or plastic in Glc free media for 4 days, followed by 2 days in the presence of 5μM EdU (A). Cells were fixed and stained with Click iT Edu Kit and Hoechst 33342. MCF10CA1 cells were seeded on 2 mg/ml collagen I, 3 mg/ml Matrigel or plastic in Glc free media for 3 (B) or 6 (C) days then media was changed to PBS containing 5μM Cell Event Caspase-3/7 Green Detection Reagent for 1 hour 30 mins. Cells were fixed and stained with Hoechst 33342. The cells were imaged using an Image Xpress micro system and the percentage of EdU- or Caspase 3/7-positive cells was quantified with MetaXpress and CME software. N≥3 independent experiments, values represent the Mean± SEM, the coloured dots for biological repeats, the black dots represent the mean of the individual experiments. Kruskal-Wallis, Dunn's multiple comparisons test. *p < 0.05, **p < 0.01, ***p < 0.001, ****p < 0.000.

4.2.4 Chemical cross-linking had a small effect on collagen I- mediated cell growth under Glc starvation

We showed that MCF10CA1 cells were able to uptake and degrade collagen I Section 3.2.3 and chemically cross-linking collagen I completely abolished collagen I uptake and ECM-dependent cell growth under AA starvation. To investigate whether collagen I crosslinking also affected MCF10CA1 cell growth under Glc or Glc and Gln starvation, cells were seeded on plastic, collagen I or crosslinked collagen I for up to 6 days. The results show that seeding cells in Glc free media on x-linked collagen I slightly reduced cell growth, but the decrease was not

statistically significant **(Figure 4-5, A-B).** Interestingly, when cells were grown in an environment deprived of both Glc and Gln, cross-linking collagen I significantly reduced ECM-dependent cell growth **(Figure 4-5, C-D)**.

Overall, these results indicate that chemically cross-linking collagen I only mildly affected cell growth under Glc starvation, but under the harsher Glc & Gln starvation cross-linking collagen I significantly impaired cell growth. Therefore, the ECM-dependent cell growth under Glc starvation might also be a result of adhesion signalling, in addition to ECM endocytosis.

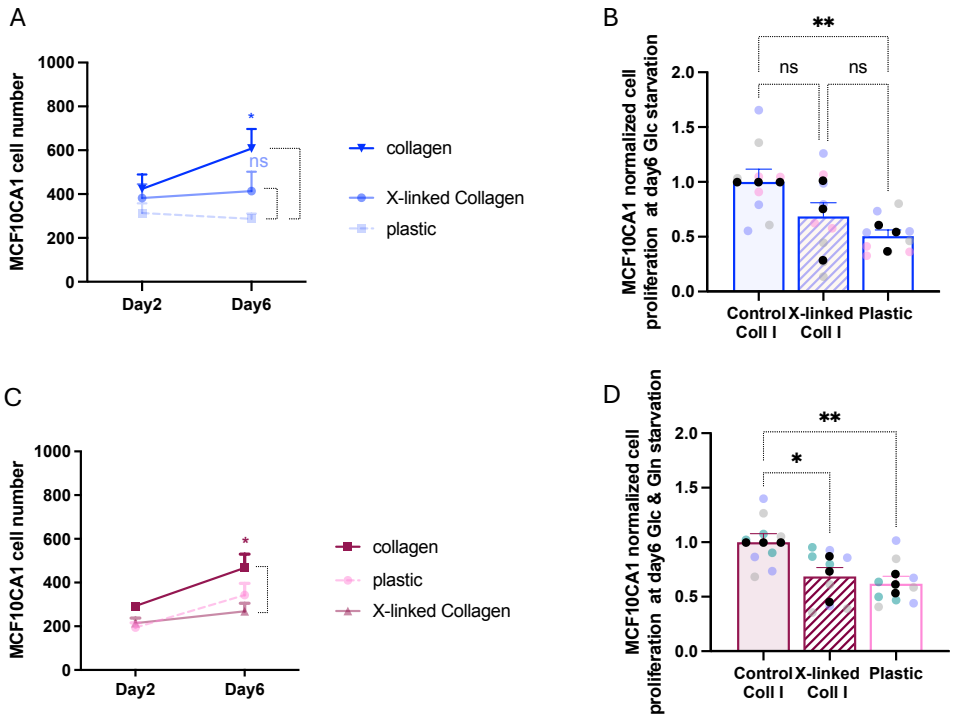

Figure 4-5 Collagen I cross-linking slightly reduced MCF10CA1 cell growth under Glc or (Glc & Gln) starvation. MCF10CA1 cells were seeded on 2 mg/ml collagen I or crosslinked collagen I (X-linked coll I) vs plastic under Glc free (A-B) or Glc & Gln free media (C-D) for 6 days. Cells were fixed at day 2, and 6 and stained with Hoechst 33342. The cells were imaged using an Image Xpress micro system and cell numbers were quantified with MetaXpress and CME software. N=3 independent experiments, values represent the Mean± SEM, the coloured dots for biological repeats, the black dots represent the mean of the individual experiments. (A) Two-Way ANOVA, Tukey's multiple comparisons test. (B) Kruskal-Wallis, Dunn's multiple comparisons test. ns: non-significant, *p < 0.05, **p < 0.01.

4.2.5 ECM-dependent cell growth might be independent of macropinocytosis

Chemically cross-linking collagen I only mildly affected cell growth under Glc starvation indicating that ECM endocytosis might not play a key role in ECM-dependent cell growth under Glc starvation. We have previously shown that ECM-dependent cell growth under AA starvation was mediated by macropinocytosis **Section 3.2.4** (Nazemi et al., 2024). To investigate whether this was the case under Glc starvation, MCF10CA1 cells were seeded on collagen I for up to 4 days in the presence of DMSO or FRAX597 under Glc starvation **(Figure 4-6,A)**. MCF10CA1 cells

were also seeded on collagen I, after performing a PAK1 siRNA knockdown, under Glc starvation (Figure 4-6,B) for up to 4 days. The results show that inhibiting PAK significantly reduced the collagen I-dependent cell growth under Glc starvation, however, knocking-down PAK1 resulted in a samll, but not statistically significant, reduction in cell growth. These results suggest that ECM-dependent cell growth under Glc starvation might mostly be regulated by adhesion signalling. Given the variability in the data, further studies are needed to investigate wether collagen I internalistaion is involved in ECM-dependent cell growth under Glc staravtion, and, if so, which endocytic mechansim is responsible for this effect.

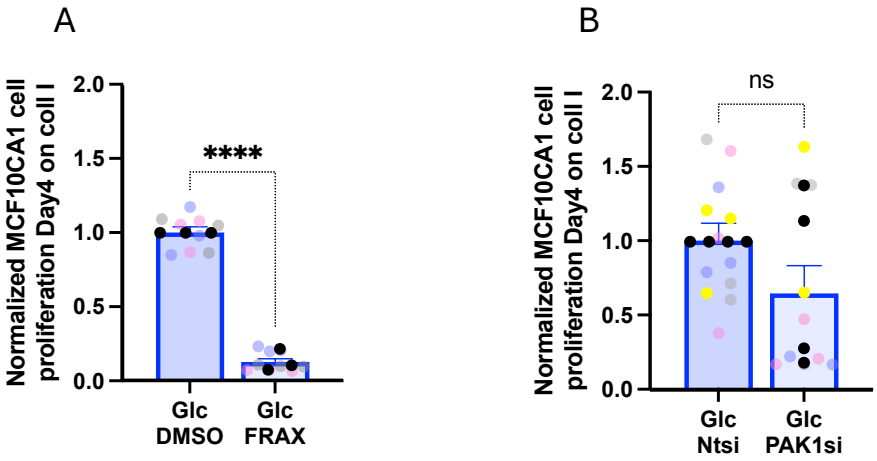

Figure 4-6 ECM-dependent MCF10CA1 cell growth might be macropinocytosis independent. MCF10CA1 cells were seeded on 2 mg/ml collagen I in Glc free media in the presence of DMSO or 1µM FRAX 597 (A). MCF10CA1 cells were seeded on 2 mg/ml collagen I, transfected with a non- targeting siRNA (Ntsi) or PAK1-siRNA (PAK1si), in Glc free media (B) for 4 days. Cells were fixed at day 4 and stained with Hoechst 33342. The cells were imaged using an Image Xpress micro system and cell numbers were quantified with MetaXpress and CME software. N≥3 independent experiments, values represent the Mean ± SEM, the coloured dots for biological repeats, the black dots represent the mean of the individual experiments. Mann-Whitney test ns: non-significant, ****$p < 0.0001$.

4.2.6 α2β1 integrin is required for ECM dependent cell growth under Glc starvation.

α2β1 integrin is the major collagen binding receptor, and its expression has been found to be upregulated in some types of cancer including invasive breast cancer (Naci et al., 2015, Moritz et al., 2021)

To investigate whether the ECM-dependent cell growth was integrin-dependent, MCF10CA1 cells were seeded on collagen I for 4 days under Glc starvation in the presence or absence of BTT-3033, a pharmacological inhibitor of α2β1 integrin which prevents its binding to collagen. The results show that inhibiting α2β1 integrin significantly inhibited ECM-dependent cell

growth **(Figure 4-7, A)**. To validate these results, the cells were seeded on collagen I for 4 days in Glc starvation media after performing an siRNA mediated knockdown of α2 integrin. Western blot analysis confirmed a significant reduction of α2 protein levels in knockdown cells **(Figure 4-7, E).** α2 downregulation significantly reduced ECM-dependent cell growth under Glc starvation **(Figure 4-7, C)**. Similarly in complete media, both pharmacological inhibition of α2β1 integrin **(Figure 4-7, B)** and siRNA-mediated knockdown of α2 subunit **(Figure 4-7,D)** significantly reduced the ECM-dependent cell growth.

Overall, these results indicate that α2β1 integrin is required for cell growth on collagen I regardless of the nutrient starvation.

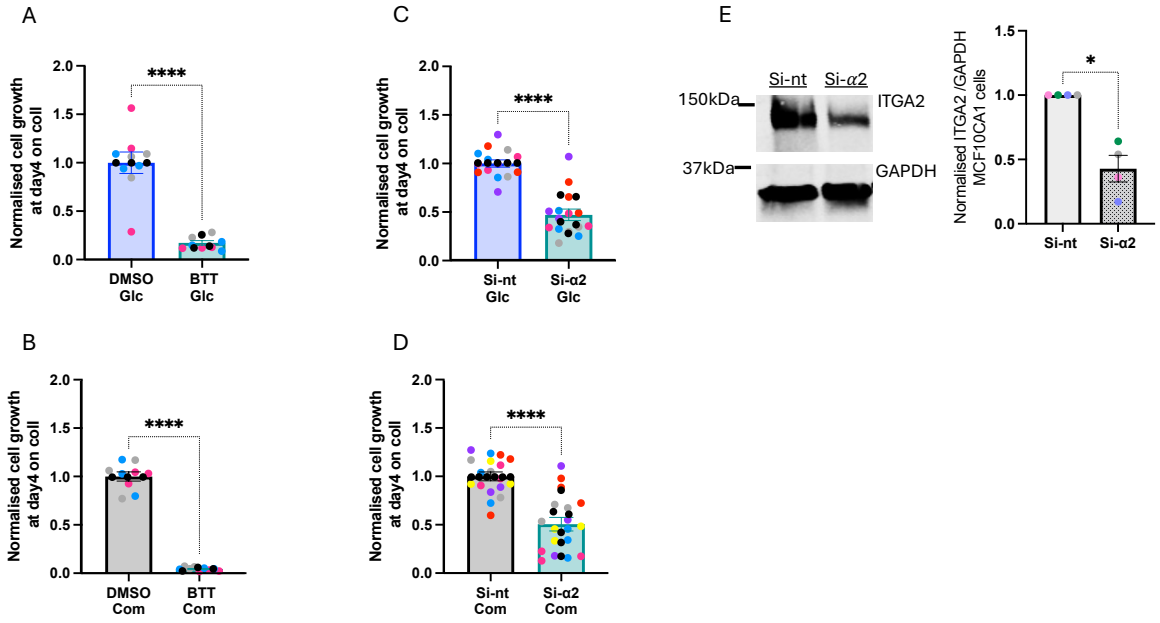

Figure 4-7 α2β1 integrin inhibition opposed the ECM-dependent cell growth. MCF10CA1 cells were seeded on 2 mg/ml collagen I in Glc free media (A) or complete media (Com, B) for 4 days in the presence of DMSO (control) or 15μM BTT-3033. MCF10CA1 cells were seeded on 2 mg/ml collagen I, transfected with an siRNA targeting α2 integrin (si-α2) or a non-targeting siRNA (si-nt) as a control, for 4 days under Glc starvation (C) or complete media (Com, D). Cells were fixed at day 4 and stained with Hoechst 33342. The cells were imaged using an Image Xpress micro system and cell numbers were quantified with MetaXpress and CME software. MCF10CA1 cells were seeded on plastic, transfected with an siRNA targeting α2 integrin (si-α2) or a non-targeting siRNA (si-nt) as a control. Cell lysates were collected after 72 hours, samples were run by Western Blotting, membranes were stained for α2 (ITGA2) and GAPDH and imaged with a Licor Odyssey system. The protein band intensity was measured with Image Studio Lite sofware (E). N≥ 3 independent experiments, values represent the Mean± SEM, the coloured dots for biological repeats, the black dots represent the mean of the individual experiments. Mann-Whitney test. *p < 0.05, ****p < 0.0001.

4.2.7 ECM-dependent cell growth under Glc starvation is associated with upregulation of amino acid-related metabolic pathways.

We have previously shown that the ECM upregulate several intracellular AA in breast cancer cells under AA starvation compared to plastic **Section 3.2.5**. To investigate whether the ECM affected the intracellular metabolite content under Glc starvation, MCF10CA1 cells were seeded on plastic or on collagen I for up to 6 days under Glc starvation and non-targeted mass spectrometry was performed to measure the intracellular metabolite content at day 1 **(Figure 4-8)** and day 6 **(Figure 4-9)** of starvation. We detected significant changes in the metabolome at both time points. Indeed, 569 metabolites and 512 metabolites were upregulated on collagen I at day 1 and day 6, respectively. The enrichment pathway analysis of the upregulated metabolites on coll I showed that glycine, serine and threonine metabolism, arginine and proline metabolism and alanine, aspartate and glutamate metabolism were among the highest metabolic pathways at both day 1 **(Figure 4-8, B)** and day 6 **(Figure 4-9, B)** under Glc starvation. Having a closer look at the intracellular AA levels, we found that most AA were upregulated on collagen I, with threonine and glycine being the most strongly upregulated **(Figure 3-8, C; Figure 4-9, C)**.

Overall, the results show that seeding cells on collagen I under Glc starvation for 6 days could upregulate intracellular metabolites involved in the amino acids metabolism.

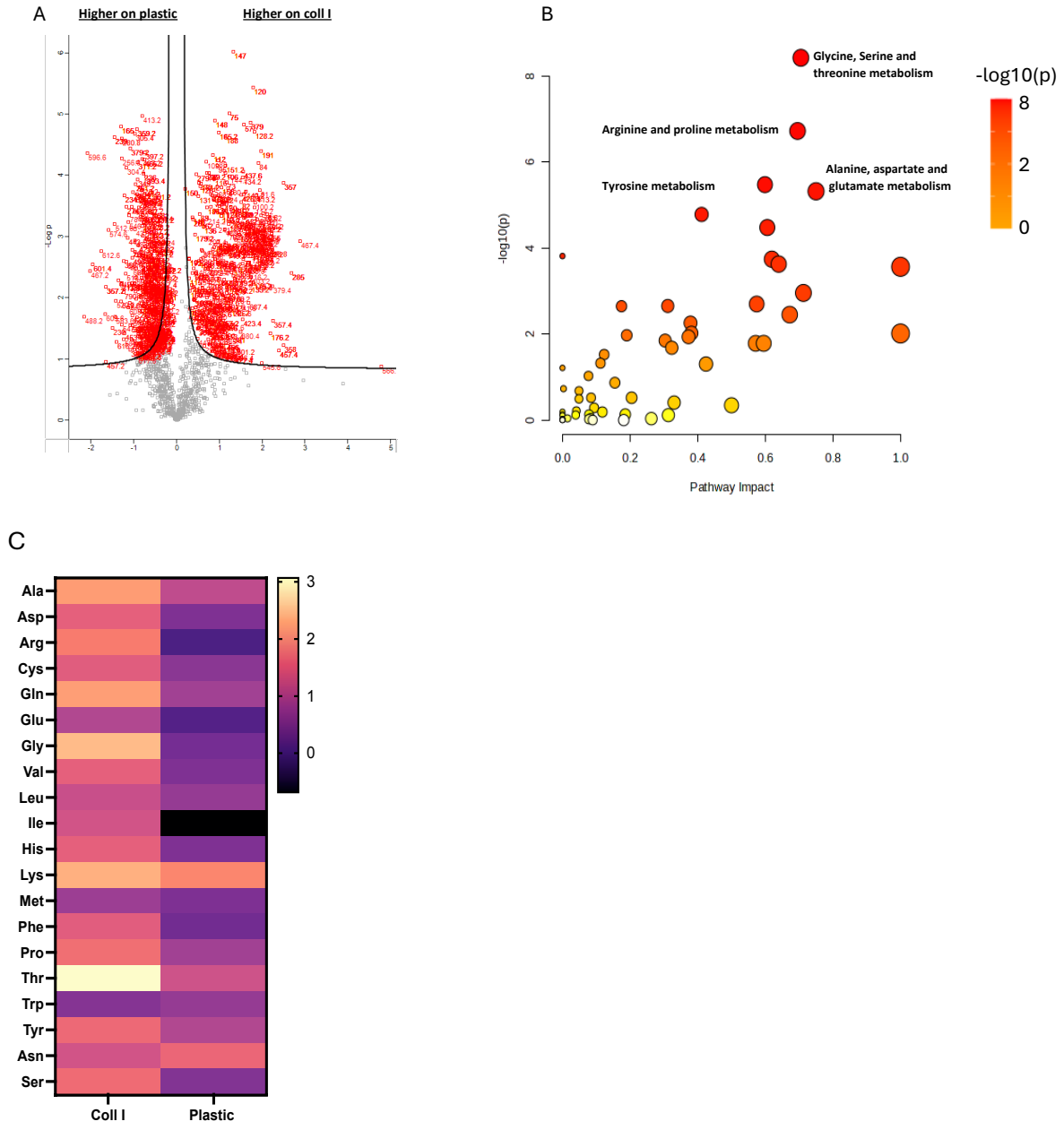

Figure 4-8 MCF10CA1 cells on collagen I switch to amino acid metabolism at day 1 of Glc starvation. MCF10CA1 cells were seeded in Glc free media on 2 mg/ml collagen I vs plastic for 1 day. Metabolites were extracted at day 1 and quantified with non-targeted mass spectrometry. Volcano blot (A) enriched metabolic pathways (B). Heatmap of amino acids changes on 2 mg/ml coll I vs plastic (C). (A) analysed using Perseus software at S0 0.1. (B) analysed using MetaboAnalyst 5.0 https://www.metaboanalyst.ca.

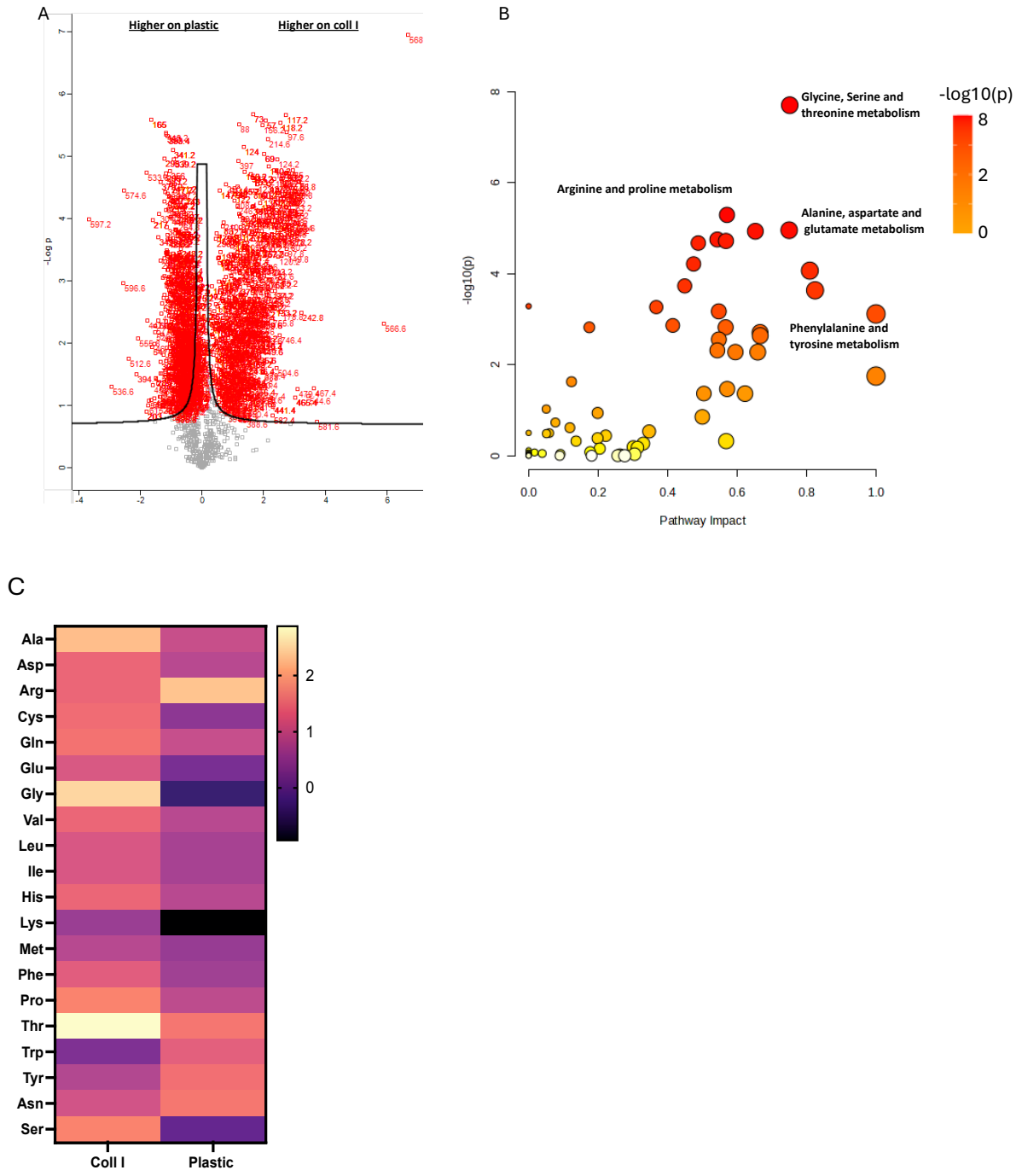

Figure 4-9 MCF10CA1 cells on collagen I switch to amino acid metabolism at day 6 of GLC starvation. MCF10CA1 cells were seeded in Glc free media on 2 mg/ml collagen I vs plastic for 6 days. Metabolites were extracted at day 6 and quantified with non-targeted mass spectrometry. Volcano blot (A) enriched metabolic pathways (B). Heatmap of amino acids level on 2 mg/ml coll I vs plastic (C). (A) analysed using Perseus software at S0 0.1. (B) analysed using MetaboAnalyst 5.0 https://www.metaboanalyst.ca.

4.3 Discussion:

In this chapter we showed that the ECM partially rescued MCF10CA1 breast cancer cell growth under Glc starvation. This ECM-dependent cell growth was due to both an increase in cell division and a decrease in cell apoptosis. Interestingly, chemically crosslinking collagen I and macropinocytosis inhibition only mildly affected ECM-dependent cell growth, while both pharmacological inhibition and siRNA-mediated knockdown of the collagen receptor $\alpha 2\beta 1$ integrin significantly reduced cell growth, suggesting that the ECM effect might be a combination of adhesion signalling and endocytosis.

A previous study showed that starving different types of cancer cells in media containing 6 mmol/l glucose and 0.6 mmol/l glutamine instead of 25.5 mmol/l and 4 mmol/l respectively affected cell growth for up to 30 days of starvation, but then the cells started to proliferate, and their growth was stabilised (Mathews et al., 2020). Thus, we performed our experiments in glucose free media. Our results showed that seeding MCF10CA1 cells on both collagen I and Matrigel partially rescued cell growth compared to plastic. Interestingly, the CDM effect was lower and transient, as the cell number was increased at day 4, then there was a reduction at 6 days. This could be due to the CDM composition and stiffness thus the different physical and mechanical properties of 2D vs 3D matrix.

Our data showed that the ECM-dependent cell growth under Glc starvation was due to both an increase in cell division and a decrease in cell apoptosis. The same results were obtained regardless of the substrate, as both collagen I and Matrigel increased MCF10CA1 cell division and decreased cell apoptosis. It is already known that Glc starvation can trigger cell death. For instance, withdrawing Glc from the media of Glc-dependent cancer cells triggered ROS mediated apoptosis (Graham et al., 2012). This has been found to be accompanied by ATP reduction (Kang et al., 2023). Interestingly, 24 hours Glc starvation of Glc-independent cancer cells, such as PDAC cells, did not cause ATP reduction or cell apoptosis. These cells generate ATP by using fatty acids; therefore, they rely on fatty acid oxidation instead of glycolysis (Lee et al., 2020). However, it is worth noting that ECM was not included in the above-mentioned studies. Entosis is another cell death mechanism where a living cell targets and internalises a neighbouring cell to obtain nutrients under starvation conditions. In a previous study, breast cancer cells were shown to survive and proliferate under Glc starvation in an entosis-dependent

manner. Glc deprivation was shown to trigger entosis via an AMP-activated protein kinase (AMPK)-dependent mechanism (Hamann et al., 2017). Therefore, it would be interesting to test whether the ECM is involved in controlling entosis under Glc starvation.

Recently we showed that breast cancer cells can internalise and degrade ECM components to survive under AA starvation **(Chapter 3)** (Nazemi et al., 2024). Here, chemically cross-linking collagen I slightly reduced collagen I-dependent cell growth under Glc starvation. This indicate that the ECM effect might be due to its internalisation, but this is not the main/only mechanism that is leading to the cell's survival. Previous studies showed that under Glc deprivation, cells can uptake extracellular components. For instance, non-small cells lung cancer (NSCLC) proliferated and survived under Glc deprivation, and this was shown to be mediated by the internalisation of extracellular proteins via macropinocytosis in a RAC-PAK dependent mechanism. The level of the AA alanine, which can feed the TCA cycle, has been shown to be increased intracellularly due to the degradation of extracellular proteins under Glc starvation. The NSCLC internalisation and degradation of extracellular proteins such as albumin was more effective and promoted cells proliferation better than free exogenous alanine (Hodakoski et al., 2019). Interestingly, alanine is one of the intracellularly upregulated amino acids in our study.

Furthermore, PTEN knockout MEFs internalised both Dextran and Albumin when they were cultured in a medium containing only 1% AA and Glc and this stimulated cell growth. Interestingly, the effect was due to Glc withdrawal rather than AA and was shown to be mediated by AMPK activation (Kim et al., 2018). Another study by Olivares et al showed that PDAC cells internalised collagen I and IV under Glc starvation and use the collagen derived proline to survive and proliferate (Olivares et al., 2017). However, in this study collagen fragments were used which does not mimic the physiological ECM while in our study we used intact collagen I. Similarly, Glc deprivation of Rab25 overexpressing ovarian cancer cells triggered the translocation of $\alpha5\beta1$ centripetally and increased its internalisation in a tensin dependent mechanism. Mimicking the nutrient starvation effect by inhibiting mTORC1 promoted fibronectin bound $\alpha5\beta1$ internalisation and localisation to the late endosomes which in turn promoted ovarian cancer cells invasion and migration (Rainero, 2016). However, in this study the cells were starved for 2 hours, while in our study, the cells were kept in Glc free media for up to 6 days, indicating that ECM internalisation might be an acute effect only. By using FRAX 597, a macropinocytosis inhibitor, collagen I dependent cell growth under Glc starvation was reduced, however, the siRNA-mediated knockdown of PAK1 did not affect the cell growth. PAK1

is a macropinocytosis regulator (Dharmawardhane S et al., 2000). FRAX597 is an inhibitor of PAK (1, 2, and 3) family members. Hence, it would be important to test an additional macropinocytosis inhibitor as well as assess the roles of other PAK family members. The fact that FRAX597 treatment resulted in much stronger inhibition of cell growth compared to nutrient cross-linking suggest that the macropinocytosis of soluble proteins, like BSA, might play a role. Consistent with this, data from our lab suggest that collagen I promotes dextran uptake (Zhe Bao, unpublished), while $\alpha 2\beta 1$ is required for dextran uptake when cells are seeded on collagen I (Martinez et al., 2024). Studies in our lab showed that MDA-MB-231 cell growth under Glc starvation was not mediated by ECM internalisation (Nazemi, 2020). Further studies are needed to confirm if MCF10CA1 breast cancer cells are able to internalise ECM components under Glc starvation and what the molecular mechanisms mediating this are.

It is already known that ECM remodelling and crosslinking increase during cancer progression and this in turn can promote ECM stiffness, adhesion clustering and integrin signalling (Levental et al., 2009). Previous studies showed that ECM stiffness can affect cancer cell metabolism (Ge et al., 2021). Seeding MDA-MB-231 breast cancer cells and A549 lung cancer cells, which are rigidity dependent cells, on a soft polyacrylamide hydrogel substrate coated with collagen I resulted in a slower growth due to an extension in the G1 phase, which led to a longer cell cycle comparing to stiff hydrogels. These observations were accompanied by a reduction in the ATP level. Interestingly, a variety of proteins showed sensitivity to changes in ECM stiffness such as proteins involved in the ATP production and in Glc metabolism (Tilghman et al., 2012). Similarly, by measuring nicotinamide adenine dinucleotide (NADH) florescence lifetime, Mah et al found that the metabolic state of MDA-MB-231 cells shifted from OXPHOS to Glycolysis when cells were plated on 3 mg/ml stiff collagen comparing to 1.2 mg/ml soft collagen**.** Interestingly, the less invasive breast cancer cells MCF7 and T-47D did not show any metabolic changes (Mah et al., 2018). On the contrary, changes in the expression of genes involved in breast cancer metabolism have been observed when metastatic breast cancer cells were plated on a high-density collagen substrate (3.5 mg/ml collagen). Both oxygen consumption and Glc metabolism were reduced, and this was not due to a change in Glc uptake but rather a change in the cell's utilization of Glc. In a higher collagen density, the cells relied on another source to fuel the TCA cycle which was Gln in this case (Morris et al., 2016). Furthermore, cells respond to stiff ECM by increasing actin fibres and focal adhesion complexes. For this to happen, the cells consume more energy leading to a drop in the intracellular ATP level and activating AMPK. Interestingly,

after few hours the intracellular ATP level recovers due to an increase in Glc uptake, YAP/TAZ nuclear localization and cell spreading (Xie et al., 2021). However, in case of Glc deprivation, we hypothesise that cancer cells rely on other extracellular nutrients to increase intracellular ATP level such as amino acids. Indeed, YAP/TAZ was shown to increase glutaminolysis by upregulating Glutaminase (GLS) and the aspartate/glutamate transporter SLC1A3 (Bertero et al., 2019). Similarly, in invasive breast cancer cells, multiple genes involved in Gln metabolism were downregulated after YAP/TAZ knockdown which in turn affected cell growth. YAP/TAZ have been shown to regulate Gln uptake and its conversion to α-ketoglutarate, therefore promoting the TCA cycle (Yang et al., 2018). Further studies are needed to investigate whether ECM stiffness is regulating ECM dependent cell growth under Glc starvation and whether this is mediated by YAP/TAZ.

Not only ECM stiffness affects cancer cell metabolism but its remodelling as well. A previous study by Sullivan et al showed a link between the ECM component Hyaluronan (HA) and glycolysis. The digestion of HA with hyaluronidase (HAase) enhanced glycolysis in different types of cells due to an increase in GLUT1 level at the plasma membrane. The addition of HAase stimulated a receptor tyrosine kinase signalling effect leading to a reduction of one of the GLUT1 regulators TXNIP. This glycolytic response to HAase showed an acceleration of MDA-MB-231 breast cancer cells migration (Sullivan et al., 2018). Overall, these studies indicate that ECM can affect Glc metabolism.

Our data show that inhibiting $\alpha2\beta1$ integrin, the major receptor of collagen, and the siRNA-mediated knockdown of the $\alpha2$ subunit significantly reduced collagen I-dependent cell growth, indicating that the ECM effect is mediated by integrins. AMPK is a metabolic sensor which gets activated when cells are under nutrient deprivation conditions (Herzig and Shaw, 2018). A previous study showed that the loss of AMPK in fibroblasts increased $\beta1$ activation in a tensin dependent mechanism which in turn enhanced the formation of fibronectin fibres, mechanical stress and cell spreading (Georgiadou et al., 2017, Georgiadou and Ivaska, 2017). On the contrary, it has been shown that a hormone secreted by adipocytes called adiponectin can increase the expression of both $\alpha5\beta1$ integrin and $\alpha2\beta1$ integrin and the migration of prostate cancer cells and chondrosarcoma cells respectively via a P38-AMPK-NF-κB signalling effect (Tang and Lu, 2009, Chiu et al., 2009). Interestingly adiponectin can increase Glc uptake, therefore it has a Glc lowering effects (Yamauchi et al., 2003). Indeed, it has been shown

previously that Glc starvation can induce cancer cell invasion and metastasis by increasing the expression of MMP9, an ECM degradation enzyme, via activating the LKB1-AMPK signalling pathway (Endo et al., 2018). In addition, ECM stiffness can also activate AMPK via Hippo kinases-AMPK pathway (Xu et al., 2024). Xu et al showed that targeting both LKB1-AMPK and Hippo Kinases-AMPK signalling pathways strongly reduced the growth of PDAC cells (Xu et al., 2024). Thus, in our study ECM-dependent cell growth under Glc starvation could be mediated by AMPK activation. However, further studies are needed to confirm this.

Our data show that breast cancer cells rely on AAs to survive under Glc starvation with serine, glycine and threonine metabolism being the most elevated pathway on collagen I. Serine can be generated from glycolysis or imported from the extracellular space and can be converted to glycine. Alternatively, glycine can also be generated from threonine **(Figure 4-10)**. The produced glycine eventually can provide carbon unites for the one-carbon metabolism, which is a fundamental pathway to provide macromolecules such as lipids and nucleic acids (Amelio et al., 2014) **(Figure 4-10)**.

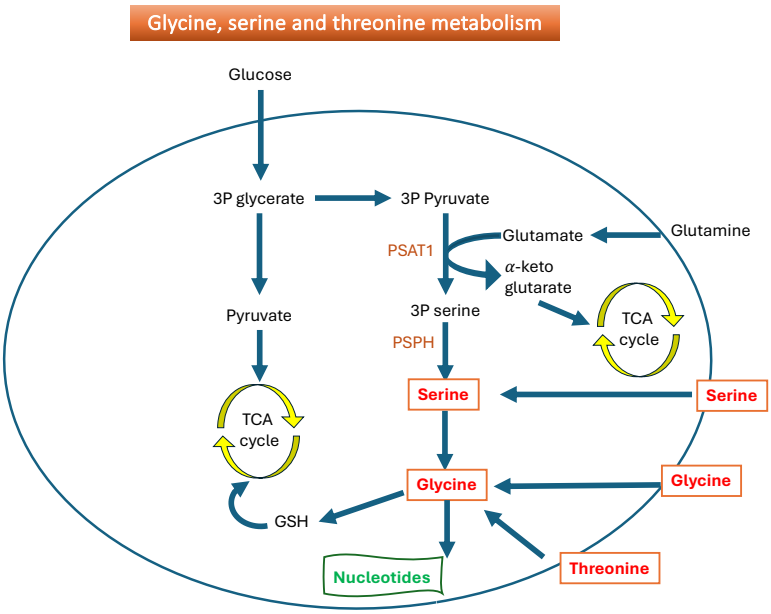

Figure 4-10 Glycine, serine, and threonine metabolism. A schematic of glycine, serine, & threonine metabolism adapted from (Amelio et al., 2014). Serine can be generated from glycolysis or imported from the extracellular space and can be converted to glycine. Alternatively, glycine can also be generated from threonine. The produced glycine can provide carbon units for one-carbon metabolism, which is a fundamental pathway to provide macromolecules such lipids and nucleic acids.

A previous study showed that glycine plays a key role in cancer cell proliferation. Using liquid chromatography-mass spectrometry, the authors identified the utilisation and the release profiles of 219 metabolites in 60 different cell lines. The study showed that glycine consumption is increased in highly proliferative cancer cells and that inhibiting glycine biosynthesis can prolong the G1 phase of the cell cycle, therefore slowing down cell proliferation (Mohit et al., 2012).

One possibility to produce serine and glycine in the absence of Glc is autophagy. Autophagy is a process where the cell recycles its cytoplasmic organelles, engulf them and degrade them into the lysosomes to release nutrients such as AAs and sugars (Lahiri et al., 2019). Indeed AMPK, under Glc starvation, can trigger selective autophagy (Endo et al., 2018). Furthermore, in our study the cells were grown in media containing AAs including serine, glycine and threonine, hence the upregulation of intracellular AAs might also be due to an increase in AA transport. Former studies showed that under nutrient deprivation, AA transport was increased due to the upregulation of AA transporters. For instance, Glc starvation stabilised the transcription factor enhancer 3 (TFE3), which was shown to activate autophagy. The stabilisation of TFE3 increased the expression of the AA transporter SLC36A1, mTOR activity and localisation to the lysosomes (Lv et al., 2024). However, it was also shown that under Gln starvation autophagy deficiency increased the transport of extracellular AAs by increasing the expression of multiple AA transporters in an activating transcription factor 4 (ATF4) dependent mechanism (Zhang et al., 2018). Our data showed that AA levels were increased on collagen I compared to plastic under Glc starvation. Studies showed that when cells are detached from ECM, they induce autophagy to avoid cell death during anoikis (Fung et al., 2008). Hence whether autophagy is involved in the survival mechanism in our study and whether autophagy is inhibited when cells are attached to the ECM under Glc starvation needs further investigation. In this chapter we showed that under Glc starvation, ECM enhanced breast cancer cell growth in a mechanism dependent on the ECM receptor $\alpha 2\beta 1$ integrin. Here we suggested that the ECM effect might promote autophagy mediated by AMPK phosphorylation or inhibit autophagy which in turn increases AA transport **(Figure 4-11)**. Further studies are needed to confirm this hypothesis.

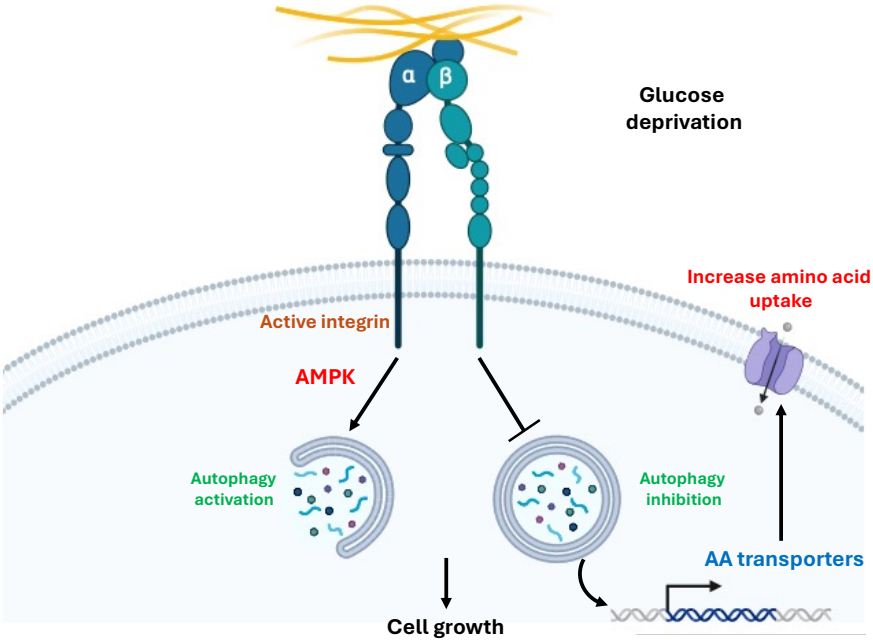

Figure 4-11 Working model of ECM-dependent cell growth under Glc starvation. Under Glc deprivation, the ECM supports cell growth in an integrin mediated mechanism We hypothesise that integrins binding to ECM might trigger signalling pathway which either 1) activate autophagy in an AMPK dependent mechanism or 2) inhibit autophagy leading to the upregulation of amino acid transports, resulting in AA uptake. "Created in BioRender.com".

5 Oncogenic RAS mutations drive a2 integrin expression under amino acid starvation

5.1 Introduction:

During cancer progression, cancer cells face different types of stress caused by either extrinsic factors such as metabolic changes, hypoxia or exposure to treatments, or intrinsic factors such as proteins accumulation. However, studies showed that cancer cells can adapt and respond to stress by activating different signalling pathways and making modifications in the gene expression machinery to survive, such as increasing the expression of genes involved in autophagy during hypoxia (Chen and Xie, 2018, Pakos-Zebrucka et al., 2016). Previous studies showed that when cells are under stress, they activate an adaptive signalling pathway called the integrated stress response (ISR). There are four ISR activators depending on the stress type; the endo-plasmic reticulum (ER) stress activates PKR-like ER Kinase (PERK), viral infection activates double-stranded RNA-dependent protein kinase (PKR), Heme deprivation activates heme-regulated eIF2a kinase (HRI) and AA deprivation activates general control non-derepressible 2 (GCN2). All of those eventually lead to the phosphorylation of eukaryotic translation initiation factor 2 alpha (eIF2α) and Activating transcription factor (ATF4) to trigger the expression of genes involved in cell survival or cell death if survival is not possible **(Figure 5-1)** (Pakos-Zebrucka et al., 2016). When cells are under AA deprivation, deacylated tRNAs accumulate intracellularly leading to the activation of GCN2, one of the ISR activators (Pakos-Zebrucka et al., 2016, Gold and Masson, 2022). Previous studies showed that GCN2 can be a cell growth regulator. For instance, a study on both human fibrosarcoma cells (HT1080) and human colorectal adenocarcinoma cells (DLD1) showed the dependency of these cells on GCN2-eIF2α-ATF4 pathway under nutrient starvation. The growth of HT1080 and DLD1 was reduced upon ATF4 knockdown cells, due to the reduction in asparagine synthetase (ASNS), an enzyme mediating the conversion of aspartate (Asp) to asparagine (ASN), as ASNS gene expression is directly regulated by ATF4. Due to the reduction in AA synthesis in the ATF4 knockdown cells, GCN2 becomes activated in a feedback loop, leading to the activation of autophagy as a survival mechanism. Interestingly, the addition of asparagine (Asn), that is

normally synthesised from Asp, to the media partially rescued cell growth. In addition, both AA starvation and Glc starvation have been reported to activate GCN2 and increase the expression of genes involved in AA transport (Ye et al., 2010). Another study by Cordova et al showed that GCN2 is important for the growth of prostate cancer (PCa) cells, where the activation of GCN2 increased the expression of ATF4 and AA transporters. Targeting GCN2 pharmacologically and genetically reduced the proliferation of PCa cells, due to reducing the uptake and the intracellular levels of multiple AA, including histidine, threonine, phenylalanine, methionine, glutamine, glutamate, asparagine, aspartate, tyrosine and alanine. Expressing the AA transporter 4F2 (SLC3A2) in particular, restored the growth of GCN2 knockdown PCa cells (Cordova et al., 2022).

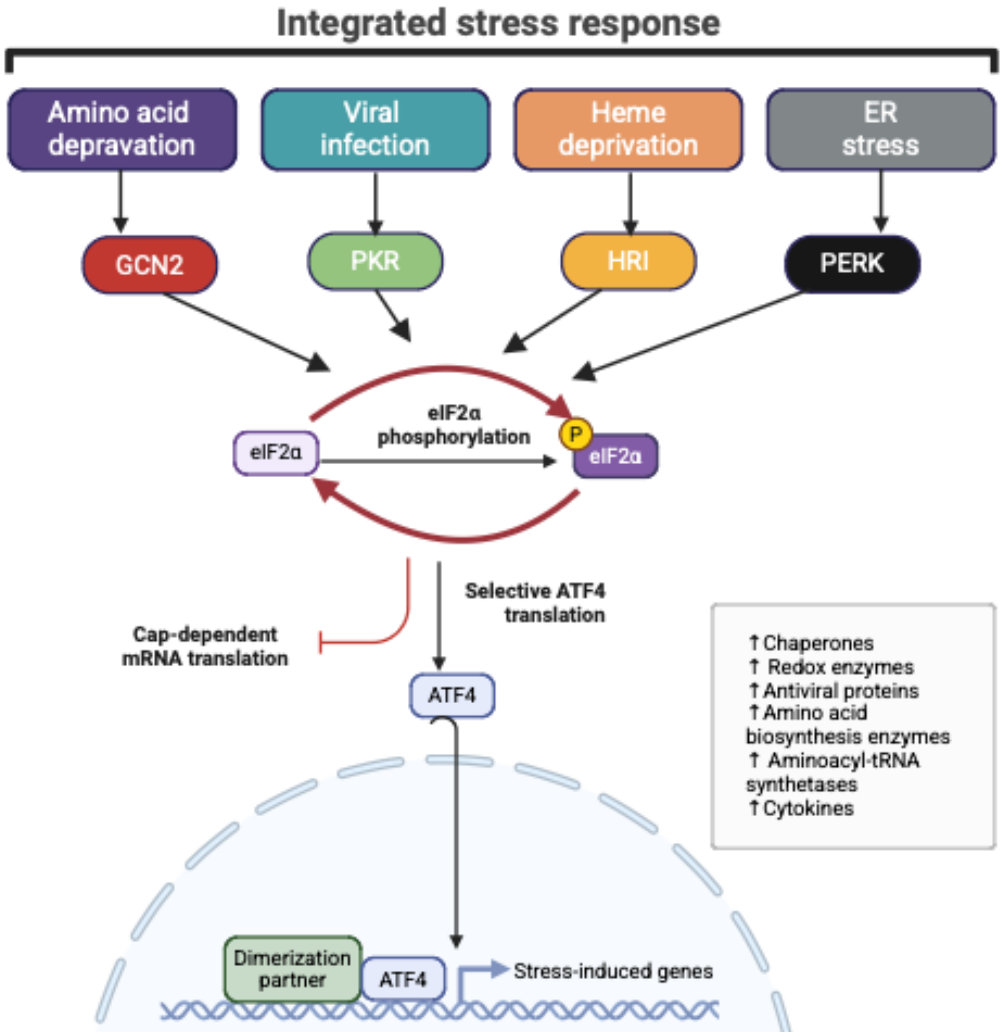

Figure 5-1 Integrated stress response signalling pathway. Four integrated stress response (ISR) pathways are activated under different types of stress. GCN2 is activated under AA starvation, PKR under viral infection, HRI under Heme deprivation and PERK under ER stress. The activation of the four pathways leads to the

phosphorylation of eIF2α and the activation of ATF4, triggering the expression of genes involved in cell survival. Adapted from (Pakos-Zebrucka et al., 2016). "Created in BioRender.com".

Our previous work showed that the ECM supports breast cancer cells growth under AAs deprivation through an ECM uptake-dependent mechanism (chapter 3) (Nazemi et al., 2024). When ECM proteins bind to their receptors, mainly integrins, they are internalised and degraded into the lysosomes. A recent publication from our lab showed that collagen I particularly binds to α2β1 integrin to be internalised and degraded (Martinez et al., 2024).

Various factors, including metabolic cues, can control the expression and trafficking of integrins. For instance, the metabolic sensor AMPK has been shown to regulate β1 integrin trafficking as β1 integrin cell surface level in RPE cells were reduced upon the activation of AMPK with the AMPK activator A-769662. This effect might be due to an increase in β1 internalisation (Ross et al., 2015). Another study showed that the inhibition of AMPK in fibroblasts increased β1 integrin activity and promoted cell adhesion in a tensin-dependent manner (Georgiadou and Ivaska, 2017, Georgiadou et al., 2017).

Here we show that collagen I-dependent cell growth under AA starvation was mediated by α2β1 integrin and that the expression of the α2 integrin subunit was increased under starvation in both breast and pancreatic cancer cells. We found that the expression of α2 was regulated by RAS-MEK-ERK pathway in cells harbouring RAS mutations, but not the GCN2 pathway. Consistently, we observed an increase in ERK phosphorylation under AA starvation. Furthermore, AA starved pancreatic cancer cells showed a faster adherence to collagen I compared to complete media. Together, these data suggest that AA starvation potentiate mutant RAS signalling, promoting α2 integrin expression, which in turn facilitate cell spreading and adhesion.

5.2 Results:

5.2.1 α2β1 integrin was required for collagen I uptake under amino acid starvation

We have previously shown that MCF10CA1 breast cancer cells uptake and degrade collagen I under AA starvation and that the uptake of collagen I was increased under AA starvation compared to complete media **(chapter 3).** α2β1 integrin is the major receptor for collagen I and we have previously showed in our lab that ECM internalisation is dependent on α2β1 integrin in complete media (Martinez et al., 2024). To investigate if collagen I uptake was mediated by α2β1 integrin under AA starvation, MCF10CA1 cells were seeded on collagen I labelled with a pH sensitive dye, pH-rodo for 6 hours in the presence or absence of BTT3033, a pharmacological inhibitor of α2β1 integrin which prevents collagen binding, in AA free media **(Figure 5-2)**. In the presence of DMSO, several pH-rodo collagen I containing endosomes can be seen inside the cells, while in the presence of BTT3033 the amount of internalised coll I was drastically reduced. Quantification of the collagen I uptake index shows that inhibiting α2β1 integrin significantly reduced collagen I uptake under AA starvation.

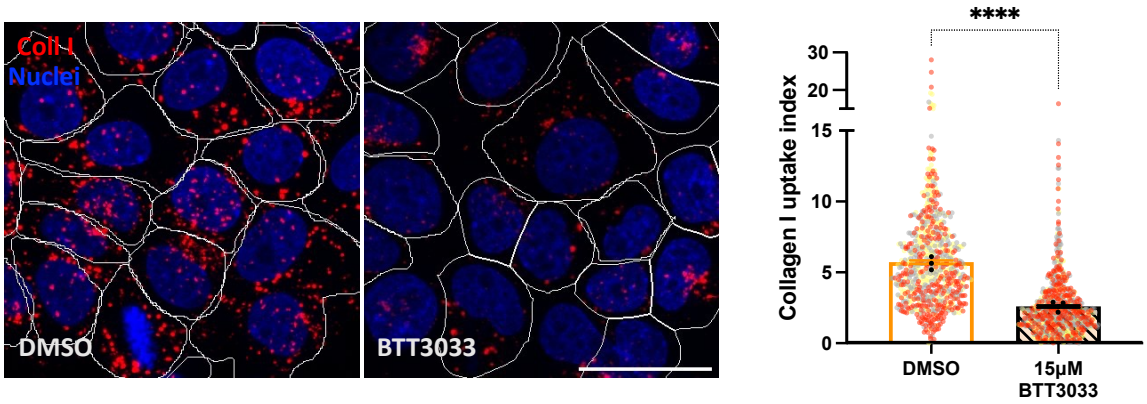

Figure 5-2 The inhibition of α2β1 integrin reduced collagen I uptake under AA starvation. MCF10CA1 cells were grown in AA free media for 18 hours and seeded in AA free media for 6 hours on 1 mg/ml collagen I labelled with pH-rodo (red). DMSO or 15 μM BTT3033 were added two hours after seeding. Cells were stained with Hoechst 33342 (Blue) and Brightfield was used to capture the cells edge (white lines). Cells were imaged live with a Nikon A1 confocal microscope, 60x magnification. Scale bar 30μm. Collagen I uptake index was calculated with Image J software. N=3 independent experiments. The graph represents the Mean ± SEM, the coloured dots for biological repeats, the black dots represent the mean of the individual experiments. Mann-Whitney test. ****p < 0.0001. These experiments were performed by Zhe Bao, PhD student in the Rainero lab.

5.2.2 α2β1 integrin was required for ECM-dependent MCF10CA1 cell growth under amino acid starvation.

To investigate whether the ECM-dependent cell growth under starvation was mediated by α2β1 integrin, MCF10CA1 cells were seeded on collagen I for 4 days under AA starvation **(Figure 5-3, A)** or Gln starvation **(Figure 5-3, B)** in the presence or absence of a BTT-3033. The results show that, while the presence of collagen I promoted cell proliferation, pharmacological inhibition of α2β1 integrin significantly prevented collagen I-dependent cells growth under both AA **(Figure 5-3, A)** or Gln starvation **(Figure 5-3, B)**. To validate the results, the cells were seeded on collagen I for 4 days under AA **(Figure 5-3, C)** or Gln starvation **(Figure 5-3, D)** in the presence of an siRNA mediated targeting α2 integrin or a non-targeting siRNA control. Similarly to the inhibitor results, α2 knockdown significantly reduced collagen I-dependent cell growth under both AA starvation **(Figure 5-3, C)** and Gln starvation **(Figure 5-3, D)**.

Overall, the results indicate that the ECM-dependent cell growth under starvation is mediated by α2β1 integrin.

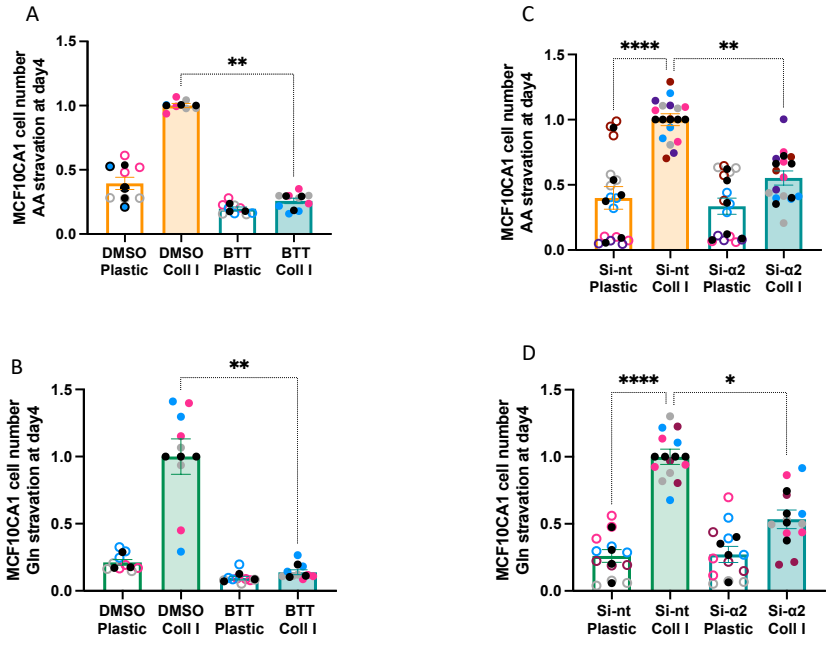

Figure 5-3 MCF10CA1 cells growth on collagen I was strongly reduced upon inhibition of α2β1 integrin under starvation. MCF10CA1 cells were seeded on 2 mg/ml collagen I under amino acid (AA) free media (A) or glutamine (Gln) free media (B) for 4 days in the presence of DMSO (control) or 15μM BTT-3033. Cells were fixed and t stained with Hoechst 33342. MCF10CA1 cells were seeded on 2 mg/ml collagen I, transfected with an siRNA targeting α2 integrin (si-α2) or a non-targeting siRNA (si-nt) as a control, for 4 days under amino acid (AA) starvation (C) or glutamine (Gln) starvation (D). Cells were fixed and stained with Hoechst 33342. The cells were imaged using an Image Xpress micro system and cell numbers were quantified with MetaXpress and CME software. N≥ 3independent experiments, values represent the Mean ± SEM, the coloured dots for biological repeats, the black dots represent the mean of the individual experiments. Kruskal-Wallis, Dunn's multiple comparisons test *p < 0.05, **p < 0.01, ****p < 0.0001.

5.2.3 Amino acid starvation strongly increased α2 integrin expression at the mRNA level

The expression of α2β1 integrin has been shown to be increased in some types of cancer including pancreatic cancer (Gregori et al., 2023), while its expression in breast cancer varies depending on cancer invasive behaviour (Moritz et al., 2021). To investigate whether AA starvation had any effect on α2 integrin expression, we performed qPCR in a panel of breast and pancreatic cancer cell lines to assess α2 mRNA levels. MCF10CA1, MDA-MB-231, and MCF7 breast cancer cells **(Figure 5-4, A, B, C),** SW1990 and Panc1 pancreatic cancer cells **(Figure 5-4, D, E)** were seeded on plastic in complete media or AA free media for 18 hours. The mRNA was extracted and α2 integrin expression was measured. The results show that starving the cells of AAs significantly boosted the mRNA levels of α2 integrin subunit in all the cell lines. Indeed, we detected a 2-fold increase in MDA-MB-231 and Panc1 cells and ~3-fold increase in MCF10CA1, MCF7, and SW1990 cells.

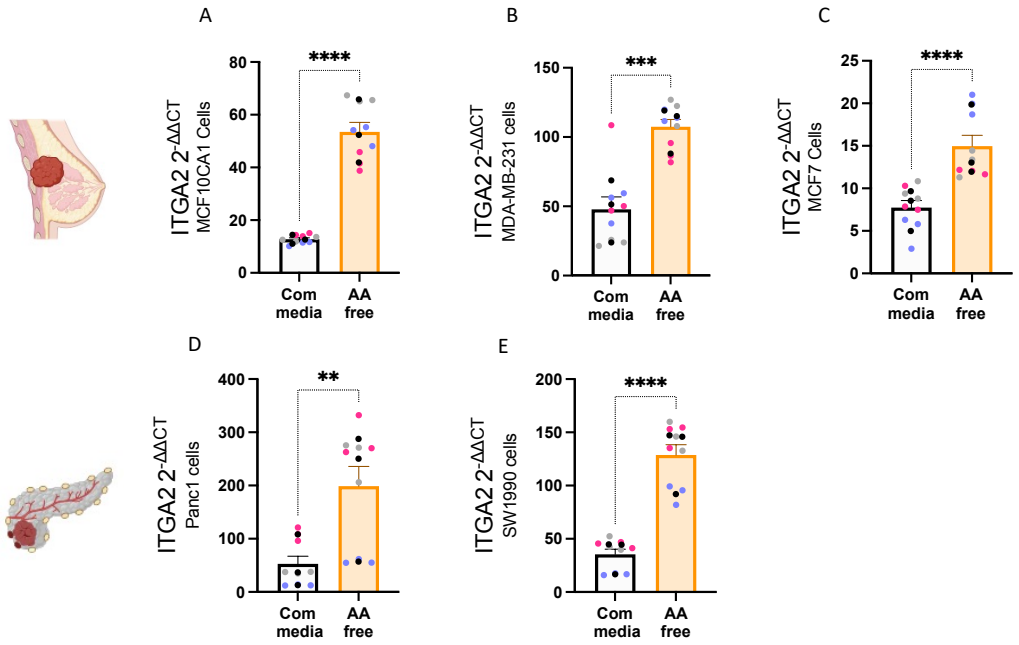

Figure 5-4 The expression of ITGA2 increased significantly at the mRNA level under AA starvation compared to complete media. Breast cancer cells MCF10CA1 (A), MDA-MB-231 (B), and MCF7 (C) and pancreatic cancer cells SW1990 (D) and Panc1 (E) were seeded on plastic in complete (Com) media or amino acid (AA) free media for 18 hrs. The cells were collected; mRNA was extracted and α2 (ITGA2) was measured by SYBR-Green qPCR. GAPDH was used as a control and the data were plotted as $2^{-\Delta\Delta CT}$. N=3 independent experiments, values represent the Mean ± SEM, the coloured dots for biological repeats, the black dots represent the mean of the individual experiments. Mann-Whitney test. **p < 0.01, ***p < 0.001, ****p < 0.0001.

5.2.4 α2 integrin expression significantly increased at the protein level under AA starvation

To investigate whether the expression of α2 integrin subunit was also increased at the protein level, MCF10CA1 and MCF7 breast cancer cells **(Figure 5-5,A,B)** and SW1990 pancreatic cancer cells **(Figure 5-5,C)** were seeded in complete media or AA free media for 18 hours, cell lysates were collected and the protein levels were measured by Western Blotting. Consistent with our qPCR data, the results show that the expression of α2 integrin was also significantly increased at the protein level under AA starvation in all the cell lines (~ 2-fold increase). To validate the results, MCF10CA1 cells were starved for 18 hours in AA free media, seeded for 1 hour on collagen I and stained for α2 integrin **(Figure 5-6)**. The results show that the localisation of α2 integrin at the cell membrane was increased under AA starvation compared to complete media. Quantification of the α2 integrin intensity shows that the intensity was significantly increased under AA starvation comparing to complete media.

Overall, our results show that AA deprivation boosted the expression of α2 integrin subunit at the mRNA and the protein levels, in both breast and pancreatic cancer cells.

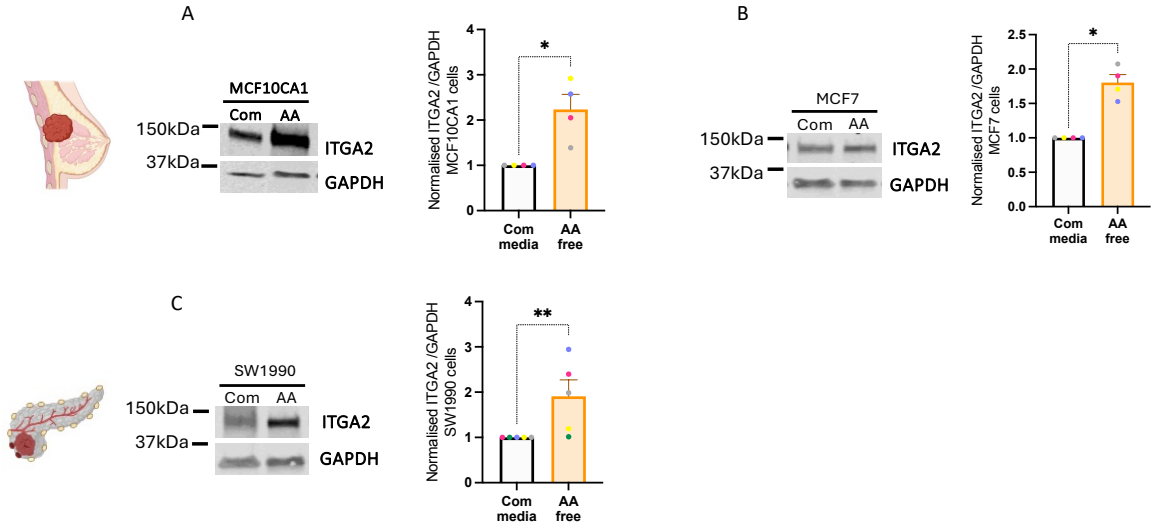

Figure 5-5 The expression of ITGA2 increased at the protein level under AA starvation. Breast cancer cells MCF10CA1 (A) and MCF7 (B) and pancreatic cancer cells SW1990 (C) were seeded on plastic in complete media (Com) or amino acid (AA) free media for 18 hours. Cell lysates were collected, samples were run by Western Blotting, membranes were stained for α2 (ITGA2) and GAPDH and imaged with a Licor Odyssey system. The proteins band intensity was quantified with Image Studio Lite software. N≥4 independent experiments, values represent the Mean± SEM, the coloured dots for biological repeats. Mann-Whitney test. *p < 0.05, **p < 0.01.

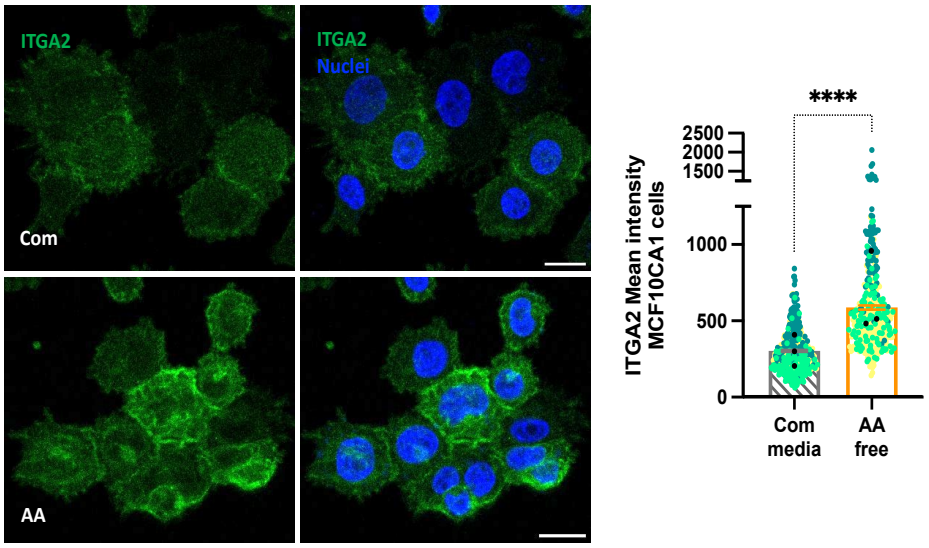

Figure 5-6 The expression of ITGA2 increased in MCF10CA1 on collagen I. MCF10CA1 cells were starved for 18 hours in amino acid (AA) free media or kept in complete (Com) media and seeded on 0.5 mg/ ml collagen I for 1 hour. Cells were fixed and stained for α2 integrin (ITGA2, green) and nuclei (blue). Cells were imaged with a Nikon A1 confocal microscope, 40x objective. Scale bar 20µm. ITGA2 mean intensity was measured using ImageJ software. N=3 independent experiments, values represent the Mean± SEM, the coloured dots for biological repeats, the black dots represent the mean of the individual experiments. Mann-Whitney test. ****p < 0.0001.

5.2.5 β1 integrin expression at the mRNA level varies under AA starvation in cancer cells

Integrins are heterodimer receptors of α and β subunits. β1 integrin subunit binds to 12 different α subunits including α2. To investigate whether β1 integrin expression was also increased under AA starvation, we performed a qPCR in the same panel of breast and pancreatic cancer cell lines. MCF10CA1, MDA-MB-231, and MCF7 breast cancer cells **(Figure 5-7, A, B, C),** and SW1990 and Panc1 pancreatic cancer cells **(Figure 5-7, D, E)** were seeded on plastic in complete media or AA free media for 18 hours. The mRNA was extracted and the β1 integrin expression was measured. Interestingly, starving the cells increased β1 mRNA level in some of the cell lines (MCF10CA1- MDA-MB-231- and Panc1) but not in others (MCF7 and SW1990). In addition, the starvation effect was smaller than the effect on the α2 subunit.

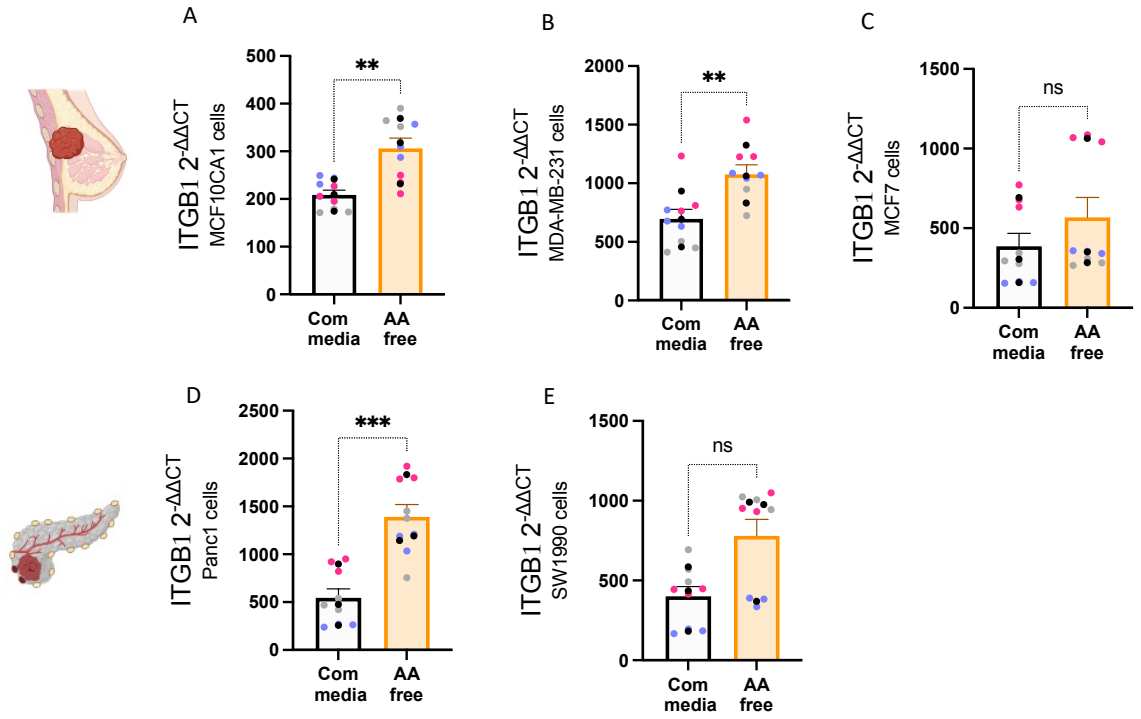

Figure 5-7 The expression of ITGB1 increased at the mRNA level under AA starvation in some cell lines. Breast cancer cells MCF10CA1 (A), MDA-MB-231 (B) and MCF7 (C) and pancreatic cancer cells SW1990 (D) and Panc1 (E) were seeded on plastic in complete media or AA free media for 18 hours. The cells were collected, mRNA was extracted and measured by SYBR-Green qPCR method. GAPDH was used as a control and the data were plotted as $2^{-\Delta\Delta CT}$. N=3 independent experiments, values represent the Mean± SEM, the coloured dots for biological repeats, the black dots represent the mean of the individual experiments. Mann-Whitney test. ns: Non-significant, **p < 0.01, ***p < 0.001.

5.2.6 α5 integrin expression increased at the mRNA level, but not at the protein level, in pancreatic but not breast cancer cells

To assess whether AA starvation triggered the expression of other integrins, we measured α5 integrin mRNA levels. MCF10CA1 breast cancer cells and SW1990 pancreatic cancer cells were seeded on plastic under complete media or AA free media for 18 hours, the mRNA was extracted and the α5 integrin expression was measured. Similarly, the cells were starved for 18 hours, cell lysates were collected, and α5 protein levels were measured by Western Blotting. **Figure 5-8** shows that the expression of α5 integrin was significantly increased at the mRNA level in SW1990 cells **(Figure 5-8, C),** while there was no change at the protein level **(Figure 5-8, D)**. On the contrary, in MCF10CA1 cells the expression of α5 was not changed either at the mRNA level **(Figure 5-8, A)** or the protein level **(Figure 5-8, B)** when starved cells were compared to complete media. Overall, AA starvation did not seem to significantly change α5 integrin levels.

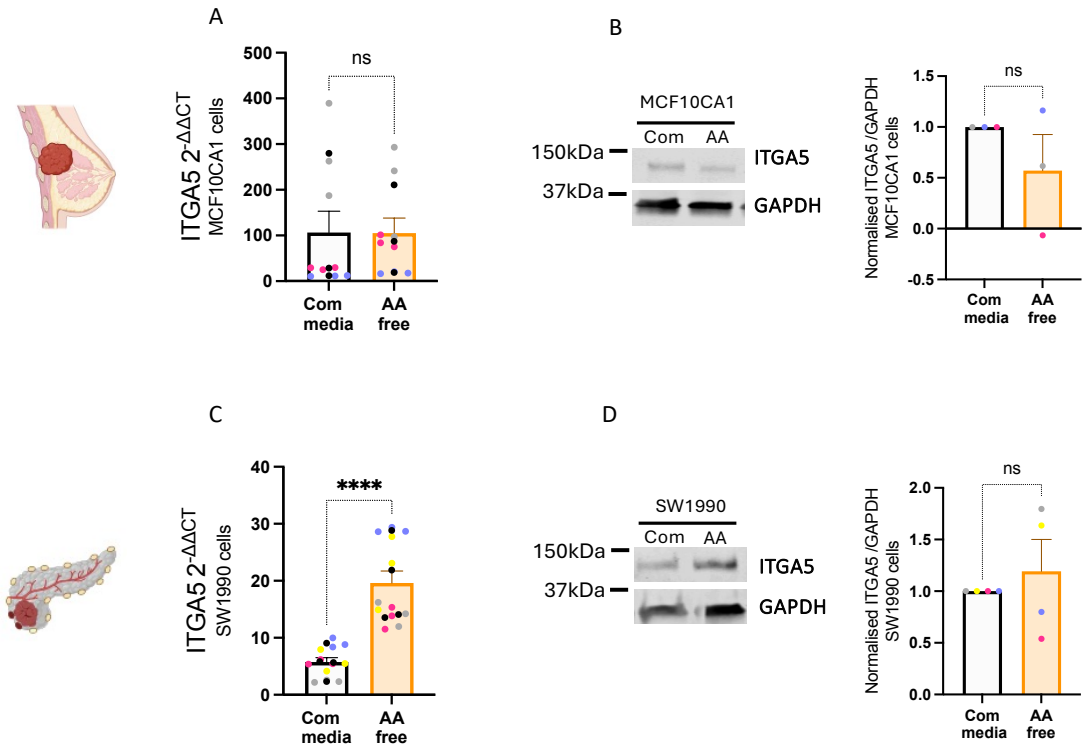

Figure 5-8 The expression of α5 integrin increased significantly at the mRNA level in pancreatic cancer cells but not at the protein level and in breast cancer cells under AA starvation Breast cancer cells MCF10CA1 (A-B) and pancreatic cancer cells SW1990 (C-D) were seeded on plastic in complete (Com) media or amino acid (AA) free media for 18 hours. (A-C) Cells were collected, mRNA was extracted and α5 integrin (ITGA5) was measured by SYBR-Green qPCR. GAPDH was used as a control and the data were plotted as $2^{-\Delta\Delta CT}$. (B-D) Cell lysates were collected, samples run by Western Blotting and membranes were stained for α5 integrin (ITGA5) and GAPDH and imaged with a Licor Odyssey system. The protein band intensity was quantified with Image Studio Lite software. N≥ 3 independent experiments, values represent the Mean ± SEM, the coloured dots for biological repeats, the black dots represent the mean of the individual experiments. Mann-Whitney test. ns: Non-significant, ****$p < 0.0001$.

5.2.7 The expression of α2, but not α5, was significantly increased in physiological starvation conditions in pancreatic cancer cells.

To confirm our results in a more physiological environment, we used the tumour interstitial fluid media (TIFM), a reconstituted media which composition recapitulates the nutrient levels detected in the interstitial fluids of pancreatic tumours. Interestingly, RNAseq experiments detected an AA-starvation signature in cells grown in TIFM (Sullivan et al., 2019a, Saab et al., 2023). SW1990 cells were seeded in complete media or TIFM media for 18 hours, mRNA was extracted and the mRNA levels of both α2 and α5 integrin subunits were measured. Interestingly, the expression of α2 was significantly increased, similarly to the AA free media **(Figure 5-9, A)**. However, the expression of α5 did not change **(Figure 5-9, B)**. Overall, our data

indicate that the intratumoral nutrient starvation conditions might specifically upregulate the α2 integrin subunit, rather than all integrins.

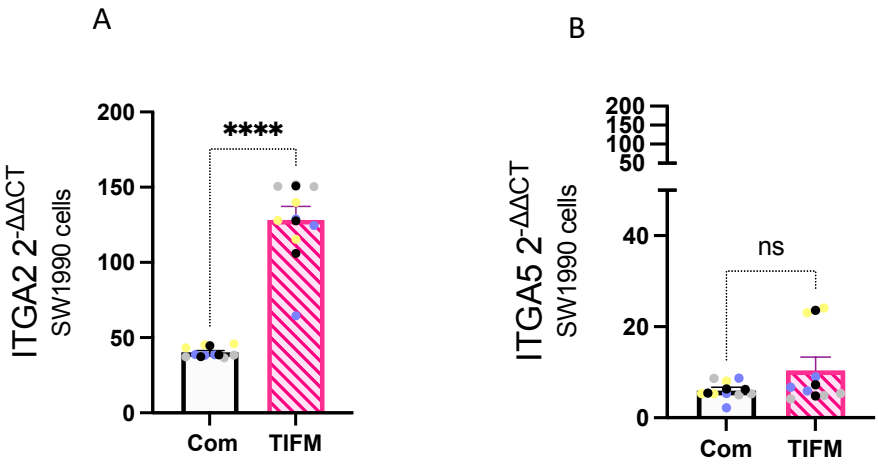

Figure 5-9 The expression of α2, but not α5, integrin increased significantly at the mRNA level in TIFM media compared to complete media. SW1990 cells were seeded on plastic in complete (Com) media or TIFM media for 18 hours. The cells were collected, mRNA was extracted and α2 (ITGA2, A) and α5 (ITGA5, B) were measured by SYBR-Green qPCR. GAPDH was used as a control and the data were plotted as $2^{-\Delta\Delta CT}$. N=3 independent experiments, values represent the Mean± SEM, the coloured dots for biological repeats, the black dots represent the mean of the individual experiments. Mann-Whitney test. ns: Non-significant, ****$p < 0.0001$.

5.2.8 Amino acid starvation promoted α2 integrin expression in a RAS-dependent and GCN2-independent manner.

AA starvation promotes the activation of the GCN2-mediated stress response (Pakos-Zebrucka et al., 2016). To test whether GCN2 was activated by AA starvation in SW1990 cells, we measured the expression of ASNS, a well-established GCN2 target (Deval et al., 2009). SW1990 cells were seeded on plastic in complete media or AA free media for 18 hours and the mRNA level of ASNS was measured by qPCR. As expected, the expression of ASNS was significantly increased under AA starvation compared to complete media **(Figure 5-10, A)**. To assess the involvement of GCN2, SW1990 cells were seeded on plastic under AA starvation for 18 hours in the presence or absence of the GCN2 inhibitor GCN2iB and the mRNA level of ASNS was measured. Consistent with the literature, the starvation-induced increase in ASNS expression was completely abolished after inhibiting GCN2 **(Figure 5-10, B)**.

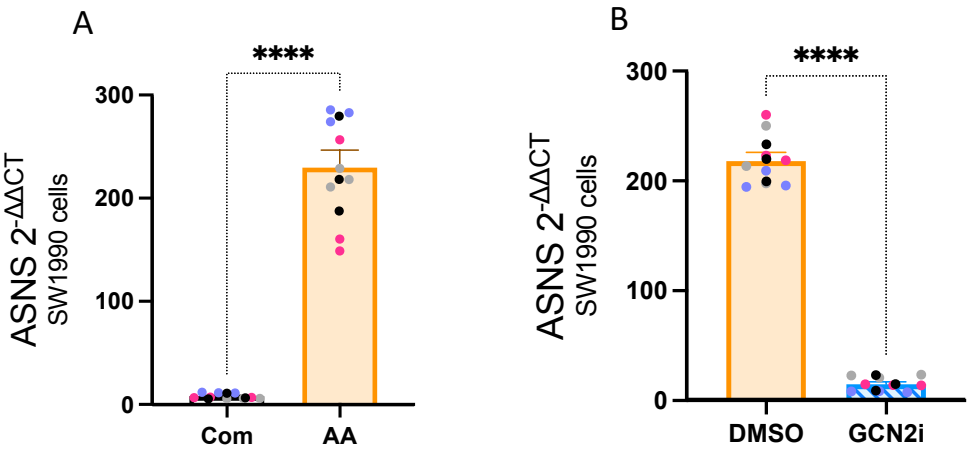

Figure 5-10 GCN2 inhibitor completely abolished the expression of ASNS under AA starvation. SW1990 cells were seeded on plastic in complete media (Com) or amino acid (AA) free media for 18 hours (A). SW1990 cells were seeded on plastic in amino acid (AA) free media for 18 hrs in the presence of (5μM GCN2iB) (GCN2i) or DMSO as a control (B). The cells were collected; mRNA was extracted and ASNS was measured by SYBR-Green qPCR. GAPDH was used as a control and the data were plotted as $2^{-\Delta\Delta CT}$. N=3 independent experiments, values represent the Mean ± SEM, the coloured dots for biological repeats, the black dots represent the mean of the individual experiments. Mann-Whitney test. ****$p < 0.0001$.

To investigate whether the increase in the expression of α2 integrin was mediated by GCN2, breast cancer cells MCF10CA1, MDA-MB-231, and MCF7 and pancreatic cancer cells Panc1, and SW1990 were seeded in AA free media for 18 hours in the presence or absence of a GCN2 inhibitor and the mRNA level of α2 integrin was measured. Interestingly, inhibition of GCN2 resulted in small but statistically significant reduction in the expression of α2 integrin

expression in MCF7 breast cancer cells **(Figure 5-11, C)** but not in MCF10CA1 cells **(Figure 5-11, A)** or MDA-MB-231 cells **(Figure 5-11, B)**. As expected, GCN2 inhibition did not affect α2 integrin expression in breast cancer cells in complete media **(Figure 5-11, D,E, F)**. The data indicate that the integrated stress response is not the main pathway promoting α2 integrin expression under AA starvation.

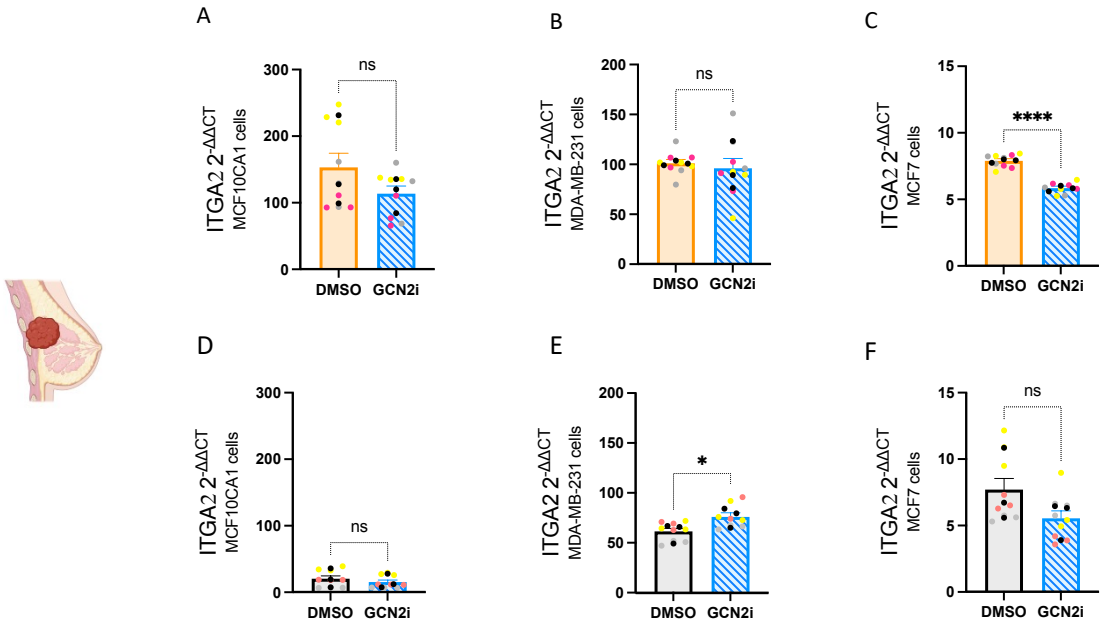

Figure 5-11 GCN2 inhibition significantly decreased the expression of α2 integrin in MCF7, but not in MCF10CA1 or MDA-MB-231 breast cancer cells under AA starvation, while no effect was detected in complete media. Breast cancer cells MCF10CA1 (A, D), MDA-MB-231 (B, E) and MCF7 (C, F) were seeded on plastic in complete media (D-F) or amino acid free media (A-C) for 18 hours in the presence of 5μM GCN2iB (GCN2i) or DMSO as a control. The cells were collected; mRNA was extracted and α2 (ITGA2) was measured by SYBR-Green qPCR. GAPDH was used as a control and the data were plotted as $2^{-\Delta\Delta CT}$. N=3 independent experiments, values represent the Mean ± SEM, the coloured dots for biological repeats, the black dots represent the mean of the individual experiments. Mann-Whitney test. ns: Non-significant, *p < 0.05, ****p < 0.0001.

RAS is an oncogene which has been found to be mutated in multiple types of cancer (Fernandez-Medarde and Santos, 2011). There are three types of RAS: HRAS, NRAS and KRAS. RAS cycles between an inactive state (GDP-bound) and an active state (GTP-bound). G12, G13, and Q61 are the most common RAS mutations and as a result of these mutations RAS becomes unable to hydrolyse GTP to GDP and therefore cannot be inactivated (Chen et al., 2021). All the cells used in this study harbour a RAS mutation, apart from MCF7 cells. MCF10CA1 cells are HRAS G12V, MDA-MB-231 cells are KRAS G13D, and both SW1990 and Panc1 cells are KRAS G12D. Interestingly, MAPK activation downstream of RAS has been reported to regulate the expression of GCN2-independent genes under AA starvation (Shan et al., 2015). To test whether

the increase in the expression of α2 integrin was driven by KRAS, Panc1, and SW1990 cells were seeded in AA free media for 18 hours in the presence or absence of a newly developed KRAS G12D inhibitor, MRTX1133 (Wang et al., 2022) and the mRNA levels of α2 integrin were measured. **Figure 5-12** shows that inhibiting KRAS significantly reduced the expression of α2 in both Panc1 **(Figure 5-12, A)** and SW1990 cells **(Figure 5-12, B)**. Consistently with our results in breast cancer cells, the inhibition of GCN2 did not affect α2 expression in either Panc1 **(Figure 5-12, A)** or SW1990 cells **(Figure 5-12, B).**

To investigate whether the expression of α2 integrin was also controlled by KRAS in complete media, Panc1, and SW1990 cells were seeded in complete media for 18 hours in the presence or absence of GCN2i, KRAS inhibitor or DMSO control and the mRNA levels of α2 integrin were measured. As expected, GCN2 inhibition did not change α2 expression in Panc1 **(Figure 5-12, C)** or SW1990 cells **(Figure 5-12, D)**. Interestingly, KRAS inhibition markedly reduced the expression of α2 integrin in SW1990 cells **(Figure 5-12, D)** but not in Panc1 cells **(Figure 5-12, C)**. Together, these data indicate that AA starvation promotes α2 expression through a KRAS-dependent signalling pathway, while in complete media the role of KRAS in controlling α2 expression might be cell line-dependent.

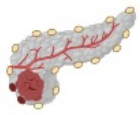

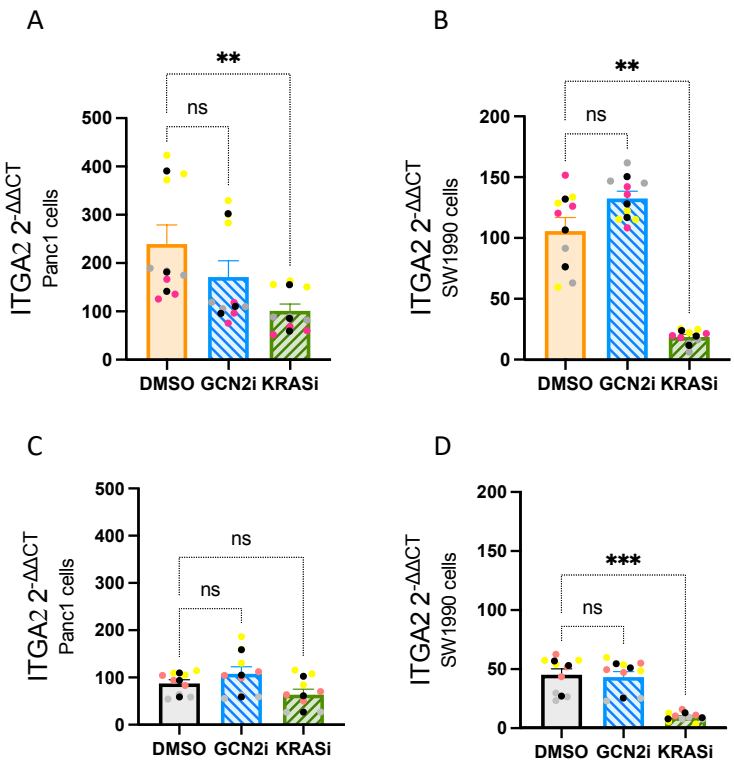

Figure 5-12 KRAS, but not GCN2, was required for α2 integrin expression in pancreatic cancer cells under AA starvation, while in complete media, KRAS inhibition decreased α2 integrin expression a cell line-dependent manner. Pancreatic cancer cells Panc1 and SW1990 were seeded on plastic in aAA free media (A-B) or complete media (C-D) for 18 hours in the presence of 5μM GCN2iB (GCN2i), 200nM MRTX1133 (KRASi) or DMSO as a control. The cells were collected; mRNA was extracted and α2 (ITGA2) was measured by SYBR-Green qPCR. GAPDH was used as a control and the data were plotted as $2^{-\Delta\Delta CT}$. N=3 independent experiments, values represent the Mean ± SEM, the coloured dots for biological repeats, the black dots represent the mean of the individual experiments. Kruskal-Wallis, Dunn's multiple comparisons test. ns: Non-significant, **p < 0.0, ***p < 0.001.

5.2.9 ERK phosphorylation rapidly increased under AA starvation in breast and pancreatic cancer cells

The activation of RAS can trigger different signalling pathways, including the RAS-RAF-MEK-ERK pathway. The final step of this pathway is the phosphorylation of ERK, which translocates to the nucleus to bind to transcription factors and induce the expression of downstream genes (Guo et al., 2020). It was previously reported that ERK can be activated under AA starvation (Franchi-Gazzola et al., 1999). Hence, to investigate the mechanism behind the increase in α2 integrin expression, we looked at the phosphorylation of ERK under AA starvation. MCF10CA1 breast cancer cells and SW1990 pancreatic cancer cells were seeded on plastic in serum-free media for 18 hours. Media was changed to AA free media without serum, cells were collected after 5, 10, and 15minutes and ERK and pERK protein levels were measured by Western Blotting. The results show that the phosphorylation of ERK increased significantly in MCF10CA1 **(Figure 5-13, A)** and SW1990 cells **(Figure 5-13, B)** within 5 min of starvation compared to complete media and then it returned to control levels. There was no difference in ERK protein levels between complete and AA free media in both cell lines. This suggests that RAS/ERK signalling might be required to promote α2 integrin expression.

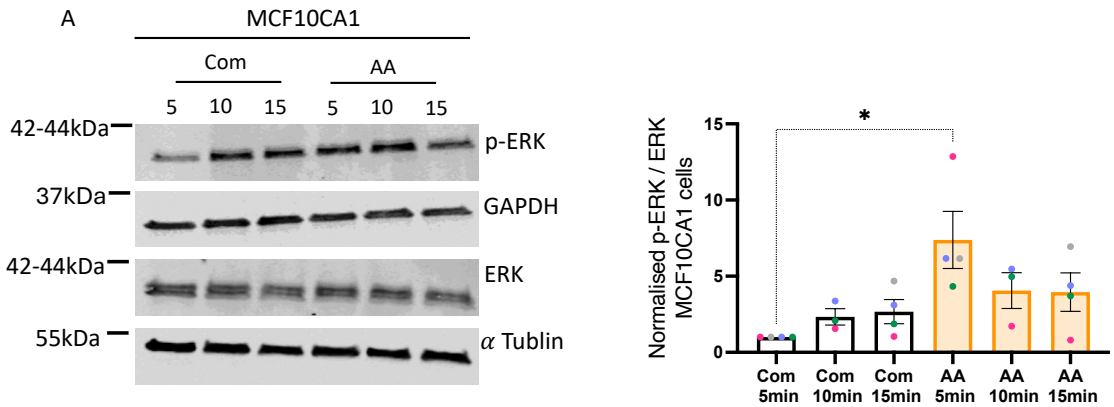

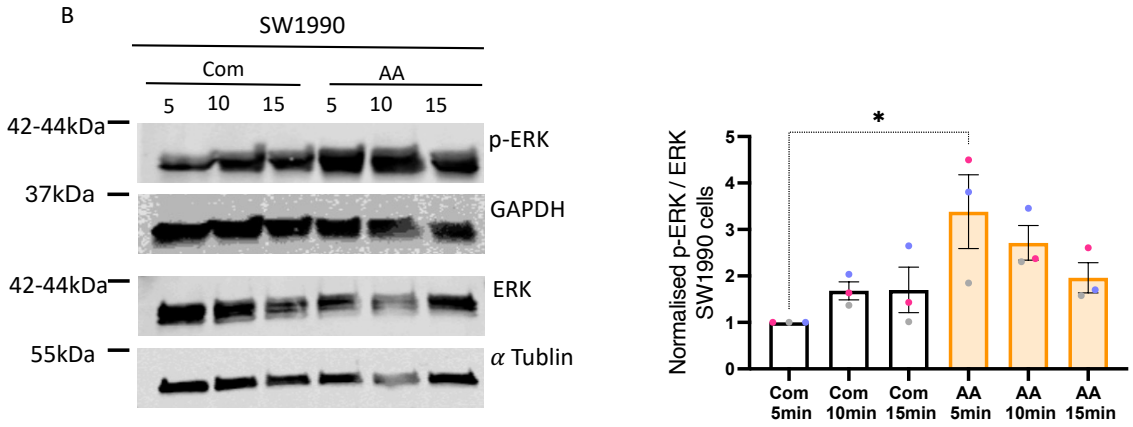

Figure 5-13 The phosphorylation of ERK was increased within 5 minutes of AA starvation in both breast and pancreatic cancer cells. MCF10CA1 cells (A) and SW1990 cells (B) were seeded on plastic in serum-free media for 18 hours then AA and serum starved for 5, 10 or 15 minutes. The cell lysates were collected, and the samples were run by Western Blotting. Membranes were blotted for ERK, phospho-ERK (p-ERK), α-tubulin and GAPDH and were imaged with a Licor Odyssey system. The protein band intensity was measured with Image Studio Lite software and the amount of p-ERK/ERK was plotted. N≥3 independent experiments, values represent the Mean± SEM, the coloured dots for biological repeats. Kruskal-Wallis, Dunn's multiple comparisons test *p < 0.05.

5.2.10 α2 integrin expression was regulated by MEK under amino acid starvation

Since our data showed that ERK signalling was activated by AA starvation, we wanted to investigate whether the MEK/ERK pathway was responsible for promoting α2 expression. MCF10CA1 breast cancer cells and SW1990 pancreatic cancer cells were seeded on plastic in AA free media for 18 hours in the presence or absence of a MEK inhibitor, Selumetinib, and the mRNA levels of α2 integrin were measured **(Figure 5-14, A, C)**. The inhibition of MEK profoundly reduced the expression of α2 integrin mRNA levels in both MCF10CA1 cells **(Figure 5-14, A)** and SW1990 cells **(Figure 5-14, C)**. Similarly, MCF10CA1 cells were seeded in AA free media in the presence or absence of Selumetinib, while SW1990 cells were treated with either Selumetinib, MRTX1133 or DMSO control. Cell lysates were collected, and the α2 integrin protein levels were measured by Western Blotting. Consistent with the mRNA results, MEK inhibition significantly reduced α2 integrin expression at the protein level in both MCF10CA1 cells **(Figure 5-14, B)** and SW1990 cells, where KRAS inhibition resulted in a similar reduction in SW1990 cells **(Figure 5-14, D)**. Overall, the data demonstrate that the expression of α2 integrin under AA starvation is regulated by KRAS and the MEK/ERK signalling pathway.

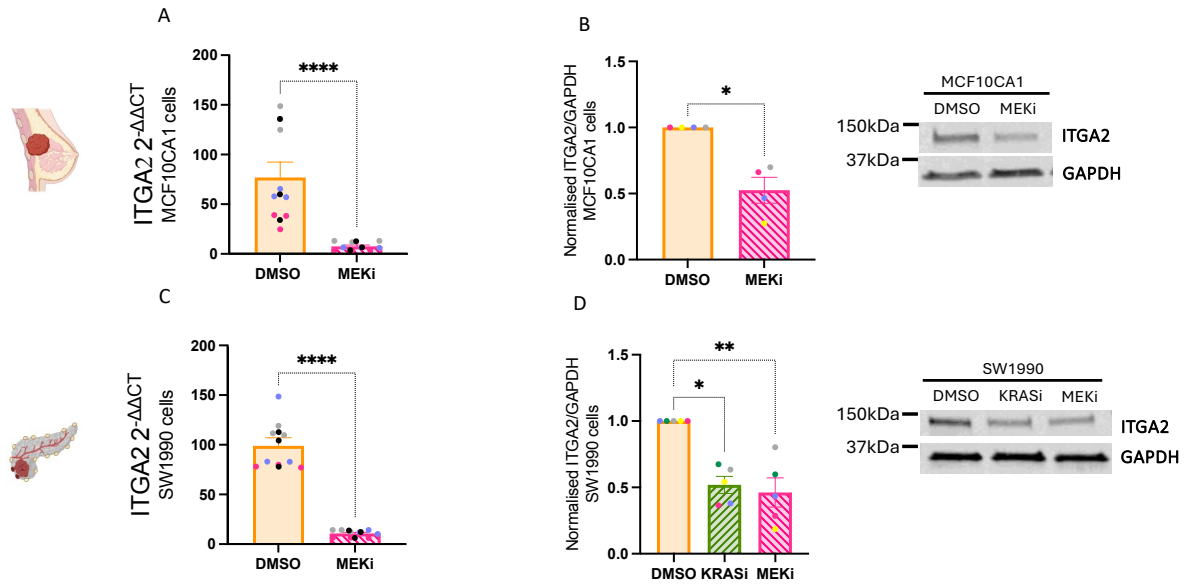

Figure 5-14 MEK inhibition reduced the expression of α2 integrin at both the mRNA and the protein level. MCF10CA1cells (A) and SW1990 cells (C) were seeded in AA free media in the presence of 10μM Selumetinib (MEKi) or DMSO as a control. The cells were collected; mRNA was extracted and α2 (ITGA2) was measured by SYBR-Green qPCR. GAPDH was used as a control and the data were plotted as $2^{-\Delta\Delta CT}$. MCF10CA1 cells (B) and SW1990 cells (D) were seeded in AA free media in the presence or absence of 10μM Selumetinib (MEKi), 200nM MRTX1133 (KRASi) or DMSO as a control. Cell lysates were collected, and the samples were run by Western Blotting. Membranes were stained for α2 integrin (ITGA2) and GAPDH and imaged with a Licor Odyssey system. The band intensity was measured with Image Studio Lite software. N≥ 3 independent experiments, values represent the Mean ± SEM, the coloured dots for biological repeats, the black dots represent the mean of the individual experiments. (A, B, C) Mann-Whitney test. (D) Kruskal-Wallis, Dunn's multiple comparisons test *p < 0.05, **p < 0.01, ****p < 0.0001.

5.2.11 The expression of α2 integrin increased in MCF10A mammary epithelial cells under AA starvation via growth factors stimulation

To investigate whether AA starvation-driven expression of α2 was associated with cancer progression or also happened in non-transformed epithelial cells, we seeded MCF10A non-transformed mammary epithelial cells on plastic and starved them for 18 hours in AA free media. Cells then were collected and α2 integrin expression was measured at the mRNA level and protein level. Interestingly, the expression of α2 integrin was increased at both the mRNA **(Figure 5-15, A)** and at the protein level **(Figure 5-15, B)** under AA starvation compared to complete media. Since MCF10A cells are RAS wild type, we hypothesised that the growth factors which are added to the growth media might be activating RAS. Hence, to determine the specific effects of AA starvation on α2 integrin expression in the absence of growth factors, MCF10A cells were seeded on plastic in media without serum and growth factors. Media was then changed to complete media or AA starvation media either with serum only, serum and growth factors (EGF and insulin) or without any supplements and incubated for 18 hours. Cells were collected and α2 integrin mRNA levels were measured. **Figure 5-15, C** shows that adding serum only or with growth factors to the complete media did not change the mRNA level of α2 integrin. However, depleting AAs from the media significantly increased the mRNA level of α2 only in the presence of serum or serum with growth factors, suggesting that growth factor signalling promoted the upregulation of α2 integrin by AA starvation.

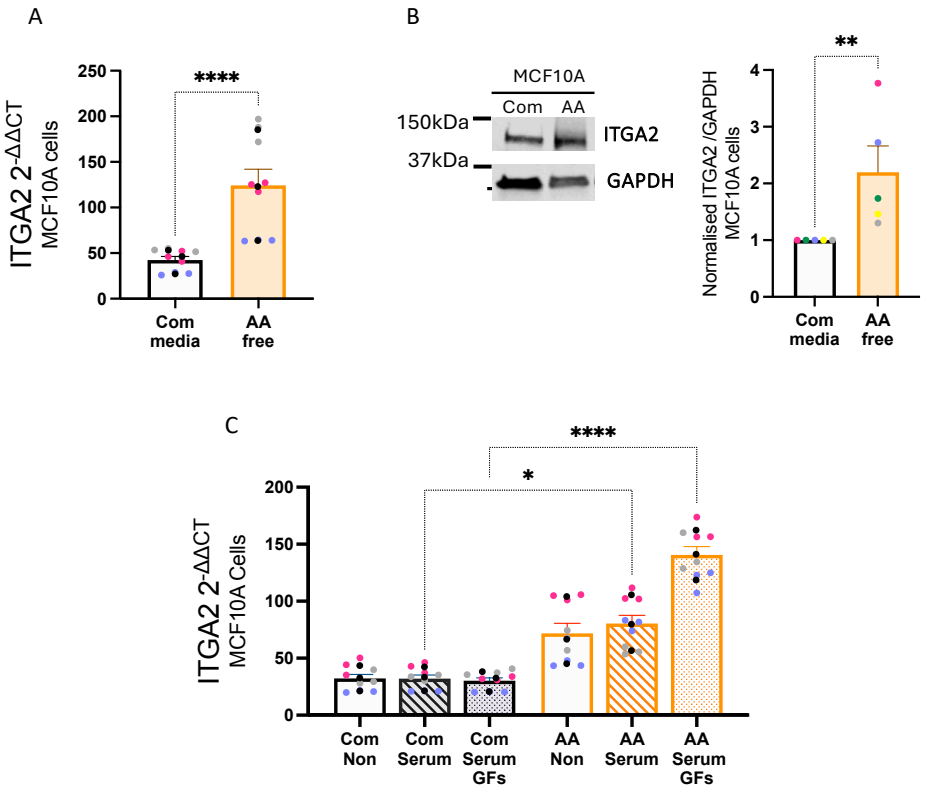

Figure 5-15 Amino acid starvation promoted α2 integrin expression in MCF10A in the presence of growth factors. MCF10A cells were seeded on plastic in complete (Com) or amino acid (AA) free media for 18 hours. The cells were collected; mRNA was extracted and α2 integrin (ITGA2) was measured by SYBR-Green qPCR. GAPDH was used as a control and the data were plotted as $2^{-\Delta\Delta CT}$ (A). MCF10A cells were seeded on plastic in complete (Com) or amino acid (AA) free media for 18 hours. Cell lysates were collected, and the samples were run by Western Blotting. Membranes were stained for α2 integrin (ITGA2) and GAPDH and imaged with a Licor Odyssey system. The protein band intensity was measured with Image Studio Lite software (B). MCF10A cells were seeded on plastic in complete (Com) or amino acid (AA) starvation media without serum, Insulin and EGF (Non), with serum but without Insulin and EGF (serum) or media with serum, Insulin and EGF (serum and GFs) for 18 hours. The cells were collected; mRNA was extracted and α2 integrin (ITGA2) was measured by SYBR-Green qPCR. GAPDH was used as a control and the data were plotted as $2^{-\Delta\Delta CT}$. N≥3 independent experiments, and values represent the Mean ± SEM, the coloured dots for biological repeats, the black dots represent the mean of the individual experiments. (A, B) Mann-Whitney test. (C) Kruskal-Wallis, Dunn's multiple comparisons test *p < 0.05, **p < 0.01, ****p < 0.0001.

5.2.12 Amino acid starvation promoted α2 integrin expression in a RAS-dependent manner in SW1990 cells grown in 3D.

To confirm our results in a more physiological context, SW1990 cells were grown in Matrigel for 24 hours in complete media, then starved for 2 days in AA free media. α2 integrin was stained, and its intensity in the acini structure was measured. Filled acini structures appear slightly irregular and smaller under AA starvation, with α2 integrin being localised at the cell surface. The quantification shows that the intensity of integrin α2 was significantly increased under AA starvation compared to complete media **(Figure 5-16, A)**. As expected, the acini area was reduced upon AA starvation **(Figure 5-16, B)**. Consistent with our 2D data, inhibiting KRAS

almost completely abrogated the expression of α2 integrin in both complete media and AA free media **(Figure 5-16, C)**. In addition, KRAS inhibition reduced the acini area under complete media, while there was no effect under AA starvation **(Figure 5-16, D)**.

These results confirm that AA starvation increased α2 integrin expression via RAS dependent mechanism, both in 2D and 3D systems

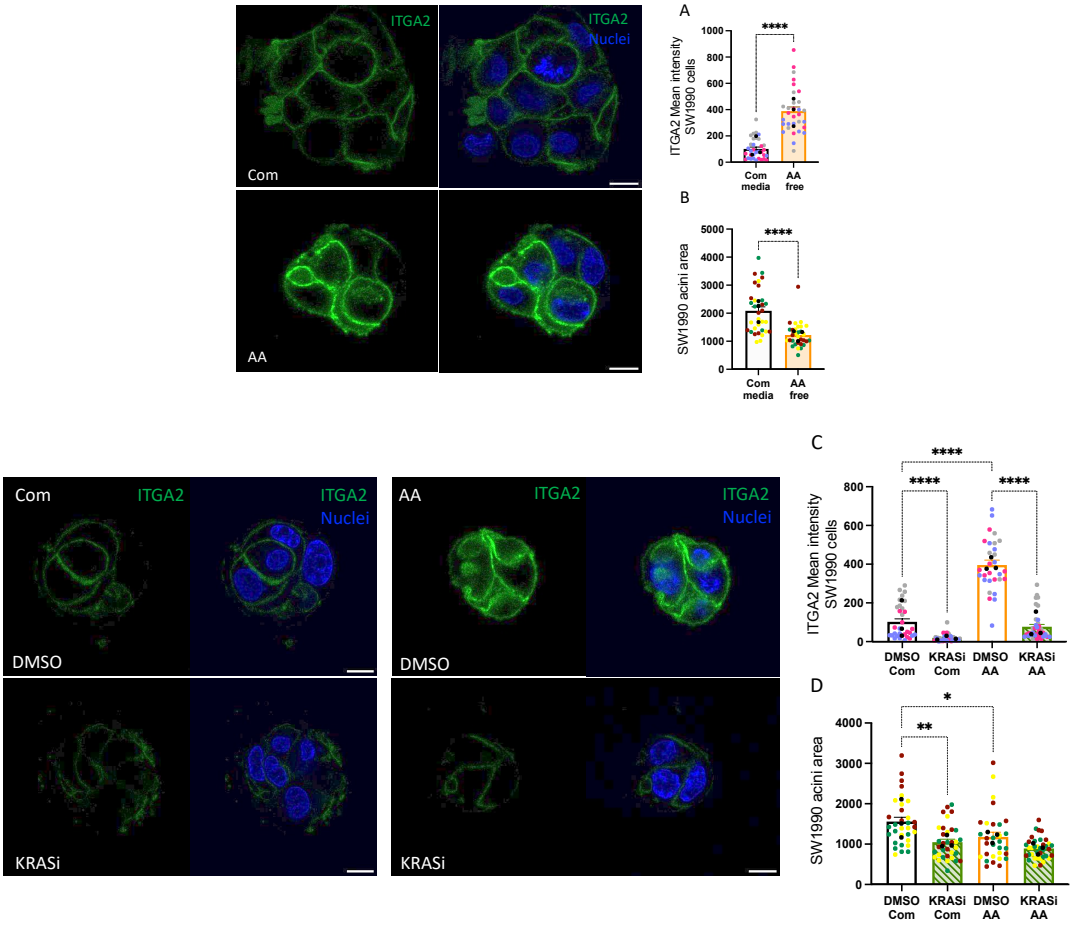

Figure 5-16 Amino acid starvation promoted α2 integrin expression in 3D, in a KRAS-dependent manner. SW1990 cells were grown in 3D Matrigel. After 24 hours, media was changed to either complete (Com) or amino acid (AA) free media (A-B). SW1990 cells were grown in 3D matrigel. After 24 hours, media was changed to either complete (Com) or amino acid (AA) free media in the presence of 200nM MRTX1133 (KRASi) or DMSO as a control (C-D). Cells were incubated for 2 days, fixed and stained for α2 integrin (ITGA2, green) and nuclei (blue). Cells were imaged with a Nikon A1 confocal microscope, 60x objective. Scale bar 10μm. (A, C) ITGA2 mean intensity and (B, D) acini area, were measured using ImageJ software. N=3 independent experiments, values represent the Mean± SEM, the coloured dots for biological repeats, the black dots represent the mean of the individual experiments. Mann-Whitney test. *$p < 0.05$, **$p < 0.01$, ****$p < 0.0001$.

5.2.13 Amino acid starvation promoted α2 integrin expression in MCF10CA1 breast cancer cells in a MAPK dependent manner in 3D.

MCF10CA1 cells were grown in Matrigel for 24 hours in complete media, then starved for 2 days in AA free media. α2 integrin was stained, and its intensity in the acini structure was measured. Similar to SW1990 cells, MCF10CA1 filled acini structures appear slightly irregular and smaller under AA starvation, with α2 integrin being localised at the cell surface and being more concentrated at the cell-cell junctions under AA starvation. The quantification shows that the intensity of integrin α2 was significantly increased under AA starvation compared to complete media **(Figure 5-17, A)**. Similarly to SW1990 cells, the acini area was decreased when cells were starved **(Figure 5-17, B)**, consistent with the fact that prolonged AA starvation reduces cell proliferation. Furthermore, MEK inhibition strongly reduced the expression of α2 integrin to almost undetectable levels under in both complete media and AA free media **(Figure 5-17, C)**. In addition, the acini area was significantly decreased under amino acid starvation compared to complete media in the presence or absence of the MEK inhibitor **(Figure 5-17, D)**. Thus, similarly to SW1990 pancreatic cancer cells, these results confirm that α2 integrin expression in MCF10CA1 breast cancer cells is mediated by the MAP/MEK pathway in 3D.

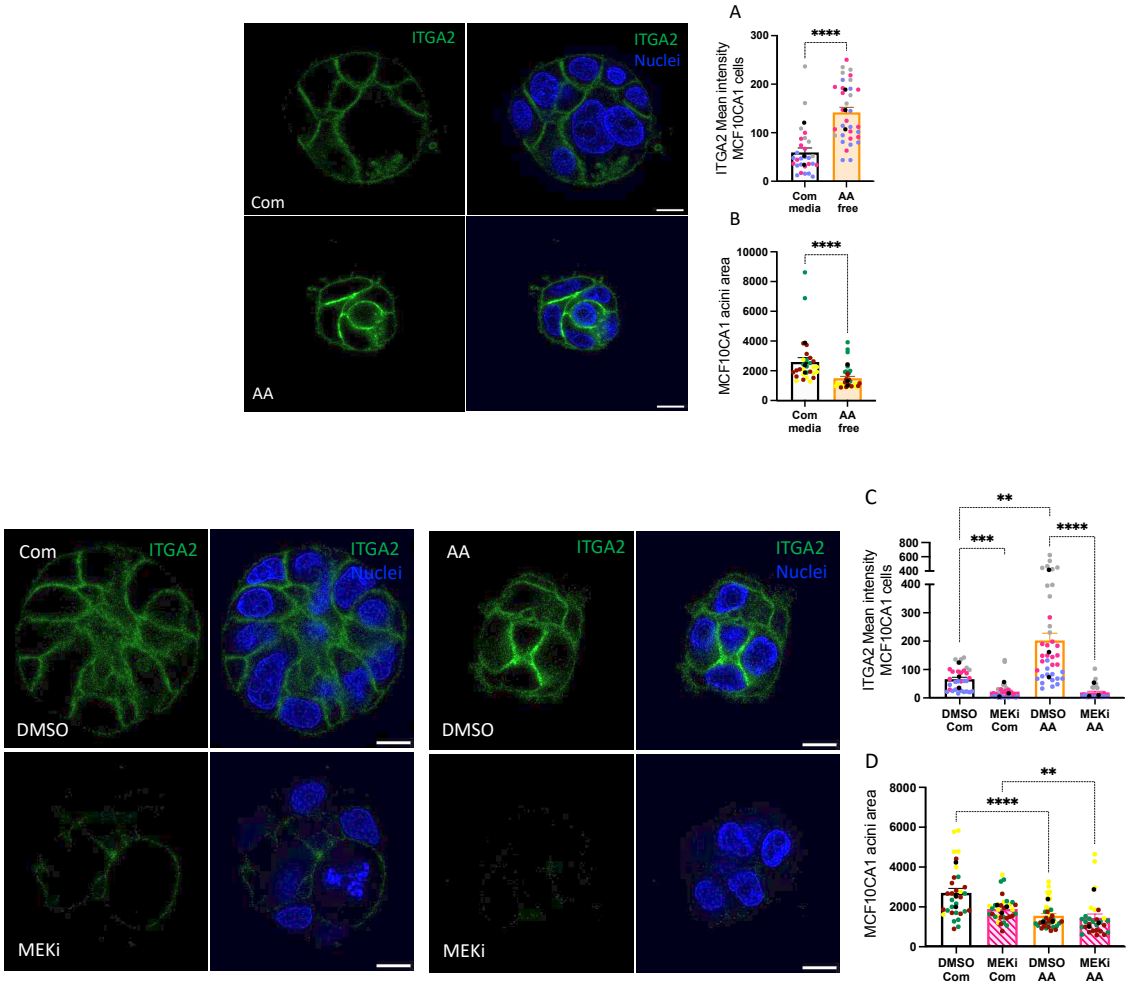

Figure 5-17 Amino acid starvation promoted α2 integrin expression in 3D, in a MAPK-dependent manner. MCF10CA1cells were grown in Matrigel. After 24 hours, media was changed to either complete (Com) or amino acid (AA) free media (A-B). MCF10CA1 cells were grown in 3D Matrigel. After 24 hours, media was changed to either complete (Com) or amino acid (AA) free media in the presence of 10μM Selumetinib (MEKi), or DMSO as a control (C-D). Cells were incubated for 2 days, fixed and stained for α2 integrin (ITGA2, green) and nuclei (blue). Cells were imaged with a Nikon A1 confocal microscope, 60x objective. Scale bar 10μm. (A, C) ITGA2 mean intensity and (B, D) acini area, were measured using ImageJ software. N=3 independent experiments, values represent the Mean ± SEM, the coloured dots for biological repeats, the black dots represent the mean of the individual experiments. Mann-Whitney test. **p < 0.01, ***p < 0.001, ****p < 0.0001.

5.2.14 Amino acid starvation promoted SW1990 pancreatic cancer cell adhesion to collagen I and spreading.

Integrins are adhesion receptors which play an important role in promoting cell adhesion (Kanchanawong and Calderwood, 2023). As the expression of α2 integrin was increased under AA starvation, we hypothesised that AA starvation promoted cell adhesion. To address this, SW1990 pancreatic cancer cells were grown in complete or AA free media for 18 hours, then seeded on plastic **(Figure 5-18, A)**, on collagen I **(Figure 5-18, B)** or on Matrigel **(Figure 5-18,**

C) for 15 minutes, 30 minutes, or 1 hour either in complete or AA free media. The show that more cells could adhered to collagen I under AA starvation compared to complete media within 30 minutes of adhesion. Interestingly, the number of cells adhered to plastic or Matrigel was similar in both complete and AA free media. To validate the results, SW1990 cells were seeded on plastic in complete or AA free media for 18hours. Cells then were seeded on collagen I for 1 hour in either complete media or AA free media. Figure 5-18, D shows the spreading of the cells on collagen I within an hour of adhesion. The cells were still rounded in complete media while in AA free media, the cells appear more spread. The quantification shows that the cell area was significantly increased under AA starvation compared to complete media (Figure 5-18, D). Overall, the data shows that AA starvation promoted adhesion to collagen I and spreading, which might be due to the increase in α2 expression.

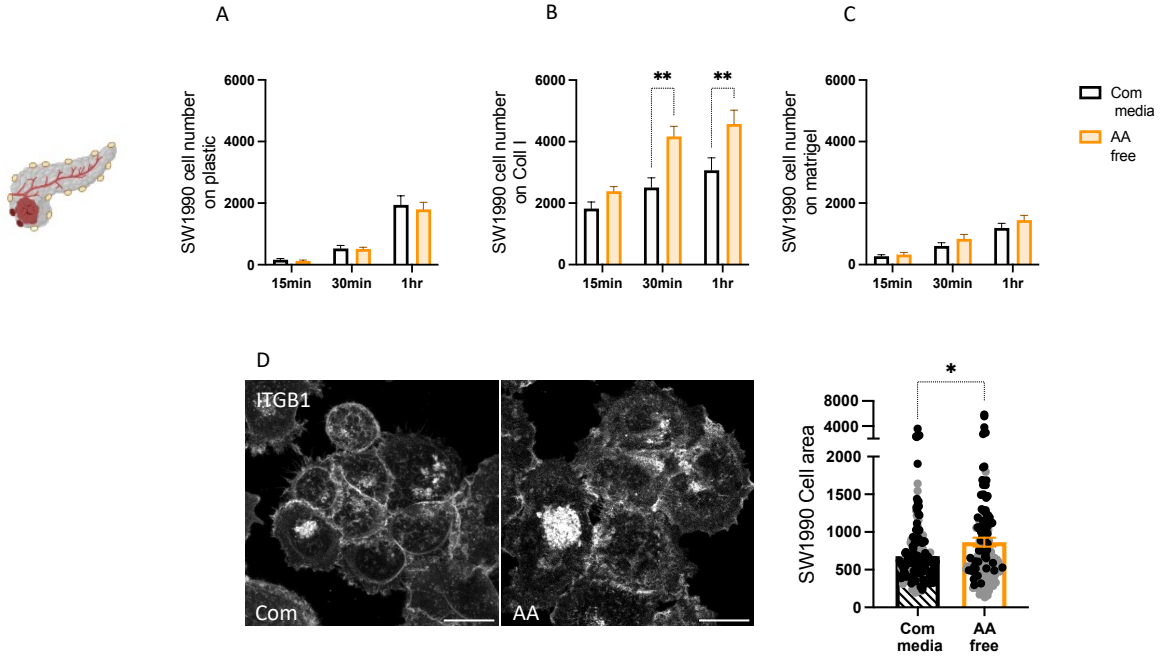

Figure 5-18 Amino acid starvation promoted SW1990 cell adhesion to collagen I and spreading. SW1990 cells were grown in complete media (Com) or amino acid (AA) free media for 18 hours then seeded on plastic (A), 2 mg/ ml collagen I (coll I, B), or 3 mg/ ml Matrigel (C). Cells were fixed after 15 minutes, 30 minutes, or 1 hour and stained with Hoechst 33342. The cells were imaged using an Image Xpress micro system and cell numbers were quantified with MetaXpress and CME software. N=3 independent experiments, values represent the Mean ± SEM. SW1990 cells were grown in complete media (Com) or amino acid (AA) free media for 18 hours and seeded on 0.5 mg/ml collagen I for 1hour. Cells were fixed and stained for β1 (ITGB1, white). The cells were imaged with a Nikon A1 confocal microscope, 40x magnification. The cell area was measured using ImageJ software. N=2 independent experiments (D). (A-B-C) Kruskal-Wallis, Dunn's multiple comparisons test. (D) Mann-Whitney test *p < 0.05, **p < 0.01.

5.2.15 Integrin α2 is upregulated in pancreatic cancer and correlates with poor prognosis

Our data show that the expression of α2 integrin is increased when cancer cells are in an AA deprived environment. The tumour microenvironment in pancreatic cancer is known for being deprived of nutrients (Kamphorst et al., 2015). Therefore, we assessed the expression of α2 integrin in pancreatic cancer patients. The data show that α2 integrin expression was highly increased in pancreatic tumours compared to healthy pancreatic tissue **(Figure 5-19, A)**. High α2 expression correlated with a reduction in the patients' overall survival **(Figure 5-19, B)** and disease free survival **(Figure 5-19, C)**. These data indicate that α2 integrin may contribute to the tumour progression and survival in pancreatic cancer patients.

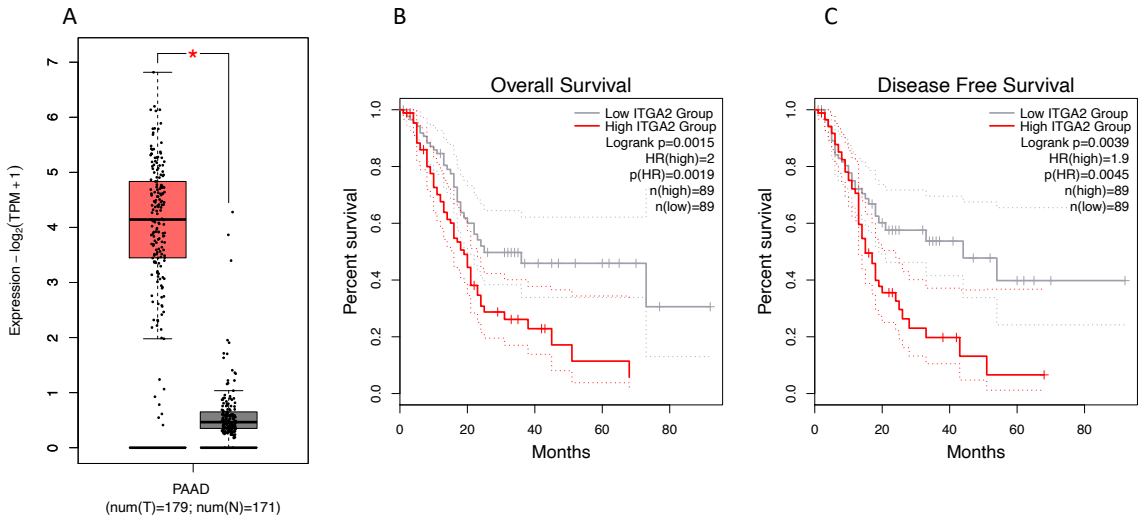

Figure 5-19 α2 integrin was over-expressed in pancreatic cancer patients and correlated with poor overall and disease-free survival. RNA sequencing analysis from pancreatic tumours (red, 179) compared to normal pancreas (grey, 171) for α2 integrin expression (A). Overall survival of patients with high (red) and low (grey) α2 integrin expression (B). Disease-free survival of patients with high (red) and low (grey) α2 integrin expression (C). The data were generated using GEPIA2 (http://gepia2.cancer-pku.cn/#index).

5.3 Discussion:

We showed that the ECM partially rescued breast cancer cell growth under AA starvation and this has been found to be due to the internalisation and degradation of the ECM **(chapter 3)** (Nazemi et al., 2024). Moreover, we found that integrins are required for ECM uptake (Martinez et al., 2024). Collagen I is the most abundant protein in the ECM and binds to its receptor $\alpha2\beta1$ integrin, which is expressed in many types of cells including epithelial cells (Heino, 2000). Here we showed that collagen I-dependent cell growth under AA starvation was mediated by $\alpha2\beta1$ integrin. In addition, we found that the expression of $\alpha2$, but not $\alpha5$, was consistently increased in breast and pancreatic cancer cells at both the mRNA and the protein level under AA starvation. Furthermore, the adhesion and spreading of pancreatic cancer cells on collagen I, but not Matrigel, was increased under AA starvation compared to complete media.

In an environment full of nutrients, we have recently shown that breast cancer cells uptake ECM components in an $\alpha2\beta1$ integrin and MAPK/p38 dependent mechanism. In addition, the downregulation of $\alpha2$ integrin significantly reduced breast cancer cells migration and invasion (Martinez et al., 2024). Here we showed that collagen I promoted the proliferation of MCF10CA1 breast cancer cells under AA starvation and Gln starvation. Collagen I-dependent cell proliferation was reduced after both pharmacologically inhibition and siRNA- mediated knockdown of $\alpha2$ integrin. Furthermore, inhibiting $\alpha2\beta1$ integrin decreased the uptake of collagen I under AA starvation. This indicate that $\alpha2\beta1$ integrin promotes cell proliferation in AA deprived environment likely by modulating ECM endocytosis. This is consistent with previous studies. For instance, Muranen et al showed that serum starvation of mammary epithelial cells triggered the internalisation of the ECM component laminin, in a $\beta4$ integrin-dependent manner. This led to an increase in intracellular amino acid content, re-activating mTORC1 and increasing cell survival under serum starvation conditions (Muranen et al., 2017). Another study showed that in a low glucose environment, fibronectin bound $\alpha5\beta1$ integrin is internalised in a tensin and Arf4 dependent mechanism. This integrin trafficking is necessary for the activation and recruitment of mTORC1 to the lysosomes under nutrient scarcity and enhanced cells migration (Rainero et al., 2015). Our previous work showed that under amino acid starvation, ECM components can be internalised via macropinocytosis (Nazemi et al., 2024). Indeed, it has been shown that integrins can be internalised via macropinocytosis. The

migration of glioblastoma cells was found to be regulated by ataxia telangiectasia and Rad 3 related kinase (ATR) mediated macropinocytosis. Interestingly α3, α5, and α6 integrins were internalised through macropinocytosis and this was required for the migration of glioblastoma cells (Derby et al., 2024). Another study showed that CYFIP-related RAC1 interacting (CYRI) proteins are macropinocytosis regulators and that α5β1 integrin can localise at the CYRI-positive macropinocytosis cups then be internalised via macropinocytosis. The loss of CYRI increased α5β1 integrin surface level which in turn promoted cell spreading and invasion (Le et al., 2021).

α2β1 integrin is one of the main collagen binding receptors and it also binds to laminin and some proteoglycans. The α2 subunit is responsible for binding to the ligand, and it determines the ligand specificity while the β1 subunit binds to the cytoskeleton (Adorno-Cruz and Liu, 2019, Naci et al., 2015). Our results showed that the expression of α2 integrin subunit was increased in a panel of breast and pancreatic cancer cells at both the mRNA and the protein level after AA starvation, while the changes in the expression of β1 and α5 were more variable. Interestingly, when SW1990 cells were seeded in the pancreatic tumour interstitial fluid media (TIFM), which more closely recapitulated the intra-tumoral nutrient levels, the expression of α2, but not α5, was increased at the mRNA level.

The expression of α2β1 integrin has been found to be upregulated in some types of cancer. A study by Mortiz et al showed that the expression of α2β1 integrin was increased in metastatic breast cancer cells compared to non-metastatic ones. Overexpressing α2 integrin subunit in MDA-MB-231 cells enhanced their invasiveness and migration but not their proliferation in vitro; however, it enhanced both their tumour growth and metastasis to the bone in vivo. Interestingly, by overexpressing α2 integrin subunit, the β1 subunit expression also increased (Moritz et al., 2021). On the contrary, another study showed that the loss of α2 in MMTV-neu mice increased tumour metastasis to the lungs in vivo without affecting tumour growth. (Ramirez et al., 2011). In this study, the authors used transgenic mice which carry the neu (c-erbB2, ERBB2) protooncogene to study the role of α2 integrin in breast cancer progression and this might be the reason why their results differ from Moritz et al. Hence the role of α2 integrin in breast cancer is still controversial and this might be due to multiple factors which affect integrins including the cancer stage, the breast cancer subtype and the tumour microenvironment. On the other hand, in PDAC, α2 integrin expression has been found to be

upregulated, and it is believed that it plays a critical role in PDAC progression. In a study by Ren et al, overexpressing α2 integrin boosted the proliferation of PDAC cells in vitro and the tumour volume in vivo (Ren et al., 2019). However, as the tumour microenvironment in both pancreatic and breast cancer is known for being nutrients deprived, studying integrins in conditions similar to the physiological ones would let us understand more accurately their role in cancer progression. Indeed, a recent study showed that β3 integrin expression increased at the mRNA and at the protein level in non-small cell lung cancer (NSCLC) cells when the cells were nutrient stressed. Starving the NSCLC cells in a Glc or serum free media upregulated the αvβ3 surface expression, which further enhanced cells viability and survival as a result of switching from glycolysis to OXPHOS / Gln metabolism. This αvβ3 effect on NSCLC metabolic reprograming was mediated by AMPK activation downstream of Src and was ECM independent, as the cells were in suspension when they were starved. The mechanism behind this increase in β3 integrin expression was not identified; however, the viability of the cells was significantly reduced by inhibiting β3 integrin or Src (Nam et al., 2024, Rainero, 2024). On the contrary, the expression of αvβ3 integrin was decreased when human glomerular epithelial cells (HGEC) were seeded in 5 mM Glc and increased when seeded in 25 mM Glc. Interestingly, also α2 integrin expression was increased when cells were seeded in 5mM Glc and cell adhesion to collagen IV was also enhanced (Kitsiou et al., 2003). Hence the upregulation in α2 integrin might not just be an AA starvation response, but it could be a more general stress response.

It is well established that when cells face stress conditions, they activate the integrated stress response (ISR) pathways. In particularly, AA deprivation triggers the GCN2 branch of the ISR (Pakos-Zebrucka et al., 2016). Here we showed that the increase in α2 integrin expression under AA starvation was partially mediated by GCN2 only in the wild-type RAS MCF7 breast cancer cells, while in both HRAS mutated cells (MCF10CA1) and KRAS mutated cells (Panc1 and SW1990), α2 integrin expression was mediated by RAS/MEK signalling pathway, in a GCN2-independent manner. A former study showed that leucin starvation of mouse embryonic fibroblast (MEF) cells for 6 hours resulted in gene expression changes. Interestingly, while the majority of genes were GCN2-depednent, 18% of the genes were GCN2-independent and 21% of the genes were partially dependent on GCN2. Hence GCN2 pathway is the main pathway that regulate gene expression under AA starvation, but it is not the only one (Deval et al., 2009).

Some studies showed that mutated RAS regulated the expression of integrins. For instance, by transforming MDCK cells with HRAS G12V or KRAS G12V mutant, α6 integrin was highly upregulated at both the mRNA and the protein level. The expression of α6 integrin was regulated by MAPK/ERK/FOSL1 pathway, which increased the cells resistance to anoikis (Zhang et al., 2017). Similarly, pharmacological inhibition of MEK1 in pancreatic cancer cells and melanoma cells decreased the expression of α6 and β3 integrins. In addition, the activation of the Raf-MEK-ERK pathway in NIH3T3 fibroblasts significantly increased the expression α6 and β3 integrin subunits. The boost in β3 integrin expression was achievable only by activating the ERK/MAPK pathway sustainably in cells expressing activated RAS-RAF-MEK-ERK but not transiently via growth factors or mitogens (Woods et al., 2001). This is in agreement with our results, where in MFC10A mammary epithelial cells, the expression of α2 integrin was not increased in complete media by adding serum or growth factors. However, starving the cells in the presence of serum or growth factors significantly increased α2 expression. Interestingly, the same study showed that the expression of α2 integrin was not increased by activating Raf-MEK-ERK pathway in fibroblasts (Woods et al., 2001). Our results also showed that the expression of α2 integrin in complete media is mediated by RAS only in one cell line (SW1990 cells) while inhibiting RAS in Panc1 cells did not affect the expression, suggesting that additional regulators contribute to the control of α2 expression in complete media. However, when cells are under stress due to the lack of AAs, the RAS-MEK pathway is triggered to increase the expression of α2. It would be interesting to investigate if this stress response mechanism is specific to AA deprivation or it is also triggered downstream of other stressors.

In multiple myeloma (MM) cells, oncogenic KRAS and NRAS interact with the AA transporter SLC3A2 and the AA sensor mTOR. This interaction regulates the translocation of SLC3A2 and mTOR to endo lysosomes and activates mTORC1. A combination of MEK inhibitor and mTORC1 inhibitor was shown to reduce MM tumour volume and promote MM patient survival. Interestingly, mTORC1 activation through this pathway was not observed in low Gln conditions, due to the reduction in SLC3A2 expression when cells were seeded in low Gln conditions for two weeks (Yang et al., 2022). In our experiments, we starved the cells only overnight and it is a full amino acid starvation. It would be interesting to determine if there is any effect of oncogenic RAS on mTORC1 activity in our system and if this in turn affect the gene expression machinery, leading to α2 upregulation. Nutrient starvation has been shown to activate AMPK,

another key metabolic sensor (Steinberg and Hardie, 2023). It has been previously shown that, the activation of AMPK by the AMPK activator AICAR led to the phosphorylation of BRAF at Ser729 in keratinocytes. The phosphorylation of BRAF promotes its binding to 14-3-3 adaptor proteins which eventually cause an inhibition to MEK-ERK signalling pathway and a reduction in cell proliferation. Interestingly, AMPK activation did not affect the mutant BRAF (Shen et al., 2013). Another study showed that, in BRAF mutant melanoma cells, the activation of AMPK by AICAR or metformin did not suppress cell growth unlike NRAS mutant cells. Here, the activation of AMPK led to the degradation of the dual-specificity protein phosphatase (DUSP6), increased ERK phosphorylation therefore accelerating cell growth (Martin et al., 2012). Hence it is worth assessing if AMPK is playing a role in the activation of ERK/MAPK pathway and the expression of α2 integrin. Wang et al showed that AA starvation or serum starvation triggered AMPK activation in human erythroleukemia K562 cells and rat hepatoma H4IIE cells, which in turn activated MEK/ERK and induced autophagy (Wang et al., 2009). However, the phosphorylation of ERK was shown at 6 hours of starvation. Our data showed that the phosphorylation of ERK was triggered after 5 minutes of AA starvation in both MCF10CA1 cells and SW1990 cells and declined after 10 and 15 minutes. Our data are in agreement with a former study showing that starving fibroblasts in AA free EBSS solution rapidly increased the phosphorylation of ERK after 5 minutes of starvation, reaching its maximum phosphorylation after 15 minutes, before gradually decreasing. The authors also showed that the volume of the cells was decreased after starving them and they suggested that the shrinkage of the cells might be the reason behind the rapid increase in ERK phosphorylation (Franchi-Gazzola et al., 1999). Interestingly, we've also seen a reduction in the 3D cell structure (acini) in AA free media compared to complete media. However, this might be also due to fewer cells being in the 3D structure, rather than individual cells being smaller. It would be interesting to investigate if the shrinkage of the cells is triggering a signalling pathway to feed in the KRAS/HRAS-MEK-ERK pathway and increase the expression of certain genes, including α2.

6 General discussion

6.1 Summary:

The TME supports tumour development at all stages of cancer. Particularly, the ECM impinges on the progression of cancer in different ways, due to its complex composition. First of all, the ECM is a reservoir for multiple essential components such as growth factors, cytokines and chemokines. Furthermore, the interaction between the ECM proteins and cancer cells triggers signalling cascades which promote cell growth, invasion and migration. The deposition and the alignment of the ECM proteins provide a highway for cancer cells to migrate. In addition, the internalisation and degradation of ECM proteins enhance cancer cells invasion and migration (Lu et al., 2012, Cox, 2021, Nazemi et al., 2024, Martinez et al., 2024).

We showed in this project that one way in which the ECM supports tumour progression is by providing nutrients for cancer cells to survive under starvation. Indeed, the ECM partially rescued breast cancer cells growth under different starvation conditions. This effect was shown to be due to an increase in cell division or a decrease in cell apoptosis depending on the starvation condition. Starved cancer cells were able to uptake and degrade ECM proteins under AA starvation, this in turn increased intracellular AA levels, while under glucose starvation the ECM promoted pro-tumorigenic signalling. However, more studies are needed to define the molecular details behind the latter **(Figure 6-1)**.

Furthermore, we showed that, under amino acid starvation, ECM dependent cell growth was mediated by ECM receptors of the integrin. Here we focused our study on $\alpha 2\beta 1$ integrin, the major collagen receptor. Interestingly, the expression of $\alpha 2$ subunit was highly increased under amino acid starvation at both the mRNA and the protein level. The expression of $\alpha 2$ integrin was shown to be regulated by active KRAS in pancreatic cancer cells and possibly active HRAS in breast cancer cells (more studies are needed to confirm this). Investigating the signalling pathway downstream of RAS showed that $\alpha 2$ expression is promoted by the MAPK (KRAS-MEK-ERK) pathway, which is stimulated by amino acid starvation.

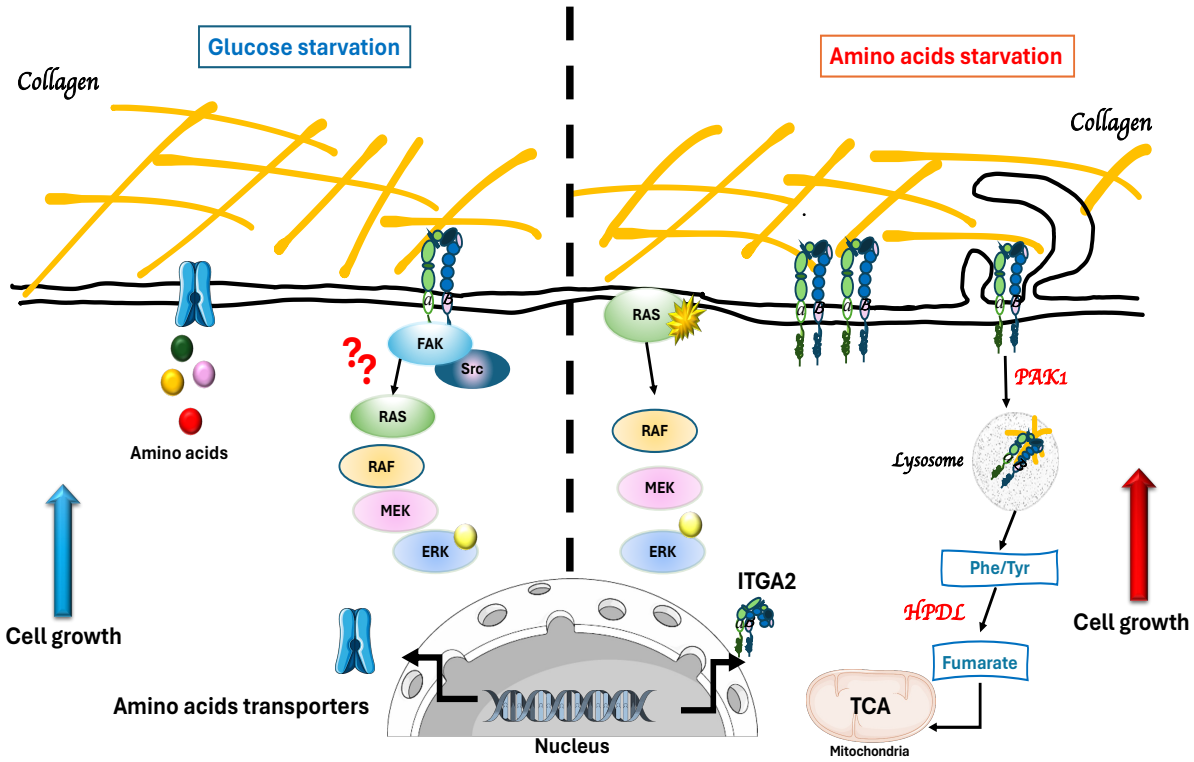

Figure 6-1 Working model. Under AA starvation, invasive breast cancer cells uptake collagen I in a PAK1 dependent mechanism and degrade it in the lysosomes. The degradation of collagen upregulates phenylalanine/ tyrosine catabolism leading to the production of fumarate which promotes cell growth. The expression of ITGA2 (α2 integrin) is increased under AA starvation in a RAS/MEK/ERK mechanism in breast cancer and pancreatic cancer cells harbouring RAS mutations. Under Glc starvation, collagen I promotes invasive breast cancer cell growth in an α2β1 dependent mechanism. α2β1 integrin binding to collagen might trigger adhesion signalling effect leading to an increase in AA transport, which enhances cell growth/survival.

6.2 ECM partially rescued highly invasive breast cancer cell growth under different starvation conditions

The growth of MCF10CA1 cells was partially rescued by collagen I, Matrigel and CAF-CDM under AA, Glc, Gln and Glc/Gln starvation. Under Gln starvation, cell growth was promoted for up to 6 days on the three types of ECM, while under AA starvation, cell growth reached a plateau after day 4. Similarly, under Glc starvation, cells grew on collagen I and Matrigel but reached a plateau after day 4. However, CAF- CDM rescued the cell growth only for 4 days, then the cell numbers started to decease gradually.

The ECM is a mixture of around 300 proteins known as the 'core matrisome'. These proteins can bind to specific receptors leading to the activation of multiple signalling pathways. In addition, the stiffness of the ECM can have a profound effect on cell behaviour. Our data showed that the effect of the simple matrices, collagen I and Matrigel, on cell growth was stronger than CAF-CDM. MCF10CA1 cells are invasive ductal carcinoma cells with high

metastatic potential (So et al., 2012), hence they have the ability to invade the basement membrane (represented by Matrigel *in vitro*) and the interstitial matrix (consisting of mainly collagen I). Since CAF-CDM is a more complex type of ECM with a dense and stiff texture (Rafaeva et al., 2023), it is possible that some ECM component specific to CAF-CDM could slower cell growth under starvation. Furthermore, the cells grew better on all types of ECM under Gln starvation compared to the other starvation conditions. ECM components are source of AAs and Glc. Collagens are the most abundant components and are enriched in proline and glycine. Proline can be an alternative to Gln, as it can be converted into pyrroline-5-carboxylate (P5C), then to glutamate and α-ketoglutarate which can feed the TCA cycle (Hsu et al., 2022). Interestingly it was previously shown that, under Gln deprivation, PDAC cells limited their Glc uptake as well, as they used collagen-derived proline as an alternative nutrient source (Olivares et al., 2017).

Overall, our data showed that both simple and complex types of matrices can partially rescued MCF10CA1 cell growth. However, the mechanism behind this might differ according to the starvation condition, and the type of ECM.

6.3 The ECM promotes cell division and prevents cell apoptosis in different starvation conditions

Various studies showed that cells use extracellular proteins to grow under starvation, such as albumin under AA starvation (Kamphorst et al., 2015), under EAA starvation (Palm et al., 2015) and under Gln starvation (Commisso et al., 2013). Furthermore, it was shown that under serum starvation, ECM proteins, both laminin (Muranen et al., 2017) and collagen I (Badaoui M et al., 2018), reduced cell apoptosis.

By performing EdU incorporation assay, we showed that ECM-dependent cell growth was associated with an increase in cell division under the three starvation conditions used. However, starvation specific effects were identified when assessing the impact of the presence of ECM on cell death. While collagen I and Matrigel did not affect cell death under AA starvation, both collagen I and Matrigel supressed cell apoptosis under Glc starvation. It was previously shown that 24 hours Glc starvation induced cell apoptosis in breast cancer cells due to an increase in reactive oxygen species (ROS) (Raut et al., 2019). Furthermore, Endo et al compared cell viability in adherent versus detached cells. They found that 24 hours Glc starvation reduced cell viability in adherent cells, but not in detached cells (Endo et al., 2020).

It is worth mentioning though that Endo et al used 2-hydroxyethyl methacrylate as a substrate, while we used collagen I and Matrigel which represent more the physiological ECMs. It is therefore possible that different substrates have differential effects on cell viability in response to Glc starvation. Our data showed that between day 3 and day 6 of Glc starvation, the number of apoptotic cells doubled on plastic, while on collagen I or Matrigel, the number of apoptotic cells did not change, indicating that ECM sustains cell survival in prolonged starvation. A previous study by Chiodi et al showed that under Glc starvation, starving transformed fibroblasts for around 48 hours resulted in cell detachment however, most of the cells were still alive. Hence Glc might be necessary for fibroblasts attachment. On the contrary, the cells survived under Gln starvation for 72 hours but started dying after prolonged starvation (CHIODI et al., 2019). However, our data showed that on ECM cells survived under Glc starvation. Despite the fact that fibroblasts could have secreted ECM during the 48 hours glucose starvation, this might not be enough for the cells to survive. Moreover, as we hypothesised that cells rely on extracellular AAs under Glc starvation, it would be interesting to refresh the media to assess if this would enhance cell proliferation.

The observation of the antiapoptotic effect of ECM under Glc starvation but not AA or Gln starvation could be due to the different mechanisms that the ECM take to support cell survival under different conditions. More studies are needed to address the role of ECM on cell apoptosis and to identify the molecular mechanisms mediating this.

6.4 The ECM promotes cell growth via different mechanisms

To overcome the TME nutrient scarcity, cancer cells reprogram their metabolism via different mechanisms, switching from glycolysis to OXPHOS, triggering signalling cascades, intercellular communication between cancer cells and TME cells including CAFs, in addition to the support from the ECM network. Hence, multiple mechanisms could be involved in promoting cancer cell survival under nutrient stress. Our data showed that breast cancer cells uptake ECM proteins via macropinocytosis and degrade them in the lysosomes under AA and Gln starvation (Nazemi et al., 2024). However, under Glc starvation, chemically cross-linking collagen I slightly reduced MCF10CA1 cell growth and it had no effect at all on MDA-MB-231 cell growth (Nazemi, 2020), while the inhibition of $\alpha 2$ integrin significantly reduced cell growth on collagen I. Hence, under Glc starvation, adhesion signalling is more likely to be involved. Integrin mediated cell adhesion plays an essential role in cell proliferation and survival. Focal adhesion kinase (FAK) is

an essential component in the adhesion complexes. FAK is one of the first recruited adhesion proteins, its activation increases when integrins bind to the ECM, which in turn triggers multiple signalling pathways (Haake et al., 2024). FAK was shown to be overexpressed in different types of cancer. ECM-integrin binding increased the phosphorylation of FAK in PDAC cells and triggered RAS/ERK signalling pathway. Furthermore, FAK was shown to be overexpressed in PDAC and malignant pleural mesothelioma (MPM) and its inhibition reduced cell proliferation and increased cell apoptosis and cell cycle arrest (Sawai et al., 2005, Kanteti et al., 2018). Hence, the phosphorylation of FAK plays a critical role in cancer cell survival. Studies in our lab showed that the inhibition of FAK significantly reduced the ECM-dependent cell growth of MDA-MB-231 cells under Glc starvation (Nazemi, Rainero lab, unpublished). It is therefore possible that ECM-dependent cell survival under Glc starvation is mediated by FAK-RAS-ERK pathway. Further studies are needed to confirm this.

It was previously shown that PDAC cells uptake and degrade collagen I and IV under both Glc and Gln starvation (Olivares et al., 2017). Normally, nutrient scarcity deactivates the metabolic sensor mTORC1 and the uptake and internalisation of extracellular proteins can reactivate it (Palm et al., 2015). Interestingly, a previous study showed that focal adhesions (FAs) are required for mTORC1 signalling where mTORC1 was shown to be in close proximity with FAs such as Paxillin. In serum starved cells, FAs were required for the activation of mTORC1 following refeeding with serum and both the knockdown and the pharmacological inhibition of FAs reduced mTORC1 activity and free amino acids uptake (Rabanal-Ruiz et al., 2021). Another study showed that under starvation, different types of cancer cells internalised collagen I, leading to the activation of mTORC1 (Yamazaki et al., 2020). These results are in agreement with what we have recently published as the uptake of collagen I reactivated mTORC1 under AA starvation in MDA-MB-231 breast cancer cells (Nazemi et al., 2024). On the contrary, collagen uptake under Glc starvation did not activate mTORC1 in PDAC cells but instead increased the phosphorylation of ERK (Olivares et al., 2017). Hence, cancer cells might react to starvation conditions in different ways.

The binding of ECM to its cell surface receptors can trigger signalling pathways to promote survival under nutrient stress. Blocking the internalisation of ECM completely reduced ECM dependent cell growth under amino acid starvation. However, under glucose starvation the growth was slightly decreased in MCF10CA1 cells and non-effective at all in MDA-MB-231 cells

(Nazemi, Rainero lab, unpublished). Hence, we suggested that ECM might promote cell survival by activating adhesion signalling under glucose starvation.

Overall, our data showed that the ECM supported cancer cells growth under starvation conditions via different mechanisms. However, within a tumour, nutrient availability could fluctuate during the tumour growth and expansion. In addition, cells at the edge of a tumour can be exposed to variety of metabolites unlike cells residing in the tumour core, where they are more exposed to hypoxic and nutrient deprived environment. Furthermore, nutrients availability for the tumour can vary according to the patient dietary nutrient intake (Altea-Manzano et al., 2020). Our data showed that the ECM supported breast cancer cell growth even in the absence of both Glc and Gln. However, studying the effect of ECM in a more physiological environment such as growing in TIFM (tumour interstitial fluid) (Sullivan et al., 2019a, Saab et al., 2023) or Plasmax (a plasma like medium) (Voorde et al., 2019) will provide more clues about the *in vivo* nutrients' availability and hence the ECM role in such an environment.

6.5 ECM modified the intracellular metabolite content under starvation

The metabolomics analysis showed that seeding breast cancer cells on collagen I under starvation conditions can upregulate multiple metabolites. **Figure 6-2** summarises the metabolic pathways upregulated on collagen I under complete media, AA, Gln and Glc starvation conditions. There are 167 metabolites upregulated on collagen I under all nutrient starvation conditions. Pathway analysis of these metabolites showed that glycine, serine, threonine metabolism; arginine, and proline metabolism; nitrogen metabolism and phenylalanine, tyrosine, and tryptophan biosynthesis were the most upregulated metabolic pathways under AA, Gln and Glc starvation conditions **(Figure 6-2).**

Phenylalanine and tyrosine metabolism was also found upregulated in MD1-MB-231 cells seeded on collagen I under AA starvation and the inhibition of macropinocytosis reduced fumarate levels, indicating that Phenylalanine and tyrosine catabolism is activated by ECM uptake (Nazemi et al., 2024). Our data showed that the ECM-dependent cell growth was reduced after the knockdown of HPDL, one of the enzymes that regulate this metabolic pathway. The expression of HPDL was found to be increased in PDAC cells and it is correlated with poor patient survival. HPDL can also localises to the mitochondria and it promotes the

production of ATP (Ye et al., 2020). Interestingly, this pathway was also upregulated on collagen in complete media. Hence, nutrient might have been partially depleted in the complete media condition. It is worth checking if refreshing the media would give the same results.

Our data showed that the level of both phenylalanine and tyrosine was increased intracellularly when the cells were seeded on collagen I and on CDM (Nazemi et al., 2024). One possibility is that some components such as albumin, which is present in the serum, might have bound to collagen to be internalised. Hence the presence of ECM components might be essential to trigger the internalisation of other extracellular components. On the other hand, phenylalanine is present in the cell culture media which can also be internalised with ECM proteins via macropinocytosis.

Purine metabolism was upregulated in breast cancer cells seeded on collagen I under AA starvation and complete media. A study showed that purine metabolism plays a role in hepatocellular carcinoma (HCC) progression as purine biosynthesis pathway was found to be upregulated in HCC and high expression of enzymes involved in purine biosynthesis pathway was correlated with poor patient survival (Chong et al., 2020).

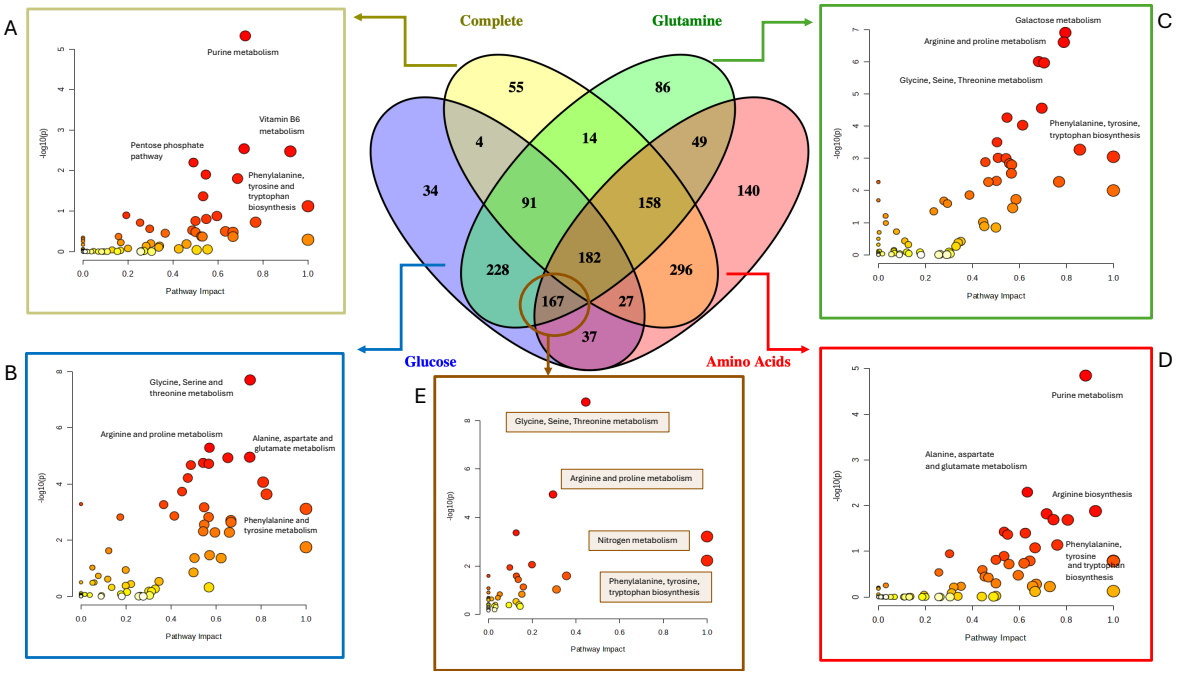

Figure 6-2 Venn diagram of the upregulated metabolites on collagen I under complete media and starvation conditions. The upregulated metabolic pathways under (A) complete media, (B) Glc starvation, (C) Gln starvation, (D) AA starvation, and (E) in common between AA, Gln and Glc starvation. Non-targeted metabolomics data analysed using MetaboAnalyst 5.0 https://www.metaboanalyst.ca.

Glycine, serine, and threonine was the most upregulated pathway on collagen I under the three starvation conditions **(Figure 6-2, E)**. Serine and glycine are linked to each other, and they can support tumour growth as they provide precursors to produce lipids, nucleic acids and proteins (Amelio et al., 2014). Serine can be synthesised from a glycolysis derived side chain, and it is the second most consumed AA by cancer cells (Amelio et al., 2014, Sullivan et al., 2019b). It was shown that the expression of phosphoglycerate dehydrogenase (PHGDH) enzyme, in the serine biosynthesis pathway, is increased in some types of cancer including breast cancer and that this can accelerate tumour growth especially in TMEs that have limited serine availability (Sullivan et al., 2019b).

The use of Nitrogen is fundamental for cancer cell growth, as nitrogen can be used for the biosynthesis of multiple biomolecules including AAs and nucleotides. AAs are the major source of nitrogen especially glutamine, glutamate and arginine (Kurmi and Haigis, 2020). Nitrogen metabolism was one of the highly upregulated metabolic pathways on collagen I under the three starvation conditions **(Figure 6-2, E)**. ECM might be supporting cancer cell growth under starvation through ECM uptake (in the case of AA and Gln starvation) or via triggering signalling pathways which can increase the intracellular AAs such as promoting autophagy or increasing the AA uptake (under Glc starvation). Indeed, preliminary data from the lab showed that under Glc starvation, collagen I promoted the survival of MDA-MB-231 via a balancing mechanism between autophagy and AA transport (Nazemi, Rainero lab, unpublished). Further studies are needed to confirm if ECM is enhancing any of these mechanisms to support MCF10CA1 cells growth.

Another interesting pathway which was upregulated under starvation was arginine and proline metabolism. A study showed that removing arginine from the cell culture media of MCF7 breast cancer cells led to a growth arrest and re-adding it to the media resumed cell proliferation (Chiaviello et al., 2012).

Further studies are needed to confirm that the upregulation of some metabolic pathways is mediated by the interaction between ECM and cancer cells and determine the molecular mechanisms behind this.

6.6 ECM-dependent cell growth is mediated by integrins

Cells interact with the ECM via cell surface receptors, mainly integrins. It is well established that integrins play multiple roles to support the progression of cancer and this includes the effect

of integrin signalling on cancer metabolism (Ata and Antonescu, 2017). Our data showed that cancer cells internalise ECM proteins under AA starvation via macropinocytosis. Furthermore, ECM-dependent cell growth was disrupted when both PAK1 and α2β1 integrin expression was inhibited or downregulated under AA and Gln starvation, while under Glc starvation, the siRNA-mediated downregulation of PAK1 did not affect the ECM dependent cell growth. This prompted us to study the expression of integrins under starvation. Indeed, our data showed that under AA starvation and Gln starvation (preliminary data, not shown), the expression of α2 was increased in a panel of breast and pancreatic cancer cells which have different morphology (epithelial and mesenchymal) and have different genetic alterations. Hence, α2 integrin upregulation was a nutrient deprivation response but not specific to certain types of cells. The expression of integrins varies across different types of cancer and according to the stage of cancer. For instance, it is possible that the expression of α2β1 is decreased during ECM detachment. However, the expression of α2β1 is increased when cancer cells start migrating especially to collagen rich organs such as bone and liver (Naci et al., 2015). Hence, the expression of α2β1 integrin tends to fluctuate during cancer cell progression. Therefore, the question is how cancer cells benefit from the upregulation of α2 integrin under nutrient starvation? a) Promoting cell adhesion. Indeed, our data showed that starved pancreatic cancer cells adhered faster on collagen I compared to non-starved cells, and this could be due to the increase in α2 integrin expression. b) Increasing the binding to ECM proteins especially collagens which in turn can trigger multiple signalling pathways. c) Promoting ECM macropinocytosis as ECM ligands need to bind to their integrin receptors to be internalised. Indeed, our data showed that the inhibition of α2β1 integrin reduced the uptake of collagen I under AA starvation. α2β1 integrin might also promote macropinocytosis via the activation of PI3-kinase (PI3K), a macropinocytosis regulator (Recouvreux and Commisso, 2017) where studies showed that PI3K is activated downstream of integrins in a mechanism dependent on FAK and Src (Wu et al., 2016) and independent of FAK and Src (Velling et al., 2004). Overall, the upregulation of α2 integrin under nutrient starvation could represent a stress response promoting cancer cell survival via multiple mechanisms. Further studies are needed to determine if the expression of α2 integrin is controlled by other stress-mediating conditions.

On the contrary to α2, the expression of α5 and β1 was variable across the tested cell lines. The variation in the integrin expression under starvation conditions could be due to the

crosstalk between integrins. This crosstalk mechanism depends on the amount of integrins expressed on the cell surface and their intracellular repository (Samarzija et al., 2020). For instance, it was previously shown that the reduction of the expression of α6 integrin reduced the expression of α2, α3 and β4 integrins in keratinocytes. The expression of α3 was shown to be regulated by α6β3/PI3K/AKT/mTOR mechanism and α3 integrin in turn regulated the expression of α2 integrin (Kligys et al., 2012). The reduction of αvβ5/αvβ6 enhanced the migration of colon cancer cells in a collagen rich environment due to the activation of α2β1 integrin in a PI3K independent mechanism (Defilles et ai., 2009). Integrins crosstalk was also shown to affect therapies, where some integrins can compensate for others when they are targeted by anticancer treatments (Samarzija et al., 2020). α2 integrin was also shown to play a role in anti-cancer drug resistance in breast cancer, pancreatic cancer and NSCLC via different mechanisms (Naci et al., 2015). Hence it would be interesting to investigate whether the increase in α2 integrin expression is linked to therapy resistance.

6.7 The expression of integrins under amino acid starvation is regulated by the RAS-MEK-Erk pathway

During cancer progression, cancer cells might experience different kinds of stress such as mechanical stress, oxidative stress, and metabolic stress (Chen and Xie, 2018). However, cancer cells must adapt and trigger mechanisms to overcome the extracellular and intracellular stress. Under AA deprivation stress, cells trigger an integrated stress response (ISR) mediated by the activation of GCN2 which leads to the upregulation of specific genes (Pakos-Zebrucka et al., 2016). Our data showed that the upregulation of α2 integrin was partially mediated by GCN2 activation only in MCF7 breast cancer cells. In the other cell lines, the expression of α2 integrin under AA starvation was mediated by mutated KRAS and its downstream MAPK/MEK pathway. The expression was also mediated by MAPK/MEK in HRAS mutated cells, and our preliminary data shows that by using a Pan-RAS inhibitor, the expression of α2 was reduced in HRAS mutated MCF10CA1 cells under AA starvation (not shown). This indicates that in mutant RAS cells under AA starvation, oncogenic RAS induces a cellular stress response, while in wild type RAS cells, GCN2 might be the main stress response regulator. A former study showed that in hepatocellular carcinoma cells, the AA stress response was mediated by both HRAS and NRAS

but not KRAS (Shan et al., 2015). Further studies are needed to confirm if the stress response is regulated by all RAS family members in breast and pancreatic cancer cells.

It is already known that RAS can regulate nutrient stress response, for instance by inducing macropinocytosis in PDAC cells (Commisso et al., 2013). Hence, RAS might regulate the ECM dependent cell survival under starvation conditions via different mechanisms: a) Increasing macropinocytosis, which is the ECM uptake mechanism that we have seen under AA starvation. b) Increasing the expression of the integrin receptors. RAS was also shown to interact with integrins causing drug resistance. For instance, αvβ3 integrin has been shown to promote Erlotinib resistance. This was identified to be mediated by an association between αvβ3 and KRAS, but not any other types of RAS. αvβ3 integrin co-localised with KRAS at the plasma membrane, which then activated RalB-TBK1-NF-kB downstream of RAS leading to the formation of highly aggressive cancer cells. Interestingly, this study was performed in the absence of ECM, hence αvβ3 integrin was unligated (Seguin et al., 2014). We have assessed the expression of α2 integrin in the absence of ECM. FAK was previously shown to support the progression of breast cancer cells carrying RAS and PI3K mutations. Silencing FAK caused growth arrest and apoptosis in mutated cells but not in normal mammary epithelial cells. The integrin ligation was shown to be essential for the activation of FAK and silencing β4 integrin had the same cell growth arrest effect (Pylayeva et al., 2009). Hence, it would be interesting to investigate whether the presence of ECM and FAK have a role in the RAS-dependent α2 integrin upregulation.

We have only explored the role of the MAPK pathway as it is known for its involvement in the induction of gene expression. It would be interesting to examine other pathways downstream of RAS to identify any other α2 integrin expression regulators.

In RAS mutated cancers, RAS is constitutively active. Previous studies showed that wildtype RAS can contribute to the activation of downstream signalling pathways. For instance, in KRAS mutated cancers, both wildtype NRAS and HRAS can increase the tumorigenesis (Sheffels and Kortum, 2021). Indeed, our data showed that AA starvation induced the expression of α2 integrin in both Panc1 and SW1990 pancreatic cancer cell lines in a KRAS mediated manner. However, in complete media, inhibiting mutated KRAS reduced the expression of α2 in SW1990 cells but not in Panc1. This suggests that the expression of α2 integrin might not be always regulated by mutated RAS as under nutrient stress both mutated RAS and possibly wildtype

RAS, which might be activated via RTKs/SOS, contribute to the upregulation of α2 integrin. Further studies are needed to confirm if wildtype RAS is activated under AA starvation and if this activation plays a role in the α2 integrin upregulation.

6.8 Therapeutic opportunities

The role of ECM in cancer progression has been of interest for decades especially for the types of cancer which are surrounded by thick ECM, such as breast and pancreatic cancer. These types of cancer can face nutrient scarcity and use extracellular macromolecules as source of nutrients to survive.

Here we showed that cancer cells uptake and use ECM proteins to survive under AA starvation. Ideally, blocking this route might be a promising target to stop cancer cell growth. The uptake of ECM proteins was shown to be mediated by α2β1 integrin and the expression of α2 subunit was shown to be increased in RAS mutated cancer cells under AA starvation.

RAS genes are among the most frequently mutated genes in various types of cancers, and they play a critical role in tumorigenesis. Thus, cancer patients with RAS mutations have poor prognosis. Lots of efforts are being dedicated towards developing cancer drugs which target RAS protein, and its upstream mediators or its downstream effectors. However, multiple drug resistance mechanisms have already been shown. Therefore, there is need to identify new approaches to overcome the drug resistance to the current treatments.

Interestingly, a recent study showed that chemoresistance in KRAS mutated PDAC cells was mediated by α2 integrin where the expression of α2 integrin was shown to be increased in Gemcitabine resistant cells and they suggested inhibiting α2 integrin to overcome chemoresistance in PDAC (Gregori et al., 2023). However, the mechanism was not identified. Similarly in MDA-MB-231 breast cancer cells, α2β1 integrin was shown to inhibit the apoptotic effect of Paclitaxel treatment in a PI3K/AKT dependent mechanism (Aoudjit and Vuori, 2001).

The KRAS mediated α2 integrin expression in our study might be a general stress response and it could be a result of activating wildtype RAS in KRAS mutated cells (further studies are needed to confirm this). Hence, we suggest a therapeutic approach for KRAS mutated cancer patients which is a combination of the following treatments.

Table 6-1 suggested treatment combinations for KRAS driven cancers

PDAC	Chemotherapy (Gemcitabine)	KRAS inhibitor (MRTX1133)	SOS inhibitors or RTKs inhibitors
Breast cancer	Chemotherapy (Paclitaxel)	RAS inhibitor	SOS inhibitors or RTKs inhibitors
PDAC/Breast cancer	α2 integrin inhibitors (bufalin or E7820)	HRAS/KRAS inhibitor	SOS inhibitors or RTKs inhibitors

6.9 Conclusion and future directions

In this research project, we identified the role of the ECM and its receptor α2β1 integrin in breast cancer cell survival under nutrient starvation conditions. Under AA starvation, ECM partially rescued the growth of invasive breast cancer cells. This effect was shown to be due to the internalisation and degradation of ECM proteins. Collagen I was shown to increase the intracellular metabolites, and multiple metabolic pathways were upregulated including phenylalanine and tyrosine metabolism. Inhibiting HPDL, an enzyme involved in phenylalanine and tyrosine catabolism, reduced the ECM mediated cell growth under AA starvation (Nazemi et al., 2024).

AA starvation was also shown to increase the expression of α2 at both the mRNA and protein level in both breast and pancreatic cancer cells harbouring mutated RAS. The upregulation of α2 integrin under AA starvation was shown to be mediated by KRAS-MAPK-ERK pathway in PDAC cells and MAPK-ERK pathway in invasive breast cancer cells, while in wildtype RAS cells, the expression of α2 integrin was shown to be mediated by GCN2 pathway.

Similarly, ECM partially rescued invasive breast cancer cell growth under Glc starvation. However, this effect was shown to be possibly mediated by adhesion signalling. Collagen I increased the intracellular metabolites and upregulated metabolic pathways mainly involved in AA metabolism, suggesting that under Glc starvation cancer cells might rely on AAs to survive.

Overall, this work highlighted the role of ECM and α2β1 integrin receptor in the nutrient deprivation stress response of RAS mutated cancer cells. Some of the remaining questions that need to be addressed are listed below:

- Is the α2 integrin upregulation in cancer a general stress response? What about other starvation conditions and therapy?

- Is the upregulation of α2 integrin under starvation mediated by KRAS only or HRAS and NRAS as well?

- Are there any other pathways downstream of RAS which also regulate the expression of α2 integrin?

- Is the AA deprivation stress response mediated by the activation of wildtype RAS in RAS mutated cancer cells or if not, what is the mechanism behind the RAS-α2 integrin expression?

- Does the RAS mediated α2 integrin expression affect cancer cell migration and invasion?

- Would the same stress response be observed in other mutated RAS cancers such as colorectal cancer and NSCLC?

- If the effect is a general stress response, would any of the drug combinations mentioned in Table 6-1 be a possible cancer therapeutic approach?

RAS oncogene is mutated in various types of cancer, and it affects cancer progression through multiple mechanisms. I hope this research could be beneficial in better understanding the role of RAS in cancer and provide a new therapeutic approach to target RAS mutated cancers.

7 References:

ADORNO-CRUZ, V. & LIU, H. 2019. Regulation and functions of integrin alpha2 in cell adhesion and disease. *Genes Dis,* 6**,** 16-24.

AKHAVAN, A., GRIFFITH, O. L., SOROCEANU, L., LEONOUDAKIS, D., LUCIANI-TORRES, M. G., DAEMEN, A., GRAY, J. W. & MUSCHLER, J. L. 2012. Loss of cell-surface laminin anchoring promotes tumor growth and is associated with poor clinical outcomes. *Cancer Res,* 72**,** 2578-88.

ALTEA-MANZANO, P., CUADROS, A. M., BROADFIELD, L. A. & FENDT, S. M. 2020. Nutrient metabolism and cancer in the in vivo context: a metabolic game of give and take. *EMBO Rep,* 21**,** e50635.

AMELIO, I., CUTRUZZOLA, F., ANTONOV, A., AGOSTINI, M. & MELINO, G. 2014. Serine and glycine metabolism in cancer. *Trends Biochem Sci,* 39**,** 191-8.

ANDERSON, N. M. & SIMON, M. C. 2020. The tumor microenvironment. *Curr Biol,* 30**,** R921-R925.

AOUDJIT, F. & VUORI, K. 2001. Integrin signaling inhibits paclitaxel-induced apoptosis in breast cancer cells. *Oncogene,* 20.

ARJONEN, A., ALANKO, J., VELTEL, S. & IVASKA, J. 2012. Distinct recycling of active and inactive beta1 integrins. *Traffic,* 13**,** 610-25.

ARORA, P. D., WANG, Y., BRESNICK, A., DAWSON, J., JANMEY, P. A. & MCCULLOCH, C. A. 2013. Collagen remodeling by phagocytosis is determined by collagen substrate topology and calcium-dependent interactions of gelsolin with nonmuscle myosin IIA in cell adhesions. *Mol Biol Cell,* 24**,** 734-47.

ATA, R. & ANTONESCU, C. N. 2017. Integrins and Cell Metabolism: An Intimate Relationship Impacting Cancer. *Int J Mol Sci,* 18.

BACCHETTI, R., YUAN, S. & RAINERO, E. 2024. ADAMTS Proteases: Their Multifaceted Role in the Regulation of Cancer Metastasis. *Dis Res,* 4**,** 40-52.

BADAOUI M, MIMSY-JULIENNE C, SABY C, VAN GULICK L, PERETTI M, JEANNESSON P, MORJANI H & OUADID-AHIDOUCH H 2018. <Collagen type 1 promotes survival of human breast cancer cells by overexpressing Kv10.1 potassium and Orai1 calcium channels through DDR1-dependent pathway.pdf>. *Oncotarget*.

BAGHBAN, R., ROSHANGAR, L., JAHANBAN-ESFAHLAN, R., SEIDI, K., EBRAHIMI-KALAN, A., JAYMAND, M., KOLAHIAN, S., JAVAHERI, T. & ZARE, P. 2020. Tumor microenvironment complexity and therapeutic implications at a glance. *Cell Commun Signal,* 18**,** 59.

BAGHBAN, R., ROSHANGAR, L., JAHANBAN-ESFAHLAN, R., SEIDI, K., EBRAHIMI-KALAN, A., JAYMAND, M., KOLAHIAN, S., JAVAHERI, T. & ZARE, P. 2020. Tumor microenvironment complexity and therapeutic implications at a glance. *Cell Commun Signal,* 18**,** 59.

BALUK, P., HASHIZUME, H. & MCDONALD, D. M. 2005. Cellular abnormalities of blood vessels as targets in cancer. *Curr Opin Genet Dev,* 15**,** 102-11.

BARTHEL, A., OKINO, S. T., LIAO, J., NAKATANI, K., LI, J., WHITLOCK, J. P., JR. & ROTH, R. A. 1999. Regulation of GLUT1 gene transcription by the serine/threonine kinase Akt1. *J Biol Chem,* 274**,** 20281-6.

BARTOSCHEK, M., OSKOLKOV, N., BOCCI, M., LOVROT, J., LARSSON, C., SOMMARIN, M., MADSEN, C. D., LINDGREN, D., PEKAR, G., KARLSSON, G., RINGNER, M.,

BERGH, J., BJORKLUND, A. & PIETRAS, K. 2018. Spatially and functionally distinct subclasses of breast cancer-associated fibroblasts revealed by single cell RNA sequencing. *Nat Commun,* 9**,** 5150.
BEKAII-SAAB, T. S., YAEGER, R., SPIRA, A. I., PELSTER, M. S., SABARI, J. K., HAFEZ, N., BARVE, M., VELASTEGUI, K., YAN, X., SHETTY, A., DER-TOROSSIAN, H. & PANT, S. 2023. Adagrasib in Advanced Solid Tumors Harboring a KRAS(G12C) Mutation. *J Clin Oncol,* 41**,** 4097-4106.
BERGAMASCHI, A., TAGLIABUE, E., SØRLIE, T., NAUME, B., TRIULZI, T., ORLANDI, R., RUSSNES, H., NESLAND, J., TAMMI, R., AUVINEN, P., KOSMA, V.-M., M´ ENARD, S. & BØRRESEN-DALE, A.-L. 2008. Extracellular matrix signature identifies breast cancer subgroups with different clinical outcome. *Journal of Pathology,* 214.
BERTERO, T., OLDHAM, W. M., GRASSET, E. M., BOURGET, I., BOULTER, E., PISANO, S., HOFMAN, P., BELLVERT, F., MENEGUZZI, G., BULAVIN, D. V., ESTRACH, S., FERAL, C. C., CHAN, S. Y., BOZEC, A. & GAGGIOLI, C. 2019. Tumor-Stroma Mechanics Coordinate Amino Acid Availability to Sustain Tumor Growth and Malignancy. *Cell Metab,* 29**,** 124-140 e10.
BRAY, F., LAVERSANNE, M., SUNG, H., FERLAY, J., SIEGEL, R. L., SOERJOMATARAM, I. & JEMAL, A. 2024. Global cancer statistics 2022: GLOBOCAN estimates of incidence and mortality worldwide for 36 cancers in 185 countries. *CA Cancer J Clin,* 74**,** 229-263.
BREASTCANCERNOW. 2024. Available: https://breastcancernow.org/about-breast-cancer/awareness/breast-cancer-risk-factors-and-causes/ [Accessed 2024].
BROECKER-PREUSS, M., BECHER-BOVELETH, N., BOCKISCH, A., DUHRSEN, U. & MULLER, S. 2017. Regulation of glucose uptake in lymphoma cell lines by c-MYC- and PI3K-dependent signaling pathways and impact of glycolytic pathways on cell viability. *J Transl Med,* 15**,** 158.
BUGLIO, G. L., CICERO, A. L., CAMPORA, S. & GHERSI, G. 2024. The Multifaced Role of Collagen in Cancer Development and Progression. *Int J Mol Sci*.
CANCER GENOME ATLAS, N. 2012. Comprehensive molecular portraits of human breast tumours. *Nature,* 490**,** 61-70.
CASWELL, P. T., SPENCE, H. J., PARSONS, M., WHITE, D. P., CLARK, K., CHENG, K. W., MILLS, G. B., HUMPHRIES, M. J., MESSENT, A. J., ANDERSON, K. I., MCCAFFREY, M. W., OZANNE, B. W. & NORMAN, J. C. 2007. Rab25 associates with alpha5beta1 integrin to promote invasive migration in 3D microenvironments. *Dev Cell,* 13**,** 496-510.
CHANG, J. & CHAUDHURI, O. 2019. Beyond proteases: Basement membrane mechanics and cancer invasion. *J Cell Biol,* 218**,** 2456-2469.
CHEN, J., CUI, L., LU, S. & XU, S. 2024. Amino acid metabolism in tumor biology and therapy. *Cell Death Dis,* 15**,** 42.
CHEN, K., ZHANG, Y., QIAN, L. & WANG, P. 2021. Emerging strategies to target RAS signaling in human cancer therapy. *J Hematol Oncol,* 14**,** 116.
CHEN, M. & XIE, S. 2018. Therapeutic targeting of cellular stress responses in cancer. *Thorac Cancer,* 9**,** 1575-1582.
CHENG, K. W., LAHAD, J. P., KUO, W. L., LAPUK, A., YAMADA, K., AUERSPERG, N., LIU, J., SMITH-MCCUNE, K., LU, K. H., FISHMAN, D., GRAY, J. W. & MILLS, G. B. 2004. The RAB25 small GTPase determines aggressiveness of ovarian and breast cancers. *Nat Med,* 10**,** 1251-6.

CHIAVIELLO, A., PACIELLO, I., VENEZIANI, B. M., PALUMBO, G. & ALOJ, S. M. 2012. Cells derived from normal or cancer breast tissue exhibit different growth properties when deprived of arginine. *Med Oncol,* 29**,** 2543-51.

CHIODI, I., PICCO, G., MARTINO, C. & MONDELLO, C. 2019. Cellular response to glutamine and:or glucose deprivation in in vitro transformed human fibroblasts. *Oncology Reports*.

CHIU, Y. C., SHIEH, D. C., TONG, K. M., CHEN, C. P., HUANG, K. C., CHEN, P. C., FONG, Y. C., HSU, H. C. & TANG, C. H. 2009. Involvement of AdipoR receptor in adiponectin-induced motility and alpha2beta1 integrin upregulation in human chondrosarcoma cells. *Carcinogenesis,* 30**,** 1651-9.

CHOI, Y. K. & PARK, K. G. 2018. Targeting Glutamine Metabolism for Cancer Treatment. *Biomol Ther (Seoul),* 26**,** 19-28.

CHONG, Y. C., TOH, T. B., CHAN, Z., LIN, Q. X. X., THNG, D. K. H., HOOI, L., DING, Z., SHUEN, T., TOH, H. C., DAN, Y. Y., BONNEY, G. K., ZHOU, L., CHOW, P., WANG, Y., BENOUKRAF, T., CHOW, E. K. & HAN, W. 2020. Targeted Inhibition of Purine Metabolism Is Effective in Suppressing Hepatocellular Carcinoma Progression. *Hepatol Commun,* 4**,** 1362-1381.

CHRISTOFORIDES, C., RAINERO, E., BROWN, K. K., NORMAN, J. C. & TOKER, A. 2012. PKD controls alphavbeta3 integrin recycling and tumor cell invasive migration through its substrate Rabaptin-5. *Dev Cell,* 23**,** 560-72.

COMMISSO, C., DAVIDSON, S. M., SOYDANER-AZELOGLU, R. G., PARKER, S. J., KAMPHORST, J. J., HACKETT, S., GRABOCKA, E., NOFAL, M., DREBIN, J. A., THOMPSON, C. B., RABINOWITZ, J. D., METALLO, C. M., VANDER HEIDEN, M. G. & BAR-SAGI, D. 2013. Macropinocytosis of protein is an amino acid supply route in Ras-transformed cells. *Nature,* 497**,** 633-7.

COMMISSO, C., FLINN, R. J. & BAR-SAGI, D. 2014. Determining the macropinocytic index of cells through a quantitative image-based assay. *Nat Protoc,* 9**,** 182-92.

CONG LI-NA, CHEN HUI, LI YUNHUA, ZHOU LIXIN, MACGIBBON MARGARET A, TAYLOR SIMEON I & QUON MICHAEL J 1997. <Physiological Role of Akt in Insulin-Stimulated Translocation of GLUT4 in Transfected Rat Adipose Cells.pdf>. *Molecular Endocrinology*

CONNOR, A. A. & GALLINGER, S. 2022. Pancreatic cancer evolution and heterogeneity: integrating omics and clinical data. *Nat Rev Cancer,* 22**,** 131-142.

COOPMAN, P., J., THOMAS, D., M., GEHLSEN, K., R. & UELLER, S., C. 1996. integrin-alpha-3-beta-1-participates-in-the-phagocytosis-of-extracellular-matrix-molecules-by-human. *Molecular Biology of the Cell,* 7.

CORDOVA, R. A., MISRA, J., AMIN, P. H., KLUNK, A. J., DAMAYANTI, N. P., CARLSON, K. R., ELMENDORF, A. J., KIM, H. G., MIREK, E. T., ELZEY, B. D., MILLER, M. J., DONG, X. C., CHENG, L., ANTHONY, T. G., PILI, R., WEK, R. C. & STASCHKE, K. A. 2022. GCN2 eIF2 kinase promotes prostate cancer by maintaining amino acid homeostasis. *Elife,* 11.

COX, T. R. 2021. The matrix in cancer. *Nat Rev Cancer,* 21**,** 217-238.

CRUK. 2017-2019a. *Breast cancer statistics* [Online]. Available: https://www.cancerresearchuk.org/health-professional/cancer-statistics/statistics-by-cancer-type/breast-cancer [Accessed 2024].

CRUK. 2017-2019b. *Pancreatic cancer statistics* [Online]. Available: https://www.cancerresearchuk.org/health-professional/cancer-statistics/statistics-by-cancer-type/pancreatic-cancer [Accessed 2024].
CUKIERMAN E, PANKOV R, R. STEVENS D & K, M. Y. 2001. <Cukierman et al.2001.Taking Cell-Matrix Adhesions to the Third dimension.pdf>. *SCIENCE*.
CURTIS, M., KENNY, H. A., ASHCROFT, B., MUKHERJEE, A., JOHNSON, A., ZHANG, Y., HELOU, Y., BATLLE, R., LIU, X., GUTIERREZ, N., GAO, X., YAMADA, S. D., LASTRA, R., MONTAG, A., AHSAN, N., LOCASALE, J. W., SALOMON, A. R., NEBREDA, A. R. & LENGYEL, E. 2019. Fibroblasts Mobilize Tumor Cell Glycogen to Promote Proliferation and Metastasis. *Cell Metabolism,* 29**,** 141-155.e9.
DE FRANCESCHI, N., HAMIDI, H., ALANKO, J., SAHGAL, P. & IVASKA, J. 2015. Integrin traffic - the update. *J Cell Sci,* 128**,** 839-52.
DE MARTINO, D. & BRAVO-CORDERO, J. J. 2023. Collagens in Cancer: Structural Regulators and Guardians of Cancer Progression. *Cancer Res,* 83**,** 1386-1392.
DEBERARDINIS, R. J. & CHANDEL, N. S. 2016. <Fundamentals of cancer metabolism.pdf>. *Sci. Adv*.
DERBY, S. J., DUTTON, L., STRATHDEE, K. E., STEVENSON, K., KOESSINGER, A., JACKSON, M., TIAN, Y., YU, W., MCLAY, K., MISQUITTA, J., ALSHARIF, S., CLARKE, C. J., GILMOUR, L., THOMASON, P., MCGHEE, E., MCGARRITY-COTTRELL, C. L., VANDERLINDEN, A., COLLIS, S. J., ROMINYI, O., LEMGRUBER, L., SOLECKI, G., OLSON, M., WINKLER, F., CARLIN, L. M., HEILAND, D. H., INMAN, G. J., CHALMERS, A. J., NORMAN, J. C., CARRUTHERS, R. & BIRCH, J. L. 2024. Inhibition of ATR opposes glioblastoma invasion through disruption of cytoskeletal networks and integrin internalization via macropinocytosis. *Neuro Oncol,* 26**,** 625-639.
DEVAL, C., CHAVEROUX, C., MAURIN, A. C., CHERASSE, Y., PARRY, L., CARRARO, V., MILENKOVIC, D., FERRARA, M., BRUHAT, A., JOUSSE, C. & FAFOURNOUX, P. 2009. Amino acid limitation regulates the expression of genes involved in several specific biological processes through GCN2-dependent and GCN2-independent pathways. *FEBS J,* 276**,** 707-18.
DENG, B., ZHAO, Z., KONG, W., HAN, C., SHEN, X. & ZHOU, C. 2022. Biological role of matrix stiffness in tumor growth and treatment. *J Transl Med,* 20**,** 540.
DEFILLES, C., LISSITZKY, J. C., MONTERO, M. P., ANDRE, F., PREVOT, C., DELAMARRE, E., MARRAKCHI, N., LUIS, J. & RIGOT, V. 2009. alphavbeta5/beta6 integrin suppression leads to a stimulation of alpha2beta1 dependent cell migration resistant to PI3K/Akt inhibition. *Exp Cell Res,* 315**,** 1840-9.
DHARMAWARDHANE S, SCHÜRMANN A, SELLS M A, CHERNOFF J, L. SCHMID S & M. BOKOCH G 2000. regulation-of-macropinocytosis-by-p21-activated-kinase-1. *Molecular Biology of the Cell*.
DOGLIONI, G., FERNANDEZ-GARCIA, J., IGELMANN, S., ALTEA-MANZANO, P., BLOMME, A., LA ROVERE, R., LIU, X. Z., LIU, Y., TRICOT, T., NOBIS, M., AN, N., LECLERCQ, M., EL KHARRAZ, S., KARRAS, P., HSIEH, Y. H., SOLARI, F. A., MARTINS NASCENTES MELO, L., ALLIES, G., SCOPELLITI, A., ROSSI, M., VERMEIRE, I., BROEKAERT, D., FERREIRA CAMPOS, A. M., NEVEN, P., MAETENS, M., VAN BAELEN, K., ALKAN, H. F., PLANQUE, M., FLORIS, G., SICKMANN, A., TASDOGAN, A., MARINE, J. C., SCHEELE, C., DESMEDT, C., BULTYNCK, G.,

CLOSE, P. & FENDT, S. M. 2025. Aspartate signalling drives lung metastasis via alternative translation. *Nature,* 638**,** 244-250.
ECKERT, L. B., REPASKY, G. A., ÜLKÜ, A. S., MCFALL, A., ZHOU, H., SARTOR, C. I. & DER, C. J. 2004. Involvement of Ras Activation in Human Breast Cancer Cell Signaling, Invasion, and Anoikis. *Cancer Res,* 64.
EFTHYMIOU, G., SAINT, A., RUFF, M., REKAD, Z., CIAIS, D. & VAN OBBERGHEN-SCHILLING, E. 2020. Shaping Up the Tumor Microenvironment With Cellular Fibronectin. *Front Oncol,* 10**,** 641.
ELIA, I., ROSSI, M., STEGEN, S., BROEKAERT, D., DOGLIONI, G., VAN GORSEL, M., BOON, R., ESCALONA-NOGUERO, C., TORREKENS, S., VERFAILLIE, C., VERBEKEN, E., CARMELIET, G. & FENDT, S.-M. 2019. Breast cancer cells rely on environmental pyruvate to shape the metastatic niche. *Nature,* 568**,** 117-121.
ELWAKEEL, E., BRUGGEMANN, M., FINK, A. F., SCHULZ, M. H., SCHMID, T., SAVAI, R., BRUNE, B., ZARNACK, K. & WEIGERT, A. 2019. Phenotypic Plasticity of Fibroblasts during Mammary Carcinoma Development. *Int J Mol Sci,* 20.
ENDO, H., OWADA, S., INAGAKI, Y., SHIDA, Y. & TATEMICHI, M. 2018. Glucose starvation induces LKB1-AMPK-mediated MMP-9 expression in cancer cells. *Sci Rep,* 8**,** 10122.
ENDO, H., OWADA, S., INAGAKI, Y., SHIDA, Y. & TATEMICHI, M. 2020. Metabolic reprogramming sustains cancer cell survival following extracellular matrix detachment. *Redox Biol,* 36**,** 101643.
ENGBRING, J. A. & KLEINMAN, H. K. 2003. The basement membrane matrix in malignancy. *J Pathol,* 200**,** 465-70.
ERDOGAN, B., AO, M., WHITE, L. M., MEANS, A. L., BREWER, B. M., YANG, L., WASHINGTON, M. K., SHI, C., FRANCO, O. E., WEAVER, A. M., HAYWARD, S. W., LI, D. & WEBB, D. J. 2017. Cancer-associated fibroblasts promote directional cancer cell migration by aligning fibronectin. *J Cell Biol,* 216**,** 3799-3816.
ERICKSEN, R. E., LIM, S. L., MCDONNELL, E., SHUEN, W. H., VADIVELOO, M., WHITE, P. J., DING, Z., KWOK, R., LEE, P., RADDA, G. K., TOH, H. C., HIRSCHEY, M. D. & HAN, W. 2019. Loss of BCAA Catabolism during Carcinogenesis Enhances mTORC1 Activity and Promotes Tumor Development and Progression. *Cell Metabolism,* 29**,** 1151-1165.e6.
EVAN, G., I. & VOUSDEN, K., H. 2001. Proliferation, cell cycle and apoptosis in cancer. *Nature,* 411.
FAN, J., KAMPHORST, J. J., MATHEW, R., CHUNG, M. K., WHITE, E., SHLOMI, T. & RABINOWITZ, J. D. 2013. Glutamine-driven oxidative phosphorylation is a major ATP source in transformed mammalian cells in both normoxia and hypoxia. *Mol Syst Biol,* 9**,** 712.
FANG, M., YUAN, J., PENG, C. & LI, Y. 2014. Collagen as a double-edged sword in tumor progression. *Tumour Biol,* 35**,** 2871-82.
FENG, Y., SPEZIA, M., HUANG, S., YUAN, C., ZENG, Z., ZHANG, L., JI, X., LIU, W., HUANG, B., LUO, W., LIU, B., LEI, Y., DU, S., VUPPALAPATI, A., LUU, H. H., HAYDON, R. C., HE, T. C. & REN, G. 2018. Breast cancer development and progression: Risk factors, cancer stem cells, signaling pathways, genomics, and molecular pathogenesis. *Genes Dis,* 5**,** 77-106.
FERNANDEZ-MEDARDE, A. & SANTOS, E. 2011. Ras in cancer and developmental diseases. *Genes Cancer,* 2**,** 344-58.

FERNANDEZ-NOGUEIRA, P., MANCINO, M., FUSTER, G., LOPEZ-PLANA, A., JAUREGUI, P., ALMENDRO, V., ENREIG, E., MENENDEZ, S., ROJO, F., NOGUERA-CASTELLS, A., BILL, A., GAITHER, L. A., SERRANO, L., RECALDE-PERCAZ, L., MORAGAS, N., ALONSO, R., AMETLLER, E., ROVIRA, A., LLUCH, A., ALBANELL, J., GASCON, P. & BRAGADO, P. 2020. Tumor-Associated Fibroblasts Promote HER2-Targeted Therapy Resistance through FGFR2 Activation. *Clin Cancer Res,* 26**,** 1432-1448.

FINICLE, B. T., JAYASHANKAR, V. & EDINGER, A. L. 2018. Nutrient scavenging in cancer. *Nat Rev Cancer,* 18**,** 619-633.

FRANCHI-GAZZOLA, R., VISIGALLI, R., BUSSOLATI, O., DALL'ASTA, V. & GAZZOLA, G. C. 1999. Adaptive increase of amino acid transport system A requires ERK1/2 activation. *J Biol Chem,* 274**,** 28922-8.

FUNG, C., LOCK, R., GAO, S., SALAS, E. & DEBNATH, J. 2008. Induction of autophagy during extracellular matrix detachment promotes cell survival. *Mol Biol Cell,* 19**,** 797-806.

GALIE, M. 2019. RAS as Supporting Actor in Breast Cancer. *Front Oncol,* 9**,** 1199.

GE, H., TIAN, M., PEI, Q., TAN, F. & PEI, H. 2021. Extracellular Matrix Stiffness: New Areas Affecting Cell Metabolism. *Front Oncol,* 11**,** 631991.

GECK, R. C. & TOKER, A. 2016. Nonessential amino acid metabolism in breast cancer. *Adv Biol Regul,* 62**,** 11-17.

GEORGIADOU, M. & IVASKA, J. 2017. Tensins: Bridging AMP-Activated Protein Kinase with Integrin Activation. *Trends Cell Biol,* 27**,** 703-711.

GEORGIADOU, M., LILJA, J., JACQUEMET, G., GUZMAN, C., RAFAEVA, M., ALIBERT, C., YAN, Y., SAHGAL, P., LERCHE, M., MANNEVILLE, J. B., MAKELA, T. P. & IVASKA, J. 2017. AMPK negatively regulates tensin-dependent integrin activity. *J Cell Biol,* 216**,** 1107-1121.

GHURA, H., KEIMER, M., VON AU, A., HACKL, N., KLEMIS, V. & NAKCHBANDI, I. A. 2021. Inhibition of fibronectin accumulation suppresses tumor growth. *Neoplasia,* 23**,** 837-850.

GOLD, L. T. & MASSON, G. R. 2022. GCN2: roles in tumour development and progression. *Biochem Soc Trans,* 50**,** 737-745.

GOPAL, S., VERACINI, L., GRALL, D., BUTORI, C., SCHAUB, S., AUDEBERT, S., CAMOIN, L., BAUDELET, E., RADWANSKA, A., BEGHELLI-DE LA FOREST DIVONNE, S., VIOLETTE, S. M., WEINREB, P. H., REKIMA, S., ILIE, M., SUDAKA, A., HOFMAN, P. & VAN OBBERGHEN-SCHILLING, E. 2017. Fibronectin-guided migration of carcinoma collectives. *Nat Commun,* 8**,** 14105.

GRAHAM, N. A., TAHMASIAN, M., KOHLI, B., KOMISOPOULOU, E., ZHU, M., VIVANCO, I., TEITELL, M. A., WU, H., RIBAS, A., LO, R. S., MELLINGHOFF, I. K., MISCHEL, P. S. & GRAEBER, T. G. 2012. Glucose deprivation activates a metabolic and signaling amplification loop leading to cell death. *Mol Syst Biol,* 8**,** 589.

GREGORI, A., BERGONZINI, C., CAPULA, M., MANTINI, G., KHOJASTEH-LEYLAKOOHI, F., COMANDATORE, A., KHALILI-TANHA, G., KHOOEI, A., MORELLI, L., AVAN, A., DANEN, E. H., SCHMIDT, T. & GIOVANNETTI, E. 2023. Prognostic Significance of Integrin Subunit Alpha 2 (ITGA2) and Role of Mechanical Cues in Resistance to Gemcitabine in Pancreatic Ductal Adenocarcinoma (PDAC). *Cancers (Basel),* 15.

GUERRERO-BARBERA, G., BURDAY, N. & COSTELL, M. 2024. Shaping Oncogenic Microenvironments: Contribution of Fibronectin. *Front Cell Dev Biol,* 12**,** 1363004.

GUO, Y. J., PAN, W. W., LIU, S. B., SHEN, Z. F., XU, Y. & HU, L. L. 2020. ERK/MAPK signalling pathway and tumorigenesis. *Exp Ther Med,* 19**,** 1997-2007.
H. MORE T, ROYCHOUDHURY S, CHRISTIE J, TAUNK K, MANE A, K. SANTRA M, CHAUDHURY K & RAPOLE S 2018. <Metabolomic alterations in invasive ductal carcinoma of breast- A comprehensive metabolomic study using tissue and serum samples.pdf>. *Oncotarget,* 9**,** 2678-2696.
HAAKE, S. M., RIOS, B. L., POZZI, A. & ZENT, R. 2024. Integrating integrins with the hallmarks of cancer. *Matrix Biol,* 130**,** 20-35.
HAMANN, J. C., SURCEL, A., CHEN, R., TERAGAWA, C., ALBECK, J. G., ROBINSON, D. N. & OVERHOLTZER, M. 2017. Entosis Is Induced by Glucose Starvation. *Cell Rep,* 20**,** 201-210.
HAMIDI, H. & IVASKA, J. 2018. Every step of the way: integrins in cancer progression and metastasis. *Nat Rev Cancer,* 18**,** 533-548.
HANAHAN, D. & WEINBERG, R. A. 2011. Hallmarks of cancer: the next generation. *Cell,* 144**,** 646-74.
HANAHAN, D. & WEINBERG, R. A. 2000. The Hallmarks of Cancer. *Cell Press,* 100.
HARBECK, N., PENAULT-LLORCA, F., CORTES, J., GNANT, M., HOUSSAMI, N., POORTMANS, P., RUDDY, K., TSANG, J. & CARDOSO, F. 2019. Breast cancer. *Nat Rev Dis Primers,* 5**,** 66.
HARIKRISHNAN, K., PRABHU, S. S. & BALASUBRAMANIAN, N. 2022. A pan-cancer analysis of matrisome proteins reveals CTHRC1 and a related network as major ECM regulators across cancers. *PLoS One,* 17**,** e0270063.
HEINO, J. 2000. The collagen receptor integrins have distinct ligand recognition and signaling functions. *Matrix Biology,* 19**,** 319-323.
HELMS, E., ONATE, M. K. & SHERMAN, M. H. 2020. Fibroblast Heterogeneity in the Pancreatic Tumor Microenvironment. *Cancer Discov,* 10**,** 648-656.
HERZIG, S. & SHAW, R. J. 2018. AMPK: guardian of metabolism and mitochondrial homeostasis. *Nat Rev Mol Cell Biol,* 19**,** 121-135.
HIRAYAMA, A., KAMI, K., SUGIMOTO, M., SUGAWARA, M., TOKI, N., ONOZUKA, H., KINOSHITA, T., SAITO, N., OCHIAI, A., TOMITA, M., ESUMI, H. & SOGA, T. 2009. Quantitative metabolome profiling of colon and stomach cancer microenvironment by capillary electrophoresis time-of-flight mass spectrometry. *Cancer Res,* 69**,** 4918-25.
HODAKOSKI, C., HOPKINS, B. D., ZHANG, G., SU, T., CHENG, Z., MORRIS, R., RHEE, K. Y., GONCALVES, M. D. & CANTLEY, L. C. 2019. Rac-Mediated Macropinocytosis of Extracellular Protein Promotes Glucose Independence in Non-Small Cell Lung Cancer. *Cancers (Basel),* 11.
HORTON, E. R., BYRON, A., ASKARI, J. A., NG, D. H. J., MILLON-FREMILLON, A., ROBERTSON, J., KOPER, E. J., PAUL, N. R., WARWOOD, S., KNIGHT, D., HUMPHRIES, J. D. & HUMPHRIES, M. J. 2015. Definition of a consensus integrin adhesome and its dynamics during adhesion complex assembly and disassembly. *Nat Cell Biol,* 17**,** 1577-1587.
HOSEIN, A. N., DOUGAN, S. K., AGUIRRE, A. J. & MAITRA, A. 2022. Translational advances in pancreatic ductal adenocarcinoma therapy. *Nat Cancer,* 3**,** 272-286.
HOSIOS, A. M., HECHT, V. C., DANAI, L. V., JOHNSON, M. O., RATHMELL, J. C., STEINHAUSER, M. L., MANALIS, S. R. & VANDER HEIDEN, M. G. 2016. Amino

Acids Rather than Glucose Account for the Majority of Cell Mass in Proliferating Mammalian Cells. *Dev Cell,* 36**,** 540-9.
HOXHAJ, G. & MANNING, B. D. 2020. The PI3K-AKT network at the interface of oncogenic signalling and cancer metabolism. *Nat Rev Cancer,* 20**,** 74-88.
HRUBAN, R. H., GOGGINS, M., PARSON, J. & KERN, S. E. 2000. Progression Model for Pancreatic Cancer. *Clinical Cancer Research,* 6.
HSU, K. S., DUNLEAVEY, J. M., SZOT, C., YANG, L., HILTON, M. B., MORRIS, K., SEAMAN, S., FENG, Y., LUTZ, E. M., KOOGLE, R., TOMASSONI-ARDORI, F., SAHA, S., ZHANG, X. M., ZUDAIRE, E., BAJGAIN, P., ROSE, J., ZHU, Z., DIMITROV, D. S., CUTTITTA, F., EMENAKER, N. J., TESSAROLLO, L. & ST CROIX, B. 2022. Cancer cell survival depends on collagen uptake into tumor-associated stroma. *Nat Commun,* 13**,** 7078.
HU, D., LI, Z., ZHENG, B., LIN, X., PAN, Y., GONG, P., ZHUO, W., HU, Y., CHEN, C., CHEN, L., ZHOU, J. & WANG, L. 2022. Cancer-associated fibroblasts in breast cancer: Challenges and opportunities. *Cancer Commun (Lond),* 42**,** 401-434.
IKENAGA, N., OHUCHIDA, K., MIZUMOTO, K., AKAGAWA, S., FUJIWARA, K., EGUCHI, D., KOZONO, S., OHTSUKA, T., TAKAHATA, S. & TANAKA, M. 2012. Pancreatic cancer cells enhance the ability of collagen internalization during epithelial-mesenchymal transition. *PLoS One,* 7**,** e40434.
KALLURI, R. 2003. Basement membranes: structure, assembly and role in tumour angiogenesis. *Nat Rev Cancer,* 3**,** 422-33.
KAMPHORST, J. J., NOFAL, M., COMMISSO, C., HACKETT, S. R., LU, W., GRABOCKA, E., VANDER HEIDEN, M. G., MILLER, G., DREBIN, J. A., BAR-SAGI, D., THOMPSON, C. B. & RABINOWITZ, J. D. 2015. Human pancreatic cancer tumors are nutrient poor and tumor cells actively scavenge extracellular protein. *Cancer Res,* 75**,** 544-53.
KANCHANAWONG, P. & CALDERWOOD, D. A. 2023. Organization, dynamics and mechanoregulation of integrin-mediated cell-ECM adhesions. *Nat Rev Mol Cell Biol,* 24**,** 142-161.
KANG, M., KANG, J. H., SIM, I. A., SEONG, D. Y., HAN, S., JANG, H., LEE, H., KANG, S. W. & KIM, S. Y. 2023. Glucose Deprivation Induces Cancer Cell Death through Failure of ROS Regulation. *Int J Mol Sci,* 24.
KANTETI, R., MIRZAPOIAZOVA, T., RIEHM, J. J., DHANASINGH, I., MAMBETSARIEV, B., WANG, J., KULKARNI, P., KAUSHIK, G., SESHACHARYULU, P., PONNUSAMY, M. P., KINDLER, H. L., NASSER, M. W., BATRA, S. K. & SALGIA, R. 2018. Focal adhesion kinase a potential therapeutic target for pancreatic cancer and malignant pleural mesothelioma. *Cancer Biol Ther,* 19**,** 316-327.
KAUKONEN, R., JACQUEMET, G., HAMIDI, H. & IVASKA, J. 2017. Cell-derived matrices for studying cell proliferation and directional migration in a complex 3D microenvironment. *Nat Protoc,* 12**,** 2376-2390.
KAUPPILA S, STENBÄCK F, RISTELI J, JUKKOLA A & RISTELI L 1998. <type I and type III collagen gene expression in human breast cancer in VIVO.pdf>. *Journal of Pathology*.
KAUSHIK, S., PICKUP, M. W. & WEAVER, V. M. 2016. From transformation to metastasis: deconstructing the extracellular matrix in breast cancer. *Cancer Metastasis Rev,* 35**,** 655-667.

KECHAGIA, J. Z., IVASKA, J. & ROCA-CUSACHS, P. 2019. Integrins as biomechanical sensors of the microenvironment. *Nat Rev Mol Cell Biol,* 20**,** 457-473.
KESSENBROCK, K., PLAKS, V. & WERB, Z. 2010. Matrix metalloproteinases: regulators of the tumor microenvironment. *Cell,* 141**,** 52-67.
KIM, S. M., NGUYEN, T. T., RAVI, A., KUBINIOK, P., FINICLE, B. T., JAYASHANKAR, V., MALACRIDA, L., HOU, J., ROBERTSON, J., GAO, D., CHERNOFF, J., DIGMAN, M. A., POTMA, E. O., TROMBERG, B. J., THIBAULT, P. & EDINGER, A. L. 2018. PTEN Deficiency and AMPK Activation Promote Nutrient Scavenging and Anabolism in Prostate Cancer Cells. *Cancer Discov,* 8**,** 866-883.
KITSIOU, P. V., TZINIA, A. K., STETLER-STEVENSON, W. G., MICHAEL, A. F., FAN, W., ZHOU, B. & TSILIBARY, E. C. 2003. Glucose-induced changes in integrins and matrix-related functions in cultured human glomerular epithelial cells. *AJP-Renal Physiol*.
KLEEFF, J., KORC, M., APTE, M., LA VECCHIA, C., JOHNSON, C. D., BIANKIN, A. V., NEALE, R. E., TEMPERO, M., TUVESON, D. A., HRUBAN, R. H. & NEOPTOLEMOS, J. P. 2016. Pancreatic cancer. *Nat Rev Dis Primers,* 2**,** 16022.
KLIGYS, K. R., WU, Y., HOPKINSON, S. B., KAUR, S., PLATANIAS, L. C. & JONES, J. C. 2012. alpha6beta4 integrin, a master regulator of expression of integrins in human keratinocytes. *J Biol Chem,* 287**,** 17975-84.
KNOTT, S. R. V., WAGENBLAST, E., KHAN, S., KIM, S. Y., SOTO, M., WAGNER, M., TURGEON, M.-O., FISH, L., ERARD, N., GABLE, A. L., MACELI, A. R., DICKOPF, S., PAPACHRISTOU, E. K., D'SANTOS, C. S., CAREY, L. A., WILKINSON, J. E., HARRELL, J. C., PEROU, C. M., GOODARZI, H., POULOGIANNIS, G. & HANNON, G. J. 2018. Asparagine bioavailability governs metastasis in a model of breast cancer. *Nature,* 554**,** 378-381.
KOORMAN, T., JANSEN, K. A., KHALIL, A., HAUGHTON, P. D., VISSER, D., RATZE, M. A. K., HAAKMA, W. E., SAKALAUSKAITE, G., VAN DIEST, P. J., DE ROOIJ, J. & DERKSEN, P. W. B. 2022. Spatial collagen stiffening promotes collective breast cancer cell invasion by reinforcing extracellular matrix alignment. *Oncogene,* 41**,** 2458-2469.
KURMI, K. & HAIGIS, M. C. 2020. Nitrogen Metabolism in Cancer and Immunity. *Trends Cell Biol,* 30**,** 408-424.
KWON, M. J. 2022. Matrix metalloproteinases as therapeutic targets in breast cancer. *Front Oncol,* 12**,** 1108695.
L. H. H. OLDE DAMINK, P. J. DIJKSTRA, M. J. A. VAN LUYN*, P. B. VAN WACHEM*, P. NIEUWENHUIS* & FEIJEN, J. 1995. Glutaraldehyde as a crosslinking agent for collagen-based biomaterials. *JOURNAL OF MATERIALS SCIENCE*.
LAHIRI, V., HAWKINS, W. D. & KLIONSKY, D. J. 2019. Watch What You (Self-) Eat: Autophagic Mechanisms that Modulate Metabolism. *Cell Metab,* 29**,** 803-826.
LAI, J. Y. & MA, D. H. 2013. Glutaraldehyde cross-linking of amniotic membranes affects their nanofibrous structures and limbal epithelial cell culture characteristics. *Int J Nanomedicine,* 8**,** 4157-68.
LARIONOVA, I., TUGUZBAEVA, G., PONOMARYOVA, A., STAKHEYEVA, M., CHERDYNTSEVA, N., PAVLOV, V., CHOINZONOV, E. & KZHYSHKOWSKA, J. 2020. Tumor-Associated Macrophages in Human Breast, Colorectal, Lung, Ovarian and Prostate Cancers. *Front Oncol,* 10**,** 566511.

LE, A. H., YELLAND, T., PAUL, N. R., FORT, L., NIKOLAOU, S., ISMAIL, S. & MACHESKY, L. M. 2021. CYRI-A limits invasive migration through macropinosome formation and integrin uptake regulation. *J Cell Biol,* 220.

LEBERT, J. M., LESTER, R., POWELL, E., SEAL, M. & MCCARTHY, J. 2018. Advances in the systemic treatment of triple-negative breast cancer. *Curr Oncol,* 25**,** S142-S150.

LEE, J. S., OH, S. J., CHOI, H. J., KANG, J. H., LEE, S. H., HA, J. S., WOO, S. M., JANG, H., LEE, H. & KIM, S. Y. 2020. ATP Production Relies on Fatty Acid Oxidation Rather than Glycolysis in Pancreatic Ductal Adenocarcinoma. *Cancers (Basel),* 12.

LEE, W., SODEK, J. & MCCULLOCH, C. A. G. 1996. Role of integrins in regulation of collagen phagocytosis by human fibroblasts. *Journal of Cellular Physiology,* 168**,** 695-704.

LEVENTAL, K. R., YU, H., KASS, L., LAKINS, J. N., EGEBLAD, M., ERLER, J. T., FONG, S. F., CSISZAR, K., GIACCIA, A., WENINGER, W., YAMAUCHI, M., GASSER, D. L. & WEAVER, V. M. 2009. Matrix crosslinking forces tumor progression by enhancing integrin signaling. *Cell,* 139**,** 891-906.

LIBERTI, M. V. & LOCASALE, J. W. 2016. The Warburg Effect: How Does it Benefit Cancer Cells? *Trends Biochem Sci,* 41**,** 211-218.

LIGORIO, M., SIL, S., MALAGON-LOPEZ, J., NIEMAN, L. T., MISALE, S., DI PILATO, M., EBRIGHT, R. Y., KARABACAK, M. N., KULKARNI, A. S., LIU, A., VINCENT JORDAN, N., FRANSES, J. W., PHILIPP, J., KREUZER, J., DESAI, N., ARORA, K. S., RAJURKAR, M., HORWITZ, E., NEYAZ, A., TAI, E., MAGNUS, N. K. C., VO, K. D., YASHASWINI, C. N., MARANGONI, F., BOUKHALI, M., FATHERREE, J. P., DAMON, L. J., XEGA, K., DESAI, R., CHOZ, M., BERSANI, F., LANGENBUCHER, A., THAPAR, V., MORRIS, R., WELLNER, U. F., SCHILLING, O., LAWRENCE, M. S., LISS, A. S., RIVERA, M. N., DESHPANDE, V., BENES, C. H., MAHESWARAN, S., HABER, D. A., FERNANDEZ-DEL-CASTILLO, C., FERRONE, C. R., HAAS, W., ARYEE, M. J. & TING, D. T. 2019. Stromal Microenvironment Shapes the Intratumoral Architecture of Pancreatic Cancer. *Cell,* 178**,** 160-175 e27.

LING, Z. N., JIANG, Y. F., RU, J. N., LU, J. H., DING, B. & WU, J. 2023. Amino acid metabolism in health and disease. *Signal Transduct Target Ther,* 8**,** 345.

LORD, S. J., VELLE, K. B., MULLINS, R. D. & FRITZ-LAYLIN, L. K. 2020. SuperPlots: Communicating reproducibility and variability in cell biology. J Cell Biol, 219.

LU, F., ZHU, L., BROMBERGER, T., YANG, J., YANG, Q., LIU, J., PLOW, E. F., MOSER, M. & QIN, J. 2022. Mechanism of integrin activation by talin and its cooperation with kindlin. *Nat Commun,* 13**,** 2362.

LU, P., WEAVER, V. M. & WERB, Z. 2012. The extracellular matrix: a dynamic niche in cancer progression. *J Cell Biol,* 196**,** 395-406.

LUAN, H., JIAN, L., HUANG, Y., GUO, Y. & ZHOU, L. 2023. Identification of novel therapeutic target and prognostic biomarker in matrix metalloproteinase gene family in pancreatic cancer. *Sci Rep,* 13**,** 17211.

LUKEY, M. J., KATT, W. P. & CERIONE, R. A. 2017. Targeting amino acid metabolism for cancer therapy. *Drug Discov Today,* 22**,** 796-804.

LV, S., ZHANG, Z., LI, Z., KE, Q., MA, X., LI, N., ZHAO, X., ZOU, Q., SUN, L. & SONG, T. 2024. TFE3-SLC36A1 axis promotes resistance to glucose starvation in kidney cancer cells. *J Biol Chem,* 300**,** 107270.

MACHADO BRANDAO-COSTA, R., HELAL-NETO, E., MAIA VIEIRA, A., BARCELLOS-DE-SOUZA, P., MORGADO-DIAZ, J. & BARJA-FIDALGO, C. 2020. Extracellular Matrix

Derived from High Metastatic Human Breast Cancer Triggers Epithelial-Mesenchymal Transition in Epithelial Breast Cancer Cells through alphavbeta3 Integrin. Int J Mol Sci, 21.
MADDOCKS, O. D. K., BERKERS, C. R., MASON, S. M., ZHENG, L., BLYTH, K., GOTTLIEB, E. & VOUSDEN, K. H. 2012. Serine starvation induces stress and p53-dependent metabolic remodelling in cancer cells. *Nature,* 493**,** 542-546.
MADSEN, D. H., INGVARSEN, S., JURGENSEN, H. J., MELANDER, M. C., KJOLLER, L., MOYER, A., HONORE, C., MADSEN, C. A., GARRED, P., BURGDORF, S., BUGGE, T. H., BEHRENDT, N. & ENGELHOLM, L. H. 2011. The non-phagocytic route of collagen uptake: a distinct degradation pathway. *J Biol Chem,* 286**,** 26996-7010.
MAH, E. J., LEFEBVRE, A. E. Y. T., MCGAHEY, G. E., YEE, A. F. & DIGMAN, M. A. 2018. Collagen density modulates triple-negative breast cancer cell metabolism through adhesion-mediated contractility. *Scientific Reports,* 8.
MAQUOI, E., ASSENT, D., DETILLEUX, J., PEQUEUX, C., FOIDART, J. M. & NOEL, A. 2012. MT1-MMP protects breast carcinoma cells against type I collagen-induced apoptosis. *Oncogene,* 31**,** 480-93.
MARTIN, M. J., HAYWARD, R., VIROS, A. & MARAIS, R. 2012. Metformin accelerates the growth of BRAF V600E-driven melanoma by upregulating VEGF-A. *Cancer Discov,* 2**,** 344-55.
MARTINEZ, J. & SMITH, P. C. 2021. The Dynamic Interaction between Extracellular Matrix Remodeling and Breast Tumor Progression. *Cells,* 10.
MARTINEZ, M. L., NAN, K., BAO, Z., BACCHETTI, R., YUAN, S., TYLER, J., GUEZENNEC, X. L., BARD, F. A. & RAINERO, E. 2024. Novel kinase regulators of extracellular matrix internalisation identified by high-content screening modulate invasive carcinoma cell migration. *PLoS Biol,* 22**,** e3002930.
MASUI, K., CAVENEE, W. K. & MISCHEL, P. S. 2014. mTORC2 in the center of cancer metabolic reprogramming. *Trends Endocrinol Metab,* 25**,** 364-73.
MATHEWS, E. H., VISAGIE, M. H., MEYER, A. A., JOUBERT, A. M. & MATHEWS, G. E. 2020. In vitro quantification: Long-term effect of glucose deprivation on various cancer cell lines. *Nutrition,* 74**,** 110748.
MEECHAM, A., CUTMORE, L. C., PROTOPAPA, P., RIGBY, L. G. & MARSHALL, J. F. 2022. Ligand-bound integrin alphavbeta6 internalisation and trafficking. *Front Cell Dev Biol,* 10**,** 920303.
MENG, X. N., JIN, Y., YU, Y., BAI, J., LIU, G. Y., ZHU, J., ZHAO, Y. Z., WANG, Z., CHEN, F., LEE, K. Y. & FU, S. B. 2009. Characterisation of fibronectin-mediated FAK signalling pathways in lung cancer cell migration and invasion. *Br J Cancer,* 101**,** 327-34.
MITRA, A. K., SAWADA, K., TIWARI, P., MUI, K., GWIN, K. & LENGYEL, E. 2011. Ligand-independent activation of c-Met by fibronectin and alpha(5)beta(1)-integrin regulates ovarian cancer invasion and metastasis. *Oncogene,* 30**,** 1566-76.
MOHIT, J., ROLAND, N., SONIA, S., NIKHIL, M., TOSHIMORI, K., AMANDA, S., RAN KAFRI, K., MARC, K., CLARY, C. & VAMSI, M. 2012. <Metabolite Profiling Identifies a Key Role for Glycine in Rapid Cancer Cell Proliferation.pdf>. *SCIENCE,* 336.
MORENO-LAYSECA, P., ICHA, J., HAMIDI, H. & IVASKA, J. 2019. Integrin trafficking in cells and tissues. *Nat Cell Biol,* 21**,** 122-132.

MORITZ, M. N. O., MERKEL, A. R., FELDMAN, E. G., SELISTRE-DE-ARAUJO, H. S. & RHOADES STERLING, J. A. 2021. Biphasic alpha2beta1 Integrin Expression in Breast Cancer Metastasis to Bone. *Int J Mol Sci,* 22.

MORRIS, B. A., BURKEL, B., PONIK, S. M., FAN, J., CONDEELIS, J. S., AGUIRRE-GHISO, J. A., CASTRACANE, J., DENU, J. M. & KEELY, P. J. 2016. Collagen Matrix Density Drives the Metabolic Shift in Breast Cancer Cells. *EBioMedicine,* 13**,** 146-156.

MURANEN, T., IWANICKI, M. P., CURRY, N. L., HWANG, J., DUBOIS, C. D., COLOFF, J. L., HITCHCOCK, D. S., CLISH, C. B., BRUGGE, J. S. & KALAANY, N. Y. 2017. Starved epithelial cells uptake extracellular matrix for survival. *Nat Commun,* 8**,** 13989.

NABA, A., CLAUSER, K. R., HOERSCH, S., LIU, H., CARR, S. A. & HYNES, R. O. 2012. The matrisome: in silico definition and in vivo characterization by proteomics of normal and tumor extracellular matrices. *Mol Cell Proteomics,* 11**,** M111 014647.

NACI, D., VUORI, K. & AOUDJIT, F. 2015. Alpha2beta1 integrin in cancer development and chemoresistance. *Semin Cancer Biol,* 35**,** 145-53.

NAGL, L., HORVATH, L., PIRCHER, A. & WOLF, D. 2020. Tumor Endothelial Cells (TECs) as Potential Immune Directors of the Tumor Microenvironment - New Findings and Future Perspectives. *Front Cell Dev Biol,* 8**,** 766.

NAGY, J. A., CHANG, S. H., SHIH, S. C., DVORAK, A. M. & DVORAK, H. F. 2010. Heterogeneity of the tumor vasculature. *Semin Thromb Hemost,* 36**,** 321-31.

NAM, A., JAIN, S., WU, C., CAMPOS, A., SHEPARD, R. M., YU, Z., REDDY, J. P., VON SCHALSCHA, T., WEIS, S. M., ONAITIS, M., WETTERSTEN, H. I. & CHERESH, D. A. 2024. Integrin alphavbeta3 Upregulation in Response to Nutrient Stress Promotes Lung Cancer Cell Metabolic Plasticity. *Cancer Res,* 84**,** 1630-1642.

NAZEMI, M. & RAINERO, E. 2020. Cross-Talk Between the Tumor Microenvironment, Extracellular Matrix, and Cell Metabolism in Cancer. *Front Oncol,* 10**,** 239.

NAZEMI, M., YANES, B., MARTINEZ, M. L., WALKER, H. J., PHAM, K., COLLINS, M. O., BARD, F. & RAINERO, E. 2024. The extracellular matrix supports breast cancer cell growth under amino acid starvation by promoting tyrosine catabolism. *PLoS Biol,* 22**,** e3002406.

NEWMAN, A. C., FALCONE, M., HUERTA URIBE, A., ZHANG, T., ATHINEOS, D., PIETZKE, M., VAZQUEZ, A., BLYTH, K. & MADDOCKS, O. D. K. 2021. Immune-regulated IDO1-dependent tryptophan metabolism is source of one-carbon units for pancreatic cancer and stellate cells. *Mol Cell,* 81**,** 2290-2302 e7.

NGUYEN-NGOC, K. V., CHEUNG, K. J., BRENOT, A., SHAMIR, E. R., GRAY, R. S., HINES, W. C., YASWEN, P., WERB, Z. & EWALD, A. J. 2012. ECM microenvironment regulates collective migration and local dissemination in normal and malignant mammary epithelium. *Proc Natl Acad Sci U S A,* 109**,** E2595-604.

NISSEN, N. I., KARSDAL, M. & WILLUMSEN, N. 2019. Collagens and Cancer associated fibroblasts in the reactive stroma and its relation to Cancer biology. *J Exp Clin Cancer Res,* 38**,** 115.

NONNAST, E., MIRA, E. & MANES, S. 2025. The role of laminins in cancer pathobiology: a comprehensive review. *J Transl Med,* 23**,** 83.

OLIVARES, O., MAYERS, J. R., GOUIRAND, V., TORRENCE, M. E., GICQUEL, T., BORGE, L., LAC, S., ROQUES, J., LAVAUT, M. N., BERTHEZENE, P., RUBIS, M., SECQ, V., GARCIA, S., MOUTARDIER, V., LOMBARDO, D., IOVANNA, J. L., TOMASINI, R., GUILLAUMOND, F., VANDER HEIDEN, M. G. & VASSEUR, S. 2017. Collagen-

derived proline promotes pancreatic ductal adenocarcinoma cell survival under nutrient limited conditions. *Nat Commun,* 8**,** 16031.

ORTH, M., METZGER, P., GERUM, S., MAYERLE, J., SCHNEIDER, G., BELKA, C., SCHNURR, M. & LAUBER, K. 2019. Pancreatic ductal adenocarcinoma: biological hallmarks, current status, and future perspectives of combined modality treatment approaches. *Radiat Oncol,* 14**,** 141.

PAKOS-ZEBRUCKA, K., KORYGA, I., MNICH, K., LJUJIC, M., SAMALI, A. & GORMAN, A. M. 2016. The integrated stress response. *EMBO Rep,* 17**,** 1374-1395.

PALM, W., PARK, Y., WRIGHT, K., PAVLOVA, N. N., TUVESON, D. A. & THOMPSON, C. B. 2015. The Utilization of Extracellular Proteins as Nutrients Is Suppressed by mTORC1. *Cell,* 162**,** 259-270.

PAVLIDES, S., WHITAKER-MENEZES, D., CASTELLO-CROS, R., FLOMENBERG, N., WITKIEWICZ, A. K., FRANK, P. G., CASIMIRO, M. C., WANG, C., FORTINA, P., ADDYA, S., PESTELL, R. G., MARTINEZ-OUTSCHOORN, U. E., SOTGIA, F. & LISANTI, M. P. 2014. The reverse Warburg effect: Aerobic glycolysis in cancer associated fibroblasts and the tumor stroma. *Cell Cycle,* 8**,** 3984-4001.

PELICANO, H., MARTIN, D. S., XU, R. H. & HUANG, P. 2006. Glycolysis inhibition for anticancer treatment. *Oncogene,* 25**,** 4633-46.

PING, Q., YAN, R., CHENG, X., WANG, W., ZHONG, Y., HOU, Z., SHI, Y., WANG, C. & LI, R. 2021. Cancer-associated fibroblasts: overview, progress, challenges, and directions. *Cancer Gene Ther,* 28**,** 984-999.

PROVENZANO, P. P., ELICEIRI, K. W., CAMPBELL, J. M., INMAN, D. R., WHITE, J. G. & KEELY, P. J. 2006. Collagen reorganization at the tumor-stromal interface facilitates local invasion. *BMC Med,* 4**,** 38.

PROVENZANO, P. P., INMAN, D. R., ELICEIRI, K. W., KNITTEL, J. G., YAN, L., RUEDEN, C. T., WHITE, J. G. & KEELY, P. J. 2008. Collagen density promotes mammary tumor initiation and progression. *BMC Med,* 6**,** 11.

PYLAYEVA, Y., GILLEN, K. M., GERALD, W., BEGGS, H. E., REICHARDT, L. F. & GIANCOTTI, F. G. 2009. Ras- and PI3K-dependent breast tumorigenesis in mice and humans requires focal adhesion kinase signaling. *J Clin Invest,* 119**,** 252-66.

P.ROMERO., J. W., M.L.GREEN., D.KAISER., M.KRUMMENACKER., AND P.D.KARP 2005. [HumanCyc04]Computational prediction of human metabolic pathways from the complete human genome. *Genome Biology,* 6.

RABANAL-RUIZ, Y., BYRON, A., WIRTH, A., MADSEN, R., SEDLACKOVA, L., HEWITT, G., NELSON, G., STINGELE, J., WILLS, J. C., ZHANG, T., ZEUG, A., FASSLER, R., VANHAESEBROECK, B., MADDOCKS, O. D. K., PONIMASKIN, E., CARROLL, B. & KOROLCHUK, V. I. 2021. mTORC1 activity is supported by spatial association with focal adhesions. *J Cell Biol,* 220.

R, M. B.-C., HELAL-NETO, E., A, M. V., BARCELLOS-DE-SOUZA, P., MORGADO-DIAZ, J. & BARJA-FIDALGO, C. 2020. Extracellular Matrix Derived from High Metastatic Human Breast Cancer Triggers Epithelial-Mesenchymal Transition in Epithelial Breast Cancer Cells through alphavbeta3 Integrin. *Int J Mol Sci,* 21.

RAFAEVA, M., JENSEN, A. R. D., HORTON, E. R., ZORNHAGEN, K. W., STROBECH, J. E., FLEISCHHAUER, L., MAYORCA-GUILIANI, A. E., NIELSEN, S. R., GRONSETH, D. S., KUS, F., SCHOOF, E. M., ARNES, L., KOCH, M., CLAUSEN-SCHAUMANN, H., IZZI, V., REUTEN, R. & ERLER, J. T. 2023. Fibroblast-derived matrix models

desmoplastic properties and forms a prognostic signature in cancer progression. *Front Immunol,* 14**,** 1154528.
RAINERO, E. 2016. Extracellular matrix endocytosis in controlling matrix turnover and beyond: emerging roles in cancer. *Biochem Soc Trans,* 44**,** 1347-1354.
RAINERO, E. 2024. Overcoming Nutrient Stress: Integrin alphavbeta3-Driven Metabolic Adaptation Supports Tumor Initiation. *Cancer Res,* 84**,** 1543-1545.
RAINERO, E., HOWE, J. D., CASWELL, P. T., JAMIESON, N. B., ANDERSON, K., CRITCHLEY, D. R., MACHESKY, L. & NORMAN, J. C. 2015. Ligand-Occupied Integrin Internalization Links Nutrient Signaling to Invasive Migration. *Cell Rep,* 10**,** 398-413.
RAMIREZ, N. E., ZHANG, Z., MADAMANCHI, A., BOYD, K. L., O'REAR, L. D., NASHABI, A., LI, Z., DUPONT, W. D., ZIJLSTRA, A. & ZUTTER, M. M. 2011. The alpha(2)beta(1) integrin is a metastasis suppressor in mouse models and human cancer. *J Clin Invest,* 121**,** 226-37.
RAUT, G. K., CHAKRABARTI, M., PAMARTHY, D. & BHADRA, M. P. 2019. Glucose starvation-induced oxidative stress causes mitochondrial dysfunction and apoptosis via Prohibitin 1 upregulation in human breast cancer cells. *Free Radic Biol Med,* 145**,** 428-441.
READER, C. S., VALLATH, S., STEELE, C. W., HAIDER, S., BRENTNALL, A., DESAI, A., MOORE, K. M., JAMIESON, N. B., CHANG, D., BAILEY, P., SCARPA, A., LAWLOR, R., CHELALA, C., KEYSE, S. M., BIANKIN, A., MORTON, J. P., EVANS, T. J., BARRY, S. T., SANSOM, O. J., KOCHER, H. M. & MARSHALL, J. F. 2019. The integrin alphavbeta6 drives pancreatic cancer through diverse mechanisms and represents an effective target for therapy. *J Pathol,* 249**,** 332-342.
RECOUVREUX, M. V. & COMMISSO, C. 2017. Macropinocytosis: A Metabolic Adaptation to Nutrient Stress in Cancer. *Front Endocrinol (Lausanne),* 8**,** 261.
REN, D., ZHAO, J., SUN, Y., LI, D., MENG, Z., WANG, B., FAN, P., LIU, Z., JIN, X. & WU, H. 2019. Overexpressed ITGA2 promotes malignant tumor aggression by up-regulating PD-L1 expression through the activation of the STAT3 signaling pathway. *J Exp Clin Cancer Res,* 38**,** 485.
REUTEN, R., ZENDEHROUD, S., NICOLAU, M., FLEISCHHAUER, L., LAITALA, A., KIDERLEN, S., NIKODEMUS, D., WULLKOPF, L., NIELSEN, S. R., MCNEILLY, S., PREIN, C., RAFAEVA, M., SCHOOF, E. M., FURTWANGLER, B., PORSE, B. T., KIM, H., WON, K. J., SUDHOP, S., ZORNHAGEN, K. W., SUHR, F., MANIATI, E., PEARCE, O. M. T., KOCH, M., ODDERSHEDE, L. B., VAN AGTMAEL, T., MADSEN, C. D., MAYORCA-GUILIANI, A. E., BLOCH, W., NETZ, R. R., CLAUSEN-SCHAUMANN, H. & ERLER, J. T. 2021. Basement membrane stiffness determines metastases formation. *Nat Mater,* 20**,** 892-903.
RHEE, D. K., PARK, S. H. & JANG, Y. K. 2008. Molecular signatures associated with transformation and progression to breast cancer in the isogenic MCF10 model. *Genomics,* 92**,** 419-28.
RICE, A. J., CORTES, E., LACHOWSKI, D., CHEUNG, B. C. H., KARIM, S. A., MORTON, J. P. & DEL RIO HERNANDEZ, A. 2017. Matrix stiffness induces epithelial-mesenchymal transition and promotes chemoresistance in pancreatic cancer cells. *Oncogenesis,* 6**,** e352.

RICARD-BLUM, S. 2010. The Collagen Family. *Cold Spring Harbor Perspectives in Biology,* 3**,** a004978-a004978.
RICK, J. W., CHANDRA, A., DALLE ORE, C., NGUYEN, A. T., YAGNIK, G. & AGHI, M. K. 2019. Fibronectin in malignancy: Cancer-specific alterations, protumoral effects, and therapeutic implications. *Semin Oncol,* 46**,** 284-290.
ROBERTSON, J., JACQUEMET, G., BYRON, A., JONES, M. C., WARWOOD, S., SELLEY, J. N., KNIGHT, D., HUMPHRIES, J. D. & HUMPHRIES, M. J. 2015. Defining the phospho-adhesome through the phosphoproteomic analysis of integrin signalling. *Nat Commun,* 6**,** 6265.
ROSS, E., ATA, R., THAVARAJAH, T., MEDVEDEV, S., BOWDEN, P., MARSHALL, J. G. & ANTONESCU, C. N. 2015. AMP-Activated Protein Kinase Regulates the Cell Surface Proteome and Integrin Membrane Traffic. *PLoS One,* 10**,** e0128013.
SAAB, J. J. A., DZIEROZYNSKI , L. N., JONKER, P. B., TABRIZI, R. A., SHAH, H., MENJIVAR, R. E., SCOTT, A. J., NWOSU, Z. C., ZHU, Z., CHEN, R. N., OH, M., SHEEHAN, C., WAHL, D. R., MAGLIANO, M. P., LYSSIOTIS, C. A., MACLEOD, K. F., WEBER, C. R. & MUIR, A. 2023. Pancreatic tumors exhibit myeloid-driven amino acid stress and upregulate arginine biosynthesis. *Elife*.
SAKAMOTO, A., KUNOU, S., SHIMADA, K., TSUNODA, M., AOKI, T., IRIYAMA, C., TOMITA, A., NAKAMURA, S., HAYAKAWA, F. & KIYOI, H. 2018. Pyruvate secreted from patient-derived cancer-associated fibroblasts supports survival of primary lymphoma cells. *Cancer Science,* 110**,** 269-278.
SAMARZIJA, I., DEKANIC, A., HUMPHRIES, J. D., PARADZIK, M., STOJANOVIC, N., HUMPHRIES, M. J. & AMBRIOVIC-RISTOV, A. 2020. Integrin Crosstalk Contributes to the Complexity of Signalling and Unpredictable Cancer Cell Fates. *Cancers (Basel),* 12.
SAWAI, H., OKADA, Y., FUNAHASHI, H., MATSUO, Y., TAKAHASHI, H., TAKEYAMA, H. & MANABE, T. 2005. Activation of focal adhesion kinase enhances the adhesion and invasion of pancreatic cancer cells via extracellular signal-regulated kinase-1/2 signaling pathway activation. *Mol Cancer,* 4**,** 37.
SEGUIN, L., KATO, S., FRANOVIC, A., CAMARGO, M. F., LESPERANCE, J., ELLIOTT, K. C., YEBRA, M., MIELGO, A., LOWY, A. M., HUSAIN, H., CASCONE, T., DIAO, L., WANG, J., WISTUBA, II, HEYMACH, J. V., LIPPMAN, S. M., DESGROSELLIER, J. S., ANAND, S., WEIS, S. M. & CHERESH, D. A. 2014. An integrin beta(3)-KRAS-RalB complex drives tumour stemness and resistance to EGFR inhibition. *Nat Cell Biol,* 16**,** 457-68.
SHAN, J., DONELAN, W., HAYNER, J. N., ZHANG, F., DUDENHAUSEN, E. E. & KILBERG, M. S. 2015. MAPK signaling triggers transcriptional induction of cFOS during amino acid limitation of HepG2 cells. *Biochim Biophys Acta,* 1853**,** 539-48.
SHEFFELS, E. & KORTUM, R. L. 2021. The Role of Wild-Type RAS in Oncogenic RAS Transformation. *Genes (Basel),* 12.
SHEN, C. H., YUAN, P., PEREZ-LORENZO, R., ZHANG, Y., LEE, S. X., OU, Y., ASARA, J. M., CANTLEY, L. C. & ZHENG, B. 2013. Phosphorylation of BRAF by AMPK impairs BRAF-KSR1 association and cell proliferation. *Mol Cell,* 52**,** 161-72.
SHI, F. & SOTTILE, J. 2008. Caveolin-1-dependent beta1 integrin endocytosis is a critical regulator of fibronectin turnover. *J Cell Sci,* 121**,** 2360-71.
SHI, F. & SOTTILE, J. 2011. MT1-MMP regulates the turnover and endocytosis of extracellular matrix fibronectin. *J Cell Sci,* 124**,** 4039-50.

SHIOVITZ, S. & KORDE, L. A. 2015. Genetics of breast cancer: a topic in evolution. *Ann Oncol,* 26**,** 1291-9.
SLEEBOOM, J. J. F., TIENDEREN, G., SCHENKE-- LAYLAND, K., VAN DER LAAN, L., W., KHALIL, A. & VERSTEGEN, M., A. 2024. The extracellular matrix as hallmark of cancer and metastasis From biomechanics to therapeutic targets. *Sci.Transl.Med*.
SO, J., Y., LEE, H., J., KRAMATA, P., MINDEN, A. & SUH, N. 2012. Differential Expression of Key signalling proteins in MCF10 cell lines. *Mol Cell Pharmacol*.
SON, J., LYSSIOTIS, C. A., YING, H., WANG, X., HUA, S., LIGORIO, M., PERERA, R. M., FERRONE, C. R., MULLARKY, E., SHYH-CHANG, N., KANG, Y., FLEMING, J. B., BARDEESY, N., ASARA, J. M., HAIGIS, M. C., DEPINHO, R. A., CANTLEY, L. C. & KIMMELMAN, A. C. 2013. Glutamine supports pancreatic cancer growth through a KRAS-regulated metabolic pathway. *Nature,* 496**,** 101-5.
SOTTILE, J. & CHANDLER, J. 2005. Fibronectin matrix turnover occurs through a caveolin-1-dependent process. *Mol Biol Cell,* 16**,** 757-68.
SPADA, S., TOCCI, A., DI MODUGNO, F. & NISTICO, P. 2021. Fibronectin as a multiregulatory molecule crucial in tumor matrisome: from structural and functional features to clinical practice in oncology. *J Exp Clin Cancer Res,* 40**,** 102.
STEINBERG, G. R. & HARDIE, D. G. 2023. New insights into activation and function of the AMPK. *Nat Rev Mol Cell Biol,* 24**,** 255-272.
STRICKLER, J. H., SATAKE, H., GEORGE, T. J., YAEGER, R., HOLLEBECQUE, A., GARRIDO-LAGUNA, I., SCHULER, M., BURNS, T. F., COVELER, A. L., FALCHOOK, G. S., VINCENT, M., SUNAKAWA, Y., DAHAN, L., BAJOR, D., RHA, S. Y., LEMECH, C., JURIC, D., REHN, M., NGARMCHAMNANRITH, G., JAFARINASABIAN, P., TRAN, Q. & HONG, D. S. 2023. Sotorasib in KRAS p.G12C-Mutated Advanced Pancreatic Cancer. *N Engl J Med,* 388**,** 33-43.
SULLIVAN, M. R., DANAI, L. V., LEWIS, C. A., CHAN, S. H., GUI, D. Y., KUNCHOK, T., DENNSTEDT, E. A., VANDER HEIDEN, M. G. & MUIR, A. 2019a. Quantification of microenvironmental metabolites in murine cancers reveals determinants of tumor nutrient availability. *Elife,* 8.
SULLIVAN, M. R., MATTAINI, K. R., DENNSTEDT, E. A., NGUYEN, A. A., SIVANAND, S., REILLY, M. F., MEETH, K., MUIR, A., DARNELL, A. M., BOSENBERG, M. W., LEWIS, C. A. & VANDER HEIDEN, M. G. 2019b. Increased Serine Synthesis Provides an Advantage for Tumors Arising in Tissues Where Serine Levels Are Limiting. *Cell Metab,* 29**,** 1410-1421 e4.
SULLIVAN, W. J., MULLEN, P. J., SCHMID, E. W., FLORES, A., MOMCILOVIC, M., SHARPLEY, M. S., JELINEK, D., WHITELEY, A. E., MAXWELL, M. B., WILDE, B. R., BANERJEE, U., COLLER, H. A., SHACKELFORD, D. B., BRAAS, D., AYER, D. E., DE AGUIAR VALLIM, T. Q., LOWRY, W. E. & CHRISTOFK, H. R. 2018. Extracellular Matrix Remodeling Regulates Glucose Metabolism through TXNIP Destabilization. *Cell,* 175**,** 117-132 e21.
SUN, Z., COSTELL, M. & FASSLER, R. 2019. Integrin activation by talin, kindlin and mechanical forces. *Nat Cell Biol,* 21**,** 25-31.
TAJAN, M., HENNEQUART, M., CHEUNG, E. C., ZANI, F., HOCK, A. K., LEGRAVE, N., MADDOCKS, O. D. K., RIDGWAY, R. A., ATHINEOS, D., SUAREZ-BONNET, A., LUDWIG, R. L., NOVELLASDEMUNT, L., ANGELIS, N., LI, V. S. W.,

VLACHOGIANNIS, G., VALERI, N., MAINOLFI, N., SURI, V., FRIEDMAN, A., MANFREDI, M., BLYTH, K., SANSOM, O. J. & VOUSDEN, K. H. 2021. Serine synthesis pathway inhibition cooperates with dietary serine and glycine limitation for cancer therapy. *Nat Commun,* 12**,** 366.

TAKACS, T., KUDLIK, G., KURILLA, A., SZEDER, B., BUDAY, L. & VAS, V. 2020. The effects of mutant Ras proteins on the cell signalome. *Cancer Metastasis Rev,* 39**,** 1051-1065.

TAKAGI, J., PETRE, B. M., WALZ, T. & SPRINGER, T. A. 2002. Global Conformational Rearrangements in Integrin Extracellular Domains in Outside-In and Inside-Out Signaling. *Cell Press,* 110.

TANG, Z., KANG, B., LI, C., CHEN, T. & ZHANG, Z. 2019. GEPIA2: an enhanced web server for large-scale expression profiling and interactive analysis. Nucleic Acids Res, 47, W556-W560.

TANG, C. H. & LU, M. E. 2009. Adiponectin increases motility of human prostate cancer cells via adipoR, p38, AMPK, and NF-kappaB pathways. *Prostate,* 69**,** 1781-9.

THOMPSON, C. B. 2011. Rethinking the regulation of cellular metabolism. *Cold Spring Harb Symp Quant Biol,* 76**,** 23-9.

TIAN, C., CLAUSER, K. R., OHLUND, D., RICKELT, S., HUANG, Y., GUPTA, M., MANI, D. R., CARR, S. A., TUVESON, D. A. & HYNES, R. O. 2019. Proteomic analyses of ECM during pancreatic ductal adenocarcinoma progression reveal different contributions by tumor and stromal cells. *Proc Natl Acad Sci U S A,* 116**,** 19609-19618.

TILGHMAN, R. W., BLAIS, E. M., COWAN, C. R., SHERMAN, N. E., GRIGERA, P. R., JEFFERY, E. D., FOX, J. W., BLACKMAN, B. R., TSCHUMPERLIN, D. J., PAPIN, J. A. & PARSONS, J. T. 2012. Matrix rigidity regulates cancer cell growth by modulating cellular metabolism and protein synthesis. *PLoS One,* 7**,** e37231.

VELLING, T., NILSSON, S., STEFANSSON, A. & JOHANSSON, S. 2004. beta1-Integrins induce phosphorylation of Akt on serine 473 independently of focal adhesion kinase and Src family kinases. *EMBO Rep,* 5**,** 901-5.

VOORDE, J. V., ACKERMANN , T., PFETZER , N., SUMPTON , D., MACKAY, G., KALNA, G., NIXON, C., BLYTH, K., GOTTLIEB, E. & TARDITO, S. 2019. Improving the metabolic fidelity of cancer models with a physiological cell culture medium. *Sci. Adv*.

WANG, J., WHITEMAN, M. W., LIAN, H., WANG, G., SINGH, A., HUANG, D. & DENMARK, T. 2009. A non-canonical MEK/ERK signaling pathway regulates autophagy via regulating Beclin 1. *J Biol Chem,* 284**,** 21412-24.

WANG, X., ALLEN, S., BLAKE, J. F., BOWCUT, V., BRIERE, D. M., CALINISAN, A., DAHLKE, J. R., FELL, J. B., FISCHER, J. P., GUNN, R. J., HALLIN, J., LAGUER, J., LAWSON, J. D., MEDWID, J., NEWHOUSE, B., NGUYEN, P., O'LEARY, J. M., OLSON, P., PAJK, S., RAHBAEK, L., RODRIGUEZ, M., SMITH, C. R., TANG, T. P., THOMAS, N. C., VANDERPOOL, D., VIGERS, G. P., CHRISTENSEN, J. G. & MARX, M. A. 2022. Identification of MRTX1133, a Noncovalent, Potent, and Selective KRAS(G12D) Inhibitor. *J Med Chem,* 65**,** 3123-3133.

WANG, X., SHANG, Y., YANG, L., TAN, X., ZHANG, H., SHAN, C. & LIU, S. 2019. <HPD overexpression predicts poor prognosis in breast cancer.pdf>. *Pathology*.

WANG, Y. & MINDEN, A. 2022. Current Molecular Combination Therapies Used for the Treatment of Breast Cancer. *Int J Mol Sci,* 23.

WANG, Z., YANG, Q., TAN, Y., TANG, Y., YE, J., YUAN, B. & YU, W. 2021. Cancer-Associated Fibroblasts Suppress Cancer Development: The Other Side of the Coin. *Front Cell Dev Biol,* 9**,** 613534.

WEI, L., LIN, Q., LU, Y., LI, G., HUANG, L., FU, Z., CHEN, R. & ZHOU, Q. 2021. Cancer-associated fibroblasts-mediated ATF4 expression promotes malignancy and gemcitabine resistance in pancreatic cancer via the TGF-beta1/SMAD2/3 pathway and ABCC1 transactivation. *Cell Death Dis,* 12**,** 334.

WHITE, D. P., CASWELL, P. T. & NORMAN, J. C. 2007. alpha v beta3 and alpha5beta1 integrin recycling pathways dictate downstream Rho kinase signaling to regulate persistent cell migration. *J Cell Biol,* 177**,** 515-25.

WIENKE, D., DAVIES, G. C., JOHNSON, D. A., STURGE, J., LAMBROS, M. B., SAVAGE, K., ELSHEIKH, S. E., GREEN, A. R., ELLIS, I. O., ROBERTSON, D., REIS-FILHO, J. S. & ISACKE, C. M. 2007. The collagen receptor Endo180 (CD280) Is expressed on basal-like breast tumor cells and promotes tumor growth in vivo. *Cancer Res,* 67**,** 10230-40.

WIENKE, D., MACFADYEN, J. R. & ISACKE, C. M. 2003. Identification and characterization of the endocytic transmembrane glycoprotein Endo180 as a novel collagen receptor. *Mol Biol Cell,* 14**,** 3592-604.

WINKLER, J., ABISOYE-OGUNNIYAN, A., METCALF, K. J. & WERB, Z. 2020. Concepts of extracellular matrix remodelling in tumour progression and metastasis. *Nat Commun,* 11**,** 5120.

WOODS, D., CHERWINSKI, H., VENETSANAKOS, E., BHAT, A., GYSIN, S., HUMBERT, M., BRAY, P. F., SAYLOR, V. L. & MCMAHON, M. 2001. Induction of beta3-integrin gene expression by sustained activation of the Ras-regulated Raf-MEK-extracellular signal-regulated kinase signaling pathway. *Mol Cell Biol,* 21**,** 3192-205.

WU, C., YOU, J., FU, J., WANG, X. & ZHANG, Y. 2016. Phosphatidylinositol 3-Kinase/Akt Mediates Integrin Signaling To Control RNA Polymerase I Transcriptional Activity. *Mol Cell Biol,* 36**,** 1555-68.

WU, K., FUKUDA, K., XING, F., ZHANG, Y., SHARMA, S., LIU, Y., CHAN, M. D., ZHOU, X., QASEM, S. A., POCHAMPALLY, R., MO, Y. & WATABE, K. 2015. Roles of the Cyclooxygenase 2 Matrix Metalloproteinase 1 Pathway in Brain Metastasis of Breast Cancer. *J Biol Chem,* 290.

XIE, J., BAO, M., HU, X., KOOPMAN, W. J. H. & HUCK, W. T. S. 2021. Energy expenditure during cell spreading influences the cellular response to matrix stiffness. *Biomaterials,* 267**,** 120494.

XIONG, X., ZHENG, L. W., DING, Y., CHEN, Y. F., CAI, Y. W., WANG, L. P., HUANG, L., LIU, C. C., SHAO, Z. M. & YU, K. D. 2025. Breast cancer: pathogenesis and treatments. *Signal Transduct Target Ther,* 10**,** 49.

XU, S., XU, H., WANG, W., LI, S., LI, H., LI, T., ZHANG, W., YU, X. & LIU, L. 2019. The role of collagen in cancer: from bench to bedside. *J Transl Med,* 17**,** 309.

XU, X., FANG, Y., NOWSHEEN, S., LI, Y. X., LOU, Z. & DENG, M. 2024. Regulation of AMPK activation by extracellular matrix stiffness in pancreatic cancer. *Genes Dis,* 11**,** 101035.

YAMAUCHI, T., KAMON, J., ITO, Y., TSUCHIDA, A., YOKOMIZOK, T., KITA, S., SUGIYAMA, T., MIYAGISHI, M., HARA, K., TSUNODAQ, M., MURAKAMIQ, K., OHTEKI, T., UCHIDA, S., TAKEKAWA, S., WAKI, H., TSUNO, N., SHIBATA, Y., TERAUCHI, Y.,

FROGUEL, P., TOBE, K., KOYASU, S., TAIRA, K., KITAMURA, T., SHIMIZUK, T., NAGAI, R. & KADOWAKI, T. 2003. Cloning of adiponectin receptors that mediate antidiabetic
metabolic effects. *Nature,* 423.

YAMAZAKI, S., SU, Y., MARUYAMA, A., MAKINOSHIMA, H., SUZUKI, J., TSUBOI, M., GOTO, K., OCHIAI, A. & ISHII, G. 2020. Uptake of collagen type I via macropinocytosis cause mTOR activation and anti-cancer drug resistance. *Biochem Biophys Res Commun,* 526**,** 191-198.

YANES, B. & RAINERO, E. 2022. The Interplay between Cell-Extracellular Matrix Interaction and Mitochondria Dynamics in Cancer. *Cancers (Basel),* 14.

YANG, C. S., STAMPOULOGLOU, E., KINGSTON, N. M., ZHANG, L., MONTI, S. & VARELAS, X. 2018. Glutamine-utilizing transaminases are a metabolic vulnerability of TAZ/YAP-activated cancer cells. *EMBO Rep,* 19.

YANG, D., LIU, J., QIAN, H. & ZHUANG, Q. 2023. Cancer-associated fibroblasts: from basic science to anticancer therapy. *Exp Mol Med,* 55**,** 1322-1332.

YANG, L., MOSS, T., MANGALA, L. S., MARINI, J., ZHAO, H., WAHLIG, S., ARMAIZ-PENA, G., JIANG, D., ACHREJA, A., WIN, J., ROOPAIMOOLE, R., RODRIGUEZ-AGUAYO, C., MERCADO-URIBE, I., LOPEZ-BERESTEIN, G., LIU, J., TSUKAMOTO, T., SOOD, A. K., RAM, P. T. & NAGRATH, D. 2014. Metabolic shifts toward glutamine regulate tumor growth, invasion and bioenergetics in ovarian cancer. *Molecular Systems Biology,* 10.

YANG, X. & WU, H. 2024. RAS signaling in carcinogenesis, cancer therapy and resistance mechanisms. *J Hematol Oncol,* 17**,** 108.

YANG, Y., BOLOMSKY, A., OELLERICH, T., CHEN, P., CERIBELLI, M., HAUPL, B., WRIGHT, G. W., PHELAN, J. D., HUANG, D. W., LORD, J. W., VAN WINKLE, C. K., YU, X., WISNIEWSKI, J., WANG, J. Q., TOSTO, F. A., BECK, E., WILSON, K., MCKNIGHT, C., TRAVERS, J., KLUMPP-THOMAS, C., SMITH, G. A., PITTALUGA, S., MARIC, I., KAZANDJIAN, D., THOMAS, C. J. & YOUNG, R. M. 2022. Oncogenic RAS commandeers amino acid sensing machinery to aberrantly activate mTORC1 in multiple myeloma. *Nat Commun,* 13**,** 5469.

YANG, Y., WANG, Y., CHE, X., HOU, K., WU, J., ZHENG, C., CHENG, Y., LIU, Y., HU, X. & ZHANG, J. 2021. Integrin alpha5 promotes migration and invasion through the FAK/STAT3/AKT signaling pathway in icotinib-resistant non-small cell lung cancer cells. *Oncol Lett,* 22**,** 556.

YAO, D., LI, C., RAJOKA, M. S. R., HE, Z., HUANG, J., WANG, J. & ZHANG, J. 2020. P21-Activated Kinase 1: Emerging biological functions and potential therapeutic targets in Cancer. *Theranostics,* 10**,** 9741-9766.

YE, J., KUMANOVA, M., HART, L. S., SLOANE, K., ZHANG, H., DE PANIS, D. N., BOBROVNIKOVA-MARJON, E., DIEHL, J. A., RON, D. & KOUMENIS, C. 2010. The GCN2-ATF4 pathway is critical for tumour cell survival and proliferation in response to nutrient deprivation. *EMBO J,* 29**,** 2082-96.

YE, X., WEI, X., LIAO, J., CHEN, P., LI, X., CHEN, Y., YANG, Y., ZHAO, Q., SUN, H., PAN, L., CHEN, G., HE, X., LYU, J. & FANG, H. 2020. 4-Hydroxyphenylpyruvate Dioxygenase-Like Protein Promotes Pancreatic Cancer Cell Progression and Is Associated With Glutamine-Mediated Redox Balance. *Front Oncol,* 10**,** 617190.

YI, W., XIAO, E., DING, R., LUO, P. & YANG, Y. 2016. High expression of fibronectin is associated with poor prognosis, cell proliferation and malignancy via the NF-

κB/p53-apoptosis signaling pathway in colorectal cancer. *Oncology Reports,* 36**,** 3145-3153.

YING, H., KIMMELMAN, A. C., LYSSIOTIS, C. A., HUA, S., CHU, G. C., FLETCHER-SANANIKONE, E., LOCASALE, J. W., SON, J., ZHANG, H., COLOFF, J. L., YAN, H., WANG, W., CHEN, S., VIALE, A., ZHENG, H., PAIK, J. H., LIM, C., GUIMARAES, A. R., MARTIN, E. S., CHANG, J., HEZEL, A. F., PERRY, S. R., HU, J., GAN, B., XIAO, Y., ASARA, J. M., WEISSLEDER, R., WANG, Y. A., CHIN, L., CANTLEY, L. C. & DEPINHO, R. A. 2012. Oncogenic Kras maintains pancreatic tumors through regulation of anabolic glucose metabolism. *Cell,* 149**,** 656-70.

YUAN, S., BACCHETTI, R., ADAMS, J., CUFFARO, D., ROSSELLO, A., NUTI, E., SANTAMARIA, S. & RAINERO, E. 2025. The protease ADAMTS5 controls ovarian cancer cell invasion, downstream of Rab25. *FEBS J*.

YUN, J., RAGO, C., CHEONG, I., PAGLIARINI, R., ANGENENDT, P., RAJAGOPALAN, H., SCHMIDT, K., WILLSON, J. K., MARKOWITZ, S., ZHOU, S., DIAZ, L. A., JR., VELCULESCU, V. E., LENGAUER, C., KINZLER, K. W., VOGELSTEIN, B. & PAPADOPOULOS, N. 2009. Glucose deprivation contributes to the development of KRAS pathway mutations in tumor cells. *Science,* 325**,** 1555-9.

ZANOTELLI, M. R., GOLDBLATT, Z. E., MILLER, J. P., BORDELEAU, F., LI, J., VANDERBURGH, J. A., LAMPI, M. C., KING, M. R. & REINHART-KING, C. A. 2018. Regulation of ATP utilization during metastatic cell migration by collagen architecture. *Mol Biol Cell,* 29**,** 1-9.

ZHANG, K., MYLLYMÄKI, S. M., GAO, P., DEVARAJAN, R., KYTÖLÄ, V., NYKTER, M., WEI, G. H. & MANNINEN, A. 2017. Oncogenic K-Ras upregulates ITGA6 expression via FOSL1 to induce anoikis resistance and synergizes with αV-Class integrins to promote EMT. *Oncogene,* 36**,** 5681-5694.

ZHANG, N., YANG, X., YUAN, F., ZHANG, L., WANG, Y., WANG, L., MAO, Z., LUO, J., ZHANG, H., ZHU, W. G. & ZHAO, Y. 2018. Increased Amino Acid Uptake Supports Autophagy-Deficient Cell Survival upon Glutamine Deprivation. *Cell Rep,* 23**,** 3006-3020.

ZHANG, Q., AN, Z. Y., JIANG, W., JIN, W. L. & HE, X. Y. 2023. Collagen code in tumor microenvironment: Functions, molecular mechanisms, and therapeutic implications. *Biomed Pharmacother,* 166**,** 115390.

ZHANG, T., REN, Y., YANG, P., WANG, J. & ZHOU, H. 2022. Cancer-associated fibroblasts in pancreatic ductal adenocarcinoma. *Cell Death Dis,* 13**,** 897.

ZHOU, K., LIU, Y., TANG, C. & ZHU, H. 2025. Pancreatic Cancer: Pathogenesis and Clinical Studies. *MedComm (2020),* 6**,** e70162.ANDERSON, N. M. & SIMON, M. C. 2020. The tumor microenvironment. *Curr Biol,* 30**,** R921-R925.